REGULATION OF GUARD CELL ANION CHANNELS

Yizhou Wang

B.Sc., M.Sc.

Thesis submitted for the degree of Doctor of Philosophy

Institute of Molecular, Cell and Systems Biology

College of Medical, Veterinary and Life Sciences

University of Glasgow

November 2012

DECLARATION

All the works presented in this thesis is my own, with the following exceptions: the gas exchange and qPCR experiments in Chapter 5 were collected jointly with Dr. Cornelia Eisenach and Ms Maria Papanatsiou, respectively. The mathematic modeling in Chapter 5 was performed and analyzed by Professor Michael Blatt.

Parts of the work described in this thesis have been published as:

WANG, Y. **and BLATT, M.R.** (2011)**.** Anion channel sensitivity to cytosolic organic acids implicates a central role for oxaloacetate in integrating ion flux with metabolism in stomatal guard cells. ***Biochemical Journal*** 439 (1): 161-170.

WANG, Y., **PAPANATSIOU, M., EISENACH, C., KARNIK, R., WILLIAMS, M., HILLS, A., LEW, V.L. and BLATT. M.R.** (2012). Systems dynamic modelling of a guard cell Cl^- channel mutant uncovers an emergent homeostatic network regulating stomatal transpiration. ***Plant Physiology*** 160: 1956-1967

Yizhou Wang

ACKNOWLEDGEMENTS

I would like to thank my supervisor Professor Mike Blatt for his never-ending patience, support and help with my study. Thank you for taking me into the world of electrophysiology, which is amazing!!!

I thank my parents for their love, support and encouragement. Without them I could have never achieved as much as I have. I also want to thank my grandparents and all family members; thank you for your understanding and support. I dedicate my thesis to all of them.

My study in Glasgow would have meant nothing without the support and friendship of everyone in Stevenson lab: Zhonghua Chen, Anna Amtmann, Cornelia Eisenach, Ben Zhang, Annegret Honsbein, Christopher Grefen, Giorgio Perella, Maria Papanatsiou, Fabian Kellermeier, Ema Sani, Amparo Ruiz-Pardo, Naomi Donald, Rucha Karnik, Vajay Kanth, Mary Williams, Adrian Hills, Craig Carr, Carla Parramona, George Boswell and all the people from Bower Building.

ABSTRACT

Stomata account for much of the 70% of global water usage associated with agriculture, and have a profound impact on the water and carbon cycles of the world. Anion channels at the plasma membrane of the guard cell are thought to comprise a major pathway for anion efflux essential for driving stomatal closure. The activity of these channels is therefore tightly linked to abscisic acid (ABA)-dependent stomatal movements.

Both the inorganic anion Cl^- and the organic acid anion malate (Mal) are transported during stomatal movements. The metabolism of organic acids, primarily Mal, plays an especially important role in these processes. However, little is known of the regulation of anion channel current (I_{Cl}) or its connection with cytosolic Mal and its immediate metabolite oxaloacetate (OAA). Work described here focuses on the relation of I_{Cl} and its connections with metabolism and signals controlling other transport at the guard cell plasma membrane. Thus the impact of Mal, OAA and of acetate on I_{Cl} in *Vicia* guard cells was examined, and results shown that all three organic acids affect I_{Cl} with different characteristics. Most prominent, the suppression of I_{Cl} by OAA within the physiological range *in vivo* indicates a capacity for OAA to co-ordinate organic acid metabolism with I_{Cl} through a direct effect of organic acid pool size.

In a second set of studies, the ABA pathway that elevates cytosolic free Ca^{2+} ($[Ca^{2+}]_i$) in order to activate I_{Cl} was explored. These studies build on the discovery of PYR/PRL ABA receptors. Previous analysis of the *pyr1/pyl1/pyl2/pyl4* mutant suggested that $[Ca^{2+}]_i$ increases are suppressed. However, direct evidence had not been forthcoming. Thus a combination of voltage clamp and fluorescent ratio analysis with the Ca^{2+}-sensitive dye Fura2 was used to show that the activity of Ca^{2+} channels (I_{Ca}) at the plasma membrane in the *pyr1/pyl1/pyl2/pyl4* mutant is not activated by ABA, with the effect that $[Ca^{2+}]_i$ increases were suppressed. Further studies showed that the normal action of ABA in promoting reactive oxygen species (ROS) was impaired, although adding H_2O_2 was sufficient to activate the I_{Ca} and trigger stomatal closure in the mutant. These results offer direct evidence that the PYR/PYL receptor proteins contribute to the activation by ABA of I_{Ca} through ROS, thus affecting $[Ca^{2+}]_i$ and its regulation of osmotic solute flux for stomatal closure.

Finally, the connection between I_{Cl} and the K^+ channel currents in the *slac1* mutant of *Arabidopsis* was studied. These studies employed systems dynamic modelling to explain the paradoxical suppression of the inward-rectifying K^+ channel current, $I_{K,in}$ and slowing of stomatal opening, by mutation that eliminated the SLAC1 anion channel. Through measuring pH_i and $[Ca^{2+}]_i$ *in vivo* confirmed the model predictions that the abnormal cytosolic pH (pH_i) and $[Ca^{2+}]_i$ suppresses $I_{K,in}$ in the *slac1* mutant, and experimental manipulation of pH_i and $[Ca^{2+}]_i$ was sufficient to recover $I_{K,in}$ and stomatal opening. These data uncover a previously unrecognised signaling network that minimises the effects of the *slac1* mutant on transpiration, and they underscore the importance of H^+-coupled anion transport for pH_i homeostasis.

ABBREVIATIONS

ABA	abscisic acid
ABI	ABA Insensitive protein
Ac	acetate
AKT	*Arabidopsis* K^+ transporter
ALMT	aluminum-activated malate transporter
AHA	*Arabidopsis* H^+-ATPase
ATP	adenosine-5'-triphosphate
BAPTA	1,2-bis(2-aminophenoxy)ethane- N,N,N',N'-tetraacetic acid
BCECF	2′,7′-bis-(2-carboxyethyl)-5-(and-6)-carboxyfluorescein
$[Ca^{2+}]_i$	cytosolic free Ca^{2+}
$[Ca^{2+}]_o$	extracellular Ca^{2+}
cADPR	cyclic ADP Ribose
CBL	calcineurin B-like protein
CDPK	calcium dependent protein kinases
CLC	H^+/Cl^- sntiporters
C_m	membrane capacitance
CO_2	carbon dioxide
CIPK	CBL-interacting protein kinase
E_{rev}	reversal potential
E_x	equilibrium potential (for a given ion,X)
Fura2	polyamino carboxylic-ethane-N,N,N',N'-tetraacetic acid
FV	fast vacuolar ion channel
GORK	guard cell outward-rectifier K^+ channel
GTP	guanosine-5'-trisphosphate
HACC	hyperpolarization-activated Ca^{2+} channel
H^+-ATPase	H^+ translocating ATPase
H_2DCFDA	2',7'-dichlorodihydrofluorescein diacetate
I_{Ca}	calcium channel current
I_{Cl}	chloride channel current

$I_{K,in}$	inward-rectifying K^+ current
$I_{K,out}$	outward-rectifying K^+ current
K_{in}	inward-rectifying K^+ channel
K_{out}	outward-rectifying K^+ channel
KAT	K^+ channel of *Arabidopsis thaliana*
KC1	K^+ rectifying channel 1
K_d	dissociation constant
K_i	half-maximal inhibition
Mal	malate
MES	2-(N-morpholino)ethanesulfonic acid
NO	nitric oxide
OAA	oxaloacetate
OST1	open stomata1
P_o	open probability
PYR/PYL/RCAR	pyrabactin resistance/ pyrabactin resistance-like protein
PP2C	protein phosphatase 2C
QUAC	quick-activating anion channel
ROS	reactive oxygen species
SLAC	slow anion channel
SLAH	SLAC1 homolog
SnRK	SNF1-related kinase
SV	slow vacuolar ion channel
$t_{1/2}$	halftime
TEA	tetraethylammonium
TPC	two-pore Ca^{2+} channel
TPK	two-pore K^+ channel
V-ATPase	vacuolar H^+-ATPase
VCL	vacuolar chloride channel
VK	vacuolar K^+ channel
V-PPase	vacuolar H^+-pyrophosphatase

TABLE OF CONTENTS

LIST OF FIGURES

LIST OF TABLES

LIST OF EQUATIONS

CHAPTER 1:

INTRODUCTION

1.1 Introduction

The stomata of plants are small pores surrounded by pairs of specialized cells, known as guard cells. Localized at the surface of leaves and stems, stomata provide the major route for gas exchange across the impermeable cuticle of leaves and stems (Hetherington and Woodward, 2003). From a physiological view, the synthesis of biomass in plants depends mainly on the balance of photosynthesis and transpiration that is mediated by adjustment of the stomatal aperture (Nilson and Assmann, 2007, Hetherington and Woodward, 2003). Stomata open to allow carbon dioxide (CO_2) enter to plant tissue for photosynthesis, and stomata close to prevent water loss from the leaf (Woodward, 2002). The role in controlling water evaporation from the plant is essential for survival of land plants: a large number of studies indicate that up to 95% of water loss from plants is through the stomatal pores (Schroeder et al., 2001b). In short, the regulation of stomata is thought to have a great impact on carbon and water cycles of the world and to contribute to ongoing climate change (Gedney et al., 2006). Clearly, understanding how stomata function is very important for agriculture, for rational using of water on arable and irrigated lands, and, of course, for future developments leading to improved crops that can deal with global climate change.

Most plants open and close their stomata during the daytime in response to changing conditions, such as light intensity, humidity, and CO_2 concentration. Guard cells regulate the aperture of the stomatal pore through changes in osmotic pressure. They swell to open and shrink to close the pore and these movements are driven by turgor changes with the osmotic content (Ehret and Boyer, 1979). The turgor pressure in guard cells is generated by ions that accumulate in the cells, including potassium (K^+), chloride (Cl^-), and malate (Mal) ions (Blatt, 2000). Increasing concentrations of these osmolites reduces the water potential (Ψ) inside the guard cells, and it leads to water influx which raises the turgor pressure. With the rise in turgor pressure, the guard cells swell and, because of the unique arrangements of the cell wall (Raschke, 1979), the cells bow, which opens the pore. Conversely, during stomatal closure much of these osmotic solutes are released from cell, reducing the turgor pressure and closing the stomatal pore. Guard cells are small on the scale of most plant cells, so the changes in K^+ ion contents is large in guard cells: in *Vicia*

for example, these changes are only 2-4 pmol K^+ per cell, but nonetheless translate to an effective change in osmotic strength equivalent to 200-300 mOsM (Blatt, 2000). Mature guard cells do not have functional plasmodesmata. Therefore, the ion fluxes must involve transport across the plasma membrane. In short, regulated ion transport is crucial for homeostasis and regulation of stomatal movements by the guard cells.

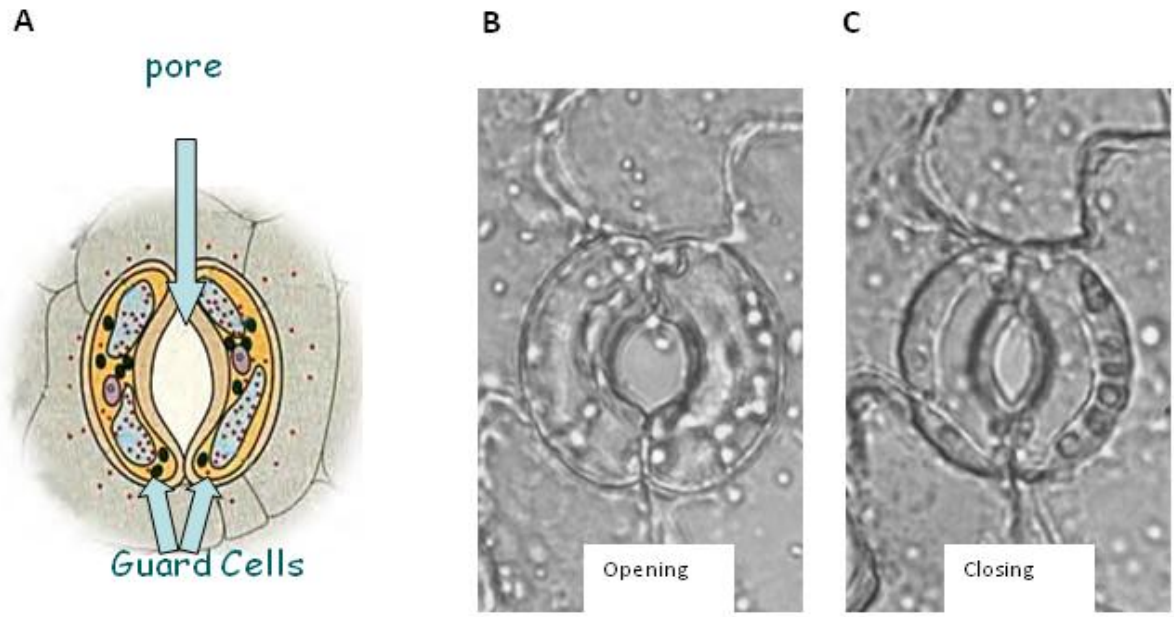

Figure 1. 1 The stoma construction.

A, Stomatal pore is surrounded by two kidney-shaped guard cells.

B and **C,** Images of *Vicia* guard cell in opening and closing stages.

1.2 Ion Transport at Plant Plasma Membrane

1.2.1 Plasma Membrane and Membrane Voltage

The plasma membrane physically separates intracellular compartments from the extracellular environment. Due to its lipid-based structure, the plasma membrane of plants, including guard cells, has a highly selective permeability that allows only non-polar molecules to pass, and it is almost impermeable to most water-soluble molecules (Alberts et al., 2002). To allow the movement of water-soluble molecules, several types of transmembrane proteins are embedded in the lipid bilayer. Several of these serve as transporters to move ions across the membrane. These proteins include ion pumps, H^+-coupled symport and antiport systems, and ion channels. The resulting permeability for ions contributes to another important biological characteristic, the membrane potential. The membrane potential, also referred to as the plasma membrane voltage (V_m), is the difference in electrical potential between inside and outside plasma membrane, and it arises from charge movement through these various ion pumps and channels. The membrane voltage is an important component of the electrochemical driving force for ion flux across the membrane. In addition, the membrane potential regulates voltage-gating channels. Voltage-gated channels are regulated by changes in membrane voltage so as to control ion permeation. In the following sections I will review some of the important properties of these various ion transporters and their relationship to membrane voltage.

1.2.2 Ion Pumps

Primary ion pumps use chemical energy, usually ATP, to drive the movement of an ionic species across the membrane. The result of this transport is to convert the chemical energy into energy gradient across the membrane. This energy is then used by secondary transporters, including ion carriers and ion channels, to drive vital cellular processes, such as accumulation of anions and elimination of Na^+ and other toxic materials. At the plant plasma membrane, primary transport is mainly energized by a family of protein known as H^+-ATPases that drive H^+ out of cell to generate a H^+ electrochemical driving force across plasma membrane and directed back into the cell (Serrano, 1989, Blatt, 1987, Morsomme and Boutry, 2000, Palmgren, 2001). In thermodynamic terms, the output of H^+-ATPase is

defined by the sum of electrical and chemical gradients, plus the energy released by ATP hydrolysis. Thus the equilibrium potential, E_p, generated by the H^+-ATPase can be described as:

$$E_p = \frac{RT}{zF}\{\ln K_{ATP} + \ln \frac{[ATP]_i}{[ADP]_i[P_i]_i} + z\ln \frac{[H^+]_i}{[H^+]_o}\} \qquad \textbf{[1. 1]}$$

where K_{ATP} is the equilibrilum constant of ATP,$[P_i]_i$ is the cytosolic inorganic phosphate concentration, $[x]_o$ and $[x]_i$ are its extra- and intracellular concentrations, R is the gas constant (8.314 J K^{-1} mol^{-1}), T is the absolute temperature in degrees Kelvin, z is the charge on H^+ and F is Faraday's constant (9.648 x10^4 C mol^{-1}). Given there is no difference in $[H^+]$, the equilibrium potential for H^+-ATPase is around -500 mV. However, the plant cell membrane voltage usually does not exceed -300 mV, because the output H^+-ATPase is used to carry out work in other energy consuming processes, such as H^+ coupled solute transport.

A number of H^+-ATPases has been indentified that generate proton electrochemical gradients over biological membranes in plants (Morsomme and Boutry, 2000). In *Arabidopsis thaliana*, 11 members of the H^+-ATPase protein family (AHA1-AHA11) are known at the plasma membrane. Genetic analyses have revealed that multiple AHAs are expressed in many tissues and organs (Gaxiola et al., 2007). AHA1 and AHA2 are highly expressed in almost all tissues and organs, suggesting that they function as the key plasma membrane H^+-ATPases in maintaining ion homeostasis (Haruta et al., 2010). Other members of this family are found expressed either developmentally and/or in subsets of tissues, including the root and vascular tissues (Palmgren, 2001). AHA1 and AHA5 are expressed in the guard cells (Ueno et al., 2005), and their activities are tightly linked with stomatal opening (Dietrich et al., 2001, Kim et al., 2010). During stomatal opening, these H^+-ATPases are activated to drive H^+ out of the guard cells and hyperpolarize the guard cell membrane. This activity gates inward-rectifying K^+ channels as well as energizing H^+-coupled anion uptake (mentioned below) needed to accumulate osmotically-active solute. Thus, the K^+ influx and accompanying anion influx results in increased cellular osmotic pressure to drive stomatal opening. Equally, inhibition of the H^+-ATPases is

important for stomatal closure. For example, over-expressing of *Arabidopsis* AHA1 results in a strong insensitivity to ABA-induced stomata closure and leads to an open stomatal phenotype (Merlot et al., 2007). Other studies indicate that reduced pump activity – and reduced H^+ extrusion from guard cells – is associated with dark and abscisic acid, both signals that are known to close stomata (Goh et al., 1996). These results are not surprising and they demonstrate that H^+-ATPases contribute directly to cellular ion homeostasis though the energetics of transport and its balance with other ions.

1.2.3 H^+-coupled Transport

The H^+-ATPase provides chemical energy and creates a $[H^+]$ gradient to facilitate H^+-coupled transporters to move ions across the membrane. In principal, the H^+-ATPase and H^+-coupled transport forms a loop in which charge cycles tightly between the outgoing and returning pathways. Indeed, early studies indicated that transport of a coupled substrate and primary transport of H^+ by the H^+-ATPase are kinetically linked (Slayman and Slayman, 1974). Notably, studies on H^+-K^+ symporter (Blatt and Slayman, 1987, Blatt et al., 1987) found the H^+-K^+ symporter and the H^+-ATPase were kinetically interdependent suggesting the two transport processes were mechanistically separate.

Many solutes were transported through coupling the flux of the solute to H^+ return across the plasma membrane. In general, the H^+ movement is accompanied with movement of negative-charged inorganics such as Cl^-, NO_3^- and PO_4^{2-}, which must be transported against a negative membrane voltage. However, such transport could proceed with the movement of positive-charged ions such as K^+ and Na^+. These transport processes are frequently characterized by a net inward current (against H^+ outward currents) and, when the membrane voltage is not clamped, by membrane depolarization. For example, Cl^- transport in *Chara* (Beilby and Walker, 1981), NO_3^- uptake in *Arabidopsis* and *Barley* (Glass et al., 1992, Meharg and Blatt, 1995). These transporters draw on both the voltage and concentration difference for H^+ that makes up the electrochemical potential for the ion, defined at equilibrium by the equation:

$$E_{HS} = \frac{RT}{(\mathrm{n}+\mathrm{m})F}\left\{\mathrm{n}ln\frac{[S]_o}{[S]_i} + \mathrm{m}ln\frac{[H^+]_o}{[H^+]_i}\right\} \qquad \textbf{[1. 2]}$$

where E_{HS} is thr equilibrium potential of H^+ coupled solute. $[S]_o$ and $[S]_i$ are its extra- and intracellular concentrations, R is the gas constant (8.314 J K^{-1} mol^{-1}), T is the absolute temperature in degrees Kelvin, n and m are the charge on solute S and H^+ separately, and F is Faraday's constant (9.648 x10^4 C mol^{-1}).

1.2.4 Ion Channels

Ion movements are not only facilitated by ion pumps, but also contributed by ion channels. In plants, a large number of different ion channels are embedded in the plasma membrane to transport various ions, including K^+, Ca^{2+}, Cl^-, and the organic anion $malate^{2-}$. The flux of any one ionic species passing through a channel is driven solely by the electrochemical gradient force for these ions defined by the Nernst equation:

$$E_x = \frac{RT}{zF} ln \frac{[X]_o}{[X]_i} \qquad \textbf{[1. 3]}$$

where E is the equilibrium or Nernst potential of the ion x, $[x]_o$ and $[x]_i$ are its extra- and intracellular concentrations, R is the gas constant (8.314 J K^{-1} mol^{-1}), T is the absolute temperature in degrees Kelvin, z is the charge on ion x and F is Faraday's constant (9.648 x10^4 C mol^{-1}). In physiological range of guard cell, the cytosolic K^+, for example, is around 200 mM. If there is 10 mM K^+ outside the membrane, the equilibrium potential for K^+, E_K is equal to -76 mV. Similar, the physiological E_{Cl} is around 30 mV, when 30 mM Cl^- outside and 10 mM inside the cell.

Unlike H^+ pumps and H^+-coupled transporters that have high selectivity for ions, ion channels are less discriminating in the ions they carry. For example, many Cl^- channels also carry NO_3^- and Mal, often better than Cl^- (Hedrich et al., 1994, Schmidt and Schroeder, 1994). Similarly, Ca^{2+} channel are generally equally permeable to Ca^{2+} and Ba^{2+} (Gelli and Blumwald, 1997, Hamilton et al., 2000). Another difference between ion channels and pumps is that most channel currents within physiological range can described by Ohm's law.

$$I = g(V - E_X) \qquad \textbf{[1. 4]}$$

Where current (I) is related to conductance (g) and the voltage difference from the equilibrium voltage of ion X. from this equation, we can clear see that ion currents pass through ion channels are regulated by three parameters (g, V and E_x). Most plant ion channels, including K^+, Cl^- and Ca^{2+} channels, are gated by voltage (V), therefore they called voltage-gated ion channels. However, other channels often identified as ligand-gated ion channels depend on the binding of ligands to affect g can also regulate channel activity. Changes in the solute contents of the cell affect E_x which will also affect the current through the open channel. Finally, some channels are also sensitive to the concentrations of specific ions on one side of the membrane or the other. In some cases, these characteristics ensure that the channel will function when there is a driving force for net ion flux in one direction only, for example for uptake, preventing the channel from opening when the driving force is for ion loss. In the following sections, the three major ion channel groups in guard cells plasma membrane that contribute to osmotic solute flux, the K^+ channels, Ca^{2+} channels and anion channels, will be introduced and main chararcteric of these channels are summarized in table 1.1

1.2.4.1 K^+ Channels

Potassium is a major element found in plant tissues and it functions in various physiological processes, including photosynthesis, protein synthesis, activation of some enzymes, phloem solute transport of photoassimilates, and maintenance of cation/anion balance in the cytosol and vacuole (Hopkins and Huner, 2004). For guard cells, K^+ is an essential osmoticum for ionic charge balance and the opening and closing of stomata. Not surprisingly, plants have evolved a large number of K^+ transporters to facilitate K^+ uptake and release across plasma membrane and its distribution around the plant. Two classes of K^+ ion channels have been well-characterized and are found in virtually all cells, namely inward-rectifying and outward-rectifying K^+ channels (Blatt, 2008, Dreyer and Blatt, 2009, Ward et al., 2009). Both classes of channels belong to the well studied K_v-channel family, a superfamily of voltage-sensitive channels found in both prokaryotes and eukaryotes (Papazian et al., 1987, Pongs et al., 1988). The K_v superfamily of K^+ channels, including the Shaker K^+ channels of *Drosophila melanogaster* and the K_v-like K^+ channels of plants, share several common structural features (Pilot et al., 2003).

These channels are all assembled of four homologous subunits, each encoded as a separate polypeptide, that coalesce to generate a central transmembrane pore and provide the permeation pathway for K^+ (Daram et al., 1997). Each of these four subunits is built of six transmembrane α-helices, designated as the S1–S6 α-helices. The pore region is formed between the S5 and S6 α-helices of the four subunits, and these two α-helices are separated by a short segment, known as the pore loop, which includes a highly conserved sequence – TxGYGD – that forms a selectivity filter for K^+ (Uozumi et al., 1995, Becker et al., 1996, Nakamura et al., 1997). In guard cells, like other plant cells, the K_v-like channels divide between two groups. The inward-rectifiers contribute to K^+ uptake and are dominated by the KAT1 (K^+ channel of *Arabidopsis thaliana* 1) and KAT2 (K^+ channel of *Arabidopsis thaliana* 2) gene products. The outward-rectifiers regulate K^+ efflux and comprise the GORK (Guard cell Outward Rectifier K^+) channel protein. The properties of each group are described below.

Inward-Rectifying K^+ Channels

The inward-rectifying K^+ channels (K_{in}) form a predominate pathway for K^+ uptake in guard cells and contribute to the most obvious K^+ current across plasma membrane (Clint and Blatt, 1989). K_{in} have been found also in roots, aleurone and mesophyll protoplasts (Lebaudy et al., 2008a, Kourie and Goldsmith, 1992). *Arabidopsis* guard cells express several of the seven K_{in} channels found in its genome, namely AKT1, AKT2, KAT1, KAT2, and the regulatory and electrically-silent subunit KC1 (Szyroki et al., 2001). Of these, the dominant subunits are KAT1 and its close homologue KAT2. These channels activate at membrane voltages negative of approximately -100 mV, and in millimolar external K^+ they facilitate K^+ influx into cytosol, thus helping to drive stomatal opening. Interestingly, the voltage-dependence of this K_{in} channel is insensitive to extracellular K^+ concentration, but its activity depends on membrane hyperpolarization by the H^+-ATPase (Schroeder, 1988, Blatt, 1992). Proton extrusion hyperpolarizes plasma membrane to create an electrical gradient for K^+ uptake (Thiel et al., 1992, Blatt et al., 1997).

Electrophysiological analyses have provided evidence that K_{in} is formed by KAT1 and KAT2 subunit (Pilot et al., 2001, Lebaudy et al., 2008a, Lebaudy et al., 2008b). KC1 is

considered to be an electrically silent subunit, as its expression does not lead to any K^+ conductance at the plasma membrane. It was activated only when coexpressed with other subunits to form heteromeric channels (Dreyer et al., 1997, Duby et al., 2008, Geiger et al., 2009a). The loss of function *Atkc1* mutant exhibits a reduction in plant biomass production and suggests AtKC1-mediated channel activity regulation is required for normal plant growth (Jeanguenin et al., 2011). Thus KC1 is considered as a regulatory subunit as it reduces the macroscopic conductance and negatively shifts the channel activation potential.

Gating of K_{in} is strongly influenced by Ca^{2+}, pH and protein phosphorylation. Elevation of cytosolic free Ca^{2+} ($[Ca^{2+}]_i$) from 0.1 to 1.5 μM strongly suppresses K_{in} channel activity (Blatt, 1999, Blatt, 2000). External Ca^{2+} ($[Ca^{2+}]_o$) is also able to decrease K_{in} currents regulated by Ca^{2+} entry across the plasma membrane (Grabov and Blatt, 1999, Hamilton et al., 2000, Blatt, 1999). Indeed, increasing extracellular Ca^{2+} concentration leads to increases in $[Ca^{2+}]_i$ and causes stomatal closing (Allen et al., 1999b). Kinetic analysis has shown that K_{in} binds four Ca^{2+} ions per channel with an apparent K_d near 300 nM in *Vicia* guard cells (Grabov and Blatt, 1999). Similarly, K_{in} channels are sensitive to external pH. It has been reported a glutamic acid residue (Glu^{240}) is involved in the extracellular acid activation mechanism of KAT1 (Gonzalez et al., 2012). Although the mechanism is still unclear, it has been found that internal pH also affects K_{in} gating (Grabov and Blatt, 1997).

Outward-Rectifying K+ Channels

Outward-rectifying K^+ channels (K_{out}) are the major route for K^+ release from the cytosol during stomatal closure (Gaymard et al., 1998, Ache et al., 2000, Clint and Blatt, 1989, Blatt and Armstrong, 1993). Unlike K_{in} channels, this class of K^+ channel is activated by membrane depolarization, and gating of K_{out} is sensitive to extracellular K^+ concentrations (Dreyer et al., 2004, Johansson et al., 2006, Blatt, 1988, Armstrong and Blatt, 1995, Blatt and Gradmann, 1997, Roelfsema and Prins, 1997). In guard cells, raising external K^+ leads to slowing in the activation halftime for K_{out} and a shift in channel gating to more positive voltages. Such unique gating properties make K_{out} channels more

adaptable to manipulating K^+ efflux independent of the K^+ concentration outside. The gating properties of K_{out} channels are strongly sensitive to internal pH (Blatt and Armstrong, 1993). It has been shown that an alkaline pH_i can increase the K^+ currents, whereas K_{out} activity is reduced on acidifying the cytosol by loading with the weak acid butyrate (Blatt and Armstrong, 1993). Unlike the K_{in} channels, K_{out} channels are insensitive to $[Ca^{2+}]_i$. For example, when $[Ca^{2+}]_i$ is elevated to micromolar concentrations, it greatly reduces K_{in}, whereas K_{out} is unaffected (Blatt and Armstrong, 1993, Grabov and Blatt, 1997, Blatt, 2000).

1.2.4.2 Anion Channels

During stomatal closing, plant cells have to depolarize the membrane to engage the activity of K_{out} channels and release K^+ to reduce turgor pressure. Unlike animal cells, plants initiate membrane depolarization by activating anion channels, which draws the membrane voltage positive (Roelfsema et al., 2012). In response to relevant external stimuli, guard cells activate anion channels releasing Cl^-, NO_3^- and Malate which drives the membrane voltage positive. Membrane depolarization is limited by the activation of the K_{out} channels thus promoting K^+ release. Membrane depolarization also deactivates the K_{in} channels, thereby inhibiting K^+ uptake. By this sequence of events, guard cells are able to release large amounts of osmotic solutes, thus reducing osmotic pressure and turgor, and closing the stomata. Anion channels at the guard cell plasma membrane divide between two major groups depending on their physiological characteristics. The first group is identified as the slow-activating, or S-type, anion channels and the second group is identified with rapid-activating, or R-type, anion channels (Hedrich et al., 1990, Linder and Raschke, 1992, Schroeder and Keller, 1992). The properties of each group are described below.

R-type Anion Channel

The R-type anion channels have also been named quick-activating anion channel (QUAC). These channels exhibit strongly voltage-dependent features: they activate on increasing membrane voltage beyond the range of -100 to -80 mV and inactivate within a few tens to hundreds of milliseconds at more negative voltages (Linder and Raschke, 1992,

Kolb et al., 1995, Dietrich and Hedrich, 1998). R-type anion channels are permeable to a large range of anions including monovalent anions, such as NO_3^- and Cl^-, as well as some divalent anions including SO_4^{2-} and malate^{2-} (Hedrich and Marten, 1993, Dietrich and Hedrich, 1998). Most important, the R-type anion channels are regulated by anion concentrations on both sides of membrane (Hedrich and Marten, 1993, Wang and Blatt, 2011). For example, external malate shifts the voltage-dependent gating characteristic of the R-type channel towards more negative membrane potentials, extending the voltage range over which the channels will open and release anions out of the cell (Wang and Blatt, 2011, Hedrich and Marten, 1993).

By contrast with the S-type channels discussed below, the molecular identity of the R-type anion channels remains unclear. It has been suggested that the ALMT12 (Aluminium-activated, Malate Transporter 12) and other members of this Aluminium-activated Malate Transporter (ALMT) family contribute to this anion flux in *Arabidopsis* (Meyer et al., 2010). AtALMT12 is highly expressed in guard cells plasma membrane and a mutant lacking AtALMT12 is impaired in dark- and CO_2-induced stomatal closure, as well as in response to abscisic acid (Meyer et al., 2010). Electrophysiological studies have shown that the *atalmt12* mutation leads to a reduced R-type current which suggests that the ALMT protein could be a candidate R-type channel subunit. Furthermore expression of AtALMT12 in *Xenopus* oocytes, shows a voltage-dependent R-type anion currents and this current can be activated by extracellular malate but not Al^{3+} (Meyer et al., 2010). However, R-type anion currents are only reduced by 40% in *almt12* mutant guard cells and, in the absence of extracellular malate, R-type currents are indistinguishable from those observed in wild-type (Meyer et al., 2010, Sasaki et al., 2010). This implies that other proteins also play a role in the formation of guard cell R-type anion channels.

S-type Anion Channel

The Slow, or S-type anion channels were originally identified with a slow-activating and largely voltage-independent current that is strongly activated by $[Ca^{2+}]_i$ in the micromolar range (Siegel et al., 2009, Chen et al., 2010b). These currents have since been

shown to associate with the SLAC1 gene product and its homologues in *Arabidopsis* (Vahisalu et al., 2008, Negi et al., 2008). The *SLAC1* gene (*SLOWANION CHANNEL 1*) is required for stomatal closure induced by either high CO_2 or ABA (Brearley et al., 1997, Grabov et al., 1997, Pei et al., 1997). The SLAC1 protein is a homologue of bacterial and fungal C4-dicarboxylate transporters, and is localized specifically to the plasma membrane of guard cells (Chen et al., 2010a). The loss-of-function *slac1* mutation showed an over-accumulation of the osmotically-active anions, especially Cl^- and Malate, and most interestingly of K^+, which was accumulated to high levels in guard cell protoplasts (Negi et al., 2008). Although loss of SLAC1 resulted in stomata that were unable to close in response to high CO_2, SLAC1 is not permeable to HCO_3^- (Geiger et al., 2009c). Functional analysis indicates that SLAC1 preferentially conducts Cl^- and NO_3^- (Chen et al., 2010a, Geiger et al., 2009c, Geiger et al., 2011). In contrast, another S-type anion channel localized on guard cell plasma membrane, the SLAH3 (the SLAC1 homolog 3), shows a high permeability to NO_3^-, furthermore, extracellular NO_3^- is required to activate SLAH3 (Geiger et al., 2011). Therefore, SLAC1 and SLAH3 appear to play complementary roles to release of Cl^- and NO_3^- during stomatal closure.

1.2.4.3 Ca^{2+} Channels

Several distinct Ca^{2+} channel activities have been characterized in the plasma membrane of plant cells. However, compared with potassium and anion channels, the corresponding genes have not yet been identified. At the guard cell plasma membrane, Hyperpolarization-Activated Ca^{2+} Channels (HACC) have been identified that mediate Ca^{2+} influx (Hamilton et al., 2000, Grabov and Blatt, 1999). Previous studies showed the activity of this type Ca^{2+} channel is enhanced by negative voltage (from approximately -120 mV to -150 mV) and by ABA (Hamilton et al., 2000). ABA activates the Ca^{2+} flux by shifting the voltage threshold for channel activation to more positive potentials (Hamilton et al., 2000). Following studies also indicated that ABA-mediated regulation of these Ca^{2+} channels can occur through second massager of reactive oxygen species (ROS) (Kaplan et al., 2007, Kwak et al., 2003). ABA induces ROS synthesis in guard cells and the elevation of ROS level directly influence on the activation of plasma membrane Ca^{2+} channels. Latter research uncovered ROS-dependent enhancement of the channels is impaired in the

Arabidopsis atrbohd and *atrbohf* mutants which encode NADPH oxidases, thus providing evidence for a role for ROS in Ca^{2+} current regulation by ABA (Kwak et al., 2003). Ca^{2+} influx is also regulated by Ca^{2+}-dependent protein kinases, especially the Ca^{2+}-dependent protein kinases CPK3 and CPK6, and by protein phosphorylation events (Mori et al., 2006). Other types of Ca^{2+} channels are also found at the plasma membrane of plants, such as depolarization-activated Ca^{2+} channels and stretch-activated Ca^{2+} channels, although their physiological characteristics are still poorly understood (Huang et al., 1994, Thuleau et al., 1994, Cosgrove and Hedrich, 1991).

Table 1. 1 Main voltage-gated ion channels on guard cell plasma membrane.

	K^+ Channel		**Anion Channel**		**Ca^{2+} Channel**
	Kin	Kout	R-type	S-type	HACC
Identified Gene	*KAT1, KAT2*	*GORK*	*ALMT12*	*SLAC1* *SLAH3*	
Activation Potential	-100 ~-200 mV	-80~-120 mV	> -100 mV	< -140 mV	< -100 mV
Selectivity	K^+>Rb^+>Na^+ >Li^+>>Cs (Blatt, 1992)	K^+>Rb^+>Na^+ >Li^+>>Cs^+ (Schroeder, 1988)	NO_3^->I^->Br^-> Cl^->>$malate^{2-}$ (Dietrich and Hedrich, 1994)	NO_3^-> Br^-> Cl^->>$malate^{2-}$ (Schmidt and Schroeder, 1994)	Ba^{2+}=Ca^{2+}>>K^+>Cl^- (Hamilton et al., 2000)
Physiological function	K^+ uptake, Stomatal opening	K^+ release, Stomatal closure	Fast electrical signaling, stomtal closing	Mediates sustained anion efflux, stomatal closing	Nutrient uptake of Ca^{2+}, Mg^{2+}, Mn^{2+}
Reversal potential (E_{rev})*	-24 mV at 30 mM K^+ outside (Pei et al., 1998)	-77 mV at 10 mM K^+ outside (Blatt, 1988)	-26 mV for Cl^- at 156 mM Cl^- and 150 mM Mal outside; (Schmidt and Schroeder, 1994)	-30 mV at 300 mM Cl^- outside (Roelfsema et al., 2004)	-34 mV with 30 mM Ba^{2+} inside, 2 mM Ba^{2+} outside (Hamilton et al., 2000)

Half activation potential ($V_{1/2}$)*	-160 mV (Grabov and Blatt, 1997)	0 or -3 mV at 10 mM K^+ (Grabov and Blatt, 1997)	-50 mV (Raschke et al., 2003)	-120 mV (Roelfsema et al., 2004)	-142 mV (Hamilton et al., 2000)
G_{max}*	38 in oocytes (Pilot et al., 2001)				
Gating charge (z_g)*	1.5 in oocytes (Pilot et al., 2001)				
Open probability*	V-dependent P_o = 0.25 at -120 mV	V-dependent P_o increases 2.5-fold when switching from pH_i 7 to 8 (Miedema and Assmann, 1996)	V-dependent P_o = 0.3 at -50 mV (Schulz-Lessdorf et al., 1996)		P_o elevated by hyperpolarization (from 0.002 at -100 to 0.18 at -160 mV) and $[Ba^{2+}]_o$. (Hamilton et al., 2000)
pH sensitivity	External and internal pH (Grabov and Blatt, 1997) (Dietrich et al., 1998)	External and internal pH (Grabov and Blatt, 1997)	External and internal pH (Schulz-Lessdorf et al., 1996)	No Affect	
Ca^{2+} sensitivity	External and internal Ca (Grabov and Blatt, 1999) (Dietrich et al., 1998)	External Ca (Miedema and Assmann, 1996)	External and internal Ca (Raschke et al., 2003)	External and internal Ca (Raschke et al., 2003)	External Ca (Kinoshita et al., 1995)

1.3 Ion Transport at Tonoplast

The guard cell vacuole makes up most of the volume of the total cell volume. During stomatal movements, the volume of guard cells can change by more than 40% mainly due to the rapid change in vacuolar volume while the volum of cytosol remains relatively steady (Louguet et al., 1990, Shope et al., 2003). These results indicate the important roles of ion and water fluxes conducted by tonoplast transporters across the tonoplast during stomatal movements. In the following sections, several major tonoplast transporters in guard cells will be brief introduced.

1.3.1 Pumps

Like plasma membrane pumps, vacuolar pumps transport H^+ across the tonoplast to modulate tonoplast membrane potential and facilitate other solutes transport between vacuoles and cytoplasm through H^+-coupled antiporters (Sze et al., 2002, Gaxiola et al., 2007). The V-ATPase and V-PPase are two primary vacuolar pumps that have been studied in detail.

The vacuolar-type H^+-ATPase (V-ATPase) is a primary-active transport protein originally discovered at the tonoplast, but later studies found they were also localized in many other internal membranes such as endoplasmic reticulum, Golgi and vesicles (Herman et al., 1994, Matsuoka et al., 1997). At the tonoplast the V-ATPase is highly expressed, making up 6.5-35% of the total tonoplast protein in different plant species (Klink et al., 1990, Fischer-Schliebs et al., 1997). V-ATPase is multisubunit protein composed of two domains: the V1 complex consisting of eight subunits responsible for ATP hydrolysis; and the V0 complex including up to six subunits responsible for proton translocation (Sze et al., 1999, Gaxiola et al., 2007). Thus the common role of the V-ATPase is to acidify intracellular compartments and maintain an H^+ electrochemical gradient across the membrane. In the vacuole, this H^+ gradient is used to energize other H^+-coupled transporters. Due to the important role of the vacuole in metabolic regulation, V-ATPases, as the primary energizing donors, are thought to help in the maintenance cellular metabolism in storage of minerals, organic acids, cytosolic pH and Ca^{2+} homeostasis.

The other major vacuolar proton pump is the V-PPase, which uses inorganic pyrophosphate (PPi) instead of ATP as an energy donor. The V-PPase is essential for maintaining the acidity of the large central vacuole (Maeshima, 2000). In addition, the V-PPase is thought to maintain cytosolic K^+ homeostasis. Vacuolar K^+ varies with cell type, but is typically around 200 mM (Leigh and Jones, 1984, Malone et al., 1991). Cytosolic K^+ is thought to be maintained homeostatically around 80-100 mM (Leigh and Jones, 1984, Maathuis and Sanders, 1994). Transport of K^+ into the vacuole against this concentration therefore depends on the V-PPase to energize the membrane. There are two types of V-PPases on the tonoplast. Type I V-PPases depend on cytosolic K^+ (Darley et al., 1998) for their activity and are moderately sensitive to inhibition by Ca^{2+}. Type II H^+-PPases are K^+-insensitive (Drozdowicz et al., 2000) but are extremely Ca^{2+}-sensitive, although the later results have not been reported for guard cells to data. It is well understood that $[Ca^{2+}]_i$ is important to regulate stomatal movements. Thus the tonoplast V-PPase not only helps to maintain K^+ homeostasis, but also provides a link between stomatal movements via changes in $[Ca^{2+}]_{i.}$

1.3.2 H^+-coupled Transporters

As mentioned above, the V-ATPase and V-PPase provide energy for H^+ coupled transporters to move other ions across tonoplast. In guard cells, a number of Cation/H^+ transporters facilitate positive charged ions, such as K^+ and Ca^{2+}, translocation. In *Arabidopsis*, one member of the CHX gene family, AtCHX20 was highly expressed in guard cells. Light-induced stomatal opening of the *Arabidopsis* mutants was insensitive to external pH and was impaired at high KCl suggest the role for CHX20 in exchanging K^+ for H^+ to maintains K^+ homeostasis (Padmanaban et al., 2007). CAX transporters are Ca^{2+}/H^+ antiporters found in central vacuole that plays an important role in translocation of Ca^{2+} into vacuole. Mutants lacking CAX1 exhibit a 50% reduction in vacuolar Ca^{2+}/H^+ antiport activity, a 40% reduction in V-ATPase activity, and an up-regulation of CAX3 and CAX4, indicating a complex regulation of vacuolar proton pump activity and a tendency to compensate for lack of CAX1 activity (Cheng et al., 2003). NHX proteins are Na^+, K^+/H^+ antiporters. In plants, NHX antiporters faciliate exchange of Na^+ and/or K^+ for H^+ by using the electrochemical H^+ gradients generated by the H^+-ATPases at the plasma membrane,

and the V-ATPase and V-PPase at the vacuole to drive either the movement of Na^+ out of the cell or the luminal movement of Na^+ or K^+ into the vacuoles and intracellular organelles. Recent results show that tonoplast-localized NHX proteins, NHX1 and NXH2, are essential for active K^+ uptake at the tonoplast, for turgor regulation, and for stomatal function in *Arabidopsis* (Barragan et al., 2012).

Earlier studies found in plants *Arabidopsis thaliana* and *Rice*, members of the large Chloride Channel (CLC) family have been proposed to encode anion channels/transporters. Proteins from the *Arabidopsis* CLC family are present in various membrane compartments. Among these proteins, AtClCa was shown to target on vacuolar membrane. Interestingly, AtCLCa mediates H^+/NO_3^- exchangers activity in the vacuolar membrane, rather than anion channel activity (De Angeli et al., 2006). Research on plant vacuoles showed that AtCLCa is energetically suited for the physiological accumulation of nitrate into vacuoles at luminal concentrations that are 50-fold higher than typical cytosolic nitrate concentrations (De Angeli et al., 2006).

1.3.3 Tonoplast Ion Channels

1.3.3.1 Cation Channels

Three cation channels have been intensively studied in guard cell vacuolar membranes including fast vacuolar (FV), K^+-selective vacuolar (VK), and slow vacuolar (SV) channels (Allen and Sanders, 1995, MacRobbie, 2006), of which two of them, the molecular identity of VK (TPK1) and SV (TPC1) (Gobert, et al. 2007; Peiter et al., 2005) have been characterized (also see table 1.2). In isolated patch-clamped vacuoles, all of these channels can mediate K^+ uptake or release, depending on the electrochemical gradient for K^+. During stomatal closure, H^+ pumping into the vacuole, causes VK mediated K^+ efflux via tonoplast depolarization, and then activates Ca^{2+} and K^+ efflux through SV (Bewell et al., 1999, Schroeder et al., 2001a).

VK channels were first identified in the guard cell vacuole membranes and are activated by elevated $[Ca^{2+}]_i$ in the range of 1 μM and highly selective for K^+ (Ward and Schroeder, 1994). They were suggested to function as a pathway for organellar K^+ release

into the cytosol in response to elevated $[Ca^{2+}]_i$ during stomatal closure (Ward and Schroeder, 1994). VK channels show a slight rectification that favors K^+ efflux from vacuoles, and its activity is also stimulated by low pH_i (Ward and Schroeder, 1994, Allen and Sanders, 1996). The *Arabidopsis* genome contains five genes that encode VK channels. The most abundantly expressed isoform of this family, TPK1, is expressed at the tonoplast where it mediates K^+-selective currents between cytosolic and vacuolar compartments.

The vacuole, which may occupy more than 90% of the volume of a plant cell, is a major source of Ca^{2+}. It is thought that Ca^{2+} efflux from the vacuole could sustain large and prolonged elevations in $[Ca^{2+}]_i$. The slow vacuolar (SV) channel was shown to be Ca^{2+} activated in vacuole. SV type vacuolar currents appear to be lost in guard cells of knockout mutants of a Ca^{2+} -induced Ca^{2+} release channel, TPC1, suggesting that SV channels not only mediate K^+ flux but also function as conducts for Ca^{2+} release (Peiter et al., 2005). TPC1 is a unique gene in plants, the only homolog of voltage-dependent Ca^{2+} channels in the *Arabidopsis* genome. Similar to TPC channels in animals (Ishibashi et al., 2000), TPC1 in plants has two pore domains rather than the four pore domains usually associated with voltage dependent Ca^{2+} channels. In plants, TPC1 is highly expressed in all tissues, consistent with the ubiquity of SV channel activity in plant vacuoles.

1.3.3.2 Anion Channels

Stomatal opening requires large rates of uptake of Cl^- and Malate into guard cell vacuole (Raschke, 1979, MacRobbie, 1990a). Tracer flux studies have shown that Cl^- uptake into guard cell vacuoles is crucial to balance K^+ uptake during stomatal opening (Macrobbie, 1981, Macrobbie, 1983, Macrobbie, 1990b). Based on thermodynamics, Cl^- accumulation into vacuoles could be largely passive ion channel-mediated during stomatal opening because both the vacuolar H^+-ATPase and the H^+-pyrophosphatase cause a negative potential on the cytosolic membrane side of vacuoles, which could drive passive anion uptake into vacuoles (Pei et al., 1996). A vacuolar chloride channel (VCL) activated mainly at negative physiological potentials on the cytosolic membrane side of guard cell vacuoles and provide a pathway for Cl^- uptake during stomatal opening (Pei et al., 1996). In addition, recent study has shown that the one member of Arabidopsis Al^{3+}-activated

malate transporters, AtALMT9, is targeted to the vacuolar membrane of plant cells and mediates low affinity malate uptake into plant vacuoles (Kovermann et al., 2007).

Table 1. 2 Main ion channels on guard cell tonoplast

	VCL	CLCa	TPC1	TPK1
Activation Potential	Activates on negative potentials (Pei et al., 1996)	Activates on positive potential for nitrate uptake (De Angeli et al., 2006)	Activates slowly by positive voltage, does not inactivates (Amodeo et al., 1994)	Activated at negative of E_K (Gobert, et al., 2007)
Selectivity	Cl^-, $malate^{2-}$ (Pei et al., 1996)	NO_3^->=I^->Br^->Cl^->SO_4^->glutamate (De Angeli et al., 2006)	K^+>TEA^+>Cl^->Gluc-><Ca^{2+} (Schulz-Lessdorf and Hedrich, 1995)	K^+>Rb^+>NH_4^+>>Li^+>Na^+>Cs^+ (Gobert, et al., 2007)
Physiological function	Kinase dependent anion uptake into the vacuole	Nitrate accumulation in the vacuole for plant nutrition;	K^+ homeostasis; CICR during stomatal responses to ABA and CO_2	K^+ homeostasis; Stomatal functioning
E_{rev}*	15 mV at 200 mM Cl^- outside (Pei et al., 1996)	-45 mV at 15 mM Cl^- outside (De Angeli et al., 2006)	10 mV at 10 mM $[Ca^{2+}]_{vac}$ (Allen and Sanders, 1994)	-15 mV at 100 mM RbCl outside. (Gobert, et al., 2007)
$V_{1/2}$*	-50 mV (Pantoja and Smith, 2002)		80 mV (Schulz-Lessdorf and Hedrich, 1995)	
z_g*			4	
Open probability*			P_o=0.15 and 0.3 at 5 and 10 mM Ca^{2+} at -70 mV (Allen and Sanders, 1994)	P_o drops steeply when $[Ca^{2+}]_{cyt}$<50 µM (Gobert, et al., 2007)
Voltage dependence	Y	Y	Y	N

1.4 Regulation of Plasma Membrane Ion Channels

Guard cell ion channels are regulated by various signals under different situations. Of these signaling events, guard cell responses evoked by the water stress hormone abscisic acid (ABA) have naturally received the greatest attention. ABA is the main hormone synthesized during drought, and it has a crucial role in mediating downstream signal cascades. A large number of second messenger molecules have been characterized in plants, including cyclic nucleotides (e.g., cAMP), ions (e.g., Ca^{2+}), phospholipid-derived molecules (e.g., inositol triphosphate), and even a gas, nitric oxide (NO), all of which play a part in ABA signalling. Indeed, much of our knowledge of these second messengers and their roles in regulating transport draws on studies of ion channel regulation in guard cells and guard cell responses to ABA. In the following sections will focus on introducing the ABA and the ABA dependent signaling.

1.4.1 ABA Regulation in Guard Cell Ion Channel

ABA is a major phytohormone that regulates a broad range of plant traits and is especially important for adaptation to environmental stresses such as drought and high salinity (Blatt and Thiel, 1993, Blatt and Grabov, 1997, Leung and Giraudat, 1998, Zhu, 2002). It promotes stomatal closure in guard cells and regulates the expression of many genes in response to water stress. In general, ABA synthesized in roots under water stress and it control guard cell triggering concerted changes in three major ion fluxes carried by inward- and outward-rectifying K^+ channels and by anion channels (Blatt and Thiel, 1993, Blatt and Grabov, 1997). To close the stoma, ABA, firstly, activates both R- and S- type anion channels, which lead plasma membrane to depolarize and prolong anion efflux. The depolarized membrane potential, in turn, activates outward K^+ channels and suppresses inward K^+ channels. The net results are a shift in the bias of transport for net solute loss to close the stoma.

To regulate ion channels by ABA, signaling is mainly achieved through two parallel pathways. The first one is mediated by cytosolic Ca^{2+}. As mentioned above, the elevation of $[Ca^{2+}]_i$ can promote anion efflux and decrease K^+ influx contributing to stomatal closing. A large body of evidence supports the idea that ABA increases in $[Ca^{2+}]_i$ through import of

Ca^{2+} from outside of cell and/or release Ca^{2+} from cellular organelles (Blatt and Grabov, 1997). At the plasma membrane, ABA affects the voltage threshold activating Ca^{2+} channels that mediate Ca^{2+} entry (Grabov and Blatt, 1999, Hamilton et al., 2000). Moreover, ABA triggers reactive oxygen species (ROS) produced by activated NADPH oxidase on plasma membrane (Kwak et al., 2003). Further studies showed ROS can activate Ca^{2+} channel and increase Ca^{2+} influx (Pei et al., 2000). Ca^{2+} influx may affect by other Ca^{2+}-associated pathways, such as inositol-1,4,5-trisphosphate, phospholipase C and lipid metabolite-mediated release, as well as the actions of inositol-hexakisphosphate (Blatt et al., 1990, Gilroy et al., 1990). In addition, the rise in $[Ca^{2+}]_i$ is caused by Ca^{2+}-induced Ca^{2+} release which is enhanced by nitric oxide and stimuled by cyclic guanosine monophosphate (cGMP)- and cyclic adenosine diphosphate (cADP)-ribose-activated Ca^{2+} channels located at one or more endomembranes (Gilroy et al., 1990, Blatt et al., 1990, Parmar and Brearley, 1993, Parmar and Brearley, 1995, Allen and Sanders, 1995, Lee et al., 1996, Muir and Sanders, 1996). The second pathway evoked by ABA is through raise in pH_i. ABA challenge leads to a rise in pH_i of 0.2–0.4 pH units, and activates outward K^+ channels (Grabov and Blatt, 1997). Experimentally, ABA evoked K^+ efflux is a $[Ca^{2+}]_i$-independent events, but inward K^+ current is sensitive to both $[Ca^{2+}]_i$ and pH_i.

Although numerous of factors related to ABA response have been reported (see Figure 1.2), many of the molecular mechanisms of ABA response are still unknown, especially how guard cells recognize the ABA signal. Previous studies have shown some ABA binding proteins such as G-protein-coupled receptors (GCR2, GTG1/2) and Mg-chelatase (CHLH) are able to bind ABA, however there is little functional data to support these observations and they remain therefore to be confirmed (Liu et al., 2007, Pandey et al., 2009, Zhang et al., 2002). Recently with the discovery of the S-type anion channel,SLAC1 and its regulator, the protein phosphatase–kinase complex PP2C-SnRK2, the PYR/PYL/RCAR proteins from START superfamily were isolated and shown to function as an ABA receptor (Ma et al., 2009, Park et al., 2009, Nishimura et al., 2010). Subsequent studies confirmed a double negative regulatory system of ABA signaling cascade: In the absence of ABA, PYR/PYL/RCARs are not bound to PP2Cs and PP2C activity is high, which prevents SnRK2 activation and followed events. However, when

ABA is present, PYR/PYL/RCARs binds to and inhibits PP2Cs, which allows accumulation of phosphorylated SnRK2s and subsequent phosphorylation of downstream anion channels (Kim et al., 2010).

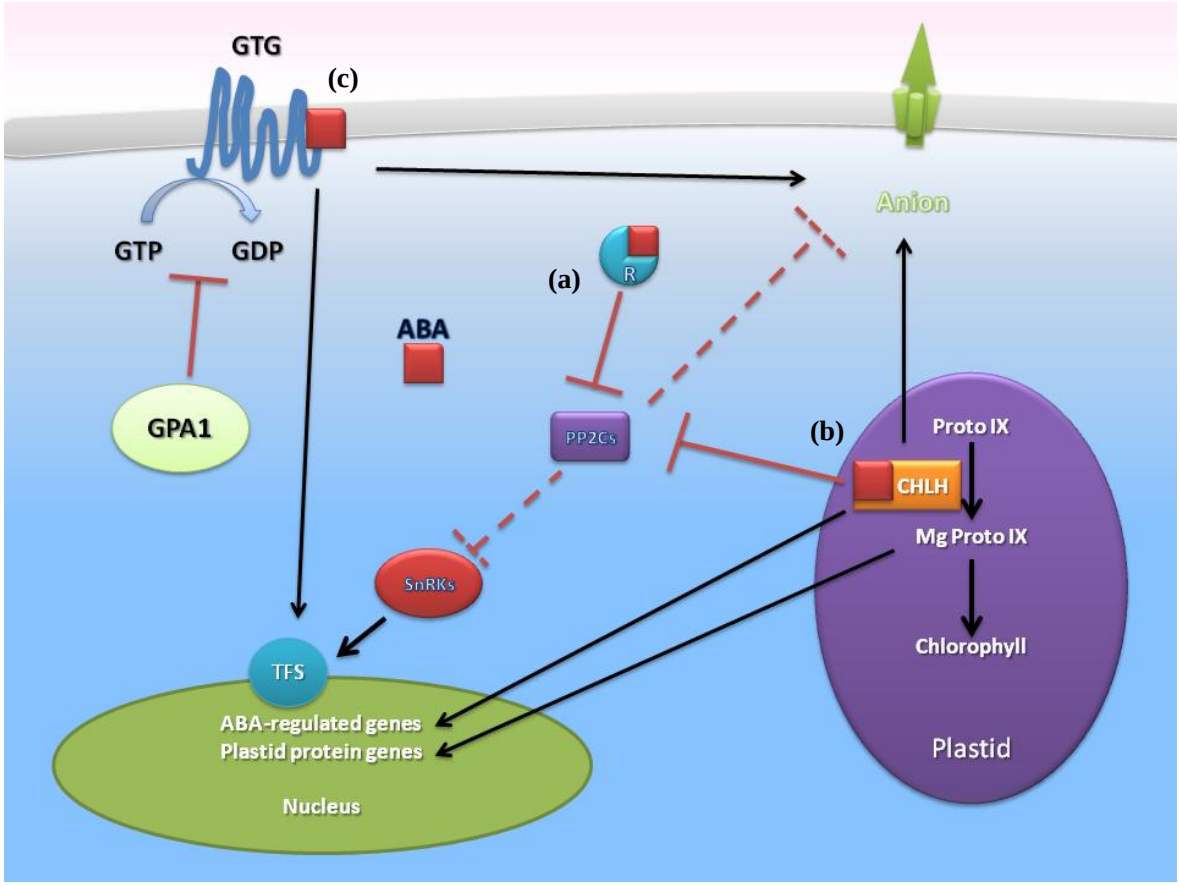

Figure 1. 2 ABA signaling factors (modified from Cutler et al., 2010)

(a) Signaling through PYR/PYL/RCAR (R) Receptor proteins. In the presence of ABA, PYR/PYL/RCARs bind to and inhibit PP2Cs, which allows accumulation of phosphorylated SnRK2s and subsequent phosphorylation of ABA-responsive element binding factors (ABFs). (b) ABA interactions with the plastid-localized magnesium cheletase (ChlH); and (c) With plasma membrane–localized GPCR type G-proteins (GTGs), Solid lines indicate activation and dotted lines indicate repression. Positive activation noted by an arrow; bars indicate repression.

1.4.2 Ca^{2+} as a Second Messenger

Cytosolic-free calcium ($[Ca^{2+}]_i$) is known to affect many cellular processes among living organism from plant to animal (Bush, 1995, Blatt, 1999, Blatt, 2000). In the guard cells of plants, changes in $[Ca^{2+}]_i$ are associated with plasma membrane ion channel regulation, especially in relation to response to ABA and biotic stimuli (Blatt and Thiel, 1993, Blatt and Grabov, 1997, Blatt, 1999, Israelsson et al., 2006). For example, inward K^+ currents ($I_{K,in}$) are greatly reduced when $[Ca^{2+}]_i$ is elevated to micromolar concentrations (Schroeder & Hagiwara 1989,Grabov & Blatt 1997). Similarly, micromolar $[Ca^{2+}]_i$ promotes anion currents (Hedrich et al 1990,Schroeder & Keller 1992). Additionally, ABA exposures leads a deactivation of $I_{K,in}$ and activation of anion currents which usually accompany with a raise of $[Ca^{2+}]_i$ (Thiel et al., 1992, Lemtiri-Chlieh and Macrobbie, 1994, Fricker et al., 1991, Irving et al., 1992, McAinsh et al., 1992, Allen and Sanders, 1994). All these evidence indicate a Ca^{2+} role in ABA signaling.

In general, the physiological range of resting $[Ca^{2+}]_i$ in guard cells is situated around 100-200 nM, as it is in most living cells (Blatt, 2000). Above this concentration, $[Ca^{2+}]_i$ has a number of effects in guard cells: once $[Ca^{2+}]_i$ reach micromolar level, it greatly reduces inward K^+ currents and promotes anion currents both of S- and R- type anion channels, leading stomatal closure (Blatt and Thiel, 1993, Blatt, 1999, Blatt, 2000). Although there is some evidence that suggests that $[Ca^{2+}]_i$ elevation may not always be required for stomatal closure in ABA (Siegel et al., 2009). Even so, a very large body of evidence supports a key role for $[Ca^{2+}]_i$. First, early studies showed that an elevation in $[Ca^{2+}]_i$ occurred within 3-5 minutes when guard cells were exposed to ABA (McAinsh et al., 1990, Garcia-Mata et al., 2003). Second, the ABA response of guard cells was sensitive to Ca^{2+} channel blockers (McAinsh et al., 1991, Cousson, 1999). Third, genetic support for ABA-induced $[Ca^{2+}]_i$ elevations in guard cells has been obtained. The ABA-insensitive *Arabidopsis* mutants *abi1-1* and *abi2-1* showed greatly reduced ABA-induced $[Ca^{2+}]_i$ elevations, which hint at a possible role for Ca^{2+} in ABA signaling (Allen et al., 1999a). Besides ABA, other stimuli were also shown to induce $[Ca^{2+}]_i$ elevation, including external Ca^{2+}, ozone, H_2O_2, Nitrate oxide (NO) and CO_2 (Clayton et al., 1999, Pei et al., 2000, Garcia-Mata et al., 2003, Webb et al., 1996).

It is widely known that elevation of $[Ca^{2+}]_i$ requires both Ca^{2+} entry across the plasma membrane and release from intracellular stores (Grabov and Blatt, 1999, Hamilton et al., 2000, Garcia-Mata et al., 2003, Blatt et al., 1990, Blatt, 1999; also see Figure 1.3). There are several pathways trigger Ca^{2+} release from intracellular stores. First, phosphoinositides can induce Ca^{2+} release. In guard cells, a range of phosphoinositides were synthesized in response to ABA. For example, Inositol-1,4,5-trisphosphate (IP3) and Inositol hexaphosphate (IP6) are produced rapidly within guard cells in response to ABA. They can initiate Ca^{2+} release and suppress $I_{K,in}$. It has also been shown that IP3 and/or IP6 probably interact with Ca^{2+} channels on endomembranes to evoke Ca^{2+} release and then raise $[Ca^{2+}]_i$ (MacRobbie, 1998, Blatt, 1999). A second mechanism of Ca^{2+} release has been shown to involove receptors sensitive to the alkaloid ryanodine and cyclic ADP-ribose (cADPR), a metabolite of nicotinamide adenine dinucleotide (Allen and Sanders, 1995, Muir and Sanders, 1996, Wu et al., 1997). These observations provided evidence for cADPR-sensitive, Ca^{2+}-permeable channels in guard cell vacuoles and observed $[Ca^{2+}]_i$ to rise following injections of guard cells with cADPR. The ABA induced stomatal closure was slowed when guard cells were preloaded with the cADPR antagonist 8-NH_2-cADPR. These or related Ca^{2+} channels may contribute to voltage- and ABA-mediated $[Ca^{2+}]_i$ signals, which are also sensitive to ryanodine (Grabov & Blatt 1999). In addition, recent studies showed nitric oxide can induce Ca^{2+} release (see below). However, Grabov & Blatt 1998 found ABA strongly influences the voltage sensitivity for $[Ca^{2+}]_i$ increases as well as affecting the kinetics for the $[Ca^{2+}]_i$ rise and its recovery. Thus ABA must act on other pathways to raise $[Ca^{2+}]_i$ in addition to releasing from internal stores. Early studies identified a low-conductance Ca^{2+} channel at the guard cell plasma membrane which provides a pathway for external Ca^{2+} entry into cells (Hamilton et al., 2000, Grabov and Blatt, 1999). In *Vicia faba*, this channel shows a sensitivity to negative membrane voltage and external as well as internal Ca^{2+} (Grabov and Blatt, 1999, Hamilton et al., 2000). It has been observed that $[Ca^{2+}]_i$ is elevated in response to hyperpolarisation of plasma membrane, and these change caused further Ca^{2+} release from internal store, suggesting a Ca^{2+} induced Ca^{2+} release (CICR) pathway initiated by Ca^{2+} influx across plasma membrane.

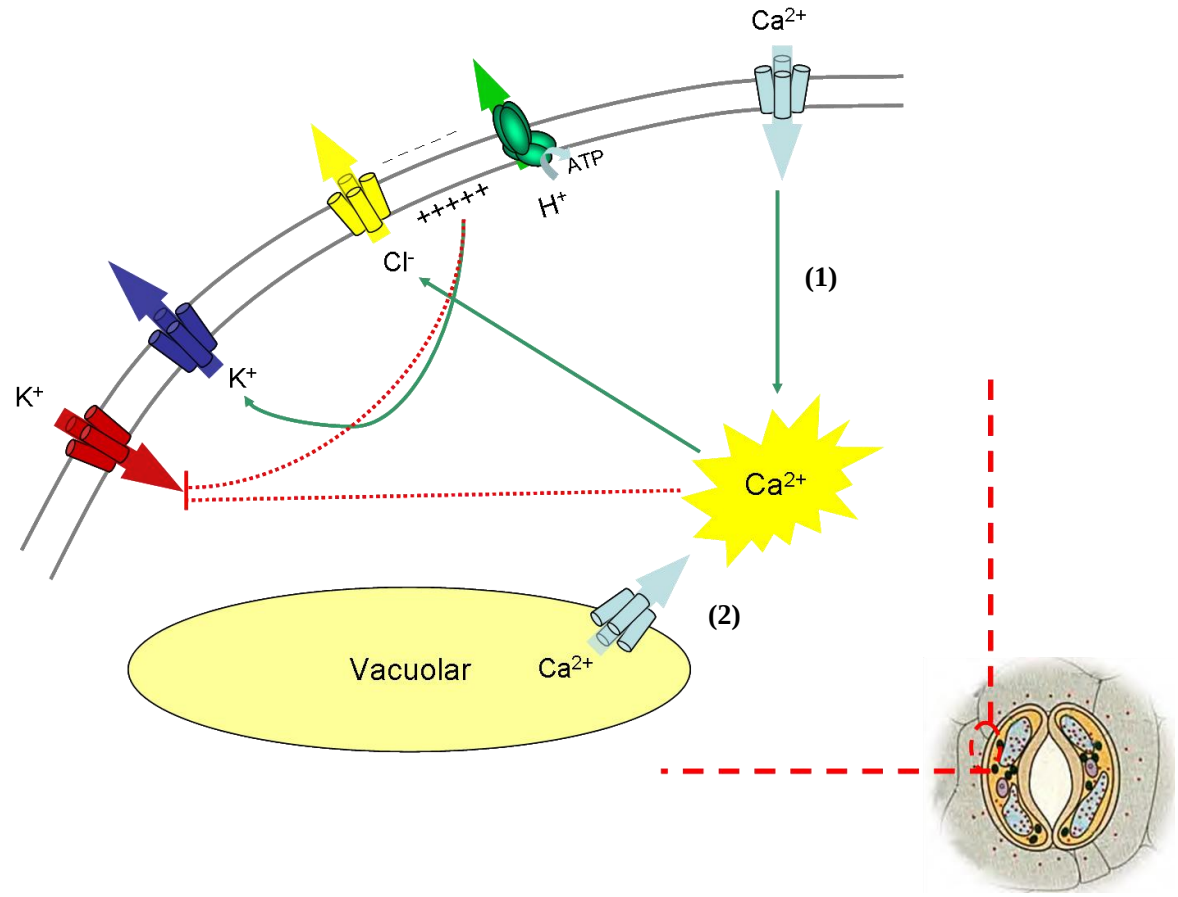

Figure 1. 3 Ion channel regulation by $[Ca^{2+}]_i$.

The elevation in $[Ca^{2+}]_i$ occurs through (1) the activation of plasma membrane Ca^{2+} channels for Ca^{2+} entry into the cell, and (2) the triggering of Ca^{2+} release from intracellular stores. The rise in $[Ca^{2+}]_i$ then activates anion channels and suppresses H^+-ATPase activity to depolarize membrane, leading in turn to a K^+ efflux and suppression of K^+ influx. Additionally, the elevation of $[Ca^{2+}]_i$ directly inactivates K_{in} channels, either via Ca^{2+} binding or through Ca^{2+}-dependent protein kinases. Positive activation noted by an arrow; bars indicate repression.

Cytosolic Ca^{2+} is involved in a number of downstream responses, many of which depend on phosphorylation events and regulate stomatal movements. Recently, a set of Ca^{2+} sensors (calcineurin B-like proteins [CBLs]) and their targets (CBL-interacting protein kinases or CIPKs) have been shown to regulate K^+ channels in *Arabidopsis* (Li et al., 2006, Luan, 2009). More than one phosphorylation cascade interacts with Ca^{2+} signaling. Members of a class of calcium dependent protein kinases (CDPK) appear to be involved in several ABA signaling cascades (Mori et al., 2006, Geiger et al., 2009b). All these observation imply that Ca^{2+} participates in stomatal regulation through series of branched pathways that involve both direct as well as indirect actions of Ca^{2+} and its binding with intermediate targets.

1.4.3 Cytosolic pH as a Second Messenger

K^+ release through K_{out} channels is not simply controlled by membrane voltage but is also regulated by chemical factors on both sides of the membrane. These channels are not sensitive to changes in $[Ca^{2+}]_i$ but they respond in activity nonetheless to various stimuli especially ABA (Blatt and Armstrong, 1993, Grabov and Blatt, 1997). Thus it was recognized early on that, at least one other signaling pathway other than $[Ca^{2+}]_i$ must be active during in ABA signal transaction. The evidence for cytosolic pH (pH_i) as a second messenger in ABA signaling arises in part from observations that ABA evokes a 0.1-0.3 pH unit elevation in guard cells (Irving et al., 1992, Blatt and Armstrong, 1993). These results were supported by experiments showing that increasing pH_i can activate K_{out} channels in a voltage independent manner (Grabov and Blatt, 1997). Additional evidence indicates that auxin treatment changes in pH_i and that the effects in this case, too, affect the K^+ channels in a complementary manner; thus changes in pH_i serve a more general role in stomatal signaling (Thiel et al., 1993, Blatt and Thiel, 1994, Woodward and Bartel, 2005). pH_i controls the K_{out} channels through H^+ binding at sites on the channel protein (Lacombe et al., 2000).

pH_i has been confirmed to affect also the characteristics of the K_{in} channels, and this action is separable from the action of $[Ca^{2+}]_i$ on the channel (Grabov and Blatt, 1997, Blatt, 1992). Indeed, decreasing pH_i (increasing the $[H^+]$ inside) increases the activity of these

inward currents, and molecular analyses have indicated at least one site for H^+ action in the K_{in} channel KAT1 is situated near the channel pore (Hoth et al., 2001, Gonzalez et al., 2012). It is less clear how pH_i acts *in vivo*, however, and it is likely that several mechanisms overlap. One target for H^+ in controlling the K^+ channels is through its effects on protein phosphatase activity. It has been shown that pH affects the activity of the ABI1 protein (Leube et al., 1998). This phosphatase plays a key role in some of the early steps in ABA signal transduction and its mutation leads to a dominant-negative (ABA-insensitive) phenotype (Leung et al., 1994, Armstrong and Blatt, 1995). Besides that, pH_i also showed an influence on both R-and S-type anion channels. It is shown that R-type and S-type anion channels at the plasma membrane are both regulated by pH_i *via* distinct mechanisms in *Arabidopsis* hypocotyl cells (Colcombet et al., 2005). Colcombet *et al* (2005) showed that R-type anion channel gating is affected by external pH, but not by internal pH. By contrast, the S-type anion channel is affected by both internal and external pH. All these results indicate that pH_i is a universal second messenger in plant cells (see Figure 1.4).

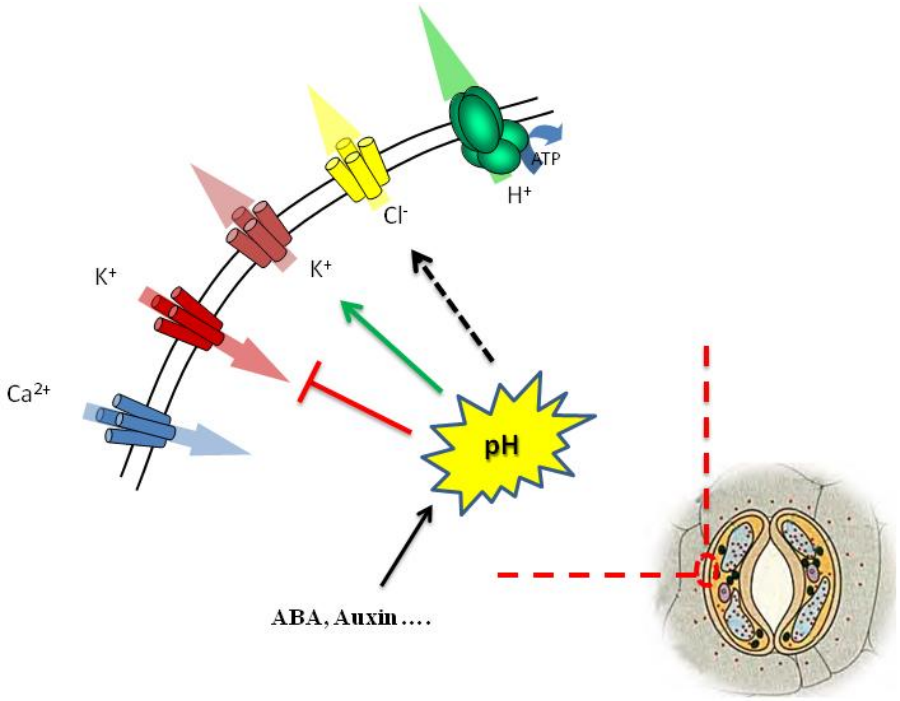

Figure 1. 4 Ion channel regulation by pH_i.

The elevation in pH_i occurs through ABA or auxin. The rise in pH_i then activates K_{out} channels and suppresses K_{in} activity. Additionally, the elevation of pH_i impact on R- and S- type anion channels with different manner. Positive activation is noted by an arrow; bars indicate repression and dotted lines indicate activated with different circumstances.

1.4.4 NO and ROS in Guard Cell Signlling

Nitric oxide (NO) is widely considered to be an important molecule in normal physiological processes in animals (Stamler et al., 2001, Mayer and Hemmens, 1997). NO was identified in the late 1990s as an important second messenger in plant defense signalling against pathogens (Delledonne et al., 1998); it was subsequently shown to be a crucial factor in the regulation of physiological processes in plants, including stomatal closure, as well as more generally in growth and development (Neill et al., 2002b, Guo et al., 2003). Generation of NO can be caused by various abiotic and biotic stresses, including ozone and UV radiation, extremes of temperature, wounding and pathogen, dehydration, and plant hormones such as ABA, auxin, cytokinin, and ethylene (Neill et al., 2002a, Neill et al., 2003). NO is synthesized by NO synthases (NOS), a family of well characterized enzymes that catalyze the conversion of L-arginine to L-citrulline and NO (Wendehenne et al., 2001). In plants, however, NO synthases have yet to be identified, and the *Arabidopsis* genome does not contain an animal NOS-like gene. A possible candidate enzymatic source of NO in plants is nitrate reductase (NR) (Yamasaki and Sakihama, 2000, Desikan et al., 2002). In *Arabidopsis*, NR encoded by the *NIA1* and *NIA2* genes (Wilkinson and Crawford, 1993). These enzymes play a central role in nitrogen assimilation and catalyse the reduction of nitrite to NO *in vitro* and *in vivo* (Desikan et al., 2002). Nitrate reductase-mediated NO synthesis has a significant impact stomatal closure in *Arabidopsis*. The *nia1nia2* double mutant is known to exhibit a greatly attenuated response to stimuli such as ABA (Lozano-Juste and Leon, 2010), and this effect correlates with a much reduced synthesis of NO. A mechanistic connection to stomatal function has been made by Garcia-Mata, et al. (2003) who showed that NO selectively regulates the Ca^{2+} sensitive K^{+} and anion channels of *Vicia* guard cells by promoting Ca^{2+} release from intracellular stores to raise $[Ca^{2+}]_i$. These studies demonstrated a clear difference in $[Ca^{2+}]_i$–related effects at the plasma membrane and within the endomembrane system, and they confirm the key role for NO in stomatal closure.

Like NO, reactive oxygen species (ROS) are highly reactive molecules containing oxygen. ROS have been found to be important in several signaling processes, notably in growth, development, and responses to biotic and abiotic environmental stimuli (Apel and

Hirt, 2004, Foreman et al., 2003, Wojtaszek, 1997). The ROS hydrogen peroxide (H_2O_2) is a significant player in ABA related stomatal movements (McAinsh et al., 1996). In *Arabidopsis*, ABA-induced stomatal closure was inhibited by the flavin analogue diphenylene iodonium (DPI) which used widely as an inhibitor of NADPH oxidase (Cross and Jones, 1986). A recent study in *Arabidopsis* guard cells shows ABA treatment enhances ROS production (Pei et al., 2000). Most important, ROS can activate a plasma membrane Ca^{2+} channels. ABA activates plasma membrane Ca^{2+} channels (Pei et al., 2000) only when NADPH is present in the cytosol, implicating NADPH oxidases in ABA signaling (Murata et al., 2001). Recent study identified the AtrbohD and AtrbohF NADPH oxidase subunits as being essential for ABA-induced stomatal closing and ABA-induced Ca^{2+} channels activation in guard cells (Kwak et al., 2003). Thus all these data provide evidence for roles of ROS and Ca^{2+} channels in ABA signaling.

1.4.5 cAMP and cGMP in Guard Cell Signlling

Cyclic Adenosine 3':5'-monophosphate (cAMP) is a key second messenger in plant cells. Much more evidence supporting the contention that cAMP plays a role in regulating plant cell function (Assmann 1995). Importantly, cAMP was found that tightly link to K^+ and Ca^{2+} (Kurosaki 1997). In this study, researchers reported that K^+ influx was stimulated by cAMP. When K^+-channel blockers were applied, K^+ influx was completely inhibited, suggesting that cAMP may regulate K^+-channels in plant cells. Furthermore they found cAMP stimulated Ca^{2+} influx which was associated with K^+ influx, suggested a cross talk in signal transduction mechanism between cAMP and cytosolic Ca^{2+} mediated by K^+ channels (Kurosaki 1997). Moreover, Volotovski et al. (1998) report that both cAMP and cGMP caused elevation of cytosolic Ca^{2+} concentration in tobacco protoplasts. These authors showed that both internal and external Ca^{2+} stores were involved in cAMP-induced cytoplasmic Ca^{2+} elevation, and that Ca^{2+}-channel blockers inhibited this cyclic nucleotide-evoked Ca^{2+} elevation, suggesting cAMP may somehow regulate Ca^{2+}-channel activities in the plasma membranes and endomembranes in plant cells.

Cyclic guanosine monophosphate (cGMP) is necessary for NO induced stomatal closure, as has been identified in pea and Arabidopsis (Neill et al., 2002a). Several lines of evidence indicate the necessity for cGMP synthesis and action for plant responses to NO.

For example, exposure to NO for 10 min caused cGMP to activate closure (Pfeiffer et al., 1994). Injection of recombinant rat NOS into tobacco leaves or treatment of tobacco suspension cultures with NO donors induced an increase in cGMP content (Hausladen & Stamler, 1998; Feelisch et al., 1999) indicating a crosslink between NO and cGMP. As mentioned above, cytosolic Ca^{2+} mediates the effects of NO leading to stomatal closure (Garcia-Mata et al., 2003). cADPR antagonists, RYR inhibitors and cGMP synthesis inhibitors have all been shown to suppress the Ca^{2+}-mobilizing actions of NO in plants, implying that NO might activate RYR through cGMP and/or cADPR (Garcia-Mata et al., 2003; Lamotte et al., 2004).

1.4.6 Protein Phosphorylation in Guard Cell Ion Channel Regulation

Protein phosphorylation and dephosphorylation events make major contributions to transport control in guard cells. These post-translational modifications usually occur at serine and threonine residues of proteins; their addition of charged groups affects protein conformations and interactions that affects enzyme activity and can modify the gating of ion channels. Recently a burst of evidence had indicated that the activity of anion channel is controlled by a kinase-phosphatase pair, PP2C and SnRK (Umezawa et al., 2009). In guard cells, 2C-type protein phosphatases (PP2Cs) and Snf1-related protein kinases (SnRK) have surfaced as some of the most important regulators of K^+ and anion channels (Geiger et al., 2009c). Among plant PP2Cs, the *ABI1* and *ABI2* gene products act as negative regulators of the ABA response (Schweighofer et al., 2004, Rodriguez et al., 1998, Klingler et al., 2010). Loss of function in these alleles leads to ABA insensitivity and a loss of stomatal closure, notably through their influence on anion channel conductance (Geiger et al., 2009c, Lee et al., 2009). Equally the Snf1-related kinase 2 (SnRK2) proteins from several plant species have been implicated in ABA signaling pathways (Wasilewska et al., 2008, Coello et al., 2011). In *Arabidopsis* guard cells, OPEN STOMATA 1 (OST1/SnRK2.6) has been confirmed to physically interact with the S-type anion channel SLAC1 and to phosphorylate its N terminus, resulting in its activation (Geiger et al., 2009c, Lee et al., 2009). These findings are supported by in vitro studies: when SLAC1 is expressed heterologously in *Xenopus oocytes* it appears electrically silent (Lee et al., 2009). However, coexpression of SLAC1 with OST1, was sufficient to give SLAC1-related anion

currents in *Xenopus oocytes* (Lee et al., 2009, Geiger et al., 2009c). These lines of evidence indicate that the OST1/SLAC1 complex is prerequisite to generating an active anion channel current. More interestingly, when coexpressed with the ABI1 protein phosphatase, the OST1/SLAC1 complex fails to show any anion currents (Lee et al., 2009, Geiger et al., 2009c). These results are consistent with protein–protein interaction assays that showed ABI1 can interact with and suppress OST1, and they demonstrate that SLAC1 is controlled by the pair of proteins ABI1 and OST1 which probably fuction in concert to regulate phosphorylation of the channel target by phosphorylation/dephosphorylation.

As mentioned above, both S- and R- type anion channels are activated by raising $[Ca^{2+}]_i$. Recent study found that I_{Cl} rises with $[Ca^{2+}]_i$ only at concentrations substantially above the mean resting value of 125 nM. The protein phosphatase antagonist okadaic acid increased I_{Cl} baseline over twofold, indicates phosphorylation enhances the Ca^{2+} sensitivity of I_{Cl} (Chen et al., 2010b). Additionally, the evidence that $[Ca^{2+}]_i$ elevation can result in activation of S-type anion channels through phosphorylation (Mori et al., 2006) suggesting a role for phosphorylation in Ca^{2+} dependent anion channel activity.The Ca^{2+}-dependent Ser/Thr protein kinases (CDPK) family are the main protein kinases activated by $[Ca^{2+}]_i$ in plants. Two members of this family, CPK3 and CPK6 have been identified involved in ABA-dependent regulation of guard cell S-type currents (Mori et al., 2006). The knock-out mutation exhibits a strongly impaired anion current (Mori et al., 2006). In addition to CPK3/6, protein-protein interaction assays indentified the CPK21 and CPK23 are potential partner of SLAC1 (Geiger et al., 2009b). Although, in *vitro* kinase assays showed that there is a difference in Ca^{2+}-sensitivities between CPK21and CPK23, it remains clear that both can activate anion channels by phosphorylation (Geiger et al., 2009b).

1.5 Ion Transport and Membrane Traffic

A large volume change and up to 60% change of the guard cell surface area, occurs in transitions between the closed and open (Homann and Tester, 1998). Because the major cell membranes can only stretch by around 2% without breakage, it is essential that material is added and removed through vesicule to and from both plasma membrane and tonoplast (Wolfe and Steponkus, 1981, Wolfe, 1982). However, membrane traffic also

serves in roles for transport control during stomatal movements. In *Nicotiana* and *Arabidopsis*, the syntaxin homologue SYP121 (=SYR1/PEN1), a member of SNARE family of proteins, has been shown to form the core of the molecular machinery for vesicle trafficking and membrane fusion and to control ion channel activities in guard cells (Leyman et al., 1999). Most interestingly, SYP121 was found to be essential for ABA signalling: disrupting SYP121 function in the guard cells prevented the normal responses of $I_{K,in}$, $I_{K,out}$ and I_{Cl} to ABA (Leyman et al., 1999). Subsequent studies showed that the SNARE also affected Ca^{2+} channel activities at the guard cell plasma membrane (Sokolovski et al., 2005). Much of the detail of how transport and traffic interact is still unresolved. Nonetheless, the recent studies have shown that the SNARE facilitates stomatal reopening through K^+ channel traffic and recycling to the plasma membrane (Eisenach et al., 2012). Additional work from this laboratory has shown that direct interactions between several K^+ channels and the SNARE are important for activating both channel gating (Honsbein et al., 2011, Honsbein et al., 2009, Grefen et al., 2010) and vesicle traffic (unpublished). These studies confirm an important role for membrane traffic and trafficking proteins in stomatal movements and in the regulation of associated ion transporters.

1.6 Aim of Research

Guard cell ion transport and signaling have been studied for the past two decades. To date, there has been significant progress in understanding the integration of guard cell K^+ channels in stomatal movements. For example, K_{out} is the major pathway for K^+ efflux during stomatal closure (Clint and Blatt, 1989, Blatt and Armstrong, 1993) and K_{in} facilitates K^+ uptake during stomatal opening. The characteristics of inward rectify K^+ channels and outward rectify K^+ channels have been well documented, as well as their features in response to various signals, notably ABA. However, the understanding of guard cell anion channels is still poor. Isolation of the SLAC1 gene has provided us an opportunity to further investigate anion channel features in guard cell. At the plasma membrane, anion channels are key elements that contribute to stomatal closing, and their activities are essential to depolarize the membrane and balance charge with K^+ during solute efflux for stomatal closure, as noted above (Schroeder et al., 2001a, Blatt, 2000,

Pandey et al., 2007). Both two type of anion channels are closely tied to Malate (Vankirk and Raschke, 1978, Raschke and Schnabl, 1978). Most important, the evidence that amount of Malate and other organic acids were over-accumulated in the *slac1* loss-of-function mutation and very high cytosolic concentrations of Mal may itself inhibit the SLAC1 current (Schmidt and Schroeder, 1994). All these results suggest a key role of Mal in S-type anion channel regulation. Equally, Mal is important for R-type anion channel. Although the molecular identity of the R-type anion channels remains uncertain, it has been suggested that ALMT12 (aluminium-activated, Malate transporter 12) and other members of this protein family may contribute to the R-type anion current in *Arabidopsis* (Meyer et al., 2010). Thus malate may well be involved in R-type anion channel regulation. Indeed, a number of lines of evidence support this role for malate. Extracellular malate alters the voltage dependence of R-type anion channels (Hedrich and Marten, 1993) and similarly of current associated with AtALMT12 (*Arabidopsis* ALMT12) (Meyer et al., 2010). Previous work focused on malate as "second signal" of CO_2 in control of the R-type channels (Hedrich and Marten, 1993), but the implied consequences of the related input from the cytosolic metabolites have been largely ignored. Therefore the first goal of this study was to explore the role of cytosolic metabolites in anion channels regulation.

A second goal of these studies was to understand the role of guard cell anion channel activity in the whole cell network. In this context, use of the *slac1* mutant offers an immediate approach. The *slac1* mutant is known to accumulate Cl^- and malate, but it also accumulates K^+ (Negi et al., 2008), suggesting additional impacts on the transport of this ion in the guard cells and possibly on other activities in the cells. Thus a major question addressed in the second theme of this research was whether eliminating Cl^- transport through the SLAC1 anion channel affected the K^+ channels directly, either as implicit in effects on charge balance, or through other, more direct mechanisms.

Finally, I was interested in understanding how the known signal of $[Ca^{2+}]_{i,}$, as an important player in ABA regulation of stomatal closure, might contribute to anion channel control. Recently, the PYR/PYL/RCAR proteins were identified as a ABA receptor family that directly interact with protein phosphatases-kinase pairs, notably through PP2Cs. The

pyr1/pyl1/pyl2/pyl4 quadruple mutant was isolated and shown to exhibit a strong ABA-insensitive phenotype. It is well known that ABA treatments results in a promotion of I_{Cl} to close stoma. However, an open question has remained whether I_{Cl} activities are impaired in *pyr1/pyl1/pyl2/pyl4* mutant directly through changes in the phosphorylation of the channel or whether the *pyr1/pyl1/pyl2/pyl4* mutant affects these changes through a Ca^{2+}-signalling pathway. I address this last question in the third experimental section of my research outlined in the following chapters.

CHAPTER 2:

MATERIALS AND METHODS

2.1 Plant Growth

Arabidopsis thaliana and *Vicia Faba* seedlings were sown onto Levington F2+S 3 (Coulders, Glasgow, UK) compost, which was treated with Intercept 70WG (Scotts, Ipswich, UK), a systemic insecticide. Seeds were stratified at 4 ℃ for 48 h and germinated under a plastic lid for one week. Plants were grown in a controlled environment growth chamber under 70 μmol m^{-2} s^{-1} light in either long day conditions (light : dark cycle 16 : 8 h, 22 : 18 ℃, 55 : 70% relative humidity (RH)) or short day conditions (9 : 15 h, 22 : 18 ℃, 60 : 70% RH). For all physiological experiments on guard cells, including stomatal aperture assays, gas exchange measurements and two-electrode voltage clamp recording, plants were grown in long day conditions. To ensure best results and reproducibility it was vital that plants were evenly watered with Hoagland solution (see table 2.1) .

Table 2. 1 Hoagland's Solution (1L)

Component	Stock Solution	Stock Solution (ml)
1M KNO_3	101.1g/L	5
2M $Ca(NO_3)_2$ x $4H_2O$	236.1g/L	7
1M KH_2PO_4	136.1g/L	2
1M $MgSO_4$ x $7H_2O$	246.5g/L	2
Microelements:		1
H_3BO_3	2.86g/L	
$MnCl_2$ x $4H_2O$	1.81g/L	
$ZnSO_4$ x $7H_2O$	0.22g/L	
$CuSO_4$	0.051g/L	
H_3MoO_4 x H_2O	0.09g/L	
Na_2MoO_4 x $2H_2O$	0.12g/L	
FeEDTA:		1
Na_2EDTA	10.4g/l	
$FeSO_4$ x $7H_2O$	7.8g/l	
KOH	56.1g/l	

All plants were kept free from any biotic and abiotic stresses. *Arabidopsis* plants were grown in individual flower pots with a diameter of 60 mm (Figure 2.1). Soil-filled pots were covered with polyester mesh (mesh width: 0.5 cm, Remnant Kings, Glasgow, UK). The mesh allowed the rosette leaves to rest on the mesh rather than the soil, preventing any biotic damage from fungus gnats (*Bradysia* ssp.) larvae in the soil. *Vicia faba* L. cv. was grown in mixture pots with a diameter of 150 mm.

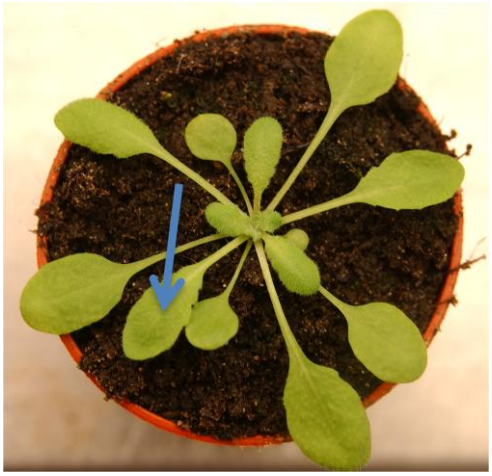

Figure 2. 1 Growth and selection of *Arabidopsis* leaves.
The selected leaf is shown by the arrow.

The Arabidopsis mutant *slac1-1* and *pSLAC1:SLAC1*-complemented lines were obtained from Jaakko Kangasjärvi (University of Helsinki). The *slac1-1* mutant was indentified by a combination of mapping, candidate gene expression in guard cell microarrays, and analyses of transfer DNA (T-DNA) insertion mutants (Vahisalu et al., 2008). The *pyr1/pyl1/pyl2/pyl3* was obtained from Sean Cutler (UC-Riverside).

2.2 Stomatal Aperture Assays

2.2.1 Preparation of Epidermal Peels

Abaxial epidermal peels were prepared from leaves of 4-5 weeks old plants. Figure 2.1 shows a typical rosette of that age for *Arabidopsis*. Epidermal peels were prepared from leaves such as the one indicated by the arrow. Young leaves have a more elliptical shape and are more serrated than other leaves, and their abaxial epidermis is stretchy and

flexible. Leaves were excised as close to the hypocotyl as possible. Details of preparing epidermal strips will be found in Chen, et al. (2012b).

2.2.2 Stomatal Movements Assay

For stomatal aperture assays epidermal peels were fixed to the glass bottom of the experimental chamber after coating the chamber surface with an optically clear and pressure-sensitive silicone adhesive. All operations were carried out on an Axiovert microscope (Zeiss, Oberkochen, Germany) fitted with Nomarski Differential Interference Contrast optics. In each experiment, photos were taken at 5 min intervals using an AxioCam digital camera combined with AxioVision software (version 3.0.6 SP4, Zeiss Vision GmbH). Stomatal apertures were determined using a calibrated eyepiece micrometer and from images using imageJ (National Institute of Health, USA). Measurements were conducted in continuous flowing solutions controlled by a gravity feeding system at a rate of ten chamber volumes of solutions per min. The standard buffer (SB) contained 10 mM KCl and 5 mM 2-(N-morpholino)propanesulfonic acid (MES), which was titrated with $Ca(OH)_2$ to a pKa of 6.1 (See Table 2.2). In experiments with ABA, Ca^{2+} and H_2O_2 treatments, these compounds were added to SB at the corresponding concentration.

Stomatal closure can be evoked by manipulation of membrane voltage and concomitant treatment with external Ca^{2+} (Grabov and Blatt, 1998). Manipulation of membrane voltage is achieved by alternating external K^+ concentrations through changing between high K^+ and low K^+ concentration solutions, hereafter referred to as Depolarising (DB) and Hyperpolarising (HB) Buffers (See Table 2.2). Treatment of DB-adapted epidermal peels with HB for a period of 20 min was shown to raise the cytosolic Ca^{2+} concentration ($[Ca^{2+}]_i$) to a plateau (Allen et al., 2001) and this process induced stomatal closure. Stomata subsequently reopened during HB washout with DB over a time course of 2.5 h (Allen et al., 2001). However, repeatedly switching between DB and HB, usually with 5 min periods for each solution, triggered a “programmed stomatal closure” response characterised by a long period of stomatal closure in the absence of further stimulus. For HB-induced closure and reopening experiments, peels were incubated in DB, for 1.5h

under 150 μmol m^{-2} s^{-1} in order to allow stomata to open. Peels were then transferred to an Axiovert200 microscope (Zeiss, Jena, Germany) with an LD Achroplan 40x/N.A. 0.6 objective. Images were taken at regular intervals over all experiments courses using an AxioCam HRc digital camera (Zeiss) and Axiovision software (version 3.0.6 SP4, Zeiss Vision GmbH). For Ca^{2+} imposed stomatal aperture measurements, peels were preincubated in DB, for 2 h under 150 μmol m^{-2} s^{-1} photosynthetically-active radiation (PAR) to open stomata, then superfused while exchanging HB and DB every 5 min for 5 times.

2.3 Water Loss and Water Content

Leaf water status is intimately related to several leaf physiological variables, such as leaf turgor, growth, stomatal conductance, transpiration, photosynthesis and respiration (Kramer and Boyer, 1995). Water content and water loss have been widely used to quantify the water deficits in leaf tissues. These parameters are useful indicators of plant water balance, since they express the relative amount of water present on the plant tissues. For water loss measurements, plant rosettes were excised from the roots and exposed to desiccation by placing them on trays on the lab bench. A piece of parafilm sealed the excised stem to avoid water loss through it. Rosettes were weighed at different time points, their fresh weight determined and the water loss calculated from the difference between the weight at each time point and the initial weight. The relative water content (RWC) of individual plants was analyzed at day 0, the day when watering stopped, day 15 and day 20 days after watering was stopped. All rosette leaves of a single plant were harvested and weighed to determine the fresh weight (FW). These leaves were incubated in a water-filled and covered Petri dish overnight, to allow maximal water absorption. These leaves were weighed again, after carefully blotting dry the leaf surfaces, to determine the turgid weight (TW). Leaves were subsequently wrapped in tin foil and dried at 70 ℃ for 72 hours followed by determination of dry weight (DW). The RWC was calculated from FW, DW and TW as shown in Equation 2.1 (Barrs and Weatherley, 1962) .

$$RWC(\%) = \frac{\mathrm{FW-DW}}{\mathrm{TW-DW}} \times 100 \qquad \textbf{[2. 1]}$$

2.4 ROS Measurements

In plants reactive oxygen species (ROS) are continuously produced as byproducts of various metabolic pathways, and have been showed to be involved in several signaling pathways such as those triggered by ABA and Ca^{2+}. There are many methods developed for measuring ROS. In my experiments, ROS production was monitored using the ROS-sensitive fluorescent probe H_2DCFDA (Molecular Probes, UK) using the method essentially described by Desikan et al. (2004). The epidermal strips were pre-treated with the opening buffer for two hours before loading NO-sensitive fluorescent probe 15 μM DAF-2DA for 20 min in the dark, followed by 20 min flushing in SB (See Table 2.2) to remove excessive dye. The strips were subsequently incubated in SB alone or in SB containing 20 μM ABA for up to 30 min, and then imagined with 10-min intervals under a confocal microscope (Zeiss, Germany). The images were collected with excitation at 488 nm and emission at 515-560 nm (Zeiss, Germany). Data are calculated as a percentage of fluorescence intensities of ABA-treated over control guard cells using ImageJ software (NIH. USA).

Table 2. 2 Solution List

Name	Component
Standard Buffer (SB)	*10 mM KCl, 5 mM MES-$Ca(OH)_2$, pH 6.15*
Depolarising Buffer (DB)	*60 mM KCl, 5 mM MES-$Ca(OH)_2$, pH 6.15*
Hyperpolarising Buffers (HB)	*0.1 mM KCl, 10mM $CaCl_2$, 5 mM MES-$Ca(OH)_2$ pH 6.15*
Openning Buffer	*50 mM KCl, 5 mM MES-NaOH, pH 6.15*
ABA and ROS treatments	*SB + ABA or H_2O_2*

2.5 Electrophysiology

Electrophysiological methods allow the study of the electrical properties of biological cells. These methods involve measurements of voltage or ionic currents on a wide variety of scales from single ion channel to whole cell tissues. In plants, electrophysiological techniques have proven especially powerful in measuring ion currents of the guard cell plasma membrane, and in understanding the mechanisms that control these currents for stomatal movements. In the following subheadings I will introduce the essential aspects of electrophysiological technology used in studies of guard cell ion currents.

2.5.1 Techniques for Studying Ion Channels.

A number of techniques are available to study ion transport across membranes. The choice of technique relies on balancing the need for physiological reality with the need for biophysical definition. Recently patch clamp methods have become a widely used technique. The patch clamp is a refinement of the voltage clamp and was developed by Erwin Neher and Bert Sakmann in the late 1970s and early 1980s. This development made it possible to record the currents of single ion channels for the first time, proving their involvement in fundamental cell processes such as action potential conduction. The patch clamp technique can be applied to a wide variety of cells from bacterial to animal and plant cells. But patch clamp methods in plants requires to removal of the cell wall in order to gain access to the plasma membrane so that a high resistance seal might be obtained. This disadvantage can be remedied through using enzymatic to digest the cell wall (Tester and Macrobbie, 1990, Ward, 1997). The original technique of the voltage clamp avoids some of the difficulties of the patch clamp with plant cells, and allows the recording of the sum of all ion currents. Like the patch clamp, the voltage clamp is used to measure ion current across the membrane, while holding the membrane voltage at a fixed value (hence, the clamp of the voltage). Cell membranes contain many different kinds of ion channels, some of which are voltage gated, as well as other types of transporters. The voltage clamp allows the membrane voltage to be manipulated independently of the ionic currents, and permits the operator to explore the current-voltage relationships of membrane under study (Kandel et al., 2000).

The two-electrode voltage clamp method was first introduced by Hodgkin and Huxley as a tool for their studies of the action potential (Hodgkin and Huxley, 1939). In this method, voltage is recorded relative to ground through a "voltage electrode" and current is passing to the cell by a "current electrode". Usually, the two electrodes are connected to an amplifier which measures membrane potential and feeds the signal into a feedback amplifier. The difference between a command voltage, V_{comm} and the recorded membrane voltage V_m is used to determine the amplitude and sign of a current that is fed back into the cell through the current electrode. Whenever the cell deviates from this command (or holding) voltage, the feedback amplifier generates a signal proportional to $V_{comm} - V_m$ and the feedback circuit passes current into the cell to reduce the V_m signal to zero. Thus, the clamp circuit produces a current equal and opposite to the ionic current. This current can be measured, giving an accurate reproduction of the currents flowing across the membrane.

2.5.2 Electronic Setup and Voltage Clamping

The total current flowing across membrane is formed of two basic parts: one is from ionic currents that derive from the movement of charged ions species across the membrane, I_{ionic}; the other is generated from the membrane capacitance, C_m. Thus the total current is based on equation:

$$I_m = I_{ionic} + C_m \frac{\delta V}{\delta t} \qquad \textbf{[2. 2]}$$

Where $\delta V/\delta t$ is the change of voltage with respect to time. When voltage is clamped by amplifier, the $\delta V/\delta t$ =0, and I_m=I_{ionic}. Thus the currents passing across the plasma membrane when the voltage change is removed in representative of the ionic currents

The voltage clamp circuit negative feedback loop is shown in Figure 2.2. The membrane voltage is measured by one electrode and recorded by the preamplifier. The high input resistance of preamplifier minimizes current leakage from the microelectrode, which otherwise introduces large errors into plasma membrane voltage measurements. The equipment generates a command voltage (V_{comm}) to compare with membrane voltage (V_m). The difference between V_{comm} and V_m is converted as a current signal and sent back via the second microelectrode.

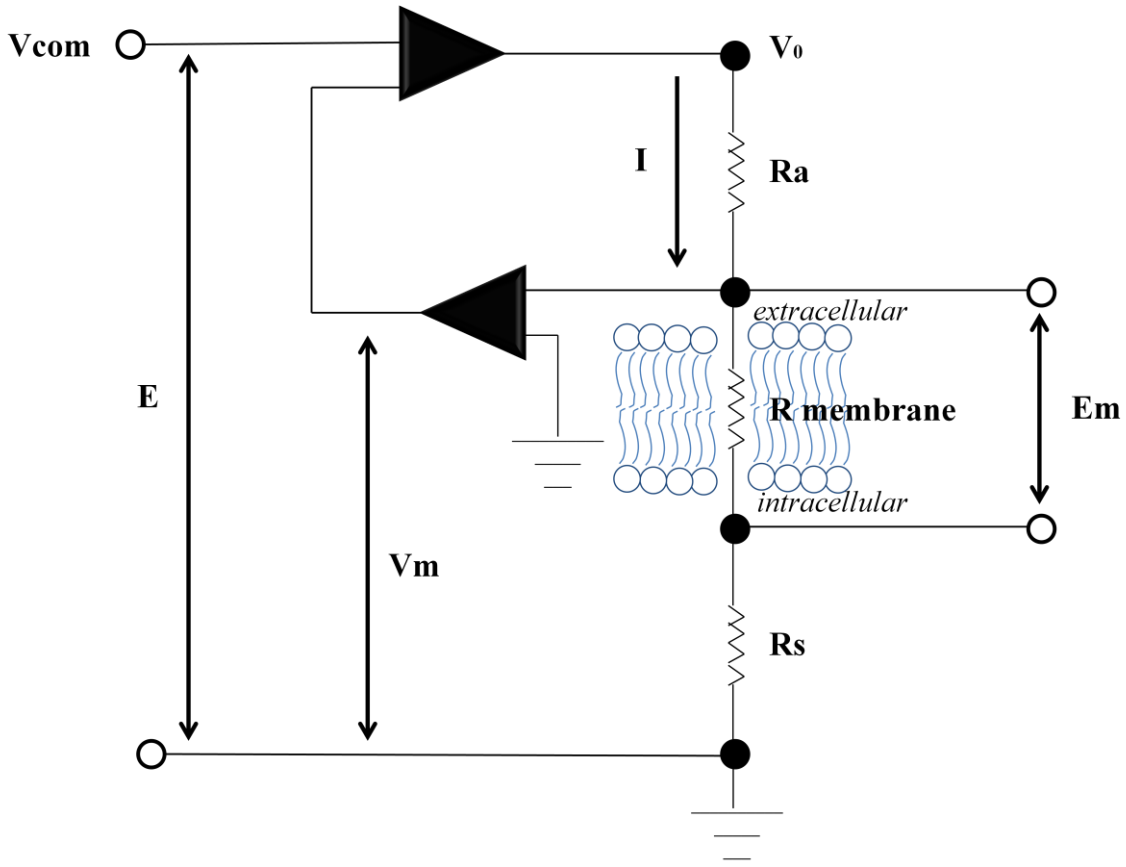

Figure 2. 2 A simplified voltage clamp circuit.

The clamping amplifier (*up*) compares the output from the preamplifer (V_m) with a command signal (E) and returns a current (I) to the cell across an access resistance (R_a). The clamp voltage, V_o, is divide across the membrane resistance ($R_{membrane}$) and a series resistance (R_s) (Modified from Blatt, 1991).

2.5.4 Microelectrodes

Microelectrodes were pulled from capillary borosilicate glass, the wall thickness is around 0.25 mm m and internal diameter is abour 1.25 mm (Dial Glassworks, Stourbridge, west Midlands, and UK). The puller was a modified two stage PD5 horizontal puller (Narashige Scientific Instrument Lab, Tokyo, Japan). All barrels were clamped into puller and then heated for 20 seconds before twisting through 360°. The barrels were cooled for 30 seconds before heating a second time and pulling. Heater and magnet settings were adjusted to optimize shape and tip size. In order for the electrodes to be inserted into half-cells, the back ends of the barrels were heated in small gas flame and shaped using forceps (Figure 2.3). Then all the electrodes were put into a sealed glass container to avoid breakage and contamination of the fine tips.

2.5.5 Half-cells

Half-cells were used to connect the microelectrodes to the amplifiers. Half-cells were home made in the lab using the methods previously described (Blatt, 1991, Chen et al., 2012b). The main body of the half-cell was constructed by cutting approximately 5 cm off a 2 ml disposable pipette. A silicone rubber bung of an appropriate size was cut and inserted into the end of pipette. A piece of 0.5 mm diameter silver wire was cut and soldered onto the end of a 2-mm socket. The wire was cleaned to remove the silver oxide layer, and then inserted through the silicone bung until the socket was seated in the back end of the pipette section. A silver chloride layer was deposited on the silver wire using a 10% solution of sodium hypochlorite by filling the half-cells overnight. This solution was then removed and carefully, the half-cell cleaned and filled with 1M KCl. Half-cells were store in 1M KCl, and most importantly, the sockets were connected together to ensure electrical equivalence between half-cells. The construction of the reference half-cell was the same. Electrical contact between the reference half-cell and cell bath solution was by a salt bridge. This bridge was made by filling polythene tubing with 2% agar dissolved in 1M KCl.

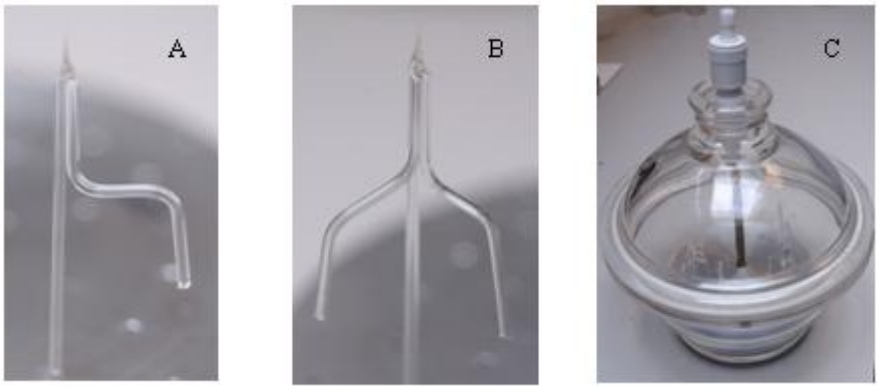

Figure 2. 3 Images of microelectrode and glass container.

Typical shape of double- and triple- barrels microelectrode (A and B); and Glass container of electrodes (C).

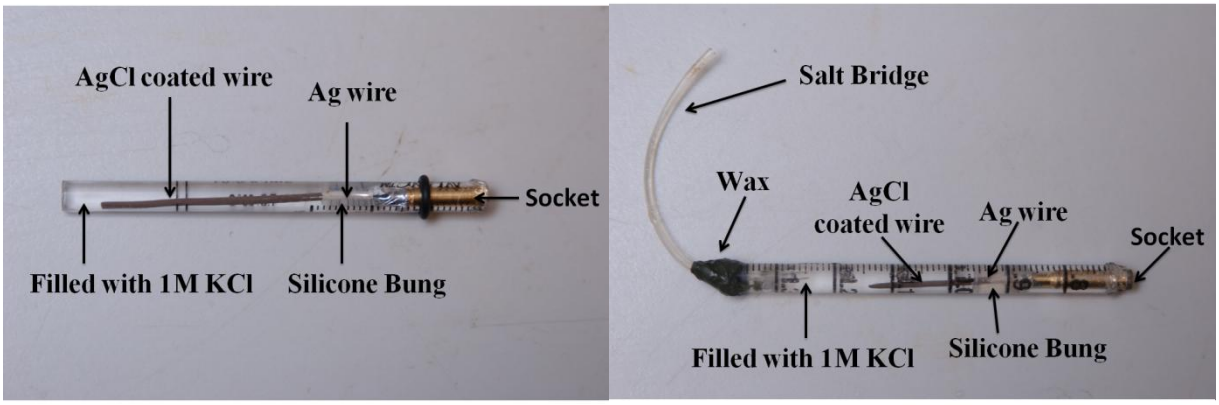

Figure 2. 4 Construction of half-cells.

Normal half-cell (*Left*); half-cell with salt-bridge (*Right*).

2.5.6 Chamber and Holder

Experiments were carried out using homemade chambers (Figure 2.5) constructed of stainless steel blocks. These blocks were glued onto a thin glass slide. The larger block had a 1.5 mm diameter hole allowing entry for the ager salt bridge into the chamber solution. The chamber was fixed into a steel holder as shown in figure 2.5 to attach the microscope stage. Solution was fed through by gravity into the chamber on one end and removed at the other near the salt bridge. Solutions were contained in flasks, each connected via PTFE tubing to a valve system giving two separate lines that allowed for rapid changing between different solutions. Solution flow rate were adjusted by a luer -lock valve.

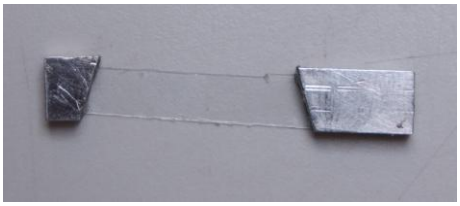

A

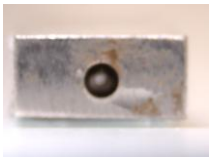

B

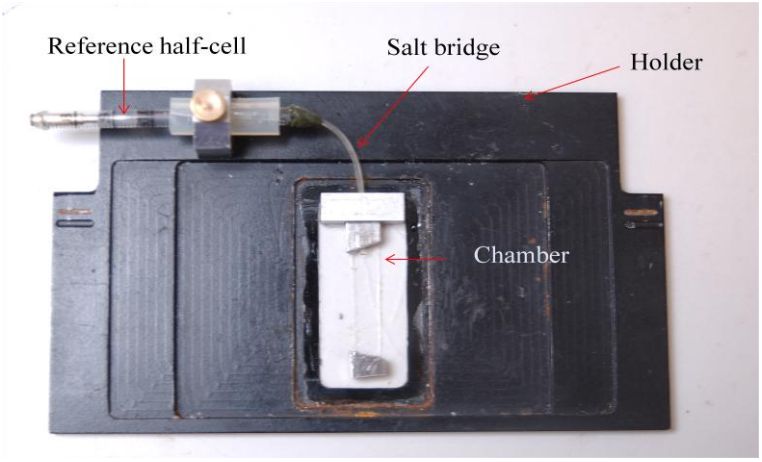

C

Figure 2. 5 Details of chamber design.

(A) and (B) Steel blocks are attached to the glass or quartz base using silicon glue. (C) Chamber was fixed on the holder and connected with salt bridge.

2.5.7 Experimental Procedure

For measurements, an epidermal strip was fixed to the chamber, and the strip was immediately bathed in the SB. A cover slip was fixed to the top of chamber, and then the chamber was secured in the holder and the agar bridge was connected to the chamber. The holder was then placed on the microscope stage. A solution delivery needle and suction pipette for removing solution were each placed in position at either end of the chamber (Figure 2.5) and solution flow was started. The tissue was examined for suitable guard cells under the microscope. Once mounted on the amplifiers, the microelectrode was moved into position using a Huxley-type micromanipulator. The cell dimensions were measured using an ocular micrometer, recorded, and cell surface area and volume were calculated assuming a cylindrical geometry. The microelectrode tips were then advanced against the cell wall of targeted cell and the cell impaled.

2.5.8 Separation of Ionic Currents

In whole cell voltage clamp experiments, recording and isolating specific ion currents from the total ionic current is a focus of much of the experimental manipulation. For example, inward current is mainly contributed by two different ionic fluxes, one carried by $I_{K,in}$ and the second by I_{Cl}. Thus it is necessary to separate these two currents in order to quantify and study each individually. One approach is to use toxins and blocking agents that eliminate one or the other of the currents. For example, tetraethylammonium ions (TEA^+) are often used to block K^+ channels (Hille, 1967) enabling the study of the anion current (Grabov et al., 1997). In my experiments, acetate was used to eliminate the background of the anion current when measuring K^+ currents and Ba^{2+} currents. For anion current recording, TEA^+ and Cs^+ were used to block K^+ channels.

2.5.9 Analysis of Ion Currents

In general, the ion channels of guard cells are voltage-dependent, including the channels examined in the studies that follow. Other transporters, such as the H^+-ATPase are active at all voltages and, consequently, their currents add to what is often called the 'instantaneous' current. The instantaneous current is defined operationally as the change in current observed within the first few milliseconds of changing membrane voltage. Thus,

currents from the anion channels and K^+ channels described in the following chapters can be identified by their slower activation and deactivation. They can be separated by subtracting the instantaneous currents recorded on stepping the membrane from voltages at which the currents of interest are normally not active. The concept behind this manipulation at one clamp voltage is shown in Figure 2.6. By repeating an analysis of this kind at many different voltages, it is then possible to build up a plot of the current-voltage (I-V) relationship for the channel; this plot represents the product of the steady-state activity of the channel and its open-channel permeability.

Analysis of the kind shown in Figure 2.6 also provides kinetic information important in the analysis of the currents. Some of this information again comes from the steady-state I-V curve of the current and can be used to separate the channel permeation properties from the voltage-dependence for its activity. For example, I-V curves for the K^+ channels were normally fitted with Boltzmann function as follows:

$$I = \frac{g_{max}(V-E_K)}{1+e^{\delta zF(V-V_{1/2})/RT}} \qquad \textbf{[2. 3]}$$

Where g_{max} is the maximum conductance, V is the commend voltage, E_K is the equilibrium voltage for K^+, $V_{1/2}$ is the voltage which half maximal current achieved, z is the ion charge, F is the Faraday constant, δ is the gating charge, R is the gas constant and T is the absolute temperature. Here the relation $g_{max}(V\text{-}E_K)$ describes the maximum current through the channel at voltage V and corresponds to the open-channel current; its product with $1/(1+\exp(\delta zF(V\text{-}V_{1/2})/RT))$ in turn describes the relative activity, sometimes called the relative open probability, of the channel at voltage V. Thus, analysis of this kind yields two key parameters that uniquely describe a channel: δ determines the change in activity with voltage, and $V_{1/2}$ determines the midpoint voltage at which this change occurs.

Finally, analysis such as shown in Figure 2.6 also provides kinetic data that can be analyzed for the rates of change in current that is the non-steady-state properties of the channels. The simplest analysis describes the halftime ($t_{1/2}$) required for the current to relax to a new steady-state following a change in voltage. This value provides information about

the channel kinetics and is related to its gating; it also provides a useful measure to quantify channel responses to a certain treatments. The $t_{1/2}$ is determined as a function of voltage using utilities provided by the Henry electrophysiology software (Y-Science, Glasgow, UK).

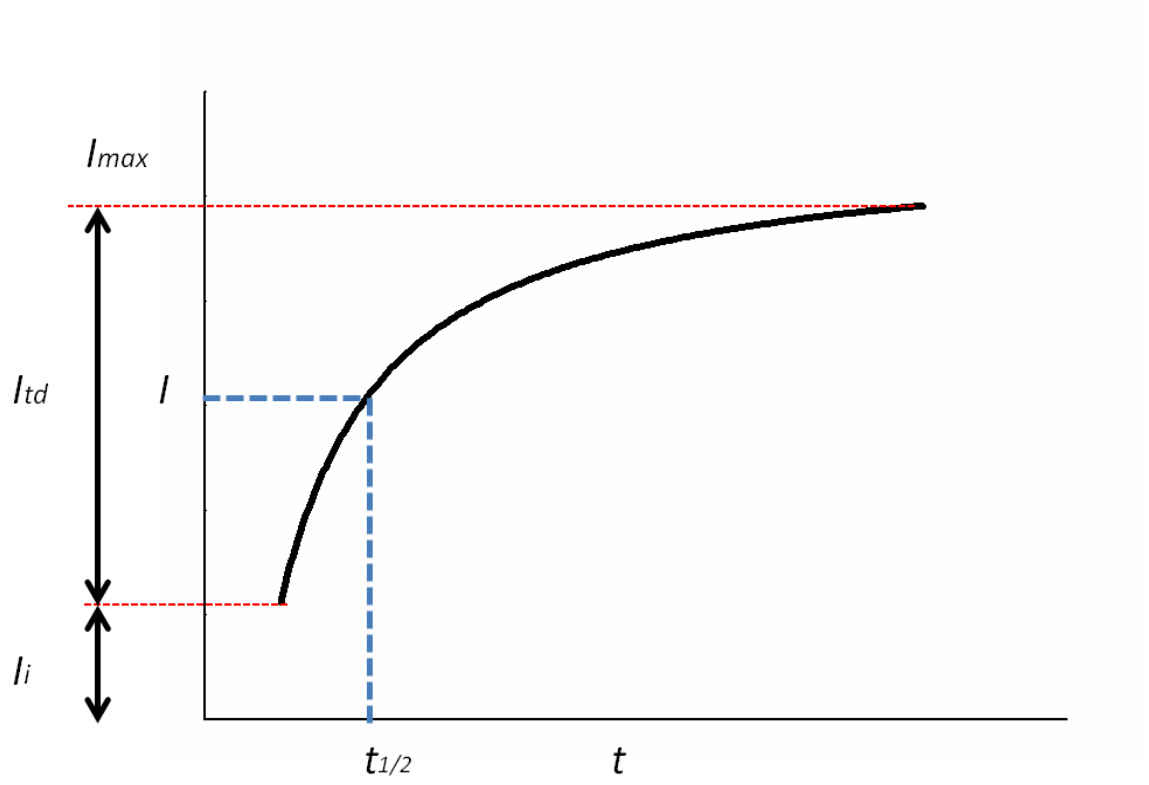

Figure 2. 6 Details of current analysis.

One current curve is shown. The instantaneous current (I_i) is subtracted from the maximal current (I_{max}) to obtain the time-dependent current (I_{td}). $t_{1/2}$ stands for halftime.

2.6 Measuring Fluorescence

Fluorescence is a powerful tool for probing biological structure and function. Nowadays, a great many of biological and chemical dyes are commercial available for measurements of cytosolic factors such as Ca^{2+} and pH. Most of these dyes are biologically inert when introduced into living cells and give a strong fluorescence which can be measured continuously. For the studies described in the chapters below, and two fluorescence dyes, Fura2 and BCECF, will be introduced later.

Fluorescence is the emission of light by a substance that has absorbed light or other electromagnetic radiation. In most cases, the emitted light has a longer wavelength than the absorbed radiation, because some energy is lost as heat. However, sometime when the absorbed electromagnetic radiation is intense, the electron absorbs two photons which lead to emission of radiation having a shorter wavelength than the absorbed radiation. The fluorescence lifetime refers to the average time the molecule stays in its excited state before emitting a photon. The intensity of the fluorescence emission (I_F) depends on the amount of incident light (I_o), on the concentration of fluorophroe (c) and on two intrinsic properties of the fluorescent molecular: extinction coefficient for light absorption (ε) and quantum yield for light output (γ). The extinction coefficient is a measure of probability of the absorption of incident light by fluorophore and the quantum yield is defined as the number of quanta of light emitted relative to the number of quanta absorbed. These parameters are related by the equation:

$$I_F = I_o \gamma \epsilon c l \qquad \textbf{[2. 4]}$$

Where l is the length of the path traversed by the light through the sample.

2.6.1 Fluorescence Dyes

There are a number of fluorescent probes available for measurement of Ca^{2+} in vivo. The most commonly-used probe is Fura-2. Fura-2, a polyamino carboxylic acid, and can be employed as a ratiometric fluorescent dye, because when Fura-2 binds to free intracellular calcium its excitation spectrum changes (Grynkiewicz et al., 1985). Fura-2 is normally excited at 340 nm and 380 nm of light, and the ratio of the emission (maximum approx.. 525 nm) derived from excitation at those wavelengths is directly correlated to the amount of intracellular calcium and independent of the amount of Fura-2 in the cell. One problem in using Fura-2 is photobleaching; like many dyes of its kind, continued excitation gradually leads to photodestruction of the fluorophore. I found that rapid data collection caused photobleaching so that the timeframe available for high temporal resolution measurements was short, normally no longer than 20 min. However, this time period was still sufficient for most experiments and permitted calculating the cytosolic-free $[Ca^{2+}]$ ($[Ca^{2+}]_i$) in stomatal guard cell during experimental challenges while recording current under voltage clamp. Other probes, such as cytosolically-expressed Yellow Cameleon protein (YC), have been shown to successfully measure $[Ca^{2+}]_i$, but using these probes requires the cells to be stably transformed with the relevant constructs. Thus a major drawback of this approach is the time required to generate the transgenic lines. In addition, the sensitivity of YC-based probes is relatively poor compared with Fura-2. For these reasons, Fura-2 was choosed for $[Ca^{2+}]_i$ measurements.

For similar reasons, I made use of the fluorescent dye 2′,7′-bis-(2-carboxyethyl)-5-(and-6)-carboxyfluorescein (BCECF) for measurement of cytosolic pH (pH_i). Because BCECF's pKa (6.97) is close to physiological pH, it can detect cytosolic pH change with high sensitivity. At low pH, the dye is weakly fluorescent but becomes more fluorescent with increasing pH. The excitation spectrum of the dye undergoes a slight shift during pH change, while the wavelength of the emission maximum remains unchanged. The pH is determined ratiometrically by the relative fluorescence intensities at 535 nm when the dye is excited at 439 nm and 505 nm respectively.

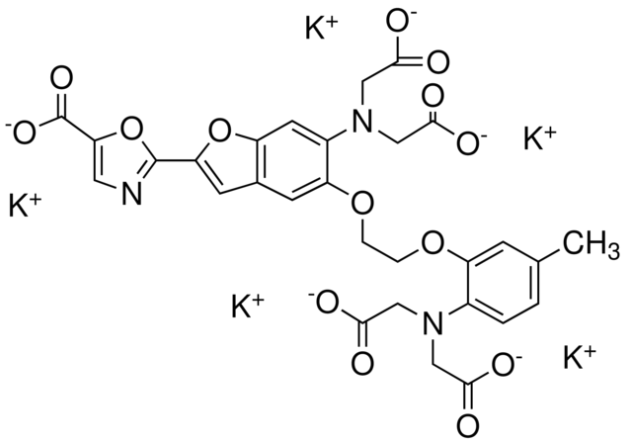

A

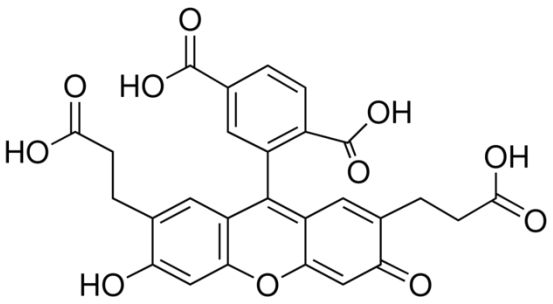

B

Figure 2. 7 The structure of Fura-2 and BCECF.

(A) Fura-2 pentapotassium salt and (B) BCECF. Taken from Sigma-Aldich company (http://www.sigmaaldrich.com).

2.6.2 Dye Loading Methods

Fluorescent dyes can be loaded into cells through several methods, including acid loading, pressure or electrophoretic microinjection into cells. Additionally, they can be chemically linked to form an acetoxymethyl ester (AM ester), which results in a membrane permeable compound, such as Fura-2 AM and BCECF AM, that is de-esterified by endogenous esterases. One difficulty of this method is that AM esters are also hydrolysed by esterases in the cell wall. As a result, treatments with AM esters of these dyes commonly results in an accumulation of dye in the wall, but not in the cytosol. Finally, some researchers have used acid loading of the free acids of the dyes; this method uses acidic solutions with the dye, which protonates the dye so that it can easily pass through cell wall and plasma membrane. Blatt et al (2007) indicated that acid loading generally leads to dye sequestration in compartments that are not part of the cytosol and rapid secretion of the compound out of the cell.

In this thesis, all experiments were carried out by iontophoretic loading. Triple barreled microelectrodes (mentioned above) were used, two barrels filled with standard electrolyte, and the third filled with a dilute solution of either Fura-2 or BCECF. Cells were observed using 63x magnifications with an additional 2.4x optivar magnifier. Prior to impalement, the target cell was centered in the field of view and five background images were collected for subsequent background subtraction. All imaging was carried out using a GenIV-intensified Pentamax-512 charge-coupled device camera (Princeton Instruments, Trenton, NJ, USA). For Fura-2, excitation wavelengths of 340 nm and 390 nm were selected using monochrometer; for BCECF, excitation wavelengths of 440 nm and 490 nm were selected. Fluorescence was excited using a xenon arc lamp (Osram, Munich, Germany) and Til Photonics monochromator. All recordings and data collection was carried out using MetaFlour (v.6.2 Universal Imaging, USA). Exposure times were adjusted to roughly balance emissions; so for Fura-2, 200 ms and 500 ms were used for 340 nm and 390 nm respectively; for BCECF, 200 ms and 400 ms wered used for 440 nm and 490 nm, respectively. These signals were employed as standards and were calibrated against known concentrations of Ca^{2+} and H^{+}. Offline analysis was carried out by using MetaFluor and ImageJ (NIH, USA).

Following impalement, cells were clamped to -50 mV and Fura-2 or BCECF was injected from the third microelectrode barrel through application of a negative running current. To prevent blocking the inject electrode's tip, the injection current was kept to a minimum and dye loading carried out over 3-5 min. Under standard conditions, Fura-2 dye loading was continued until the fluorescence intensity monitored at 340 nm was between 400 and 750 above background (estimated concentration of Fura-2 in cytosol was under 10 μM); for BCECF a similar protocol was used, except that dye loading was monitored at 490 nm and continued until this signal was between 2000-3000 above background (estimated concentration of BCECF in cytosol was near 50 μM).

2.6.3 $[Ca^{2+}]_i$ Calibration

The mathematical relationship between the measured fluorescence ratio (R) and the free calcium ion concentration is expressed as follows:

$$[Ca^{2+}] = K_d \left(\frac{Sf}{Sb}\right) \frac{(R - R_{min})}{(R_{max} - R)} \qquad \textbf{[2. 5]}$$

The evaluation of this expression requires the values for the so-called calibration constants (K_d, R_{max}, R_{min}, S*f*, and S*b*) to be inserted. The values of R_{max} and R_{min} are the ratio values measured under conditions of saturating calcium levels and in the absence of calcium, respectively. The values of S*b* and S*f* are proportional to the fluorescence excited by the denominator wavelength (normally 390 nm) again under conditions of saturating calcium levels (the "b" referring to the bound state) and in the absence of calcium (the "f" referring to the free calcium) respectively. A value of 225 nM is normally used for the dissociation constant for fura2 calcium binding (K_d). The ratio equation then generates calcium values in nanomolar concentration.

In vitro calibration constants were obtained from solutions of Fura-2 and a background solution containing no Fura-2. The calibration solutions were typically made to mimic the intracellular condition. The Ca^{2+} free solution contained 10 mM KCl, 50 mM BAPTA, 5 mM HEPES (pH 7.5) and 10 μM Fura-2. The high Ca^{2+} solution contained 10 mM KCl, 1 mM $CaCl_2$, 5 mM HEPES (pH 7.5) and 10 μM Fura-2. Gives a minimum and maximum ratio of 0.5 and 3 respectively, and with S*f* and S*b* was 3 and 1, respectively.

2.6.4 pH_i Calibration

Calibration of BCECF was carried out similarly to that for Fura-2, but using dual wavelength ratio measurements with standard monochromator and collection settings (above) with solutions titrated to pH values of 5.3, 5.9, 6.3, 6.9, 7.4, 7.9 and 8.4 using a series of Good pH buffers and KOH *in vitro*. The titration curve for BCECF curve is shown in Figure 2.8 and was used for all further calculations.

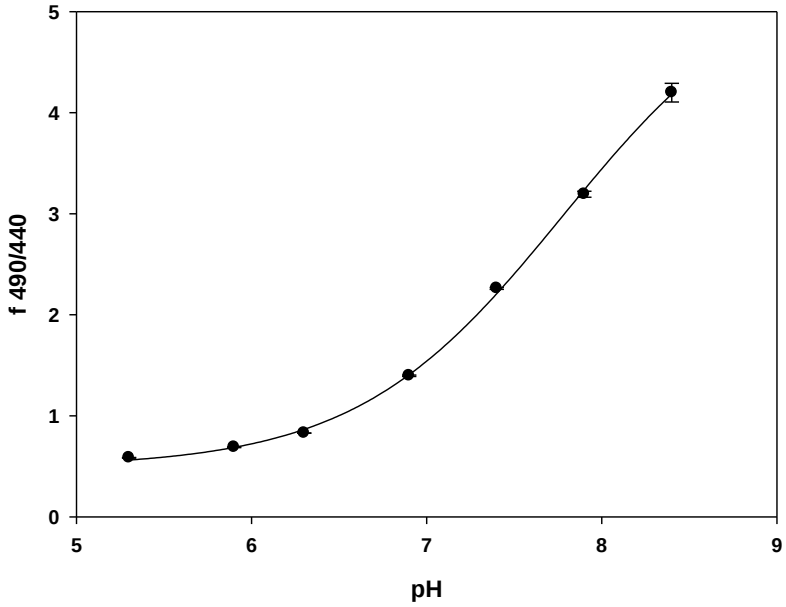

Figure 2. 8 BCECF fluorescence titration curve.

In some experiments, manipulations were carried out to change the pH_i. These experiments generally made use of weak acid loading by adding a weak acid to the external solution. The protonated weak acid then equilibrated across the plasma membrane and deprotonation led to a release of H^+ in the cytosol. Under these circumstances, it is possible to calculate the capacity of the cell to buffer pH_i. Cytoplasmic H^+ buffer capacity, β, was determined according to the function:

$$\beta = -\delta \frac{\delta [A^-]_i}{\delta pH_i} \qquad \textbf{[2. 6]}$$

where $[A^-]_i$ is the concentration of the acid anion in the cytoplasm on adding the weak acid to the bath. The calculation requires only that values for pH_i, pH_o, the pK_a for each weak acid (=4.82 for butyrate) and the concentration of weak acid added outside are known. It was assumed that the initial concentration of the acid anion was zero in the cytoplasm and $[HA]_i = [HA]_o$ on adding the weak acid. Then, from the Henderson-Hasselbalch equation,

$$[A^-]_i = \frac{[A_{tot}]}{10^{pK_a - pH_i} + 10^{pH_o - pH_i}} \qquad \textbf{[2. 7]}$$

where pH_i is the final cytoplasmic pH, and $[A_{tot}]$ is the total weak acid added (= $[HA]_o$+ $[A^-]_o$).

2.7 Gas Exchange Measurements

The basic principle of gas exchange measurements lies in determining how much H_2O and CO_2 is used or produced by plant tissue. In this study the LI-6400XT system (LI-COR Bioscience GmbH, Bad Homburg, Germany) was used to measure H_2O and CO_2 differentials between incoming and outgoing air of a whole rosette enclosed in a Whole Plant Arabidopsis Chamber (LI-COR 6400-17). Pots containing single plants were sealed with saran wrap before mounting in the whole plant chamber to prevent water vapour and CO_2 diffusion from the soil. Chamber CO_2 concentration was set to 380 ppm. The whole plant chamber top was sealed with transparent Propafilm (LI-COR, 250-01885) allowing ambient light to be used as a light source. Chamber temperature and humidity also matched the ambient conditions. Sample and reference signals from the IRGA were matched before each measurement, and data were recorded for 2–3 min in each case. Data for each genotype and condition were collected on at least three separate days at similar times of day.

2.8 Data Analysis

All currents recordings were analysed and leak currents subtracted using standard methods (Blatt, 2004) with Henry IV software. Data analysis and curve fittings were carried out by using SigmaPlot 11 (Systat Software, Inc., USA). Where appropriate, data are presented as means ± S.E.M. of n observations. Significances were determined using Students' T-test or ANOVA for pairwise comparisons.

CHAPTER 3:

THE EFFECT OF CYTOSOLIC ORGANIC ACIDS ON ANION CHANNELS

3.1 Introduction

Respiration in plant leaves is one of the most important processes contributing to carbon exchange between the plants and atmosphere. Combined with photosynthesis, it has a major impact on biomass production in plants. Both photosynthesis and respiration lead to the production of three-carbon compounds which feed into the tricarboxylic acid (TCA) cycle and, from there, into a variety of synthetic pathways leading, for example, to organic acid and amino acid synthesis. The TCA cycle begins with the condensation of oxaloacetate (OAA) and acetyl CoA, and proceeds via a series of oxidative steps that release two carbon atoms as CO_2; it ends with the regeneration of OAA (Figure 3.1). OAA is an intermediate of the TCA cyle and gluconeogenesis. It forms upon oxidation of Mal, catalysed by malate dehydrogenase, and it reacts with Acetyl-CoA to form citrate, catalysed by citrate synthase (Figure 3.1). OAA also forms in the mesophyll of plants by the condensation of CO_2 with phosphoenolpyruvate, catalysed by PEP carboxykinase. It can arise from pyruvate *via* an anaplerotic reaction. Although well-studied beyond these biochemical processes, the role of OAA in stomatal function and ion tansport has yet to be explored at the start of this research. By contrast, the dicarboxylic acid malate (Mal) is well-known to have a multitude of functions in plant metabolism and osmotic homeostasis. It plays a key role not only in TCA cycle, but also in crassulacean acid metabolism (CAM) and C4 metabolism, in osmotic regulation, in pH homeostasis, and also appears as an important root exudate (Martinoia and Rentsch, 1994). In guard cells, much of Mal is synthesized by the carboxylation of phosphoenolpyruvate and the rest often accompanies K^+ during the uptake of solutes into the guard cells to maintain electrical balance. Increased apoplastic Mal levels can be observed at high CO_2 levels when stomata are closed (Hedrich et al., 1994) suggest Mal could be form a link between environmental CO_2 and stomatal movements.

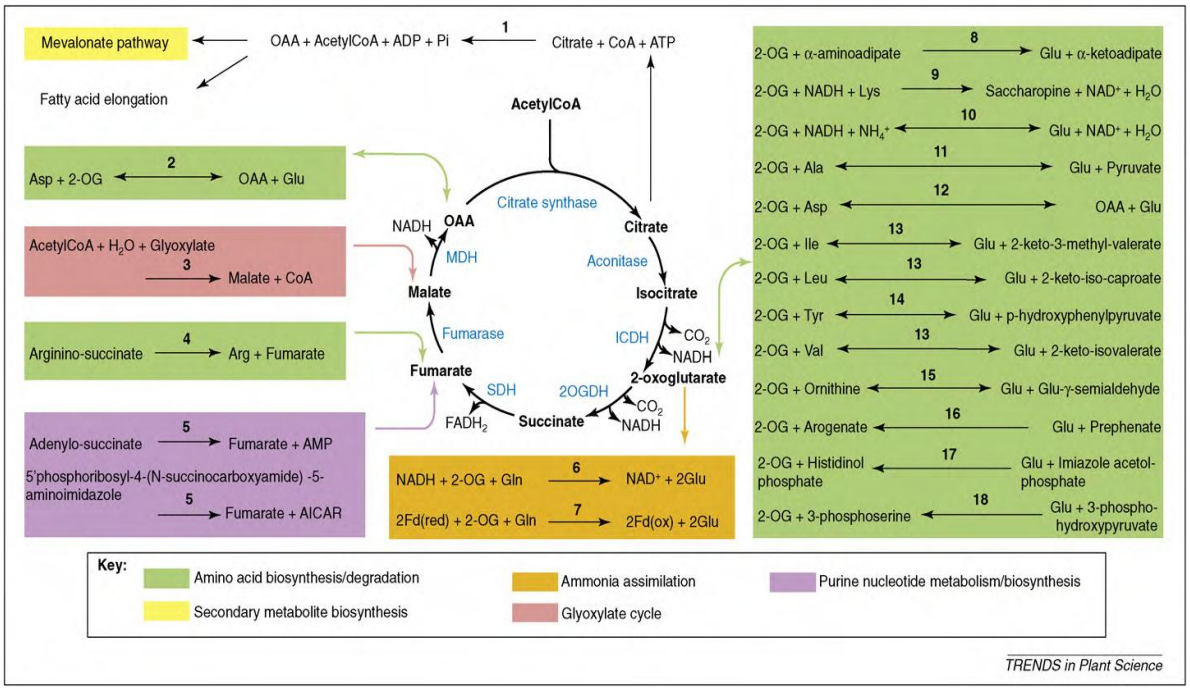

Figure 3.1 The TCA cycle is embedded in a larger metabolic network (Taken from Sweetlove et al., 2010)

Several important network connections involved in biosynthetic processes are indicated by the coloured boxes below and to the left and right of the TCA cycle. Abbreviations: ICDH, isocitrate dehydrogenase (NAD(P) dependent); MDH, malate dehydrogenase (NAD+ dependent); 2OGDH, 2-oxoglutarate dehydrogenase; PDH, pyruvate dehydrogenase; and SDH, succinate dehydrogenase. Metabolite abbreviations: AICAR, aminoimidazole carboxamide ribonucleotide; CoA, coenzyme A; Fd(ox), oxidised ferredoxin; Fd(red), reduced ferredoxin; 2-OG, 2-oxoglutarate; OAA, oxaloacetate; and Pi, inorganic phosphate. Numbered reactions are catalysed by the following enzymes: 1, ATP citrate lyase; 2, aspartate transaminase; 3, malate synthase; 4, arginosuccinate lyase; 5, adenylosuccinate lyase; 6, glutamate synthase (NADH); 7, glutamate synthase (ferredoxin); 8, 2-aminoadipate transaminase; 9, saccharopine dehydrogenase (NADH, L-lysine forming); 10, glutamate dehydrogenase; 11, alanine transaminase; 12, aspartate transaminase; 13, branched chain amino acid transaminase; 14, aromatic amino acid transaminase; 15, ornithine transaminase; 16, glutamate-prephenate aminotransferase; 17, histidinol-phosphate transaminase; and 18, phosphoserine aminotransferase.

It is widely recognized that ionic fluxes and some metabolites such as Mal across both plasma membrane and tonoplast are mainly contributors for regulation of osmotic content and turgor pressure that drive stomatal open and close (Hetherington and Woodward, 2003, Schroeder et al., 2001, Blatt, 2000, Blatt et al., 2007, Willmer and Fricker, 1996). Among these ionic fluxes, transport of Mal across the plasma membrane of guard cells is an important process in the regulation of stomatal movements. Although many details of Mal transport are still largely unknown, it has been reported that Mal efflux is associated with plasma membrane anion channels (Hedrich et al., 1994). At the plasma membrane, anion channels are key elements that contribute to stomatal closing, and their activities are essential to depolarize the membrane and balance charge with K^+ during solute efflux for stomatal closure (Blatt, 2000, Schroeder et al., 2001). Guard cell anion channels divide between two large groups according to their physiological characteristics, as noted in Chapter 1. The first group, the slow or S-type anion channels, was identified with a slow-activating current. These channels are strongly activated by micromolar range of $[Ca^{2+}]_I$ (Schroeder and Keller, 1992, Schroeder and Hedrich, 1989). Recently, a homologue of fungal and bacterial dicarboxylate/malic acid transport proteins, SLAC1, has been identified as an S-type channel in the *Arabidopsis* (Negi et al., 2008, Vahisalu et al., 2008). The other group of anion channel was first characterized by a strongly voltage-dependent current that activated on increasing membrane voltage beyond the range −100 to −80 mV and inactivated within a few tens to hundreds of milliseconds at more negative voltages (Schroeder and Keller, 1992, Hedrich et al., 1990, Hedrich and Marten, 1993). This current was identified with rapid, or R-type, anion channels.

Despite their differences, both of these anion channels are indentified to transport Mal and so most likely contribute to its homoeostasis and to regulating stomatal movements (Vankirk and Raschke, 1978a, Vankirk and Raschke, 1978b). The recently isolated *slac1* loss-of-function mutation was shown to associate with over-accumulations of Mal and other organic acids, as well as K^+ (Vahisalu et al., 2008). Additionally, a very high cytosolic concentration of Mal may itself inhibit the S-type currents (Schmidt and Schroeder, 1994). Although the molecular identity of the R-type anion channels has remained uncertain until now, it has been shown that R-type currents are Mal sensitive

(Hedrich and Marten, 1993, Raschke et al., 2003). Moreover, a controversial R-type anion channel, ALMT12 (aluminium-activated, Mal transporter 12), and other members of this aluminium-activated Mal transporter family have been shown contribute to the R-type anion currents in *Arabidopsis* (Meyer et al., 2010); the currents generated from AtAlMT12 when expressed in *Xenopus oocytes* exhibit a sensitivity to extracellular Mal concentration. Indeed, extracellular Mal has long been found to alter the voltage dependence of R-type anion channels (Hedrich and Marten, 1993) in effect promoting anion efflux through the channels in response to the organic anion outside. These observations have been interpreted as an indirect 'feedforward' mechanism for CO_2 control of the channels (Hedrich and Marten, 1993). However, the effect of Mal and other organic acids in the cytosol from metabolism on these channels has largely been ignored.

To bridge this gap in knowledge, I examined the anion channel current (I_{Cl}), and its regulation by metabolically related organic acid anions through experimental manipulations both outside and inside guard cells of *Vicia faba*. I show here that Mal action exhibits a biphasic characteristic, with higher Mal concentrations outside suppressing I_{Cl}. I also find that Mal, as well as its precursor oxaloacetate (OAA), suppresses I_{Cl} in a voltage-independent manner when present on the cytosolic side of the membrane. Furthermore, I show that the effect of OAA is evident well within its physiological concentration range. These findings point to control of the anion channels by OAA, indicating the capacity for feedback control from cellular metabolic activity and a much more subtle 'fine tuning' of the anion channels by metabolism than previously anticipated.

3.2 Material and Methods

Single and double-barrelled microelectrodes were prepared and coated with paraffin to reduce capacitance as described in Chapter 2.

For an open channel, the current is commonly described as a linear conductance with the I-V curve passing across the voltage axis at E_{rev}, the reversal voltage for the current. In the case of the guard cell anion or Cl^- -selective channel, E_{rev} will be close to E_{Cl} and at more negative voltage the channel will carry a net inward (negative) current as it allows anions to pass across the plasma membrane. In Figure 3.2A, the current is described by Ohm's law (Equation 1.4) for the open channel, and the inward current (outward flux of Cl^-) is indicated by the shading. In the steady-state, channel gating dependent on voltage superimposes on this current to adjust its absolute amplitude according to the voltage-dependence of the relative conductance. The relative conductance is proportional to the steady-state open probability (P_o) of the channel population, and can be described as a function with values between zero (no channel is open) and one (the maximum number of channels is open). Typically, this behavior is well-described with a sigmoidal dependence on voltage (Figure 3.2B). The actual steady-state I-V curve of anion channel (Figure 3.2C) is therefore the product of the open channel I-V curve (Figure3.2A) times the relative conductance of the channel population (Figure 3.2B).

For analysis of the anion current, I used both the steady-state and instantaneous currents. Because voltage transitions under clamp are fast compared to the response of P_o, changing voltage gives rise to current relaxations which provide useful information about the properties of the channels involved. Both the S- and R-type channels (see Chapter 1) activate at positive voltages (see Figure 3.2 and 3.3), thus the instantaneous current I-V curve is roughly equivalent to the open channel I-V curve and incorporates components of both channel currents. The R-type current deactivates rapidly at voltages negative of -60 mV, whereas the S-type current deactivates slowly and only partially at these voltages. Therefore the steady-state I-V curve represents largely this current, especially at the more negative voltages.

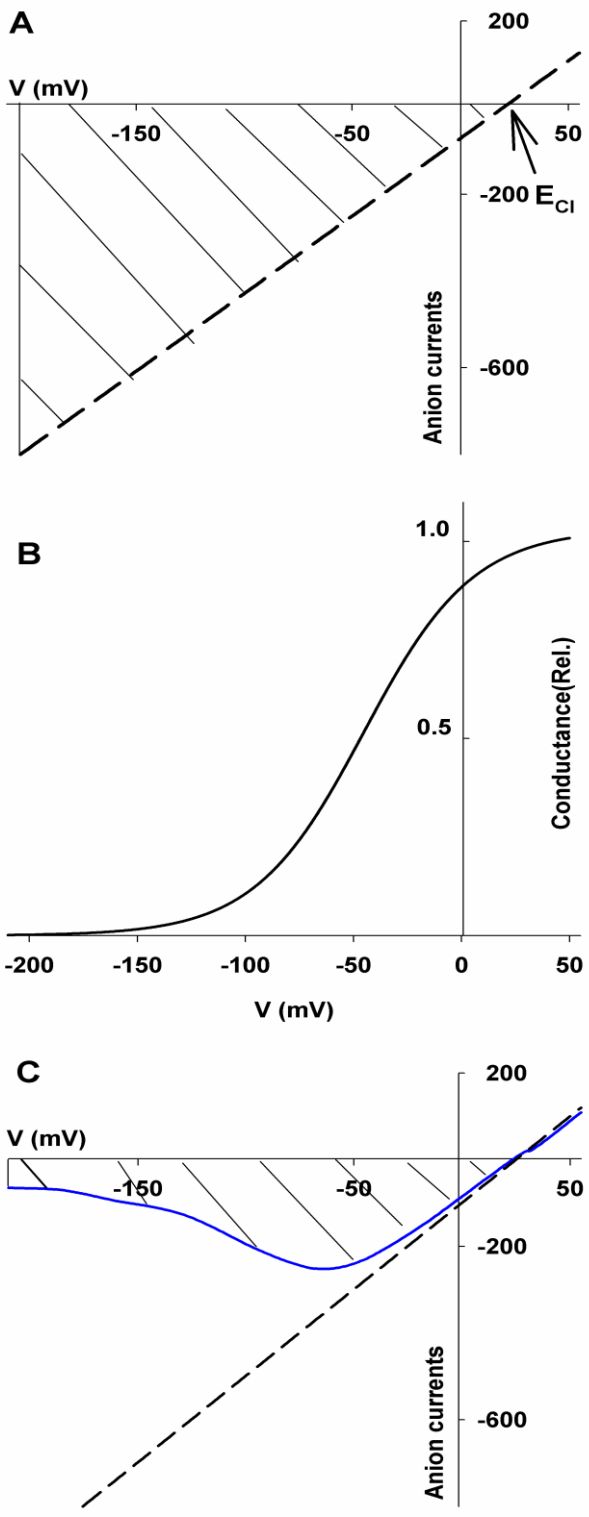

Figure 3.2 Steady-state I-V curve of anion channels.

(A)The open channel I-V curve. E_{Cl} defines the equilibrium voltage for Cl^-. (B) The relative conductance of channel population takes on values between zero (roughly zero channels open) and one (the maximum number of channels open) with a sigmoidal dependence on voltage. (C) The steady-state I-V curve (blue line). The shaded area indicates anion efflux.

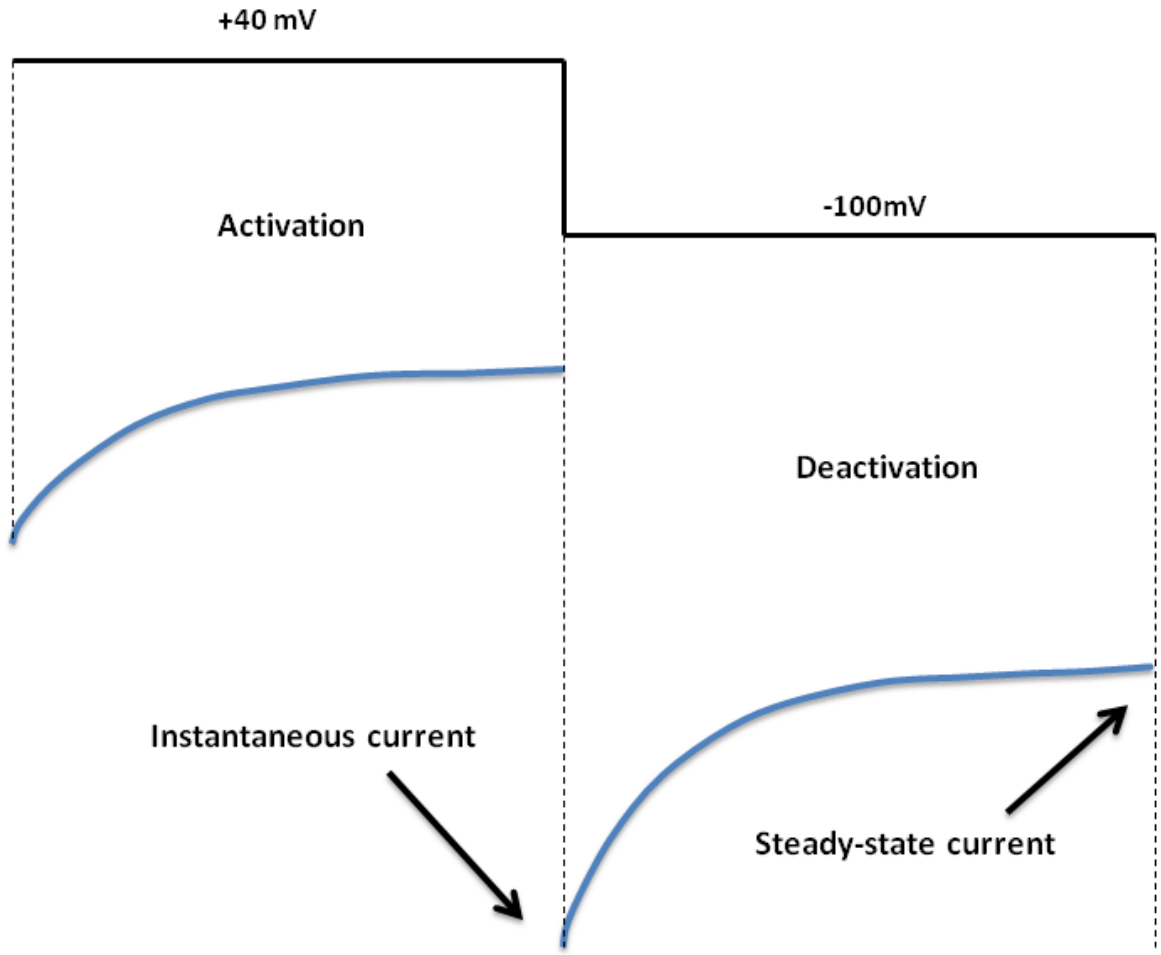

Figure 3.3 Analysis anion current.

Instantaneous and steady-state currents from one voltage clamp cycle shown with activation step (+40 mV) followed by deactivation step (-100 mV). Current shown in blue and voltage cycles in black.

3.3 Results

3.3.1 The Effect of Mal on I_{Cl}

3.3.1.1 Biphasic Activation of I_{Cl} by External Mal

Firstly, the effects of Mal outside were examined. Guard cells from epidermal strips were superfused with Mal concentrations up to 20 mM. Figure 3.4 summarizes the mean current-voltage (I-V) curves of the effect of 0, 1 and 10 mM Mal on anion currents from ten independent experiments. Voltage was clamped to a conditioning step to +40 mV and subsequent clamp steps to voltages more negative than approximately -40 mV yielded substantial inward-directed and instantaneous I_{Cl} that relaxed to steady-state values near -5 to -10 $\mu A \cdot cm^{-2}$ within 3-5 s. Figure 3.4 shows that both mean instantaneous and steady-state (inset above) I_{Cl} were enhanced by 1 mM external Mal. Amplitudes of the instantaneous current increased by 70-75% at voltages negative from -100 mV (from -52 ± 7 to -91 ± 9 $\mu A \cdot cm^{-2}$ at -220 mV) and near the negative maximum at -75 mV the steady-state current increased by approximately 60% from -13 ± 1 to -22 ± 3 $\mu A \cdot cm^{-2}$. However, in 10 mM Mal both instantaneous and steady-state I_{Cl} were reduced close to control values in the absence of Mal. Additionally, a maximum steady-state I_{Cl} were found around -50 mV in 1 mM Mal, and in 10 mM Mal with a great reduced amplitude (inset above).

To further investigate external Mal action on I_{Cl} gating, I_{Cl} relaxations were fitted to derive the halftime, $t_{1/2}$, for current deactivation at voltages more negative than -40 mV for all three sets of data. Figure 3.5 shows the voltage-dependence of $t_{1/2}$ for I_{Cl} and display a biphasic action of external Mal on the current. It clear exhibit that 1 mM Mal resulted in an increase in $t_{1/2}$ (inset), consistent with a slowing of its relaxation, especially at move negative voltages (approximately two times greater halftime compared to the control at -200 mV). However, up to 10 mM Mal yielded $t_{1/2}$ values statistically indistinguishable from the control at all voltages. All these results indicate that I_{Cl} shows a biphasic activation of I_{Cl} by external Mal: at low concentrations Mal results in an increasing I_{Cl}, and at high concentration Mal I_{Cl} is reduced.

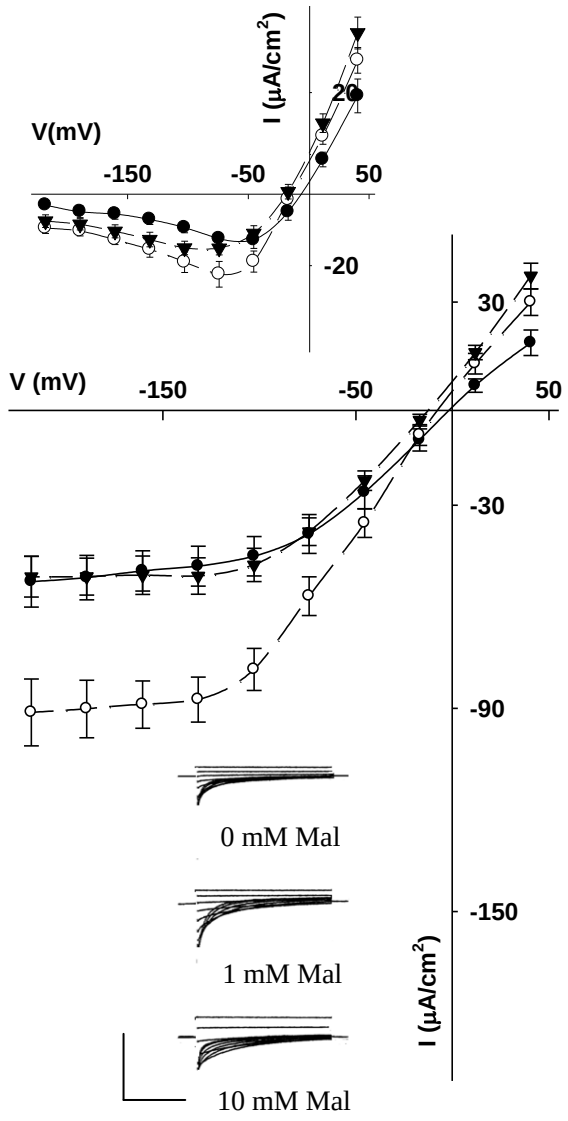

Figure 3. 4 External Mal shows a biphasic modulation of I_{Cl} in *Vicia* guard cells.

Instantaneous anion current as a function of voltage from ten independent experiments as means ± S.E.M. Measurements were carried out in 5 mM Ca^{2+}-Mes buffer (pH 6.1), with 15 mM TEA-Cl and 15 mM CsCl alone and with additions of 1-20 mM Mal. Data for 0 (●), 1 (○) and 10 mM (▼) Mal only are shown for clarity. Voltages were clamped from a conditioning voltage of +40 mV to voltages between +40 and -220 mV in 10s steps. Inset (*above*): steady-state current–voltage curves derived from the same measurements (cross-referenced by symbol). Inset (below): representative current traces. Scale: 100 µA • cm^{-2} (vertical), 5 s (horizontal).

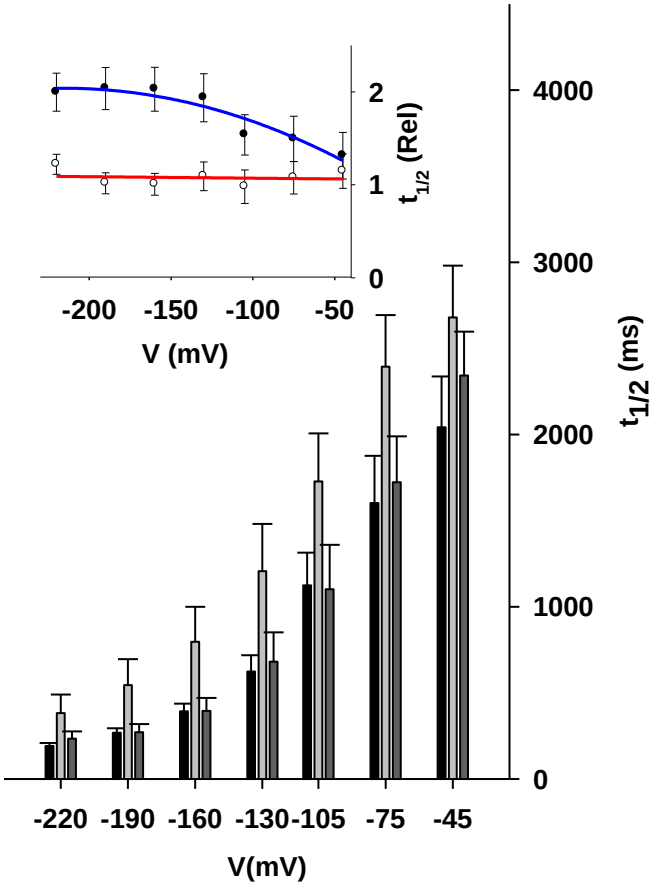

Figure 3. 5 Half time value of external Mal on I_{Cl}.

Current relaxation halftimes ($t_{1/2}$) as a function of voltage. Values are means ± S.E.M. from the same ten independent experiments (as Figure 3.4) for 0 mM (*black bars*), 1 mM (*grey bars*) and 10 mM Mal (*dark grey bars*). Inset: relaxation halftimes plotted relative to the control without Mal for 1 mM (*blue line*) and 10 mM (*red line*) Mal.

3.3.1.2 Cytosolic Mal Suppresses I_{Cl}

Guard cells of many species, including *Vicia*, accumulate high concentrations of Mal to balance K^+ uptake during stomatal opening (Willmer and Fricker, 1996, Raschke and Schnabl, 1978, Vankirk and Raschke, 1978a). Usually, Mal is distributed to the vacuole, but concentrations of 1-8 mM have been estimated in the cytosol (Willmer and Fricker, 1996, Martinoia and Rentsch, 1994). Moreover, Mal as an important metabolite is wildly recognized from biochemical level. Thus Mal has been seen as a common point linking cellular metabolism and stomatal anion channel gating. But to date, little knowledge is available about the influence of Mal on I_{Cl} from the cytosolic side of the membrane.

To explore the effect of Mal on I_{Cl} from the inside, I impaled guard cells with double barrelled microelectrodes as before, but with concentrations between 1 mM and 20 mM Mal in addition to 100 mM CsCl filling the microelectrode barrels to load the cytosol by diffusion from the microelectrode. Figure 3.6 summarizes data from ten or more independent experiments with each loading solution. In each case I allowed at least 10 min following impalements for loading from the microelectrode (see Chapter 2). Results from guard cells impaled with 1 mM Mal in the microelectrodes showed a statistically significant increase around maximum I_{Cl} between -40 mV and -100 mV in the steady-state (Figure 3.6), but the effect on the instantaneous current amplitude was marginal (inset above) and there are no significant changes in mean $t_{1/2}$ values for I_{Cl} deactivation at any voltage (Figure 3.7). By contrast, the instantaneous I_{Cl} from guard cells impaled with 10 mM Mal in the microelectrodes showed a signification reduction and a smaller effect on the steady-state current was obtained (Figure 3.6). In addition, about half reduced of $t_{1/2}$ was recorded (Figure 3.7) independent of membrane voltage.

To further analyze, the results from various concentration of Mal were fitted to a hyperbolic function for the $t_{1/2}$ and amplitude of I_{Cl} (Figure 3.12). The analysis yielded apparent K_i values for Mal of 3 ± 1 mM and 10 ± 3 mM respectively. Thus Mal suppressed I_{Cl} on transition to negative voltages, accelerating deactivation and reducing the magnitude of the current, but the effect on current amplitude was evident primarily at the upper end of the physiological range of Mal concentrations found in the cells.

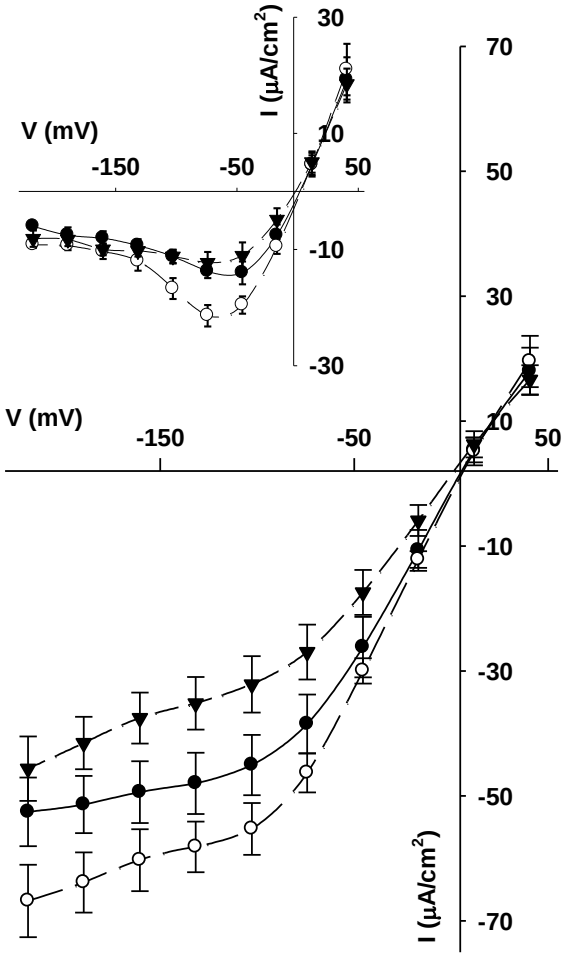

Figure 3. 6 Internal Mal shows a marginal stimulation of I_{Cl} at low millimolar concentrations.

Steady-state anion current as a function of voltage as means ± S.E.M. from ten or more independent experiments at each Mal concentration. Measurements were carried out in 5 mM Ca^{2+}-Mes buffer (pH 6.1), with 15 mM TEA-Cl and 15 mM CsCl. Guard cells were impaled with double-barrelled microelectrodes filled with 100 mM CsCl alone (●) and with additions of 1–20 mM Mal; data for 1 mM (○) and 10 mM (▼) Mal. Voltages were clamped from a conditioning voltage of + 40 mV to voltages between +40 and −220 mV in 10s steps as in Figure 1. Inset (*above*): instantaneous current–voltage curves derived from the same measurements (cross-referenced by symbol).

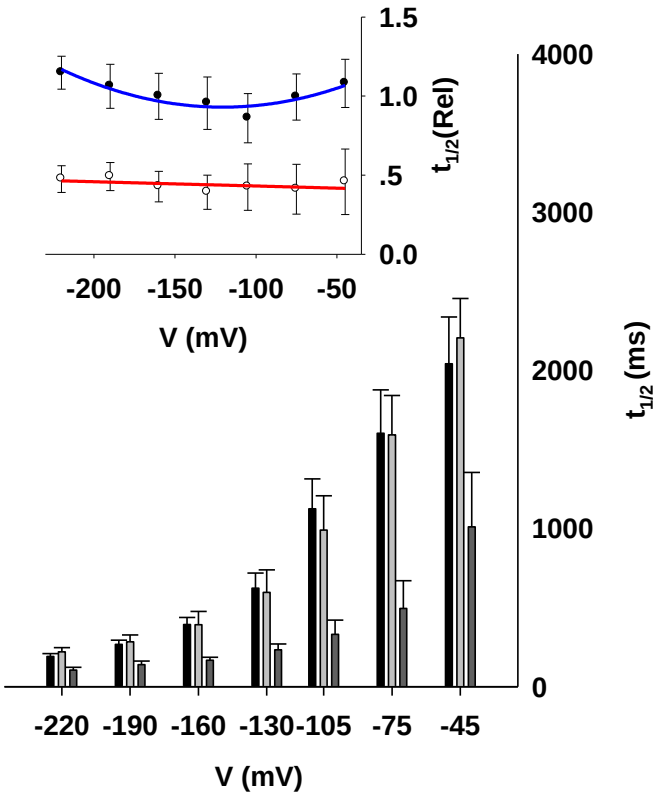

Figure 3. 7 Half time value of internal Mal on I_{Cl}.

Current relaxation halftimes ($t_{1/2}$) as a function of voltage. Values are means ± S.E.M. from the same experiments (as Figure 3.6) for 0 mM (*black bars*), 1 mM (*grey bars*) and 10 mM Mal (*dark grey bars*). Inset: relaxation halftimes plotted relative to the control without Mal for 1 mM (*red line*) and 10 mM (*blue line*) Mal.

3.3.2 The Effect of OAA on I_{Cl}

OAA is the four-carbon precursor in the formation of cytosolic Mal from phosphoenolpyruvate and is the immediate product of Mal oxidation; it is an intermediate in several metabolic pathways, including glycolysis, amino acid synthesis and in the mitochondrial tricarboxylic acid cycle, and it exchanges with Mal across both chloroplast and mitochondrial membranes (Willmer and Fricker, 1996, Martinoia and Rentsch, 1994). As an important intermediate in metabolism in guard cells, it is to be expected that the cytosolic concentration of OAA fluctuates according to changes in metabolic activity. Direct measurements of steady-state OAA concentration in the cytosol are not available, but estimates based on energy charge and Mal/OAA exchange transport equilibrium suggest values of 0.1-0.5 mM and possibly as high as 3 mM in the light (Heineke et al., 1991). Given its central importance to Mal balance, as well as the role of Mal on I_{Cl} regulation, I next examined whether OAA is involved in regulating I_{Cl}.

3.3.2.1 External OAA Does Not Affect I_{Cl}

Firstly, I examined the effects on I_{Cl} of OAA from outside of the guard cells. I found that OAA concentrations as high as 10 mM added outside the cells had no appreciable effect on instantaneous or steady-state I_{Cl} (Figure 3.8). Additionally, there was no change in channel gating, in mean $t_{1/2}$ values for I_{Cl} deactivation at any voltage (Figure 3.9). The relative $t_{1/2}$ showed a difference only in the very negative voltage range (insert) but is not significant ($P>0.05$).

3.3.2.2 Cytosolic OAA Blocks I_{Cl}

By contrast, cytosolic OAA loads introduced from the microelectrodes had a measurable effect on all three parameters. Adding 1 and 10 mM OAA inside greatly suppressed the instantaneous I_{Cl} by approximately 58% and 70% respectively, compared with the control and independent of membrane voltage (Figure 3.10). A similar block of steady-state I_{Cl} was observed in each case, the amplitude was decreased about 23% and 43% at -50 mV respectively (Figure 3.10, inset). Furthermove I_{Cl} kinetics analysis showed a substantial acceleration in current deactivation, even with 1 mM OAA and again largely independent of membrane voltage (Figure 3.11).

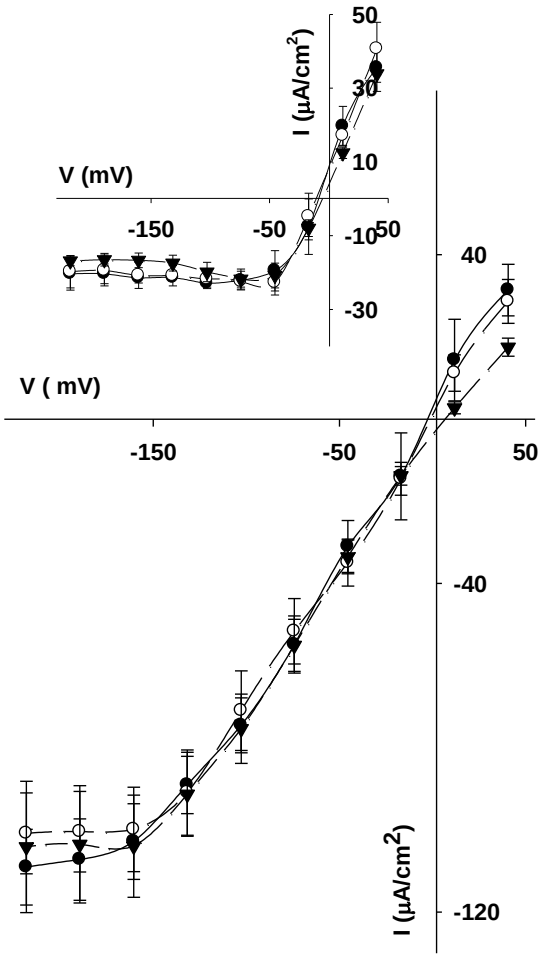

Figure 3. 8 I_{Cl} shows no appreciable sensitivity to external OAA.

Instantaneous anion current as a function of voltage from 15 independent experiments as means ± S.E.M. Measurements were carried out in 5 mM Ca^{2+}-Mes buffer (pH 6.1), with 15 mM TEA-Cl and 15 mM CsCl alone and with additions of 1-10 mM OAA. Data for 0 (●), 1 (○) and 10 (▼) mM OAA only are shown for clarity. Voltages were clamped from a conditioning voltage of +40 mV to voltages between +40 and -220 mV in 10s. Inset (*above*): steady-state current–voltage curves derived from the same measurements (cross-referenced by symbol).

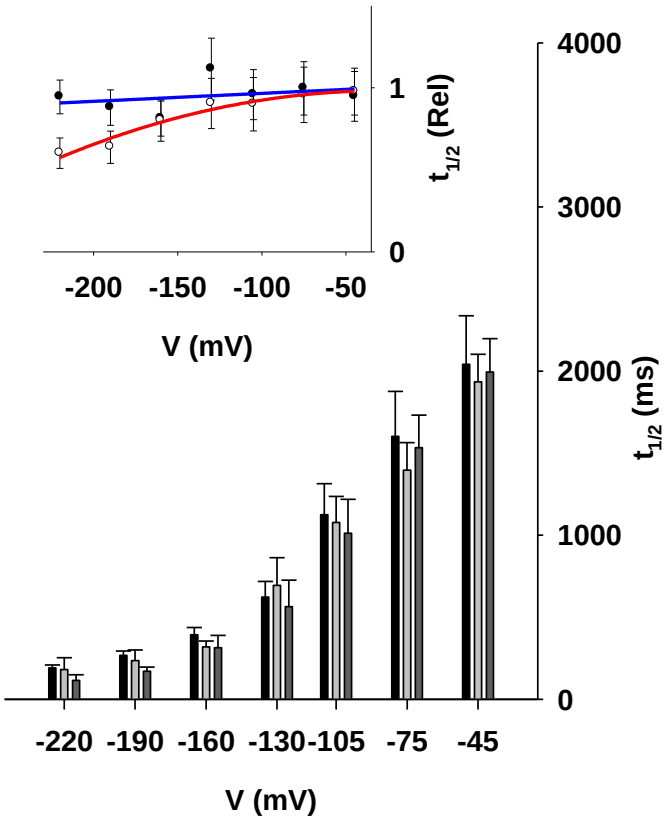

Figure 3. 9 Half time value of external OAA on I_{Cl}.

Current relaxation halftimes ($t_{1/2}$) as a function of voltage. Values are means ± S.E.M. from the same experiments (as Figure 3.8) for 0 mM (*black bars*), 1 mM (*grey bars*) and 10 mM Mal (*dark grey bars*). Inset: relaxation halftimes plotted relative to the control without OAA for 1 mM (*red line*) and 10 mM (*blue line*) OAA.

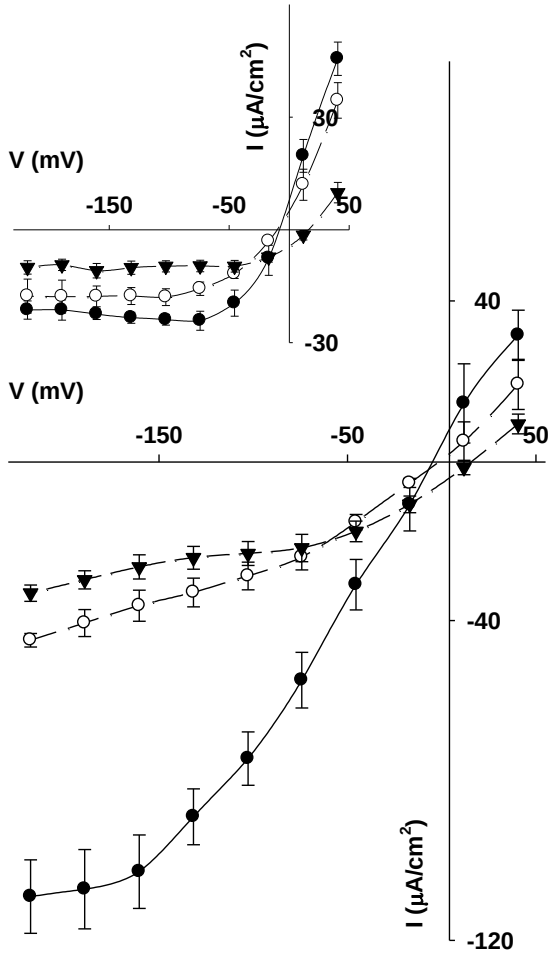

Figure 3. 10 Internal OAA suppresses I_{Cl} at low millimolar concentrations.

Instantaneous anion current as a function of voltage from 13independent experiments as means ± S.E.M. Measurements were carried out in 5 mM Ca^{2+}-Mes buffer (pH 6.1), with 15 mM TEA-Cl and 15 mM CsCl. .Guard cells were impaled with double-barrelled microelectrodes filled with 100 mM CsCl alone (●) and with additions of 1–10 mM OAA; data for 1 (○) and 10 (▼) mM OAA only are shown for clarity. Voltages were clamped from a conditioning voltage of +40 mV to voltages between +40 and -220 mV in 10s. Inset (*above*): steady-state current–voltage curves derived from the same measurements (cross-referenced by symbol)

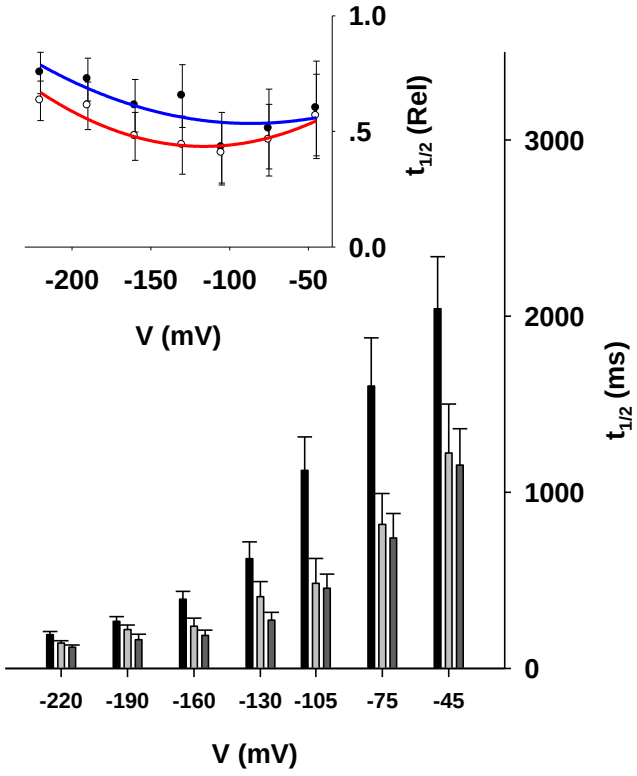

Figure 3. 11 Half time value of internal OAA on I_{Cl}.

Current relaxation halftimes ($t_{1/2}$) as a function of voltage. Values are means ± S.E.M. from the same experiments (as Figure 3.10) for 0 mM (*black bars*), 1 mM (*grey bars*) and 10 mM Mal (*dark grey bars*). Inset: relaxation halftimes plotted relative to the control without OAA for 1 mM (*red line*) and 10 mM (*blue line*) OAA.

To further analyze, the results from various concentration of OAA were fitted to a hyperbolic function for the $t_{1/2}$ and amplitude of I_{Cl} (Figure 3.12). The analysis yielded apparent K_i values for OAA in accelerating I_{Cl} deactivation and reducing the current amplitude of 0.17 ± 0.08 mM and 0.21 ± 0.05 mM respectively, which is well within the physiological range of OAA concentrations I noted before. Additions of OAA, both inside and outside the guard cells, had no effect on the reversal voltage for I_{Cl}, as was evident from lack of significant difference in currents recorded either side of the apparent reversal voltage, indicating that the relative permeability of the channels for OAA is very low compared with that for Cl^- and Mal.

3.3.3 The Effect of Present Both of OAA and Mal on I_{Cl}

Given the potentially counteractive effects of the organic acids in the cytosol, I also examined whether OAA suppression of I_{Cl} was rescued in the presence of low concentration of Mal which enhance I_{Cl}. In this case, epidermal strips were bathed in standard buffer of 5 mM Ca^{2+} -Mes buffer (pH 6.1), with 15 mM TEA-Cl and 15 mM CsCl. Guard cells were impaled with microelectrodes containing 1 mM OAA and 1 mM Mal, and I_{Cl} was recorded as described above. As mentioned above, 1 mM OAA strongly suppressed I_{Cl}, but with 1mM Mal I_{Cl} showed a largely increased. Thus I was interested to see if the suppression of 1mM OAA on I_{Cl} was also seen when 1 mM Mal was present.

Figure 3.13 summarizes results from 11 independent experiments with both organic acids. Results from guard cells impaled with 1 mM Mal in the microelectrodes showed a statistically significant increase in both instantaneous and steady-state I_{Cl} (Figure 3.13). But this effect was partially reduced by the presence of low OAA concentrations which supressed I_{Cl} (Figure 3.13)

Kinetic analysis shows an accelerated current deactivation with additional 1 mM OAA (Figure 3.14) and the influence of both organic acids was voltage-independent (Figure 3.14, inset). These results suggest that the immediate metabolic partner of Mal may have an important role in control of I_{Cl} under normal physiological conditions.

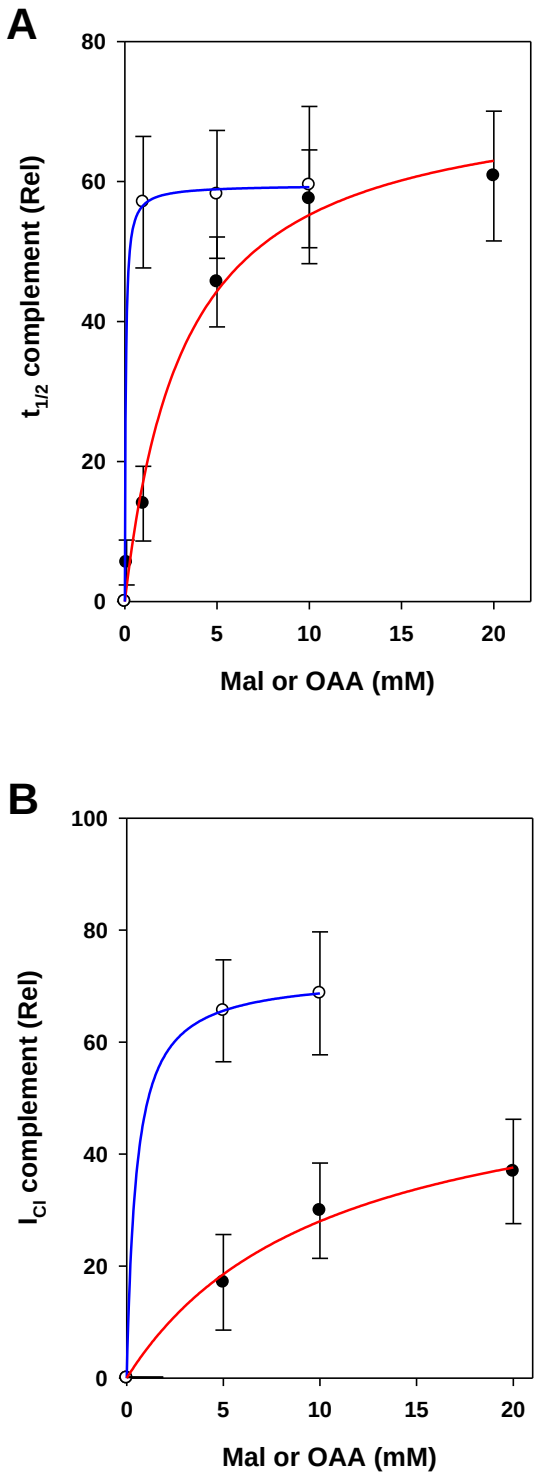

Figure 3. 12 I_{Cl} shows a high relative sensitivity to OAA (*blue line*) within the physiological concentration range compared with that for Mal (*red line*).

Means±S.E.M. for I_{Cl} inactivation halftimes (A) and current amplitudes (B) determined as the complement values relative to the controls (=1-X/X_0) at -75 mV, where X_0 is control and X is the acid concentration added in control solution. Data were fitted independently by non-linear least-squares to a hyperbolic function to derive apparent K_i values.

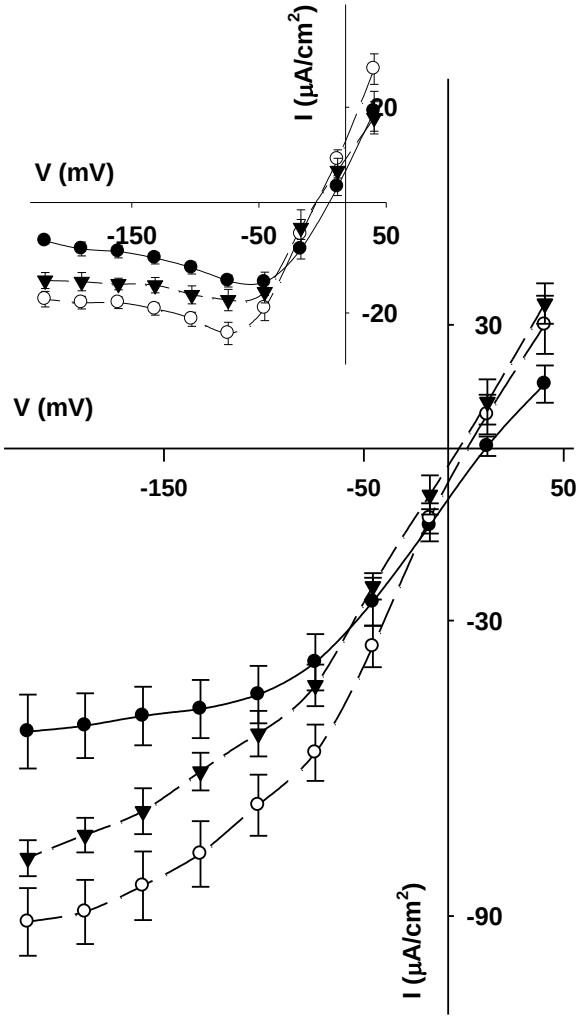

Figure 3. 13 Internal OAA suppresses I_{Cl} in the presence of Mal.

Instantaneous anion current as a function of voltage as means ± S.E.M. from 11 or more independent experiments for each combination of treatments. Measurements were carried out in 5 mM Ca^{2+}-Mes buffer (pH 6.1) with 15 mM TEA-Cl and 15 mM CsCl. Guard cells were impaled with double-barrelled microelectrodes filled with 100 mM CsCl alone (●) and with additions of 1 mM Mal without (○) and with (▼) 1 mM OAA . Inset (*above*): steady-state current–voltage curves derived from the same measurements (cross-referenced by symbol).

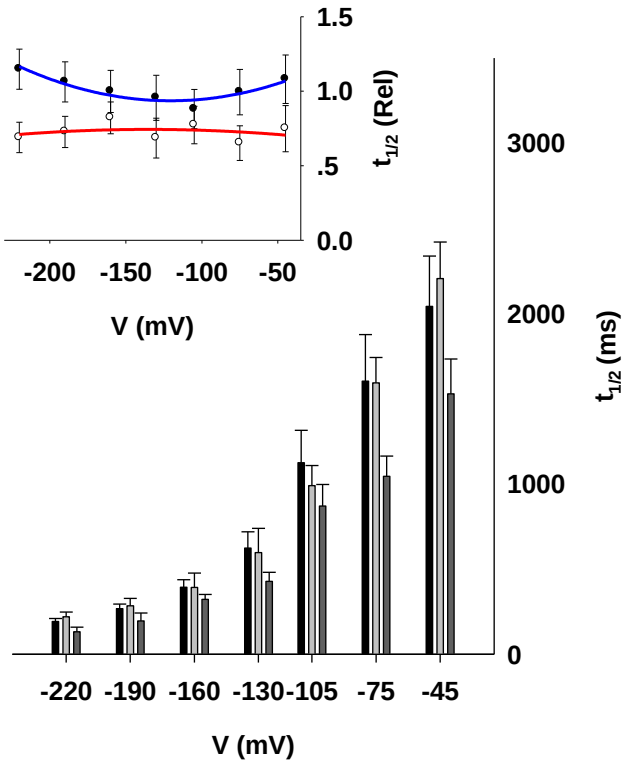

Figure 3. 14 Half time value of internal OAA on I_{Cl} in the presence of Mal.

Current relaxation halftimes ($t_{1/2}$) as a function of voltage. Values are means ± S.E.M. from the same experiments (as Figure 3.13) for 0 mM Mal and OAA (*black bars*), 1 mM Mal without (*grey bars*) and with 1 mM Mal (*dark grey bars*). Inset: relaxation halftimes plotted relative to the control without additions for 1 mM Mal alone (*red line*) and with 1 mM OAA (*blue line*).

3.3.4 The Effect of Acetate (Ac) on I_{Cl}

Ac is a common anion in biology. This two-carbon acid anion is a substrate for the tricarboxylic acid cycle and fatty acid synthesis, but in a thioester complex with co-enzyme A, and it normally occurs as the free acid at concentrations of 0.5-1.5 mM (Roughan, 1995). Like OAA, its influence on I_{Cl} is largely unknown. Nonetheless, previous electrophysiological studies have used the free acid anion in microelectrode filling solutions to avoid cytosolic Cl^- loading and its consequences for solute balance and background Cl^- leakage across the membrane (Blatt, 1987). Therefore, the influence of Ac on I_{Cl} was explored.

3.3.4.1 External Ac Suppressed I_{Cl}

In the absence of information on the Ac-sensitivity of I_{Cl}, I challenged guard cells with 1 and 10 mM Ac by additions outside. Figure 3.15 summarize results of 13 or more independent experiments for each treatment. The results showed that increasing Ac concentrations suppressed the instantaneous and steady-state I_{Cl} at voltages between -40 and -100 mV. Kinetic analyses indicate that external Ac accelerated current deactivation (Figure 3.16). Unlike the effects of Mal and OAA, however, Ac showed a pronounced voltage-dependence in its effect on I_{Cl} kinetics: a reduction in $t_{1/2}$ was clearly seen at voltages near and more positive than -100 mV and when Ac was added to cytosol, and it led to a shift in the apparent reversal potential for I_{Cl} (Figures 3.15).

3.3.4.2 Cytosolic Ac Blocks I_{Cl}

Cytosolic Ac loads were introduced from the microelectrodes as before, and showed that Ac had a substantial effect on the current. Adding 1 and 10 mM Ac inside greatly suppressed the instantaneous I_{Cl} by approximately 24% and 48% respectively, compared with the control and the effect was independent of membrane voltage (Figure 3.17). A similar block of steady-state I_{Cl} was observed in each case: the current amplitude was decreased about 44% and 47% at -50 mV, respectively (Figure 3.17, inset). Furthermore, kinetic analysis of I_{Cl} showed a substantial acceleration in current deactivation. Like external Ac, the effect of internal Ac on I_{Cl} was largely dependent of membrane voltage (Figure 3.18).

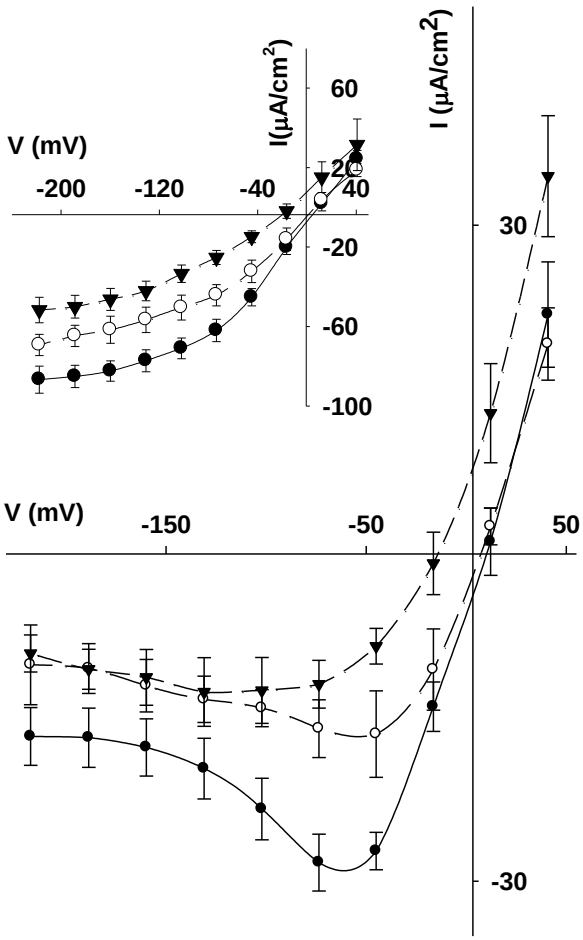

Figure 3. 15 I_{Cl} shows sensitivity to external Ac.

Steady-state anion current as a function of voltage from 13 independent experiments as means ± S.E.M. Measurements were carried out in 5 mM Ca^{2+}-Mes buffer (pH 6.1) with 15 mM TEA-Cl and 15 mM CsCl alone (●) and with additions of 1 mM (○) and 10 mM (▼) Ac. Voltages were clamped from a conditioning voltage of +40 mV to voltages between +40 and -220 mV in 10s steps. Inset (*above*): instantaneous current–voltage curves derived from the same measurements (cross-referenced by symbol).

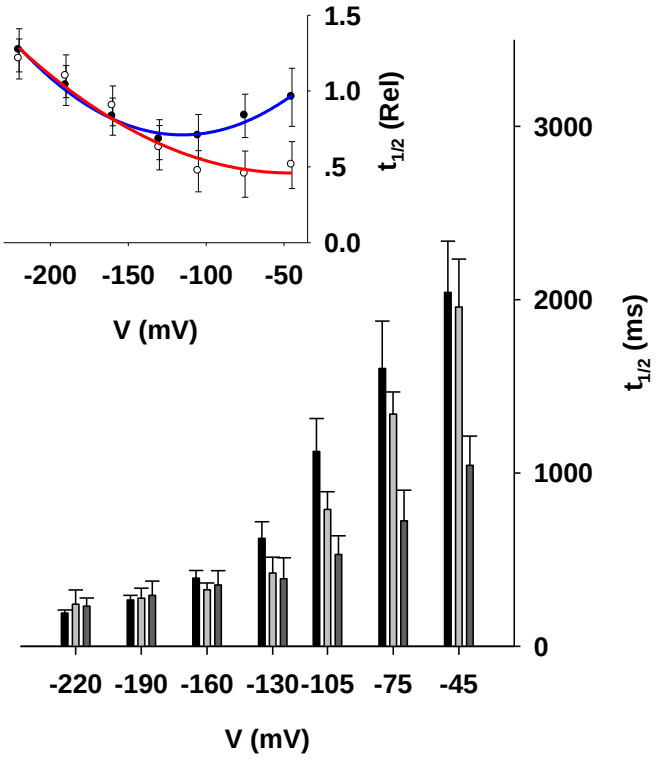

Figure 3. 16 Half time value of external Ac on I_{Cl}.

Current relaxation halftimes ($t_{1/2}$) as a function of voltage. Values are means ± S.E.M. from the same experiments (as Figure 3.15) for 0 mM Mal and Ac (*black bars*), 1 mM Ac (*grey bars*) and 10 mM Ac (*dark grey bars*). Inset: relaxation halftimes plotted relative to the control without additions for 1 mM Ac (*red line*) and 10 mM Ac (*blue line*).

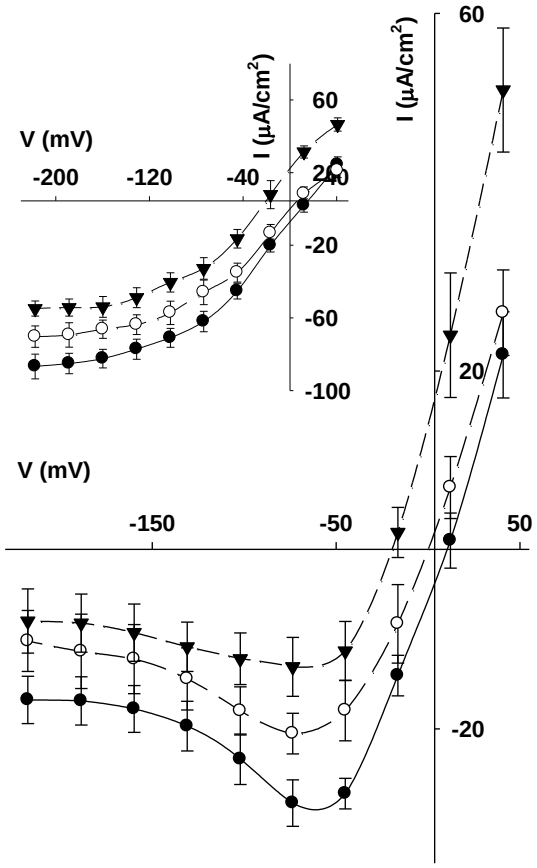

Figure 3. 17 I_{Cl} suppressed by internal Ac.

Steady-state anion current as a function of voltage from 13 independent experiments as means ± S.E.M. Measurements were carried out in 5 mM Ca^{2+}-Mes buffer (pH 6.1) with 15 mM TEA-Cl and 15 mM CsCl alone (●) and with additions of 1 mM (○) and 10 mM (▼) Ac. Voltages were clamped from a conditioning voltage of +40 mV to voltages between +40 and -220 mV in 10s steps. Inset (*above*): instantaneous current–voltage curves derived from the same measurements (cross-referenced by symbol).

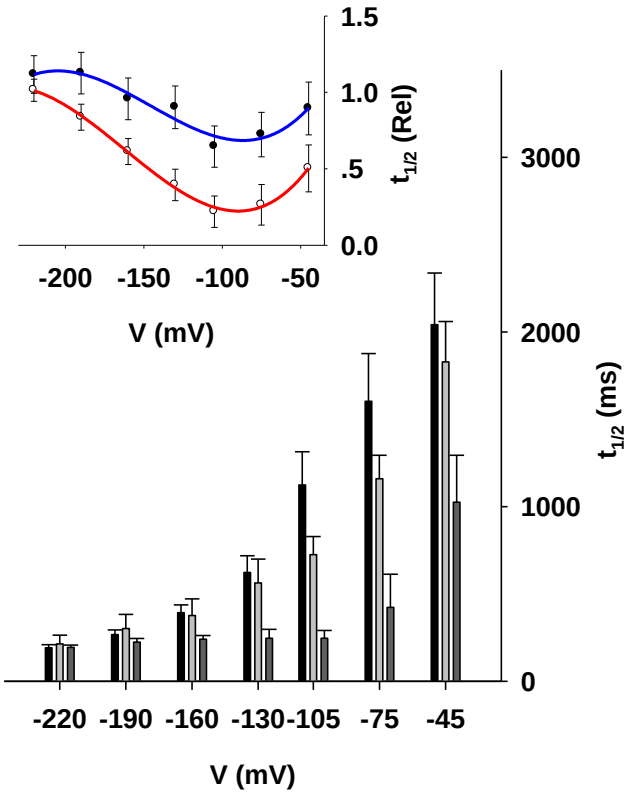

Figure 3. 18 Half time value of internal Ac on I_{Cl}.

Current relaxation halftimes ($t_{1/2}$) as a function of voltage. Values are means ± S.E.M. from the same experiments (as Figure 3.16) for 0 mM Mal and Ac (*black bars*), 1 mM Ac (*grey bars*) and 10 mM Ac (*dark grey bars*). Inset: relaxation halftimes plotted relative to the control without additions for 1 mM Ac (*red line*) and 10 mM Ac (*blue line*).

3.4 Discussion

It is well known that both inorganic ion transport and organic acid metabolism make major contributions to the changes in osmotic content of the guard cells that drives stomatal movements (Blatt, 2000, Schroeder et al., 2001, Roelfsema and Hedrich, 2005, Shimazaki et al., 2007). Stomata open and close by accumulating and losing K^+, and Cl^- and Mal accompany these fluxes over the diurnal cycle (Talbott and Zeiger, 1993, Talbott and Zeiger, 1996, Asai et al., 1999). Up to date, the understanding of transport of inorganic ions, mainly of K^+ and Cl^-, in guard cells is much better known than of organic metabolites such as Mal. Yet these organic compounds are not only important as metabolic intermediates, but are also essential as osmotica. Among these organic acids, Mal is a key contributor in guard cells movements and, from its position at the junction of cellular metabolism, environmental CO_2 responses and ion transport, it is an obvious link between all three processes. Much of the Mal synthesized in the light or in response to high concentration of CO_2, is transported and accumulated in vacuole (Martinoia and Rentsch, 1994). However, much of the Mal transported out of vacuole is released across the plasma membrane when the stomata close (Vankirk and Raschke, 1978a, Dittrich and Raschke, 1977). Thus these processes must be regulated in concert with metabolism, both as Mal is synthesized for transport to the vacuole and again as it reenters the cytosol for export and to feed into the metabolic pools of other organic acids. Very little is known of the mechanisms behind this regulation, although it is clearly central to the osmotic homoeostasis of guard cells.

In this study, I examined the impact of cytosolic Mal, its immediate metabolite OAA, and of Ac on I_{Cl} of *Vicia* guard cells. Although it cannot be ruled out that some degree of metabolic conversion of the acid anions took place during these experiments, both the extracellular medium and the microelectrode represent virtually infinite volumes, the latter exchanging with the cytosol directly. Thus at steady-state the membrane surface will have been exposed to organic acid concentrations effectively ‘clamped’ close to that of the corresponding solutions (Blatt and Slayman, 1983, Blatt et al., 1987). Results showed all three organic acids affected I_{Cl}, but with markedly different characteristics and sidedness to

their activities. Most prominent was the suppression of I_{Cl} with OAA evident even at low millimolar concentrations. These findings indicate a capacity for coordinating organic acid metabolism with I_{Cl} through the direct effect of organic acid pool size and they suggest that the effects may be exerted as much by Mal metabolites as by Mal itself.

3.4.1 Mal and OAA in I_{Cl} Regulation

As previously reported (Hedrich and Marten, 1993, Schmidt and Schroeder, 1994), low concentrations of Mal outside the cells affected the voltage dependence of I_{Cl}. To further investigate, I examined the effects of cytosolic Mal. These studies showed an enhancement of I_{Cl}, although elevation of cytosolic Mal to higher concentrations led to measurable declines in I_{Cl} relative to the control (Figure 3.13). Subsequent findings uncovered that I_{Cl} is more sensitive to OAA in the cytosol than it is to Mal (Figure 3.12). Additions even of 1 mM OAA resulted in a significant block of I_{Cl}, consistent with an apparent K_i near 0.1 mM and well within the dynamic concentration range for OAA *in vivo* (Heineke et al., 1991).

In guard cells, Mal synthesis in the cytosol is driven largely from metabolism cycles of phosphoenolpyruvate and OAA (Willmer and Fricker, 1996). Part of Mal from these metabolites will be transported across through tonoplast and accumulated in the vacuolar to open stoma, especially in the second half of the diurnal cycle (Willmer and Fricker, 1996, Talbott and Zeiger, 1993). By contrast, during stomatal closing at the end of the day or following stimulation with abscisic acid, guard cells export of much of the Mal in the vacuole and release it across the plasma membrane (Willmer and Fricker, 1996, Roelfsema and Hedrich, 2005). These observations are generally consistent with previously reports of variations in the low millimolar range of the pool of cytosolic Mal in leaves (Martinoia and Rentsch, 1994). However, this cycling of Mal between vacuole and apoplast implies a substantial hysteresis in Mal flux control overall, and requires a fine control over Mal export both at the tonoplast and at the plasma membrane during the course of the day.

If the cytosolic Mal pool remains within the bounds of 0.5-10 mM, how might I_{Cl} be regulated to prevent undue Mal efflux during stomatal opening, yet provide a major

pathway for its loss during stomatal closure? One potential mechanism is through regulating cytosolic free Ca^{2+} which enhances both R- and S-type anion channels to activated of I_{Cl} (Schroeder and Keller, 1992, Hedrich and Marten, 1993, Chen et al., 2010, Grabov and Blatt, 1997, Geiger et al., 2009), in effect promoting Mal (and Cl^-) efflux across the plasma membrane. This mechanism is certainly important for guard cells in the response to abscisic acid and drought stress (Blatt, 2000, Schroeder et al., 2001), but it is more difficult to reconcile the diurnal cycle of $[Ca^{2+}]_i$ with that of Mal synthesis and accumulation in the day and release at night. Usually, the diurnal changes in $[Ca^{2+}]_i$ in guard cells are in the range of free concentrations in the steady-state (Dodd et al., 2007, Dodd et al., 2005) which is substantially below the $K_{1/2}$ of 600–700 nM for I_{Cl} activation by $[Ca^{2+}]_i$ (Chen et al., 2010). Furthermore, the diurnal oscillation in $[Ca^{2+}]_i$ is in opposite with the changes that might be expected to regulate Mal in guard cells (Dodd et al., 2005): $[Ca^{2+}]_i$ increases in the day and declines at night, whereas the opposite would be required to facilitate Mal accumulation in the day and its efflux through the anion channels at night. In short, the diurnal changes in Mal do not sit well with the characteristics of I_{Cl} modulation by $[Ca^{2+}]_i$ in guard cells.

However, the sensitivity of I_{Cl} to OAA does provide another mechanism to explain how Mal flux is regulated over the diurnal cycle. It is generally thought that much of the fixed carbon in guard cells is imported and passes through glycolysis before condensation with bicarbonate to form OAA and Mal (Willmer and Fricker, 1996, Asai et al., 2000, Outlaw, 2003). OAA is formed through the action of phosphoenolpyruvate carboxylase, which is activated by its phosphorylation in the light thus suppressing its sensitivity to inhibition by Mal (Outlaw et al., 2002, Cotelle et al., 1999). Thus I might anticipate that sucrose uptake and metabolism to form Mal in the light will be accompanied by an elevation in the cytosolic OAA pool, even if NAD-Mal dehydrogenase is activated by light (Gotow et al., 1985); conversely, carbon passage through Mal and OAA to phosphoenolpyruvate and pyruvate, and transfer of both Mal and pyruvate to the mitochondria at the end of the day (Willmer and Fricker, 1996) is likely to be accompanied by a relative depletion of this same OAA pool. In other words, diurnal variations in cytosolic OAA are potentially in phase with the expected oscillation between Mal retention

and stomatal opening during the day and I_{Cl} -mediated Mal release and stomatal closure at night. The K_m for OAA of cytosolic NAD-Mal dehydrogenase (Gotow et al., 1985) is very close to the apparent K_i for OAA of I_{Cl} in *Vicia* guard cells (Figures 3.10- 3.12), thereby ensuring a close coordination between the two kinetic processes. I note, too, that low millimolar OAA inside suppresses I_{Cl} even in the presence of Mal (Figures 3.10-3.11 and 3.13-3.14). So it is conceivable that diurnal variations in the cytosolic OAA could play an important role in regulating I_{Cl} and Mal efflux across the plasma membrane. Indeed, in this context it is of interest to note that the diurnal oscillation of the OAA pool in various CAM (crassulacean acid metabolism) species is also in phase with stomatal movements (Chen et al., 2002), albeit with the higher OAA concentration and stomatal opening at night.

3.4.2 Electrophysiological Studies with Ac Electrolytes

Finally it is of interest that I_{Cl} showed sensitivity to Ac. The monocarboxylic acid is normally present at low concentrations (Roughan, 1995) relative to its action on the current (Figures 3.15-3.18), and is therefore unlikely to have an impact on I_{Cl} activity in vivo. Effects of weak-acid loading with Ac can also be ruled out because, in contrast with the evidence shown in Figures 3.15-3.18, cytosolic acidification enhances anion channel activity (Schulz-Lessdorf et al., 1996). The action of higher Ac concentrations is relevant, however, because the caboxylic acid anion is commonly used as an electrolyte substitute to avoid the consequences of Cl^- loading via the microelectrode (Blatt et al., 1987, Blatt and Slayman, 1983, Schulz-Lessdorf et al., 1996, Blatt et al., 1990, Garcia-Mata et al., 2003, Roelfsema and Prins, 1997). It is clear that this practice does more than simply avoiding the effects of elevating Cl^- in the cytosol: Ac loading leads to a block of I_{Cl}. The results of the present study, including parallel effects for Ac added outside and inside, the apparent shift in instantaneous current and current reversal voltage, and the strong voltage-dependence to its action on $t_{1/2}$ (Figures 3.16 and 3.18), implies a complex dependence on Ac residence within the channel pore itself; furthermore, the voltage-dependence to Ac action (Figures 3.16 and 3.18) and the more pronounced effect on instantaneous I_{Cl} when added outside (Figure 3.15) may indicate a greater sensitivity of the R-type anion channels to Ac. Regardless, however, the block of I_{Cl} has had the serendipitous advantage of simplifying the kinetic analysis of the guard cell K^+ channels

and other currents through their isolation from anion flux through I_{Cl}

From a physiological standpoint, the block of I_{Cl} by Ac will not influence other membrane currents under voltage clamp. However, it may well affect the balance of ionic currents under free-running (non-clamped) conditions. For example, suppressing I_{Cl} might be expected to promote Ca^{2+} entry and $[Ca^{2+}]_i$ elevation initially by favouring membrane hyperpolarization, even with low millimolar concentrations of K^+ outside (Asai et al., 2000, Pandey et al., 2007, Blatt and Thiel, 1993). Raising $[Ca^{2+}]_i$ above 500–600 nM normally promotes a burst in I_{Cl} activity (Chen et al., 2010), but this activity is likely to be much suppressed by an Ac load with a consequent loss of the 'damping' effect of I_{Cl} in promoting membrane depolarization. In short, Ac loading may have led to an overestimate of the normal dynamic range for $[Ca^{2+}]_i$ in its coupling with oscillations with membrane voltage (Sokolovski et al., 2005, Grabov and Blatt, 1998). Indeed, preliminary analysis using quantitative kinetic modeling of guard cell ion transport and homoeostasis has suggested that $[Ca^{2+}]_i$ oscillations are likely to be constrained with an upper limit near 600 nM largely as a result of I_{Cl} activation (Hills et al., 2012).

3.4.3 Summary

In conclusion, I find that the anion channel current of *Vicia* guard cells shows a compound dependence, from the cytosolic side of the membrane, on several organic acids. Most notably, suppression of I_{Cl} by OAA is consistent with a role for this dicarboxylic acid in modulating channel activity for a diurnal cycle of Mal accumulation and release that parallels the cycle of stomatal opening and closing. Additionally, block of I_{Cl} by the monocarboxylic acid Ac demonstrates that its use in electrophysiological studies has serendipitous consequences for the study of other ion channels at the guard cell plasma membrane.

CHAPTER 4:

ABA REGULATES ANION CHANNELS THROUGH REACTIVE OXYGEN SPECIES-MEDIATED PLASMA MEMBRANE Ca^{2+} CHANNELS

4.1 Introduction

The stoma is a small pore surrounded by a pair of guard cells in the epidermis of plant leaves. It is the primary route for gas exchange, enabling CO_2 entry for photosynthesis, at the same time presenting a major pathway for water loss by transpiration. The guard cells regulate the aperture of the stomatal pore to balance the often conflicting demands for CO_2 and for water conservation. Stomatal opening and closing are driven by the uptake and loss, respectively, of osmotic solutes, principally K^+, Cl^- and malate (Mal) (Blatt, 2000, Kim et al., 2010) through a complex network of interacting transporters at the plasma membrane and tonoplast (Hills et al., 2012, Chen et al., 2012). These transporters are regulated by a number of well-defined signals, including light, CO_2, drought and the water stress hormone abscisic acid (ABA). Much research has focused on ABA-mediated stomatal closure, demonstrating that the process incorporates both Ca^{2+}-independent and Ca^{2+}-dependent signalling elements. Of the latter, elevated free cytosolic Ca^{2+} concentration ($[Ca^{2+}]_i$) plays a critical and early role by inactivating inward-rectifying K^+ channels ($I_{K,in}$), preventing K^+ uptake, and by activating Cl^- (anion) channels (I_{Cl}) at the plasma membrane, thereby driving membrane depolarization and engaging K^+ efflux through outward-rectifying K^+ channels ($I_{K,out}$) (Blatt et al., 1990, McAinsh et al., 1990, Thiel et al., 1992, Lemtiri-Chlieh and Macrobbie, 1994, Schmidt et al., 1995). The complementary efflux of K^+ and anions results in a net loss of osmotic content, reducing the turgor and the volume of guard cells and leading the stomata to close.

Abscisic acid elevates $[Ca^{2+}]_i$ through the combined effects of Ca^{2+} entry at the plasma membrane and Ca^{2+} release from endomembrane stores, what has often been coined as Ca^{2+}-induced Ca^{2+} release (Blatt, 2000, MacRobbie, 2000). ABA activates Ca^{2+} channels (I_{Ca}) at the plasma membrane, even in isolated membrane patches, facilitating Ca^{2+} influx (Grabov and Blatt, 1998, Grabov and Blatt, 1999, Hamilton et al., 2000, Hamilton et al., 2001). The rise in $[Ca^{2+}]_i$ is linked in part to reactive oxygen species (ROS) (Pei et al., 2000, Kwak et al., 2003), as the NADPH oxidase mutant, *atrbohD/atrbohF*, impairs ROS production and I_{Ca} activation in ABA (Kwak et al., 2003). In parallel, the rise in $[Ca^{2+}]_i$ depends on a second pathway leading through cyclic ADP-ribose to a rise in nitric oxide (Leckie et al., 1998, Neill et al., 2002, Garcia-Mata et al., 2003).

A large body of evidence also supports protein (de-)phosphorylation in ABA signalling (Armstrong et al., 1995, Li and Assmann, 1996, Grabov et al., 1997, Allen et al., 1999). Abscisic acid activates members of the SNF1-related 2 protein kinase family (SnRK2s), notably SnRK2.6/OST1 which promotes ABA regulation of guard cell transport and is able to phosphorylate both anion and K^+ channels directly (Mustilli et al., 2002, Geiger et al., 2009, Sato et al., 2009). The 2C protein phosphatases (PP2Cs) ABI1 and ABI2 were identified initially to function upstream of SnRK2s, their activity suppressing ABA action, subsequent evidence showed that they inactivate SnRK2 kinases by direct dephosphorylation (Umezawa et al., 2009, Geiger et al., 2009). The discovery of the START PYR/PYL/RCAR protein family of ABA receptors, which interact directly with PP2C-type protein phosphatases, places these receptor proteins squarely at the front of a protein kinase/phosphatase signal cascade initiated by ABA (Park et al., 2009). Significantly, the quadruple *pyr1/pyl1/pyl2/pyl4* mutant shows a strong insensitivity to ABA in stomatal closing and ABA inhibited stomatal opening, although the mutant stomata close if selected signalling elements are engaged, for example by driving $[Ca^{2+}]_i$ oscillations with changes in extracellular K^+ and Ca^{2+} concentrations (Nishimura et al., 2010). These observations imply that the $[Ca^{2+}]_i$ intermediate is subject to ABA binding with the PYR/PYL/RCAR receptors. They are consistent, too, with evidence that protein phosphorylation is a prerequisite for Ca^{2+} channel activation (Kohler and Blatt, 2002) or Ca^{2+} release (Sokolovski et al., 2005) in ABA. Lacking nonetheless is direct evidence connecting the PYR/PYL/RCAR receptors with $[Ca^{2+}]_i$ elevation *in vivo,* and whether their action is necessarily associated with Ca^{2+} channels at the plasma membrane or with another pathway to raise $[Ca^{2+}]_i$ remains an open question.

Here I describe a novel strategy for recording I_{Ca} at the plasma membrane of intact guard cells, and have used it along with voltage-clamp measurements of $I_{K,in}$ and I_{Cl}, and with Fura2 fluorescence imaging of $[Ca^{2+}]_i$, to explore the response to ABA in wild-type and *pyr1/pyl1/pyl2/pyl4* mutant *Arabidopsis*. I report that ABA-induced I_{Ca} and $[Ca^{2+}]_i$ increases – and the consequent changes in gating of $I_{K,in}$ and I_{Cl} – were reduced in *pyr1/pyl1/pyl2/pyl4* mutant and that the effect could be ascribed to a loss in activation of the dominant Ca^{2+} channels at the plasma membrane in ABA. Additional studies showed

that *pyr1/pyl1/pyl2/pyl4* mutant is impaired in ROS production, although adding H_2O_2 rescued both Ca^{2+} channel activation and stomatal closing in the mutant. These results demonstrate that the PYR/PYL/RCAR receptors contribute to ROS-mediated activation by ABA of I_{Ca}, thus affecting $[Ca^{2+}]_i$ and its regulation of osmotic solute flux for stomatal closure.

4.2 Materials and Methods (see Chapter 2)

4.3 Results

4.3.1 The *pyr1/pyl1/pyl2/pyl4* Quadruple Mutant Exhibit a Strong ABA Insensitivity

The *pyr1/pyl1/pyl2/pyl4* quadruple mutant was recently shown to cause strong ABA insensitivities in seed germination, root growth and ABA-induced gene expression (Park et al., 2009). In guard cells, the *pyr1/pyl1/pyl2/pyl4* mutant shows a strong ABA insensitive phenotype, preventing stomatal closing (Figure 4.1) and ABA inhibition of stomatal opening (Nishimura et al., 2010). Thus the *pyr1/pyl1/pyl2/pyl4* mutant shows an ABA hyposensitive phenotype in response to drought stress. The lower water content and faster water loss in *pyr1/pyl1/pyl2/pyl4* quadruple mutant leaf compared to wild-type implicate there is higher leaf transpiration in this mutant during drought stress (Figure 4.2). In other words, the drought stress induced stomatal closure is largely impaired in *pyr1/pyl1/pyl2/pyl4* mutant. These phenomena led me to investigate further properties of the PYR/PYL receptors in stomatal regulation.

4.3.2 The Deactivation of I_{Kin} by ABA Is Largely Impaired in *pyr1/pyl1/pyl2/pyl4* Mutant.

Guard cells close the stoma by regulating plasma membrane K^+ and anion channels. Indeed, ABA results in a fast activation of I_{Cl} and inactivation of $I_{K,in}$ (Blatt, 1990). To explore the activity of $I_{K,in}$ and I_{Cl}, I used the two-electrode voltage clamp to record these ion currents during ABA treatments. Figure 4.3 shows current traces and means steady-state current–voltage (I-V) curves of $I_{K,in}$ from wild-type and *pyr1/pyl1/pyl2/pyl4* mutant guard cells recorded before and after 3 min treatment with 20 μM ABA. In wild-type guard cells, ABA dramatically reduced the amplitude of $I_{K,in}$. Similar results were obtained in each of 12 independent experiments. However, in *pyr1/pyl1/pyl2/pyl4* mutant, I did not observe a significant change in $I_{K,in}$ in the presence of ABA. The average reduction of steady-state $I_{K,in}$ in the wild-type was around 90-95% at voltages negative from -165 mV (from -355 ± 55 to -15 ± 4 μA cm^{-2} at 210 mV), whereas in *pyr1/pyl1/pyl2/pyl4* mutant this reduction was marginal (from -290 ± 22 to -245 ± 19 μA cm^{-2}) at the same voltage (Figure 4.3).

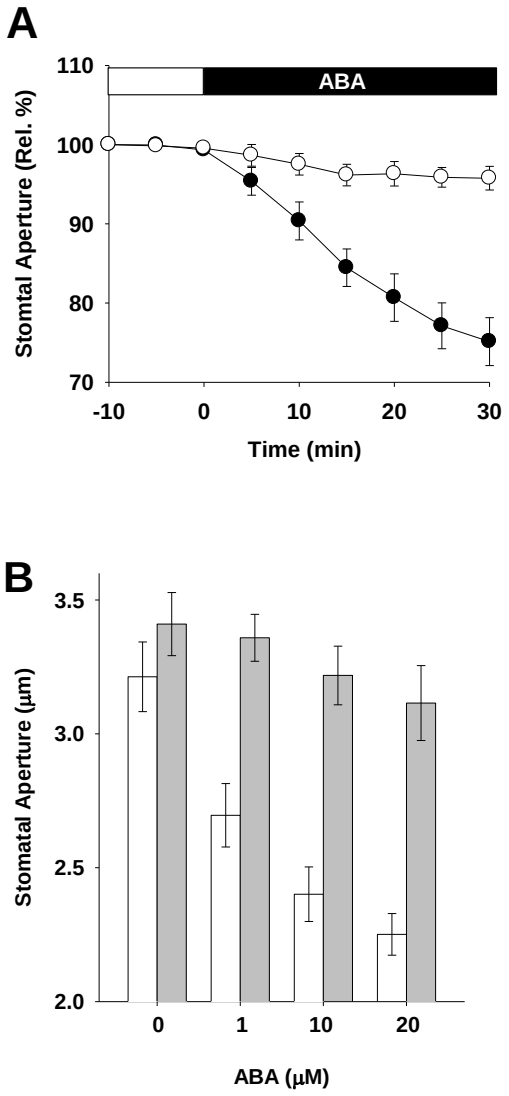

Figure 4. 1 The *pyr1/pyl1/pyl2/pyl4* mutant exhibits a drought insensitive phenotype.

(A) 20 µM ABA-induced stomatal closure in wild-type (*black circles*) and *pyr1/pyl1/pyl2/pyl4* (*open circles*) mutant guard cells. Apertures normalised on a cell-by-cell basis to values at time -10 min for each cell. Data are means ± SE of n = 34 stomata pooled from at least four independent experiments for each line.

(B) ABA-induced stomatal closure in *pyr1/pyl1/pyl2/pyl4* mutant and wild type rosette leaves treated with the indicated ABA concentrations for 30 min (n=30-50 stomata in each experiment)

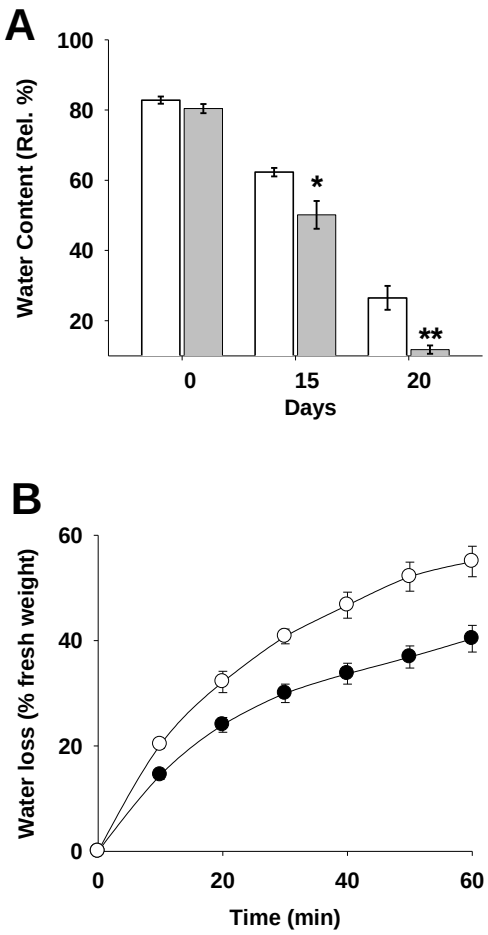

Figure 4. 2 Different concentration of ABA-induced stomatal closing.

(A) Water content in wild-type (*open bars*) and *pyr1/pyl1/pyl2/pyl4* mutant (*grey bars*) plants are shown as means ± SE (n = 8-10). * denotes significant differences (P<0.05) and ** denotes significant differences (P<0.01) between *pyr1/pyl1/pyl2/pyl4* mutant and wild-type.

(B) *pyr1/pyl1/pyl2/pyl4* mutant plants exhibit enhanced water loss from excised rosettes. Plants were grown for 60 d and then rosettes were excised and placed on trays on the lab bench. Weight loss (mainly water) from rosettes was followed with time, and is represented as the percentage of the initial fresh weight, wild-type (*black circles*) and *pyr1/pyl1/pyl2/pyl4* (*open circles*) mutant plants.

4.3.3 The Activation of I_{Cl} by ABA Is Impaired in *pyr1/pyl1/pyl2/pyl4* Mutant.

I recorded I_{Cl} from both wild-type and *pyr1/pyl1/pyl2/pyl4* mutant guard cells. Figure 4.4 shows anion currents from both before and after applying 20 μM ABA. The steady-state I_{Cl} was obviously increased in the wild-type, but, in *pyr1/pyl1/pyl2/pyl4* mutant the change was marginal. The I-V curves summarize the mean value of steady-state I_{Cl} and show in the wild-type a significant increase in response to ABA between -75 mV and -220 mV; there was no significant change in the *pyr1/pyl1/pyl2/pyl4* mutant across this voltage range (Figure 4.4). Thus, all of these results indicate a concerted block of the ABA response of $I_{K,in}$ and I_{Cl} in *pyr1/pyl1/pyl2/pyl4* mutant.

4.3.4 A Reduced ABA- Evoked $[Ca^{2+}]_i$ Elevation in *pyr1/pyl1/pyl2/pyl4* Mutant.

The abnormal reaction of these Ca^{2+} sensitive channels in response to ABA implicate the possibility that ABA induced $[Ca^{2+}]_i$ elevation might be affected in *pyr1/pyl1/pyl2/pyl4* mutant. Although previous studies (Nishimura et al., 2010) suggest Ca^{2+} signal is downstream of the PYR/PYL/RCAR receptor, there is no direct experimental evidence to support this conclusion. To close this gap in knowledge, I quantified $[Ca^{2+}]_i$ by fluorescence ratio imaging after iontophoretic injections of the Ca^{2+}-sensitive dye fura2 into individual guard cells. Fluorescence image pairs were collected at 10-sec intervals using a 535-nm interference filter (±20 nm) after excitation with light at 340 and 390 nm, and were corrected for background fluorescence collected prior to dye injections. Fluorescence ratio (f340/f390) images were calibrated against known standards (Garcia-Mata et al., 2003, Grabov and Blatt, 1998; also see Chapter 2) and were used to estimate $[Ca^{2+}]_i$ near the plasma membrane during voltage clamp cycles. Ratiometric $[Ca^{2+}]_i$ measurements showed a significant elevation in responses to 20 μM ABA stimulus (Figure 4.5). ABA application drove an increase of $[Ca^{2+}]_i$ over 282 ± 32 nM in the wild-type from resting concentration 192 ± 20 nM to maximum value 473 ± 50 nM (Figure 4.5B). However, a dramatically reduced ABA-induced $[Ca^{2+}]_i$ elevation was obtained in *pyr1/pyl1/pyl2/pyl4* mutant (Figure 4.5A). The mean $[Ca^{2+}]_i$ increase in the mutant was only 80 ± 14 nM (Figure 4.5B). These results directly confirm that *pyr1/pyl1/pyl2/pyl4* mutant impairs ABA induced $[Ca^{2+}]_i$ elevations.

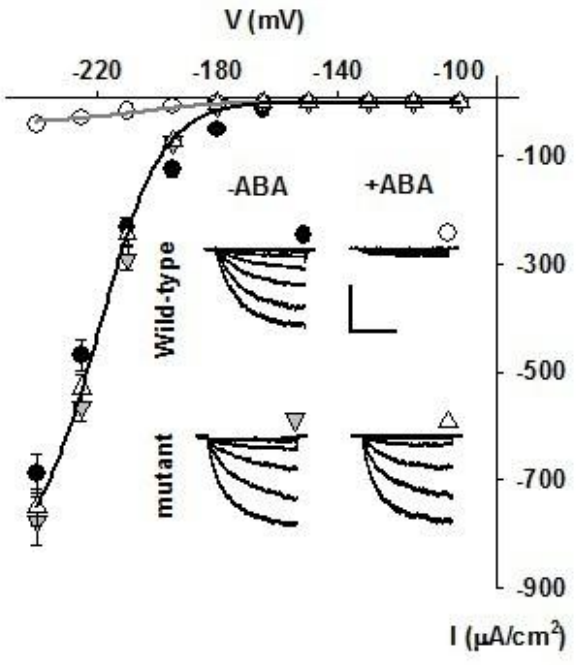

Figure 4. 3 Characteristics of $I_{K,in}$ of wild-type and *pyr1/pyl1/pyl2/pyl4* Mutant in response to 20 μM ABA.

Mean steady-state I-V curves were extracted from K_{in} measurements in wild-type (n=13) and *pyr1/pyl1/pyl2/pyl4* mutant guard cells (n=10). Data points are means ±SE. Data sets were fitted individually to a Boltzmann function (see Chapter 2). For fitted parameters see table 5.1. *Inset*: Shown are examples of $I_{K,in}$ current traces determined from ten-step voltage protocol with holding voltage, -100 mV for 2 s, and test voltage steps from -120 to -240 mV for 4 s. Wt in absence of ABA (●) and presence of ABA (○); *pyr1/pyl1/pyl2/pyl4* mutant in absence of ABA (▼) and presence of ABA (△). Scale: 200 μA cm^{-2} (vertical), 2 s (horizontal).

Table 4. 1 $I_{K,in}$ gating parameters in response to ABA.

The *pyr1/pyl1/pyl2/pyl4* mutant has no effect on the macroscopic gating parameters of the inward-rectifying K^+ current in present of ABA. Non-linear least-squares fitting of $I_{K,in}$ data in Figure 4.3 to Boltzmann Equation. Maximum ensemble conductance, g_{max}; half-maximal voltage, $V_{1/2}$; gating charge, δ. Data points are means ±SE.

	Wild-type		***pyr1/pyl1/pyl2/pyl4* mutant**	
	-ABA	+ABA	-ABA	+ABA
g_{max} (μS/cm^2)	4.8 ±0.2	0.2 ±0.1	4.7 ±0.3	4.1 ±0.5
$V_{1/2}$ (mV)	-208.5 ±1.5	-200.0 ±6.7	-216.0 ±0.3	-210.0 ±7.9
δ	2.0 ±0.4	2.0 ±0.3	1.9 ±0.1	2.0 ±0.1

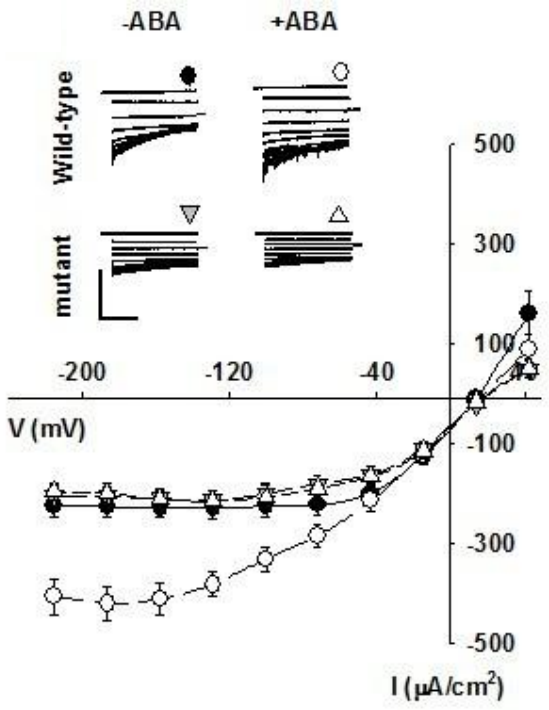

Figure 4. 4 Characteristics of anion channels of wild-type and *pyr1/pyl1/pyl2/pyl4* mutant guard cells in response to 20 µM ABA.

Mean steady-state I-V curves were extracted from anion measurements in wild-type (n=15) and *pyr1/pyl1/pyl2/pyl4* mutant guard cells (n=13). Data points are means ±SE. *Inset*: examples of anion current traces determined from a ten-step voltage protocol designed to activate the current at a voltage of +40 mV for 5 s followed by steps from +40 to -220 mV for 8 s. Symbols refer to the wild-type in absence of ABA (●) and presence of ABA (○); *pyr1/pyl1/pyl2/pyl4* mutant in absence of ABA (▲) and presence of ABA (▽). Scale: 200 µA cm^{-2} (vertical), 2 s (horizontal).

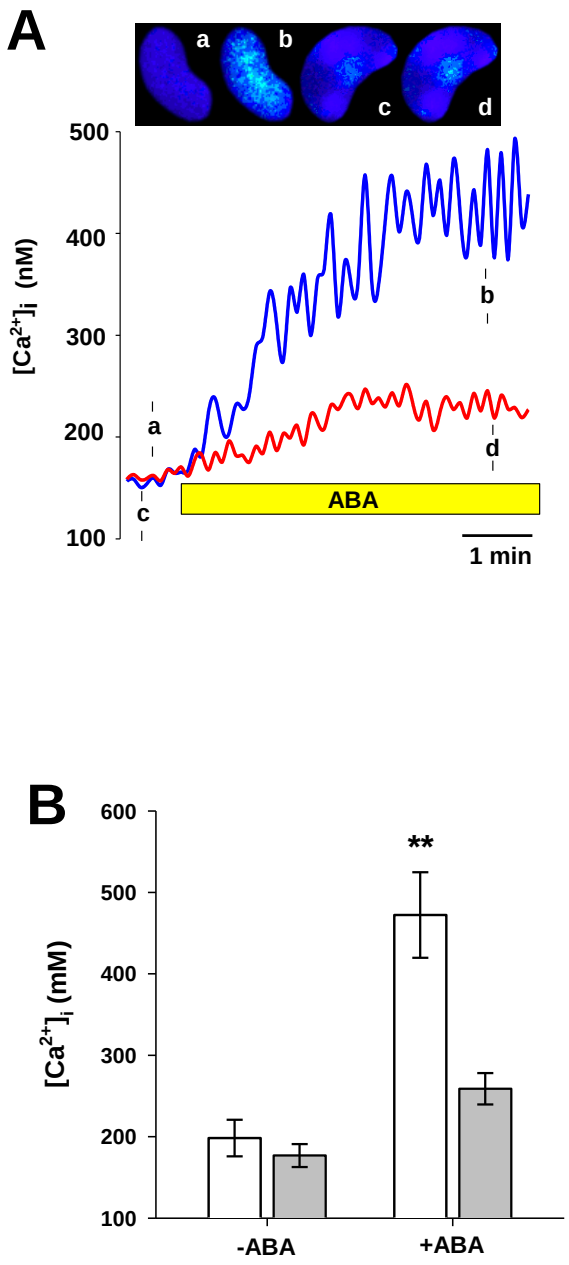

Figure 4. 5 ABA promotes evoked $[Ca^{2+}]_i$ increases.

(A) One example of the difference of $[Ca^{2+}]_i$ increases between guard cells of the wild-type (*blue line*) and *pyr1/pyl1/pyl2/pyl4* mutant (*red line*) plants after 20 μM ABA application. Fura2 fluorescence images were collected at 10-s intervals. *Above*: Selected ratio images for guard cells of wild-type (*a–b*) and the *pyr1/pyl1/pyl2/pyl4* mutant (*c-d*) correspond to the time points indicated. Scale: 1 min.

(B) $[Ca^{2+}]_i$ before and after ABA in wild-type (*open bars*) and *pyr1/pyl1/pyl2/pyl4* mutant guard cells (*grey bars*) are shown as means ± SE (n = 9–12). ** denotes significant difference (P<0.01) between *pyr1/pyl1/pyl2/pyl4* mutant and wild-type.

4.3.5 Elevating External Ca^{2+} Causes Stomatal Closure in Both Wild-type and *pyr1/pyl1/pyl2/pyl4* Mutant.

External Ca^{2+} ($[Ca^{2+}]_o$) can trigger $[Ca^{2+}]_i$ increases (Allen 1999) and result in a deactivation of $I_{K,in}$ and enhanced of I_{Cl}. Thus I examined stomatal response and the activity of $I_{K,in}$ and I_{Cl} with external Ca^{2+} ($[Ca^{2+}]_o$) to examine whether both these channels are still sensitive to Ca^{2+} in *pyr1/pyl1/pyl2/pyl4* mutant guard cells.

First of all, I examined stomatal response with $[Ca^{2+}]_o$. Figure 4.6A shows similar closing processes in both the wild-type and *pyr1/pyl1/pyl2/pyl4* mutant with 5 mM $[Ca^{2+}]_o$. Closing also occurred when $[Ca^{2+}]_o$ was increased from 0 to 1, 5 or 10 mM (Figure 4.6B). Furthermore, programmed Ca^{2+}-induced stomatal closure was reported through repetitive addition and removal of $[Ca^{2+}]_o$ to the extracellular solution shifting the K^+ equilibrium potential in guard cells (Allen et al., 2001). Such Ca^{2+}-programmed stomatal closing was observed also in both the *pyr1/pyl1/pyl2/pyl4* mutant and wild-type plants (Nishimura et al., 2010) also see Figure 4.7). These observations suggest that the *pyr1/pyl1/pyl2/pyl4* mutant exhibits a normal response to external Ca^{2+}.

In Addition, I recorded the changes of $I_{K,in}$ and I_{Cl} in response to $[Ca^{2+}]_o$. 5 mM $[Ca^{2+}]_o$ strongly suppressed $I_{K,in}$ and activated I_{Cl} in both wild-type and *pyr1/pyl1/pyl2/pyl4* mutant guard cells (Figure 4.8A and B). Figure 4.9 summaries the change of the corresponding currents in each case. The summary clearly shows that the current response in wild-type and *pyr1/pyl1/pyl2/pyl4* mutant guard cells was similar. In conclusion, all of these results point to the role of the PYR/PYL protein upstream of the Ca^{2+} signal.

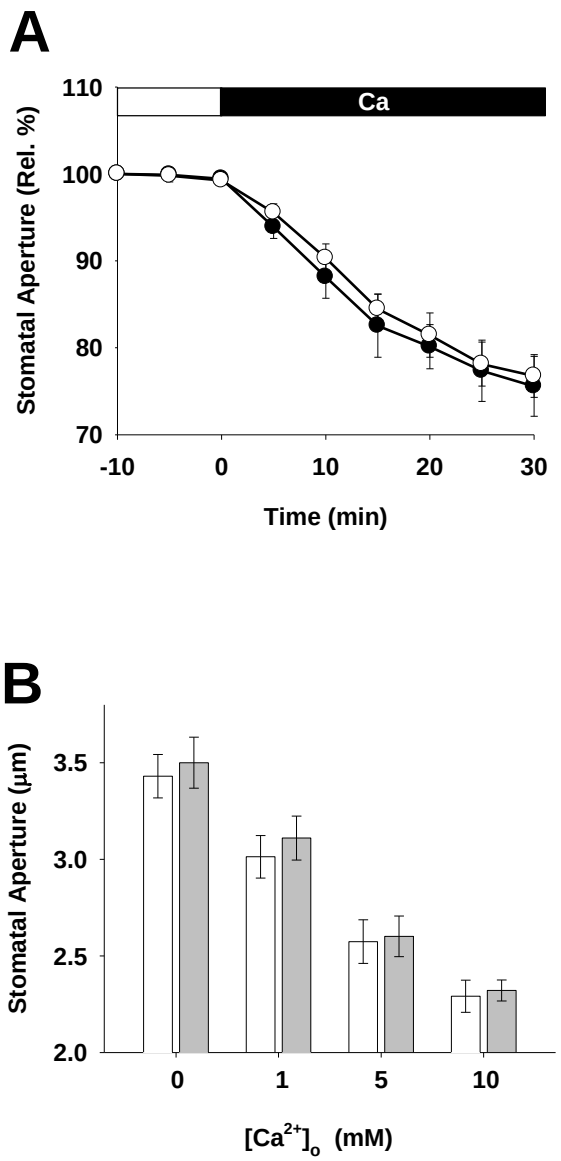

Figure 4. 6 External Ca^{2+}-induced stomatal closing.

(A) Ca^{2+}-induced stomatal closure in wild-type (*black circle*) and *pyr1/pyl1/pyl2/pyl4* mutant (*open circle*) rosette leaves treated with the 5 mM $[Ca^{2+}]_o$ for 30 min (n=30-50 stomata in each experiment).

(B) Different $[Ca^{2+}]_o$ caused similar stomatal closure in wild-type and *pyr1/pyl1/pyl2/pyl4* mutant stomata (wild-type : *open bar*; *pyr1/pyl1/pyl2/pyl4* mutant :*grey bar*; n ≥20).

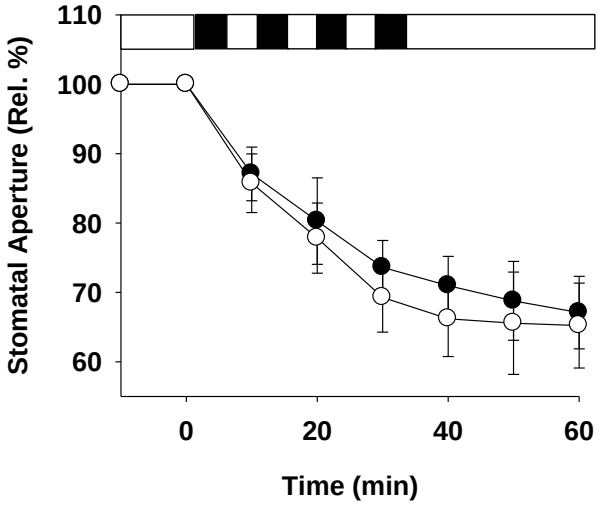

Figure 4. 7 Programmed Ca^{2+}-induced stomatal closing.

Ca^{2+}-induced stomatal closure in wild-type (*black circle*) and *pyr1/pyl1/pyl2/pyl4* mutant (*open circle*) rosette leaves treated with repetitive exchanges between depolarizing (*white bar*) and hyperpolarizing (*black bar*) buffers (n=15-20 stomata in each experiment).

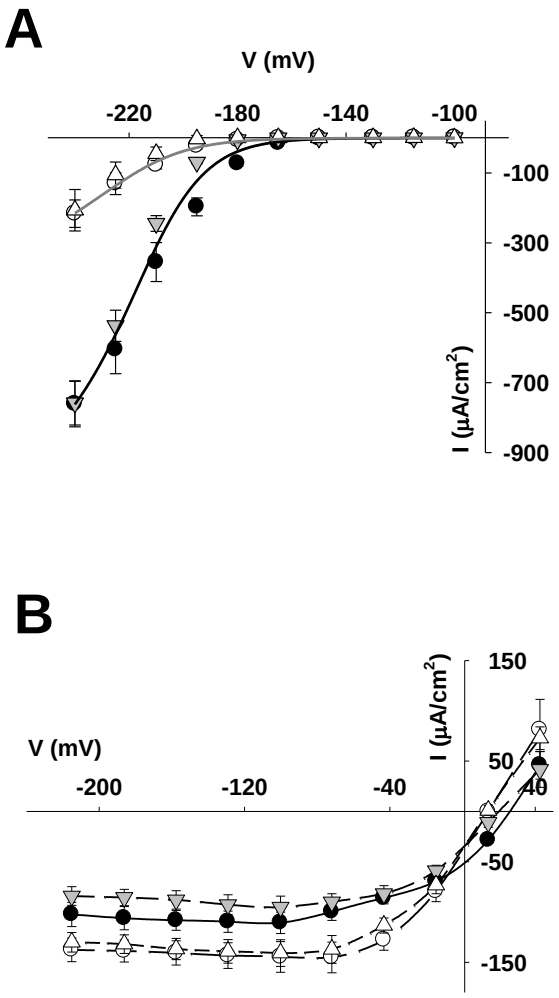

Figure 4. 8 Characteristics of $I_{K,in}$ and I_{Cl} of wild-type and *pyr1/pyl1/pyl2/pyl4* mutant guard cells in response to 5 mM external Ca^{2+}.

(A) Mean steady-state I-V curves were extracted from $I_{K,in}$ measurements in wild-type (n=12) and *pyr1/pyl1/pyl2/pyl4* mutant guard cells (n=11). Data points are means ±SE. Data sets were fitted individually to a Boltzmann function. Parameter see table 5.2.

(B) Mean steady-state I-V curves were extracted from anion measurements in wild-type (n=15) and *pyr1/pyl1/pyl2/pyl4* mutant (n=13) guard cells. Data points are means ±SE. Wild-type in absent of Ca^{2+} (●) and presence of Ca^{2+} (○); *pyr1/pyl1/pyl2/pyl4* mutant in absent Ca^{2+} (▼) and presence Ca^{2+} (△).Scale: 200 µA cm^{-2} (vertical), 2 s (horizontal).

Table 4. 2 $I_{K,in}$ gating parameters in response to Ca^{2+}.

The *pyr1/pyl1/pyl2/pyl4* mutant has a similar effect on the macroscopic gating parameters of the inward-rectifying K^+ current as wild-type in present of Ca^{2+}. Non-linear least-squares fitting of $I_{K,in}$ data in Figure 4.8 to Boltzmann Equation. Maximum ensemble conductance, g_{max}; half-maximal voltage, $V_{1/2}$; gating charge, δ. Data points are means ±SE.

	Wild-type		***pyr1/pyl1/pyl2/pyl4* mutant**	
	$-Ca^{2+}$	$+Ca^{2+}$	$-Ca^{2+}$	$+Ca^{2+}$
g_{max} (μS/cm^2)	4.8 ± 0.2	1.6 ± 0.2	4.6 ± 0.2	1.6 ± 0.2
$V_{1/2}$ (mV)	-208.5 ±1.5	-225.3 ± 3.4	-216.0 ± 0.3	-226.3 ± 2.7
δ	1.9 ± 0.1	1.7 ± 0.2	2.0 ± 0.1	1.8 ± 0.2

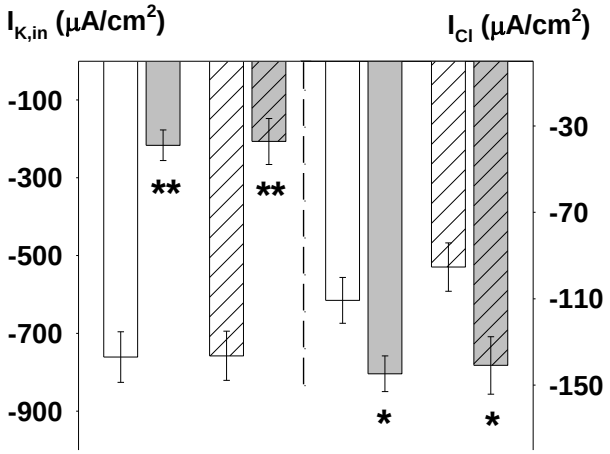

Figure 4. 9 The *pyr1/pyl1/pyl2/pyl4* mutant exhibits a similar reaction as wild-type in response external Ca^{2+}.

Inactivation of $I_{K,in}$ and activation of I_{Cl} in response to 5 mM external Ca^{2+}. Steady-state current determined as described for Figure 4.8 for $I_{K,in}$ at -240 mV and I_{Cl} at -100 mV in wild-type (*open bars*) and *pyr1/pyl1/pyl2/pyl4* mutant (*shaded bars*) guard cells. The effects of a 5-min exposure to Ca^{2+} (*grey bars*) are shown as means ± SE (n = 15–20). * denotes significant differences at $P<0.05$, and ** denotes significant differences at $P<0.01$ between with and without external Ca^{2+}.

4.3.6 ABA Activation of Plasma Membrane I_{Ca} is Impaired in *pyr1/pyl1/pyl2/pyl4* Mutant.

ABA triggers $[Ca^{2+}]_i$ elevation mainly through activating plasma membrane I_{Ca} (Hamilton et al., 2000, Pei et al., 2000). Thus I wondered if the PYR/PYL protein could affect on the activity of plasma membrane I_{Ca} in response to ABA. To explore the question, I use the two-electrode voltage clamp to measure I_{Ca}. Due to the difficulty of voltage clamping measurements of I_{Ca}, all previous studies were based on patch clamp. To bridge this gap, I develop a new method for I_{Ca} recording based on voltage clamp in intact guard cells. I used 150 mM Ba-Acetate (pH 7.5) to fill electrode barrels and bathed guard cells in 5 mM MES-$Ba(OH)_2$ at pH 6.1. The activity of guard cell Cl^- channels is suppressed by milimolar acetate (Wang and Blatt, 2011) and the K^+ channels are blocked by millimolar Ba^{2+}. Ba^{2+} also permeates the Ca^{2+} channels (Hamilton et al., 2001, Hamilton et al., 2000). Thus, my strategy was to minimize the interference of K^+ and Cl^- channels with the Ca^{2+} currents. Figure 4.10 and 4.11 confirmed that the recordings gave measurements of Ca^{2+} currents, based on current reversal and block by La^{3+}. Based on this new method, I recorded an increasing inward current in wild-type guard cells under negative voltages (currents from -302 $\pm$31 to -527 $\pm$ 40 $\mu A\ cm^{-2}$ at -200 mV) when 20 μM ABA was applied (Figure 4.12). By contrast, ABA activation of these currents was largely absent in *pyr1/pyl1/pyl2/pyl4* mutant guard cells (Figure 4.12). Thus ABA failed to activate plasma membrane Ca^{2+} channels *pyr1/pyl1/pyl2/pyl4* mutant.

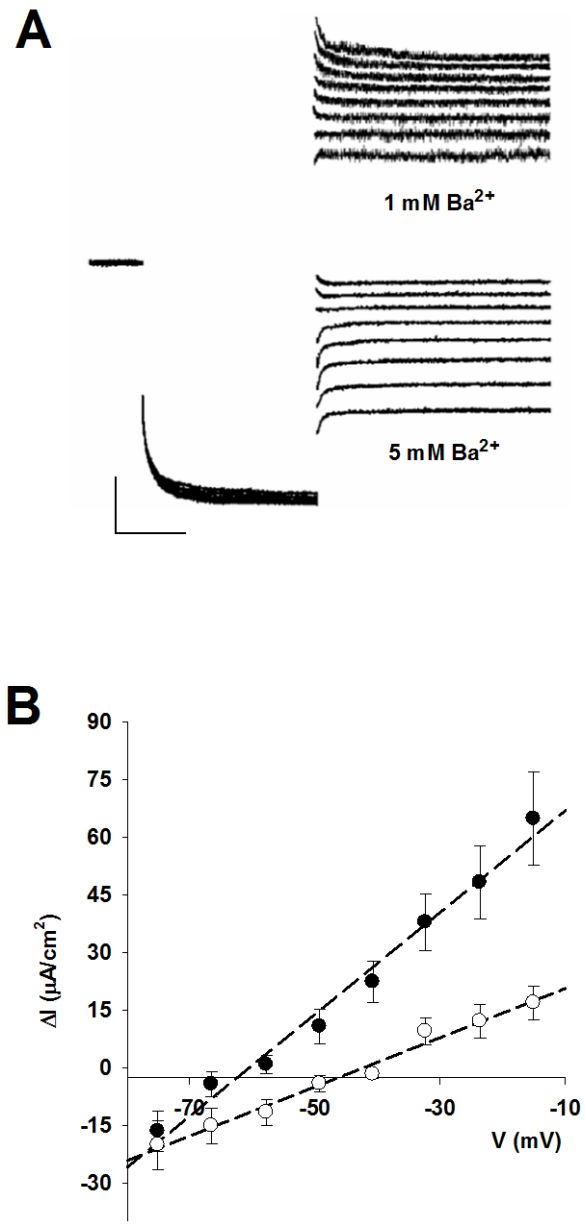

Figure 4. 10 I_{Ba} tail currents measurement in wild-type guard cells.

(A) I_{Ba} tail currents recording in different Ba^{2+} concentrations. The current was activated at -100 mV and, then, the voltage was stepped from -15 mV to voltages negative of approximately -80 mV. Scale: 200 μA cm^{-2}, 0.5 s (horizontal).

(B) Reversal voltage derived from ΔI-V curve plotting using tail current data, including that of (A). 1 mM Ba^{2+} outside (*black circles*) led to a negative reversal voltage around -57 ± 5 mV, while 5 mM Ba^{2+} shifted the reversal to a more positive voltage about -35 ± 4 mV. The change in reversal voltage is consistent with the predicted shift for E_{Ba} with a 5-fold change in concentration of 13 mV.

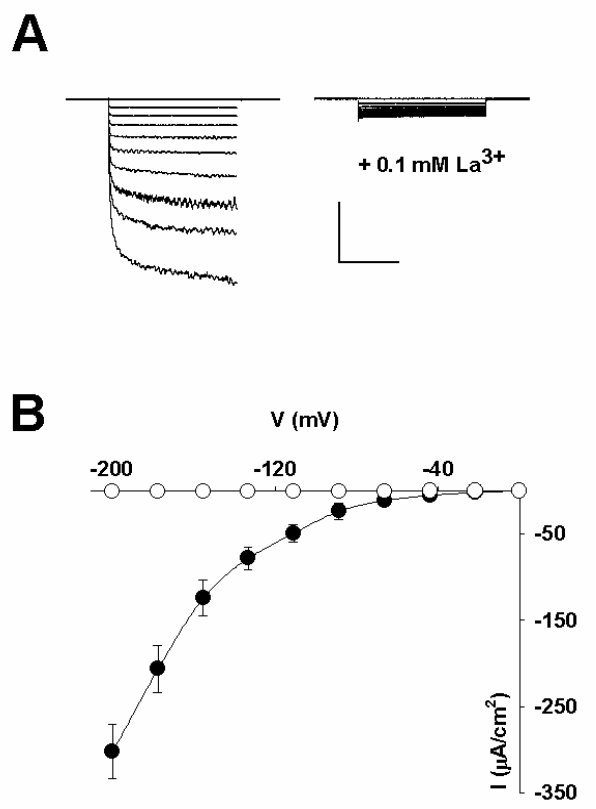

Figure 4. 11 Characteristics of I_{Ba} of wild-type and *pyr1/pyl1/pyl2/pyl4* mutant in response to La^{3+}.

(A) Typical Ba^{2+} current block by La^{3+}. Currents recorded from the same cell before (*left*) and after (*right*) adding 100 mM $LaCl_3$. Scale: 200 μA cm^{-2}, 1 s (horizontal).

(B) Mean steady-state I/V curves were extracted from I_{Ba} measurements in wild-type (n=11) and *pyr1/pyl1/pyl2/pyl4* mutant (n=10). Data points are means ±SE. Wild-type in absence of La^{3+} (●) and presence of La^{3+} (○).

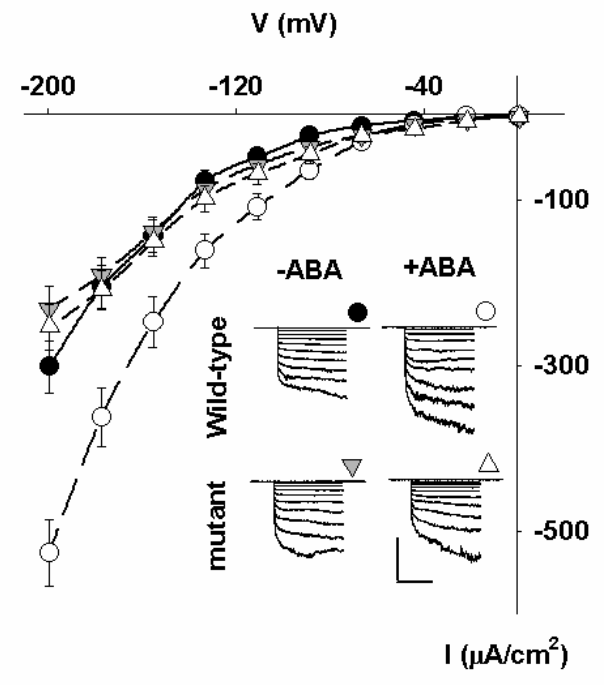

Figure 4. 12 ABA-activation of I_{Ca} channels is impaired in *pyr1/pyl1/pyl2/pyl4* mutant guard cells.

Mean steady-state I/V curves were extracted from I_{Ca} measurements in wild-type (n=10) and *pyr1/pyl1/pyl2/pyl4* mutant (n=8) guard cells. Data points are means ±SE. *Inset*: Shown are examples of Ba^{2+} current traces determined from ten-step voltage protocol designed with activation an voltage of 0 mV for 3 s, and steps to test voltages between 0 and -200 mV for 1.5 s. Wt in absent ABA (●) and presence ABA (○); *pyr1/pyl1/pyl2/pyl4* mutant in absent ABA (▼) and presence ABA (△).Scale: 200 μA cm^{-2}, 1 s (horizontal).

4.3.7 ABA-induced H_2O_2 Activates Plasma Membrane I_{Ca} and -ROS Production Is Impaired in *pyr1/pyl1/pyl2/pyl4* Mutant.

ABA stimulates reactive oxygen species (ROS) production in guard cells and ROS can activate plasma membrane I_{Ca} (Pei et al., 2000). Therefore I next examined whether or not ROS activation of I_{Ca} occurs in *pyr1/pyl1/pyl2/pyl4* mutant. Again, measurements were carried out under voltage clamp before and during treatments with H_2O_2. Figure 4.13 clearly shows increasing I_{Ca} in wild-type guard cells with 100 μM H_2O_2,the amplitude increasing from -302 ± 31 to -697 ± 50 μA cm^{-2} at -200 mV. Unlike the results in ABA exposure, H_2O_2 also activated I_{Ca} currents in the *pyr1/pyl1/pyl2/pyl4* mutant comparable to wild-type – from -231 ± 26 to -636 ± 42 μA cm^{-2} at -200 mV (Figure 4.13) – indicating that there is no effect on ROS-dependent I_{Ca} activation in the mutant. To further investigate, external H_2O_2 was used to induce stomata closure. Figure 4.14 shows that 100 μM external H_2O_2 triggered a similar closing progression in both wild-type and mutant guard cells. These findings suggest ABA-induced ROS production might be affected in the *pyr1/pyl1/pyl2/pyl4* mutant.

I analyzed ABA-dependent ROS production using the fluorescent dye 2,7-dichlorofluorescin diacetate (H_2DCF-DA). As shown in Figure 4.14B, the fluorescence increased after treatment of wild-type guard cells with 20 μM ABA. However, only a slightly increase in ROS was obtained in *pyr1/pyl1/pyl2/pyl4* mutant. Thus, compared with the wild-type, ABA-induced ROS production was dramatically reduced in *pyr1/pyl1/pyl2/pyl4* mutant. These results indicate an impaired ROS-associated pathway lies behind the failure of ABA to induce I_{Ca} in the *pyr1/pyl1/pyl2/pyl4* mutant.

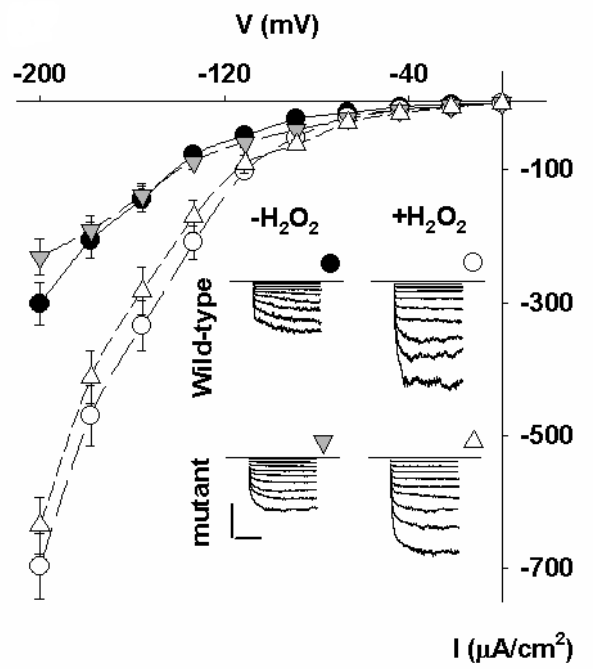

Figure 4. 13 H_2O_2-activation of I_{Ca} channels in both wild-type and *pyr1/pyl1/pyl2/pyl4* mutant guard cells.

Mean steady-state I/V curves were extracted from I_{Ca} measurements in wild-type (n=11) and *pyr1/pyl1/pyl2/pyl4* mutant (n=9) guard cells. Data points are means ±SE. (*insert*) Shown are examples of Ba^{2+} current traces determined from ten-step voltage protocol was designed to activation voltage of 0 mV for 3 s and stepped to -200 mV for 1.5 s. Wild-type in absence of H_2O_2 (●) and presence of H_2O_2 (○); *pyr1/pyl1/pyl2/pyl4* mutant in absence of H_2O_2 (▼) and presence of H_2O_2 (△).Scale: 200 µA cm^{-2}, 1 s (horizontal).

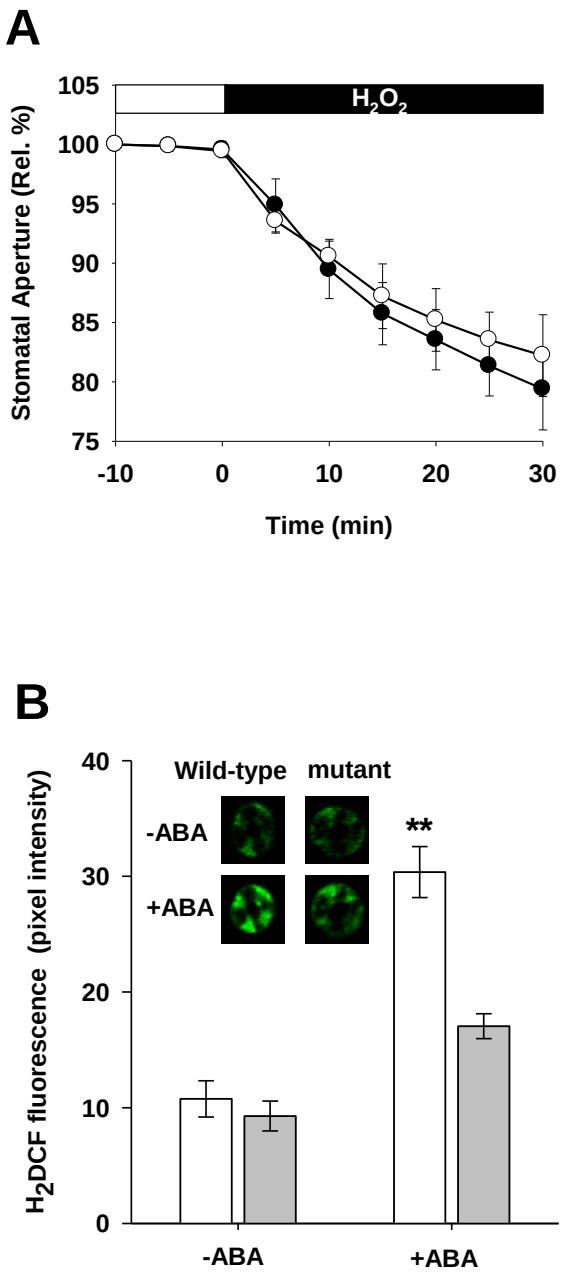

Figure 4. 14 Exogenous H_2O_2 rescues stomatal closing in *pyr1/pyl1/pyl2/pyl4* mutant and ABA-induced ROS generation are disrupted in the *pyr1/pyl1/pyl2/pyl4* mutant.

(A) 100 μM H_2O_2-induced stomatal closure in wild-type (*black circles*) and *pyr1/pyl1/pyl2/pyl4* mutant (*open circles*) mutant guard cells. Apertures were normalised on a cell-by-cell basis to values at a time point 10 min before treatments. Data are means ± SE of n = 33 stomata pooled from at least four independent experiments for each line.

(B) ROS level before and after ABA in wild-type (*open bars*) and *pyr1/pyl1/pyl2/pyl4* mutant guard cells (*grey bars*) are shown as means ± SE (n=20-24). ** denotes significant difference (P<0.01) between *pyr1/pyl1/pyl2/pyl4* mutant and wild-type.

4.4 Discussion

ABA signalling is general recognized as critical for transduction of water stress. Abscisic acid is usually synthesized in roots during drought and transported to the leaf tissues, evoking stomata closure and reducing transpirational water loss (Blatt and Armstrong, 1993). This effect is achieved through a net loss of osmotically active solutes from the guard cells, including K^+ and anions Cl^- and malate from cytosol across the plasma membrane, and consequently a decline guard cell turgor. Guard cells respond to ABA through stimulation of an inward-directed current, mainly mediated by I_{Cl}, which depolarizes the membrane to generate a driving force for K^+ efflux; it also inactivates $I_{K,in}$ that normally mediates in K^+ uptake (Blatt, 2000). It has been known that both Ca^{2+}-dependent and -independent pathways can regulate $I_{K,in}$ and I_{Cl} in guard cells in response to ABA. But it is still unclear the relationship between these two pathways. Whether they are two separate, parallel regulation routes, or whether they exist as a "feed-back" for fine mediation in ABA signalling is still largely unknown. Recently, the PYR/PYL/RCAR proteins were identified as new ABA binding targets and signalling proteins (Ma et al., 2009, Park et al., 2009) supplying us with an opportunity to explore this question. The most remarkable finding described above is that the *pyr1/pyl1/pyl2/pyl4* mutant cannot evoke a $[Ca^{2+}]_i$ increase in response to ABA, suggesting that PYR/PYL proteins are directly involved in $[Ca^{2+}]_i$ regulation. I used voltage clamp to explore this question and provide the first measurements of plasma membrane I_{Ca} in vivo. From these studies, I found that the ABA-promoted Ca^{2+} entry current was impaired and that the effect can be connected to reduce ROS levels with ABA in *pyr1/pyl1/pyl2/pyl4* mutant. Thus I am able to build a link between ABA perception and $[Ca^{2+}]_i$ regulation via ROS-mediated activation of Ca^{2+} channels.

4.4.1 Impaired ABA-evoked $[Ca^{2+}]_i$ Elevation in *pyr1/pyl1/pyl2/pyl4* Mutant

My initial experiments showed ABA cannot close stoma in *pyr1/pyl1/pyl2/pyl4* mutants (Figure 4.1), in line with the evidence that silence of ABA activated I_{Cl} and inactivated $I_{K,in}$ in this mutant (Figure 4.3). The results suggested the failure of ABA to induced stomatal closing is due to loss of control of the corresponding ion channels. In

ABA signalling, upstream regulation of $I_{K,in}$ and I_{Cl} is through drought stress phosphatases-kinase pairs, PP2Cs and SnRKs. It has been indentified that PP2Cs and SnRKs directly interact with S-type anion channel *in vitro* (Umezawa et al., 2009, Geiger et al., 2009). Similarly, OST1, a member of SnRKs, also interacts with KAT1, a dominant inward-rectifying K^+ channel in guard cell (Sato et al., 2009). In *pyr1/pyl1/pyl2/pyl4* mutants, without these cytosolic ABA receptors, the phosphatases-kinase pairs do not work as usual in response ABA. Therefore, not surprisingly, there is little change in $I_{K,in}$ and I_{Cl}.

More interestingly, the *pyr1/pyl1/pyl2/pyl4* mutant showed a normal response to external Ca^{2+} (Figure 4.6-4.8). Elevating $[Ca^{2+}]_o$ can obviously increase $[Ca^{2+}]_i$ (Allen et al., 1999). Indeed, both $I_{K,in}$ and I_{Cl} appeared sensitive to $[Ca^{2+}]_I$ under these conditions. According to this published work, we observed a normal change in $I_{K,in}$ and I_{Cl} in the *pyr1/pyl1/pyl2/pyl4* mutant treated with $[Ca^{2+}]_o$. It is well known that ABA control of $I_{K,in}$ depends on an early rise in $[Ca^{2+}]_i$ and elevated $[Ca^{2+}]_i$ also activates I_{Cl} (Blatt, 2000; also see Figure 4.8). Thus, all these results suggest that PYR/PYL proteins localize upstream of $[Ca^{2+}]_i$ regulation. To confirm that the PYR/PYL proteins regulate $[Ca^{2+}]_i$, I examined ABA induced $[Ca^{2+}]_i$ elevation in the *pyr1/pyl1/pyl2/pyl4* mutant (Figure 4.5). Although there was still a small increase in $[Ca^{2+}]_i$ in *pyr1/pyl1/pyl2/pyl4* mutant, the effect might be related to other ABA signalling events, the reduced $[Ca^{2+}]_i$ rise in the mutant compared to wild-type clearly underscores the functional importance of $[Ca^{2+}]_i$ elevation, and its imparement in the *pyr1/pyl1/pyl2/pyl4* mutant. Indeed, earlier studies had indicated ABA-mediated activation of I_{Ca} is accelerated when ABA is added to the inner surface of the membrane (Hamilton 2000) and pointed out that activation of I_{Ca} by ABA required protein phosphorylation (Kohler and Blatt, 2002, Sokolovski and Blatt, 2004, Sokolovski et al., 2005). All these data suggest ABA control of I_{Ca} is mediated through protein (de-)phosphorylation from the cytosolic side of the membrane. With the finding of the dominant negative mutants *abi1* and *abi2*, which reduced ABA-induced $[Ca^{2+}]_i$ increases, the importance of protein (de-)phosphorylation events becomes more clear. Thus, there is no doubt that phosphatases-kinase pairs of PP2Cs and SnRKs participate directly in ABA-regulated $[Ca^{2+}]_i$. My results, together with previous studies, confirm the role for PYR/PYL at an early stage of $[Ca^{2+}]_i$ regulation.

4.4.2 A Link Between ABA Perception and Cytosolic Ca^{2+} Regulation

ABA induces both Ca^{2+} release from intracellular stores and Ca^{2+} influx from the extracellular space. However, the detail is remain unclear how the PYR/PYL receptor proteins regulate $[Ca^{2+}]_i$ elevation in response to ABA. Evidence that ROS activates plasma membrane I_{Ca} and promotes extracellular Ca^{2+} influx (Pei et al., 2000, Murata et al., 2001) led me to consider the role of PYR/PYL in the activation of I_{Ca} through ROS production. In agreement with previous studies (Pei et al., 2000, Murata et al., 2001), fluorescence measurements of ROS indicated that it increased after ABA treatment in wild-type guard cells (Figure 4.13). By contrast, ABA had little effect in promoting ROS levels in *pyr1/pyl1/pyl2/pyl4* mutant (Figure 4.13B). However, the loss of ROS production could be overcome with externally applied H_2O_2, which elicited the same degree of stomatal closure in *pyr1/pyl1/pyl2/pyl4* mutant as in the stomata of wild-type plants (Figure 4.13A). Likewise, increased extracellular Ca^{2+} induced a similar stomatal closing response in both wild-type and *pyr1/pyl1/pyl2/pyl4* mutant guard cells (Figure 4.6). These data support the idea that the *pyr1/pyl1/pyl2/pyl4* mutation disrupts ABA signalling at a point upstream of ROS production. Again, a parallel can be drawn to mutants that affect protein (de-)phosphorylation pathways in the guard cells: Like the *pyr1/pyl1/pyl2/pyl4* mutant, the ABA-insensitive *abi1-1* and *ost1* mutations impair ABA-induced ROS production and stomatal closure (Murata et al., 2001). Furthermore, earlier studies showed that PYL1 interacts directly with ABI1, and ABI1 also can inhibit the activation of OST1 (Nishimura et al., 2010). Thus, my data indicate that PYR/PYL proteins act at a point upstream of the protein phosphatases-kinase pairs in the signalling cascade linking ABA to $[Ca^{2+}]_i$ through ROS synthesis.

It is well know that $[Ca^{2+}]_i$ elevation occurs through a combination of Ca^{2+} entry and intracellular Ca^{2+} release. How might PYR/PYL proteins affect Ca^{2+} release from intracellular stores? Previous studies showed ROS can induce Nitric Oxide (NO) synthesis in *Arabidopsis*, and NO selectively regulates Ca^{2+}-sensitive ion channels of *Vicia* guard cells by promoting Ca^{2+} release from intracellular stores to raise $[Ca^{2+}]_i$ (Garcia-Mata et al., 2003). Thus it is highly possible that ABA-induced NO synthesis is also impaired in *pyr1/pyl1/pyl2/pyl4* mutant. Whether this process is directly caused through lack of ROS

production or PYR/PYL protein related phosphatases-kinase pairs still needs to be explored. In addition, other factors such as plant phospholipase C isoforms also affect I_{Ca} activation and Ca^{2+} -induced Ca^{2+} release via slow vacuolar (SV) channels (Ward and Schroeder, 1994, Bewell et al., 1999). Whether PYR/PYLs influence the SV channel directly or through phosphatases-kinase pairs is also a question that remains unanswered.

4.4.3 A New Method to Measure I_{Ca} *in vivo.*

I_{Ca} measurements have been reported for many years, but all of these measurements in plants are based on the patch clamp. In guard cells, there are no reports about I_{Ca} in vivo so far. I used two-electrode voltage clamp technology to measure plasma membrane I_{Ca} after devising conditions that allowed its isolation in the intact guard cells. At plasma membrane there are, at least, three types of inward currents. Two channel classes carry positive charges, K^+ and Ca^{2+}, and one class carries negative charge, that of Cl^- and Mal. Because Ba^{2+} permeates many Ca^{2+} channels, and guard cell K^+ channels are blocked by millimolar Ba^{2+} (Hamilton et al., 2000, Hamilton et al., 2001), use of this divalent is ideal for measuring I_{Ca}. Therefore, I used MES-$Ba(OH)_2$ buffer to bathe cells, thus eliminating K^+ currents and providing a permeant divalent, and also buffering external pH. Furthermore, I used 150 mM Ba-Acetate (pH 7.5) filled electrodes. Previous studies indicate high concentration of acetate can block the Cl^- channels (See Chapter 3 and Wang and Blatt, 2011). Thus the dominant currents across plasma membrane in my experiments were limited to those carried by Ba^{2+}.

An interesting question to ask is ‘How many functional Ca^{2+} channels reside at the plasma membrane in the intact guard cell?’ Previously this question could not be answered. I now can calculate the number of Ca^{2+} channels on plasma membrane, following relation describes the measured current: $I=N\gamma P_o(V_m-V_x)$. Where I is ionic current experimentally observed; N is the number of channels; γ is the single-channel conductance; P_o is the probability of the channel open, which is a function of time and membrane potential; V_m is the membrane potential; and V_x is the reversal potential of the current. If we assume P_o =0.2, and γ=13 based on Hamilton et al. (2000) results. Selected data from my results, for

example, I= -800 pA, V_x = -64 mV. Therefore the estimate number of Ca^{2+} channel per cell is around 2000 to 3000.

In conclusion, my results identify an impaired ABA-induced stomatal phenotype associate with the lack of ABA perception protein PYR/PYL/RCAR. I interpret these abnormal stomatal movements in *pyr1/pyl1/pyl2/pyl4* mutant through its influence on ABA-induced guard cell plasma membrane I_{Ca} and the consequences for downstream $I_{K,in}$ and anion channels regulation. I suggest that PYR/PYL/RCAR proteins are required for ABA induced stomatal closure and has an important role in evoking $[Ca^{2+}]_i$ elevation. These findings underline the significance of the PYR/PYL/RCAR proteins for the early ABA signal transduction in stomatal guard cells and build the link between ABA perception and $[Ca^{2+}]_i$ regulation.

CHAPTER 5:

SYSTEMS DYNAMIC MODELLING OF GUARD CELL Cl^- CHANNEL MUTANT UNCOVERS AN EMERGENT HOMEOSTATIC NETWORK REGULATING STOMATAL TRANSPIRATION

5.1 Introduction

Guard cells open the pore by transport and accumulation of osmotically active solutes - mainly K^+ and Cl^-, and the organic anion malate^{2-} (Mal) -to drive water uptake and cell expansion; they close the pore by coordinating the release of these solutes through K^+ and anion channels at the plasma membrane. The past half century has generated a wealth of knowledge for guard cell transport, signalling and homeostasis, resolving the properties of the major transport processes and metabolic pathways for osmotic solute uptake and accumulation, and many of the signalling pathways that control them (Blatt, 2000, Schroeder et al., 2001, McAinsh and Pittman, 2009, Hills et al., 2012). Even so, much of stomatal dynamics remains unresolved, especially how the entire network of transporters in guard cells works to modulate solute flux for a dynamic range of stomatal apertures. This gap in understanding is most evident in a number of often unexpected observations, many of which have led necessarily to ad hoc interpretations. Among these, recent studies highlighted a diurnal variation in the free cytosolic concentration of $[Ca^{2+}]_i$, high in the daytime despite the activation of primary ion-exporting ATPases, and have been interpreted to require complex levels of regulation (Dodd et al., 2007). Other findings wholly defie intuitive explanation. For example, the *tpk1* mutant of Arabidopsis removes a major pathway for K^+ flux across the tonoplast and suppresses stomatal closure, yet the mutant has no significant effect on cellular K^+ content (Gobert et al., 2007). Similarly, the *Arabidopsis clcc* mutant eliminates the H^+-Cl^- antiporter at the tonoplast; it affects Cl^- uptake, reduces vacuolar Cl^- content and slows stomatal opening; but, counterintuitively, it also suppresses stomatal closure (Jossier et al., 2010).

The recently isolated *SLAC1* anion channel is a major pathway for anion loss from the guard cells during stomatal closure (Vahisalu et al., 2008, Negi et al., 2008). Its mutation leads to incomplete and slowed closure of stomata in response to physiologically relevant signals of dark, high CO_2, and the water-stress hormone abscisic acid. The loss of function in the *slac1* mutant leads to guard cells accumulating Cl^- and Mal but also K^+ (Negi et al., 2008), consistent with additional impacts on K^+ transport. In work leading to this study, I observed that the *slac1* mutant paradoxically altered the activities of the predominant K^+ channels at the guard cell plasma membrane. However, a straightforward explanation for

these findings was not forthcoming.

Quantitative systems analysis offers one approach to such problems. Efforts to model stomatal function generally have been driven by a 'top-down' approach (Farquhar and Wong, 1984, Eamus and Shanahan, 2002) and have not incorporated detail essential to understanding the molecular and cellular mechanics that drive stomatal movement. Only recently, we elaborated a quantitative systems dynamic approach to modelling the stomatal guard cell that incorporates all of the fundamental properties of the transporters at the plasma membrane and tonoplast, the salient features of osmolite metabolism, and the essential pH_i and $[Ca^{2+}]_i$ buffering characteristics (Hills et al., 2012). The model resolved with this approach (Chen et al., 2012a) successfully recapitulated a wide range of known stomatal behaviours, including the diurnal changes in free cytosolic Ca^{2+} concentration ($[Ca^{2+}]_i$) (Dodd et al., 2007) and oscillations in membrane voltage and $[Ca^{2+}]_i$ thought to facilitate stomatal closure (Blatt, 2000, McAinsh and Pittman, 2009, Chen et al., 2012a). I used this approach to resolve the mechanism behind the counterintuitive alterations in K^+ channel activity uncovered in the *slac1* mutant of *Arabidopsis*. Here I report that anion accumulation in the mutant affects the H^+ and Ca^{2+} load on the cytosol, elevating cytosolic pH and $[Ca^{2+}]_i$, and in turn regulating the K^+ channels. I validated the key predictions of the model and, in so doing; uncovered a previously unrecognised homeostatic network that reduces the effects of the *slac1* mutant on water loss from the plant.

5.2 Materials and Methods

The methods of plant growth, aperture measurements, electrophysiology, gas exchange, $[Ca^{2+}]_i$ and pH_i measurements used here are detailed in Chapter 2.

5.2.1 Gene Expression Analysis

Total RNA was extracted from mature leaves and transcript levels determined by quantitative PCR as before (Chen et al., 2012a). Unique primers (Table 5.1) were designed for the VH^+-ATPase C subunit (Dettmer et al., 2006), the plasma membrane H^+-ATPases, *AHA1*, *AHA2* and *AHA5* (Blatt, 2004) and the K^+ channels *KAT1*, *KAT2*, *KC1*, *GORK*, *AKT1*, *AKT2* (Pilot et al., 2001, Hosy et al., 2003, Honsbein et al., 2009), the vacuolar channels *TPK1* (Gobert et al., 2007), and *TPC1* (Peiter et al., 2005). The *TUB9* (At4g20890) and *ACT2* actin genes (At3g18780) (9) served as an internal controls.

Table 5. 1 Primers used for quantitative PCR analysis of transcript abundance.

Gene	AGI	Forward Primer (5' to 3')	Reverse Primer (5' to 3')
AHA1	AT2G18960	CACAACCAAGAAAGATTACGG	CTTCTCTTGGCTTGCTCTG
AHA2	AT4G30190	CACTTCACGGTTTACAGCC	GCTTCACGACTGATTCCAC
AHA5	AT2G24520	CAGTGAACTCTCTCAGATTGCTG	GAATCGTGTCAATGTCAAGTCC
AKT2	AT4G22200	CCTCCTTCACTTGATGACCTC	CTCCATCTTCATTCGTCACC
GORK	AT5G37500	GCTCAGTCGTCTATCTACCCG	CGTGCTTTCTACTACGCTCTTC
KAT1	AT5G46240	TCTCAAATACTGCGGATAAGC	TCTATTGCTATTGACTGTTGCC
KAT2	AT4G18290	GCTGATAATCCTTCCTGCTTC	CATCTTCATCATCTATTTCTGCG
KC1	AT4G32650	GATTCCAACGGATTTCTACG	TGTTCACTCACACCCTTGG
TPC1	AT4G03560	TGTCAAGGACAGGATTCTCAAG	AAGTGGAACACTCTGGTTTGC
TPK1	AT5G55630	AAACAGAGGGCGTTGGTG	CGAACTCATCCATTATCCCAG
TUB9	AT4G20890	AGTGTCCCTGAGCTAAC	AGTGGGAGCTATATCGC
VHAc	AT1G12840	GAACGCTTGTGTGATTCTACC	AGCAAGGTTGATAGTGAAGGAG
YLS8	AT5G08290	ACTGGGATGAGACCTGTATG	TGTTGTTGTTACCAGTTCCA

5.2.4 OnGuard Modelling

The OnGuard software and model was driven through a diurnal 12:12 h light:dark cycle as described previously (Chen et al., 2012a) and all model outputs derived from this cycle. Model parameters (Hills et al., 2012) were adjusted to reflect the physical dimensions of the *Arabidopsis* stomatal complex and transporter numbers scaled accordingly. Light sensitivity was assigned solely to the plasma membrane H^+-ATPase and Ca^{2+}-ATPase, the vacuolar VH^+-ATPase, H^+-PPase and Ca^{2+}-ATPase, and to sucrose synthesis in accordance with experimental observation (Chen et al., 2012a). All other model parameters were fixed, the properties of the individual transporters and buffering reactions thus responding only to changes in model variables arising from the kinetic features encoded in the model. The OnGuard software is available at *www.psrg.org.uk*.

5.3 Results

5.3.1 Both Instantaneous and Steady-state Cl^- Currents Are Impaired in *slac1* Mutant

SLAC1 anion channel is a major pathway for anion loss from the guard cells during stomatal closure (Vahisalu et al., 2008, Negi et al., 2008). The mutant shows a dramatically reduced S-type Cl^- current but little change in R-type currents when analysed by patch clamp in guard cell protoplasts (Vahisalu et al., 2008). To test the Cl^- currents *in vivo*, I measured currents in wild-type (Wt), *slac1-1* mutant and pSLAC1 plants by voltage clamp. Figure 5.1 summarizes the mean current-voltage (I-V) curves of the anion currents from ten independent experiments from each of these lines. Voltage was clamped to conditioning steps to +40 mV and subsequent clamp steps were made to voltages more negative than approximately −40 mV. Test clamp steps yielded substantial inward-directed and instantaneous I_{Cl}. Figure 5.1 shows that both of mean instantaneous and steady-state (inset above) I_{Cl} were dramatic reduced in the *slac1-1* mutant Compared with Wt and *pSLAC1* plants, the mean instantaneous current in *slac1-1* guard cells decreased by 70–80% at voltages negative from -100 mV (-451 ± 39 in Wt; -479 ± 47 in *pSLAC1* and -153 ± 14 μA • cm^{-2} at -220 mV in *slac1-1*). Similarly, near the negative maximum at -75 mV the mean steady-state current decreased by approximately 70% in *slac1-1*.

5.3.2 Altered the Activities of K^+ Channels in *slac1-1* Mutant.

Uptake and release of K^+ across the guard cell plasma membrane is mediated largely by two subsets of Kv-like K^+ channels. Channels mediating K^+ uptake are dominated by the KAT1 K^+ channel gene product in *Arabidopsis*, and they give rise to an inward-rectifying (inward-directed) K^+ current ($I_{K,in}$) that activates at voltages near and negative of -120 mV. K^+ release occurs through the GORK K^+ channel that gives rise to an outward-rectifying (outward-directed) K^+ current ($I_{K,out}$) at voltage positive of the K^+ equilibrium voltage (Blatt, 1988, Schachtman et al., 1992, Blatt, 2000, Schroeder et al., 2001, Hosy et al., 2003). On recording $I_{K,in}$ and $I_{K,out}$ under voltage clamp (Chen et al., 2012b), I observed (figure 5.2 and figure 5.3) the suppression of $I_{K,in}$ and a moderate enhancement of $I_{K,out}$ in intact guard cells of the *slac1-1* mutant *Arabidopsis* compared with currents from guard cells of wild-type and *pSLAC1* plants (Vahisalu et al., 2008).

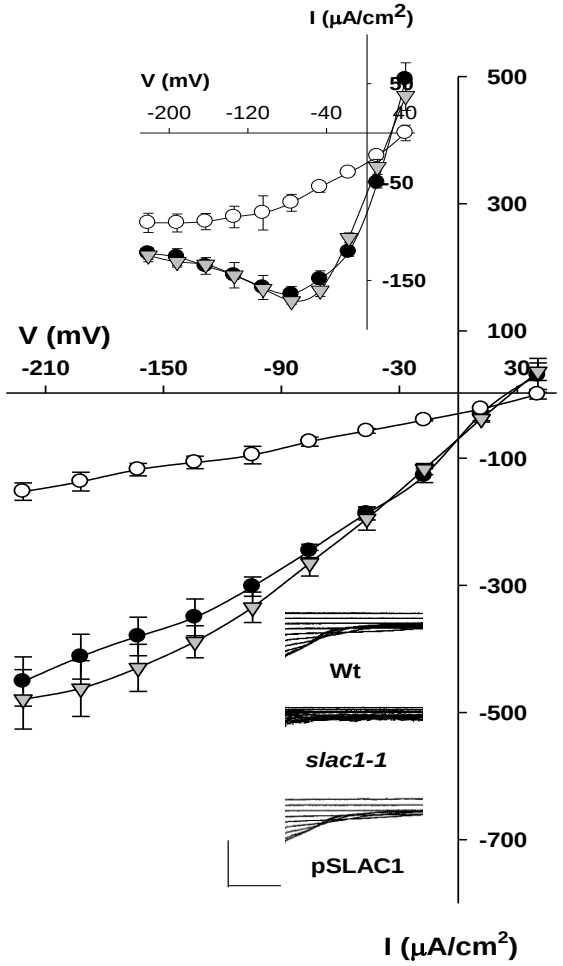

Figure 5. 1 *slac1-1* shows a reduced I_{Cl}.

Instantaneous anion current as a function of voltage from ten independent experiments as means ± SE. Measurements were carried out in 5 mM Ca^{2+} -MES buffer (pH 6.1), with 15 mM TEA-Cl and 15 mM CsCl. Data are for Wt (●), *slac1-1* (○) and pSLAC1 (▼). Voltages were clamped from a conditioning voltage of +40 mV to voltages between +40 and -220 mV in 10 s steps. Scale: 500 µA • cm^{-2} (vertical), 2 s (horizontal). Inset (*above*): steady-state current–voltage curves derived from the same measurements (cross-referenced by symbol).

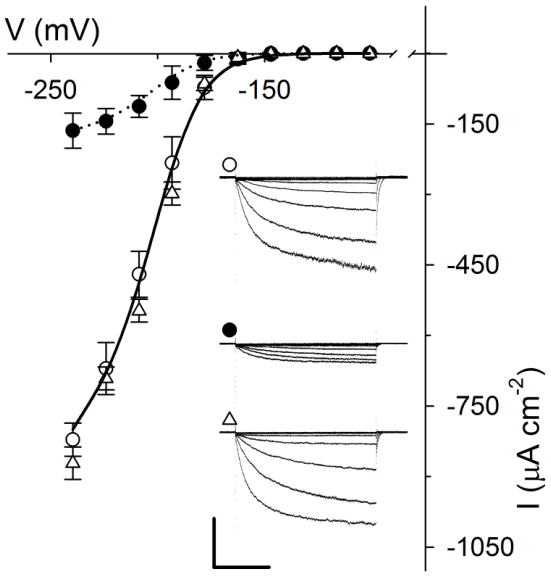

Figure 5. 2 The *slac1* mutant of *Arabidopsis* alters currents carried by inward- ($I_{K,in}$) K^+ channels.

Steady-state current recorded under voltage clamp for $I_{K,in}$ show a roughly an 80% suppression of channel current. Curves are fittings of Wt (solid line) and *slac1-1* currents (dotted line) to a Boltzmann function. *Inset*: Current traces recorded under voltage clamp and cross-referenced by symbol. *Scale*: vertical, 500 μA • cm^{-2}; horizontal, 2 s. *slac1-1* currents are significantly different ($P<0.001$) for all points negative of -180 mV. Data are means ±SE of n≥12 independent experiments for Wt (○), *slac1-1* (●), and *pSLAC1* plants (△).

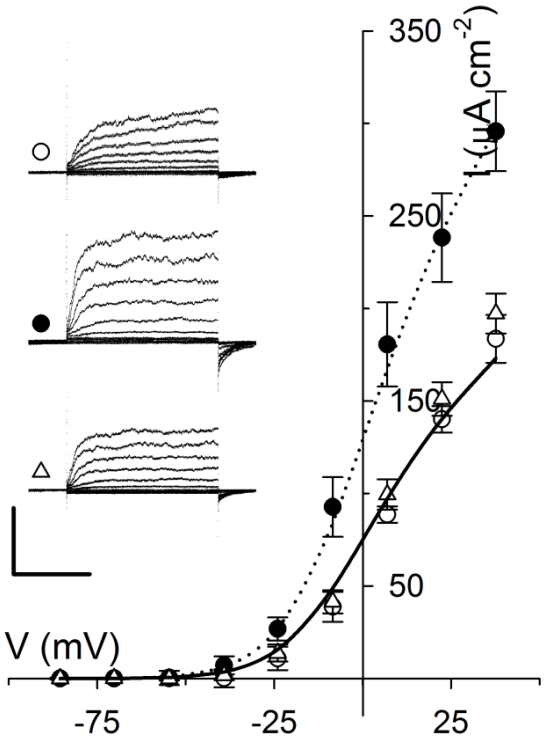

Figure 5. 3 The *slac1* mutant of *Arabidopsis* alters currents carried by outward- ($I_{K,out}$) K^+ channels.

Steady-state current recorded for $I_{K,out}$ under voltage clamp show a roughly an 50% enhancement of channel current. Curves are fittings of wild-type (solid line) and *slac1-1* currents (dotted line) to a Boltzmann function. *Inset*: Representative current traces recorded under voltage clamp and cross-referenced by symbol. Scale: vertical, 200 μA cm^{-2}; horizontal, 2 s. *slac1-1* currents are significantly different ($P<0.001$) for all points positive of -20 mV. Data are means ±SE of n≥12 independent experiments for Wt (○), *slac1-1* (●), and *pSLAC1* plants (∆).

Guard cells of wild-type and *pSLAC1* plants showed similar K^+ currents, with Wt plants yielding mean steady-state values for $I_{K,in}$ at -240 mV and $I_{K,out}$ at +40 mV of -821±35 (n=15) and +183±13 μA cm^{-2} (n=12), respectively; guard cells of the *slac1-1* mutant, however, gave currents of -164±37 (n=14) and +295±22 μA cm^{-2} (n=12) corresponding to an 80% reduction and 61% increase at these voltages respectively.

5.3.3 *slac1-1* Guard Cells Exhibit More Negative Membrane Voltage.

The membrane voltage is an important component of the electrochemical driving force for ion flux across the membrane. In turn, the membrane potential also can regulate voltage-gating channels, which are activated by changes in membrane voltage. In guard cells, the SLAC1 channel contributes to the sum of inward-directed currents which, in principle, depolarize membrane voltage. Thus in *slac1-1*, the plasma membrane voltage should be more negative than Wt. However, the abnormal K^+ currents in *slac1-1* led me to question how the membrane voltage changed in this mutant. To answer this question, I recorded membrane voltage in Wt, *slac1-1* and pSLAC1. Figure 5.4 shows the mean membrane voltage of *slac1-1* mutant guard cells was displaced negative relative to values recorded from guard cells of Wt and *pSLAC1*, consistent with loss of inward current through the SLAC1 channel

5.3 4 Slowed Stomatal Opening in *slac1-1* Mutant.

Energetic considerations rule out the idea that the SLAC1 channel contributes to anion uptake and stomatal opening (Blatt, 2000, Vahisalu et al., 2008, Barbier-Brygoo et al., 2011); indeed, eliminating the SLAC1 current was expected to accelerate opening by eliminating an efflux shunt opposing anion accumulation via H^+-coupled transport that might otherwise slow anion accumulation. By contrast, $I_{K,in}$ is a dominant pathway for K^+ uptake during opening (Blatt, 2000, Hills et al., 2012) and its suppression in the *slac1-1* mutant was expected to impair stomatal opening. Thus I expected that the reduced $I_{K,in}$ might lead to slowed stomatal opening.

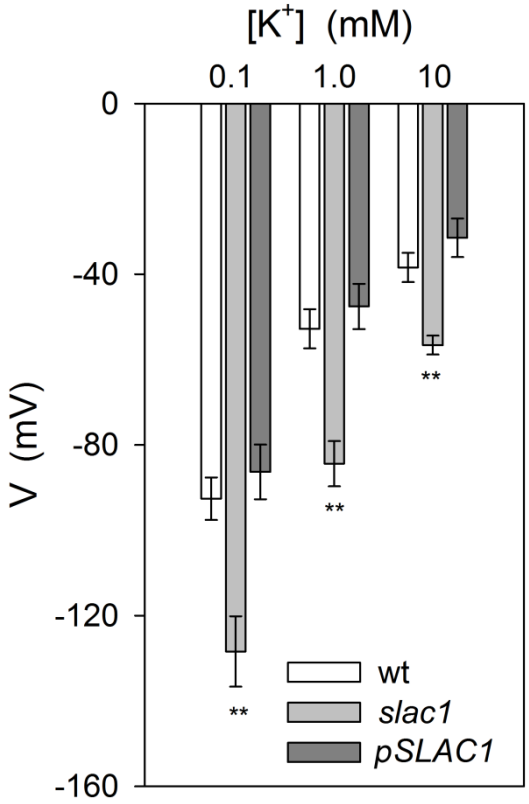

Figure 5. 4 Membrane voltage is hyperpolarised in guard cells of *slac1-1* mutant of *Arabidopsis*.

Free-running voltages recorded from wild-type, *slac1-1*, and pSLAC1:SLAC1 complemented *slac1-1* mutant Arabidopsis with 0.1, 1 and 10 mM KCl outside. Data are Means ±SE from ≥15 guard cells for each line. Values for the *slac1-1* mutant differ significantly ($P<0.001$) from that of wild-type and *pSLAC1* guard cells at all three KCl concentrations.

To explore this question, I compared the stomatal opening processes in Wt, *slac1-1* and pSLAC1. To monitor opening, I measured apertures from stomata in situ and in isolated in epidermal peels, and I recorded transpiration from intact *Arabidopsis* plants in response to step changes in light. Figure 5.5 shows gas exchange measurements yielded rates of change in transpiration that were slowed in the mutant. Although *slac1-1* showed a larger apertures and conductances than Wt and pSLAC1, the opening rate of *slac1-1* was significantly slower when compared with the Wt and pSLAC1 plants on transitions to light. Due to loss of most of Cl^- current, the closing rate was also slower than Wt and pSLAC1. Aperture measurements from epidermal peels showed same results (Figure 5.6). The stomatal aperture of Wt and pSLAC1 guard cells was faster in response light. Stomata of the *slac1-1* mutant opened with halftimes roughly 2-fold greater than either the wild-type or *pSLAC1* plants (Figure 5.6). Additionally, we traced stomatal aperture movements during whole day. Over a 24-h period, stomata of failed to close fully, opened and closed sluggishly, and responded over an elevated range of apertures in the *slac1-1* mutant when compared with the wild-type or pSLAC1 plants (Figure 5.7). These data confirm an unexpected and moderating effect of the *slac1* mutation on water loss as a result of slowed stomatal opening.

5.3.5 Altered K^+ Channel Activities Are Not Reflected in Channel Gene Transcription

The expression of several ion channel genes in *Arabidopsis* is subject to environmental cues, and potentially to homeostatic regulation (Amtmann and Blatt, 2009). One possible explanation for the altered K^+ channel currents was that the *slac1* mutation affects expression of these channels. Therefore with help from Maria Papanatsiou, I tested whether the *slac1-1* mutation might affect K^+ channels gene transcription. In the *Arabidopsis* guard cell there are several K^+ channel expressed on plasma membrane including KAT1, KAT2, KC1, GORK, AKT1 and AKT2. Thus transcripts for these K^+ channel genes were assayed by quantitative PCR using mRNA isolated from plants grown together and harvested 2 h after the start of daylight. Because *slac1-1* showed overaccumulations in K^+, we also assayed for transcripts of the predominant vacuolar K^+ channel TPK1 (Gobert et al., 2007), and the K^+- and Ca^{2+}-permeable channel, TPC1 (Peiter

et al., 2005), as well as for the vacuolar VH^+-ATPase C subunit, VHA-C, and the plasma membrane H^+-ATPases, AHA1, AHA2 and AHA5 that could affect energisation of the membranes (Haruta and Sussman, 2012). Figure 5.8 summarises results that showed there is no difference between the three plant lines, thus discounting homeostatic feedback via transcription.

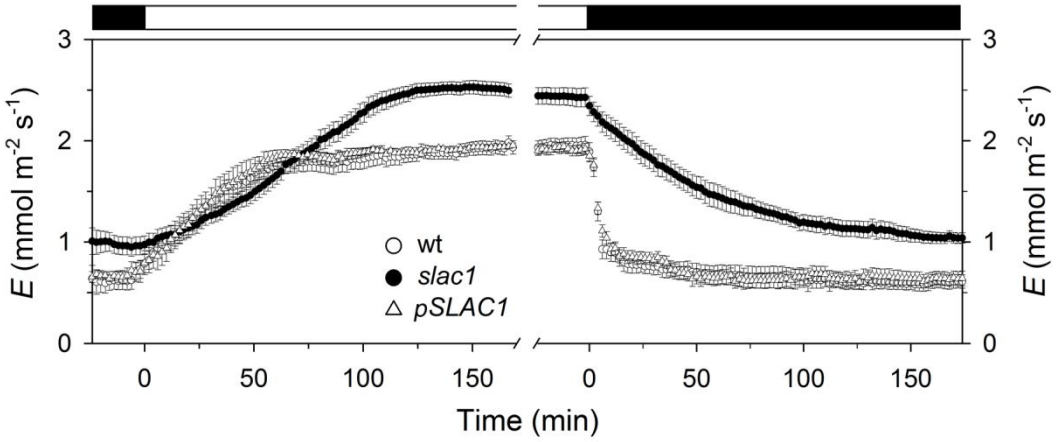

Figure 5. 5 The *slac1* mutant of *Arabidopsis* alters stomatal opening and closing on light-dark transitions.

Transpiration rates recorded from intact Arabidopsis on transition from dark to 300 μmol $m^{-2}s^{-1}$ light (left) and back to dark (right). Fitted halftimes for opening (sigmoid) and closing (single-exponential): Wt, 22.4±0.5 and 5.5±0.2 min; *slac1-1*, 65.6±0.4 and 50.7 ±0.4 min; pSLAC1, 27.1±0.4 and 6.3±0.1 min.

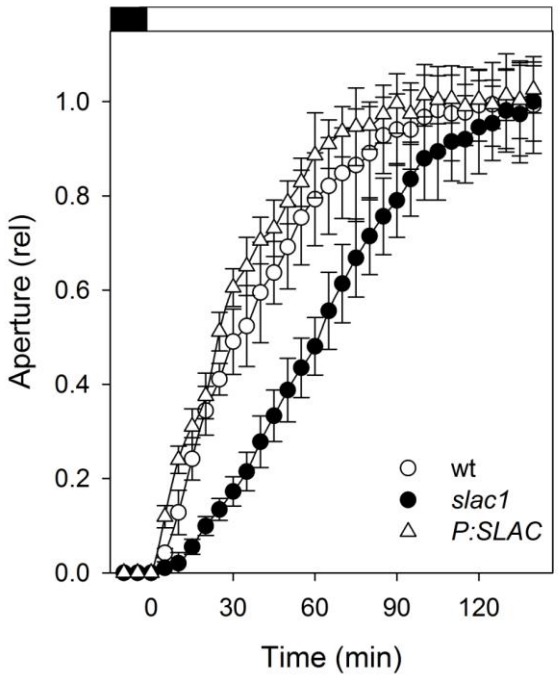

Figure 5. 6 The *slac1* mutant of *Arabidopsis* alters stomatal opening on light-dark transitions.

Stomatal apertures from epidermal peels. Data normalised to initial and final apertures on transition to 300 μmol $m^{-2}s^{-1}$ light. Opening halftimes: Wt, 38±5 min; slac1-1, 74±8 min; pSLAC1, 34±7 min. Apertures (initial/final in μm): Wt, 2.6±0.2 / 4.2±0.4; *slac1-1*, 4.0 ±0.3 / 4.8±0.4; pSLAC1, 2.6±0.2 / 4.0±0.4. Data are means ±SE of n≥12 independent experiments for Wt (○), *slac1-1* (●), and pSLAC1 plants (△).

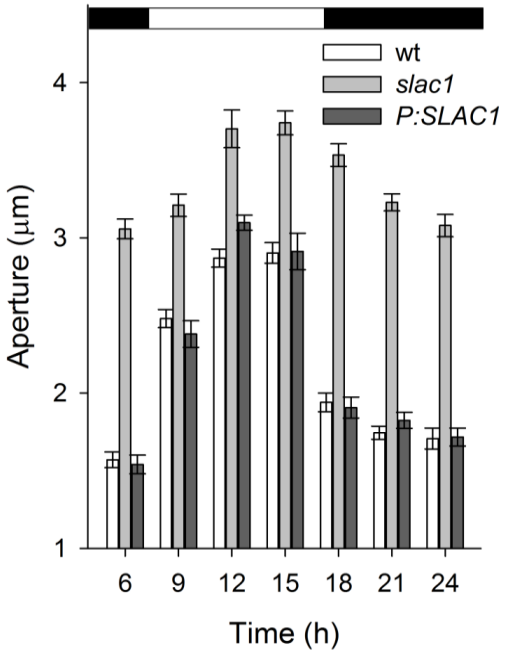

Figure 5. 7 The *slac1* mutant of *Arabidopsis* alters stomatal opening and closing.
Stomatal opening and closing recorded in leaves at 3-h intervals over 24 h. Note the slower response in the first three daylight hours for the mutant. *slac1-1* apertures are significantly different ($P<0.001$) at all times.

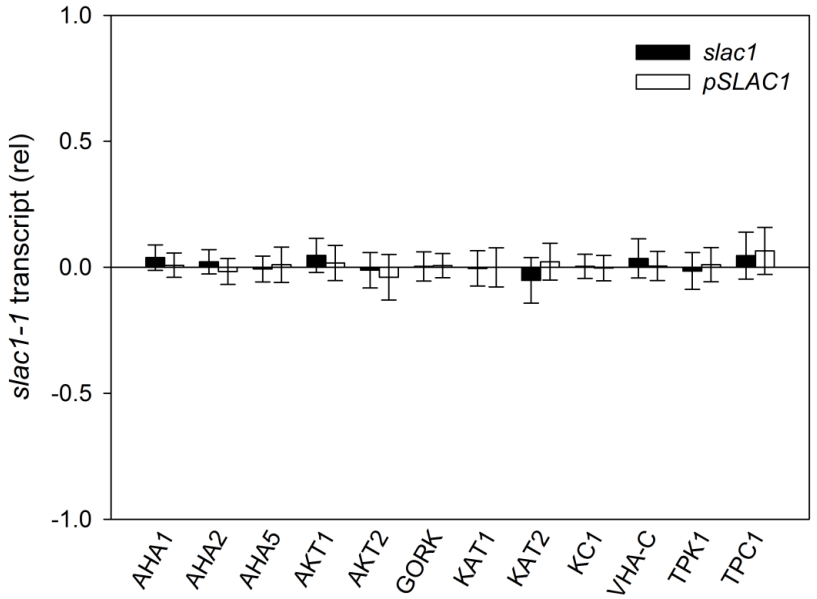

Figure 5. 8 Transcript levels for selected plasma membrane and tonoplast transporters from *slac1-1* and pSLAC1 *Arabidopsis* assayed by quantitative PCR.

Data are means ±SE of three independent experiments and are reported as the change in expression relative to Wt levels (=0) after normalising to the housekeeping *ACT2* actin gene and *TUB9* tubulin gene transcripts.

5.3.6 OnGuard Model Successfully Reproduced Stomatal Behaviors of Wt and *slac1-1*

Comparing model outputs with observed macroscopic characteristics (See Appendix) showed that the model successfully reproduced all of the major features of the slac1 mutant. As shown in Appendix Figure 4, simulated stomatal apertures, cytosolic and vacuolar solute concentrations were consistent with published experimental data. Notably, the model simulated *slac1-1* with a larger aperture than Wt and high accumulation of Cl^-, Mal and K^+ in line with our experimental data and previous published data (Negi et al., 2008). Moreover, the model also exhibited roughly a 5-fold increase in the halftime for closure and a slower rate of stomatal opening (Figure 5.9B), and similar gas exchange and aperture measurements were obtained. Most importantly, model simulated the enhanced $I_{K,out}$, and greatly reduced $I_{K,in}$ activities in the *slac1-1* simulation (Figure 5.9 C and D), much as observed experimentally. Thus the model successfully reproduced the behaviour of the Wt and *slac1-1 Arabidopsis* stomata.

5.3.7 *slac1* Is Predicted to Elevate pH and $[Ca^{2+}]_i$ Affecting K^+ Channels and Stomatal Opening

To explore the physiological context of the slac1-1 mutation, we next made use of quantitative systems modelling of the guard cell, incorporating all of the known transporters at the plasma membrane and tonoplast, their biophysical and kinetic characteristics, the salient features of sucrose and malic acid (Mal) metaboism, as well as the homeostatic parameters of Ca^{2+} and pH buffering (Hills et al., 2012). We used an equivalent ensemble of model parameters (Chen et al., 2012a) to simulate the diurnal cycle of stomatal movements after scaling guard cell volume and stomatal aperture to the dimensions of the *Arabidopsis* stomatal complex while maintaining transporter surface densities. An essential feature of this modelling approach is that the system is defined by a set of model components (transporters, metabolic and buffering reactions), the parameters of which are fixed constants defined experimentally. Thus, all of the dynamic behaviour of the system arises from the emergent interactions between model components and associated dependent variables, notably of ion and solute concentrations, and of the voltages across the two membranes (Chen et al., 2012a). Simulations were carried out first with the full complement of membrane transporters including the SLAC1 current, and then

with the SLAC1 current omitted. The model reproduced the behaviour of the wild-type *Arabidopsis* stomata and all of the salient features of the *slac1-1* mutant, notably the elevated range of stomatal apertures and accumulation of Cl^-, Mal and K^+ (Figure 5.16A); it returned roughly a 5-fold increase in the halftime for closure and a slowed rate of stomatal opening (Figure 5.9B); and it enhanced $I_{K,out}$, and greatly reduced $I_{K,in}$ activities in the *slac1-1* simulation (Figure 5.9C,D), much as observed experimentally (see Figure 5.2 and 5.3).

In addition to successfully simulating stomatal behaviors, the OnGuard model also yielded two predictions for the *slac1-1* mutant: it showed (1) roughly a 0.2 unit elevation in pH_i above the means in the Wt, both day and night, and (2) a rise in the daytime $[Ca^{2+}]_i$, to values near 400 nM (Figure 5.9E). Significantly, both elevated pH_i and $[Ca^{2+}]_i$ are known to suppress $I_{K,in}$. In *Vicia* guard cells $[Ca^{2+}]_i$ inactivates $I_{K,in}$ with a K_i of 330 nM and a Hill coefficient of 4 (Grabov and Blatt, 1999) and the current activates with $[H^+]_i$ (decreasing pH_i), showing an apparent $K_{1/2}$ near 400 nM (pH 6.4) and Hill coefficient of unity (Blatt, 1992, Grabov and Blatt, 1997). By contrast, raising pH_i enhances $I_{K,out}$, the current exhibiting a K_i for H^+ near 40 nM (pH 7.4) and a Hill coefficient of 2 (Blatt and Armstrong, 1993, Grabov and Blatt, 1997). Such quantitative detail is not available for *Arabidopsis*, but all evidence (Hoth and Hedrich, 1999, Hosy et al., 2003, Siegel et al., 2009) indicates similar pH_i and $[Ca^{2+}]_i$ sensitivities. Thus, I suspected that the elevations in pH_i and $[Ca^{2+}]_i$ predicted for the *slac1-1* guard cells might explain the altered K^+ currents of the mutant.

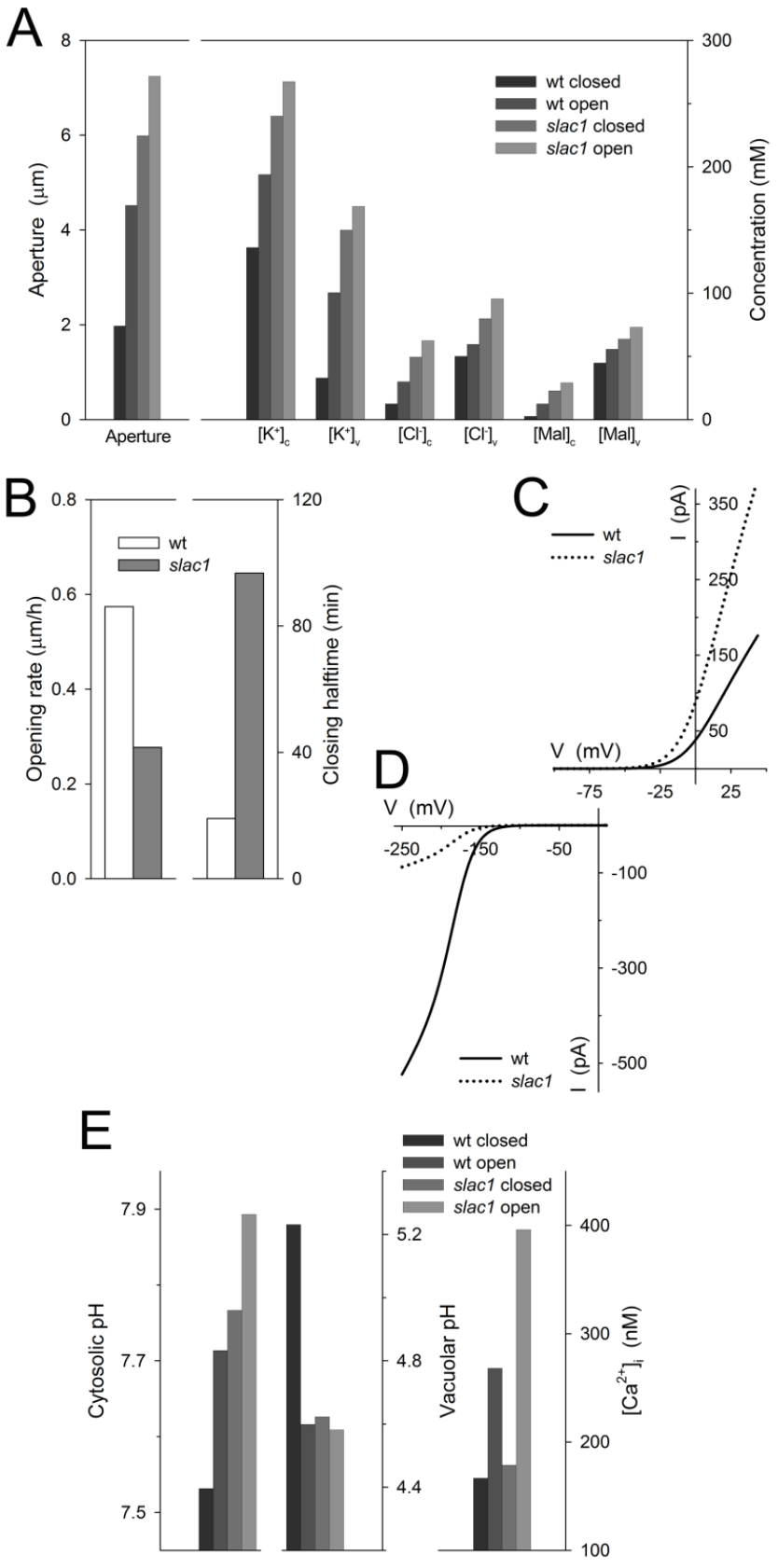
A
Aperture (µm)
Concentration (mM)
wt closed
wt open
slac1 closed
slac1 open
Aperture
[K+]c
[K+]v
[Cl-]c
[Cl-]v
[Mal]c
[Mal]v
B
Opening rate (µm/h)
Closing halftime (min)
wt
slac1
C
I (pA)
V (mV)
wt
slac1
D
V (mV)
I (pA)
wt
slac1
E
Cytosolic pH
Vacuolar pH
[Ca2+]i (nM)
wt closed
wt open
slac1 closed
slac1 open

Figure 5. 9

Figure 5.9. Quantitative systems modelling reproduces characteristics for *slac1-1* guard cells and accounts for altered K^+ channel activities through predicted elevations of pH_i and $[Ca^{2+}]_i$.

(A) Mean stomatal aperures and cytosolic and vacuolar solute concentrations for the closed and open stoma. Outputs for each variable (left to right, Wt closed and open, *slac1* closed and open).

(B) Stomatal opening rates (left) and closure halftimes (right), determined from simulated apertures during the first 3 h (opening) and the final 3 h (closing) of the daylight period (compare Figure 5.5-5.7).

(C,D) Current-voltage curves for $I_{K,out}$ (C) and $I_{K,in}$ (D) in wild-type (solid line) and slac1 (dotted line) simulations taken at 3 h into the daylight period (compare Figure 5.2-5.3).

(E) Predicted outputs (left to right, outputs for Wt closed and open, *slac1* closed and open) for cytosolic (*left*) and vacuolar pH (*right*), and for free cytosolic $[Ca^{2+}]$ ($[Ca^{2+}]_i$).

5.3.8 Direct pH and $[Ca^{2+}]_i$ Measurements and Manipulations Validate Model Predictions

To test these predictions, I recorded pH_i and $[Ca^{2+}]_i$ *in vivo* by ratiometric fluorescence imaging using the H^+-sensitive dye BCECF and the Ca^{2+}-sensitive dye Fura-2 after iontophoretic injection into guard cells. Recordings of BCECF fluorescence yielded pHi near 7.6 in Wt and *pSLAC1*, similar to guard cells of *Vicia* (Blatt and Armstrong, 1993, Grabov and Blatt, 1997); recordings from *slac1-1* guard cells showed an elevated pH_i, around 8.0 (Figure 5.10), consistent with, even exceeding, model predictions. Using butyrate treatments (Figure 5.11), I calculated a cytosolic buffer capacity of 84±6 mM H^+/pH unit for guard cells of Wt *Arabidopsis*, close to that for *Vicia* guard cells (Grabov and Blatt, 1997), and almost a 2-fold higher buffer capacity of 143±13 mM/pH unit in the *slac1-1* mutant (Figure 5.10). This increase in buffer capacity is consistent with an elevated content of organic acids (Negi et al., 2008). Measurements of $[Ca^{2+}]_i$ from guard cells of Wt and *pSLAC1* gave values near 220 nM, whereas *slac1-1* showed significantly elevated $[Ca^{2+}]_i$ with a mean value near 450 nM (Figure 5.12-13). Thus, in *slac1-1*, pHi and $[Ca^{2+}]_i$ alone appeared sufficient to explain both $I_{K,in}$ suppression and the enhancement of $I_{K,out}$, assuming kinetic sensitivities similar to those for the K^+ channels in *Vicia*.

To validate this conclusion, I tested the capacity to recover Wt activities of $I_{K,in}$ and $I_{K,out}$ in the *slac1-1* mutant when $[Ca^{2+}]_i$ and pH_i were chemically 'clamped' to suppress their elevation. *slac1-1* mutant were impaled as before, but with electrolyte including 10 mM of the Ca^{2+} buffer BAPTA (K_d 130 nM) for direct loading from the microelectrode; following impalements, the guard cells were challenged with 3 mM butyrate to lower pH_i near a value of 7.5, close to that of Wt (Figure 5.14). Analysis of five independent experiments with *slac1-1* (Figure 5.14-5.15) showed that these manipulations were sufficient to recover both $I_{K,in}$ and $I_{K,out}$ in the *slac1-1* mutant with characteristics that were quantitatively equivalent to those observed in Wt. I used a similar strategy in measurements of stomatal opening. Buffering elevated $[Ca^{2+}]_i$ by BAPTA loading was not possible in this case, so guard cells in epidermal strips were treated with butyrate to suppress pH_i as before. The results yielded rates of stomatal opening statistically equivalent to those of Wt (Figure 5.16).

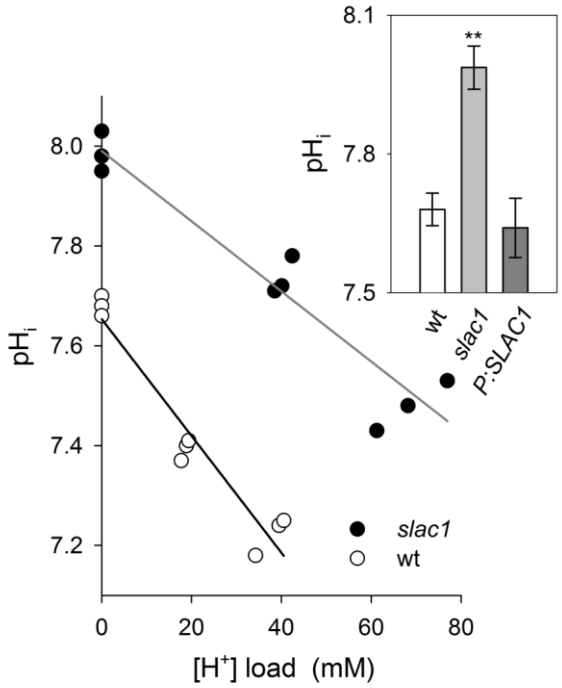

Figure 5. 10 Altered K^+ channel currents are consequent on elevation of pH_i.

Mean±SE for pH_i (inset, n≥7) and pH buffering analysis (n=3) from guard cells of wildtype (○) and *slac1-1* mutant (●) *Arabidopsis* using BCECF fluorescence ratio analysis and before and during acid loading with 1 mM and 3 mM butyrate. Buffering determined by linear fitting (solid lines, see (Grabov and Blatt, 1997)) gave 84±6 mM H^+/pH unit (wild-type), and 143±13 mM/pH unit (*slac1-1*). pH_i values from *slac1-1* guard cells differed significantly ($P<0.001$) from that of wild-type and pSLAC1.

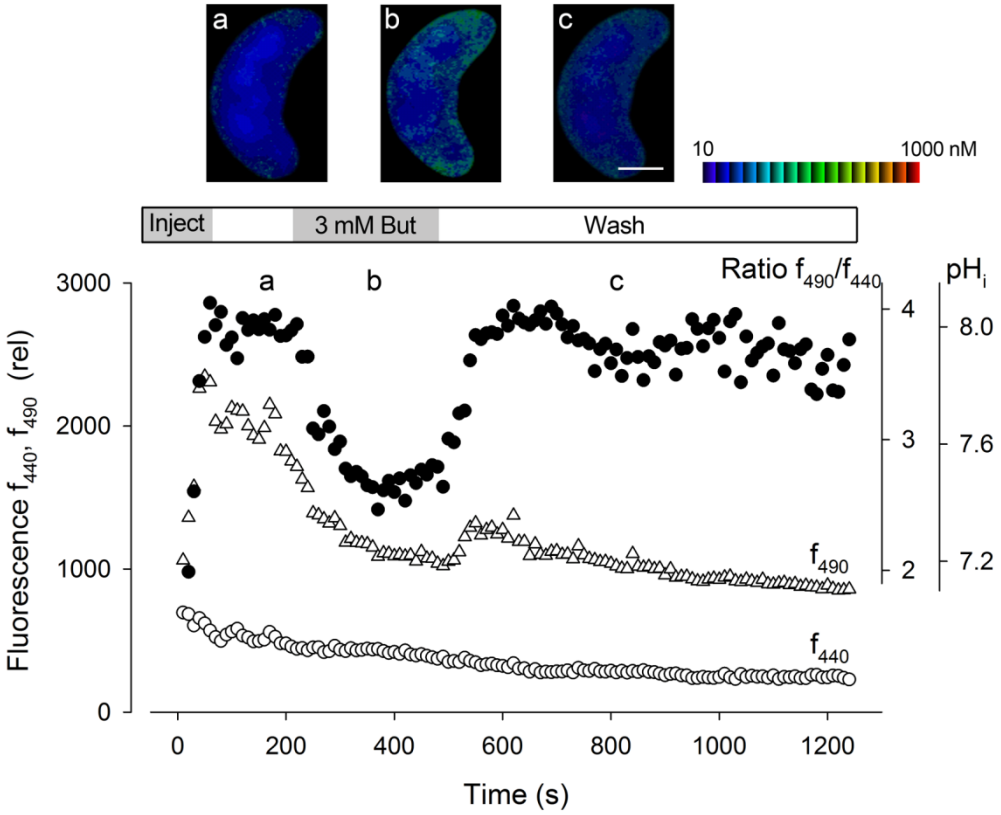

Figure 5. 11 pH_i recording from one *slac1-1* mutant guard cell using BCECF fluorescence ratiometry.

Fluorescence at 440 nm (f440, ○), 490 nm (f490, ∆), and the fluorescence ratio (f490/f440 and calibrated pH_i, ●) recorded at 10-s intervals from 1.5-µm depth around the cell periphery. Representative images (above) taken at time points indicated (a,b and c). Intensity modulated pseudocolor scale (left to right), pH 8 to pH 6. Period of BCECF injection, exposure to 3 mM butyrate, and butyrate washout as indicated.

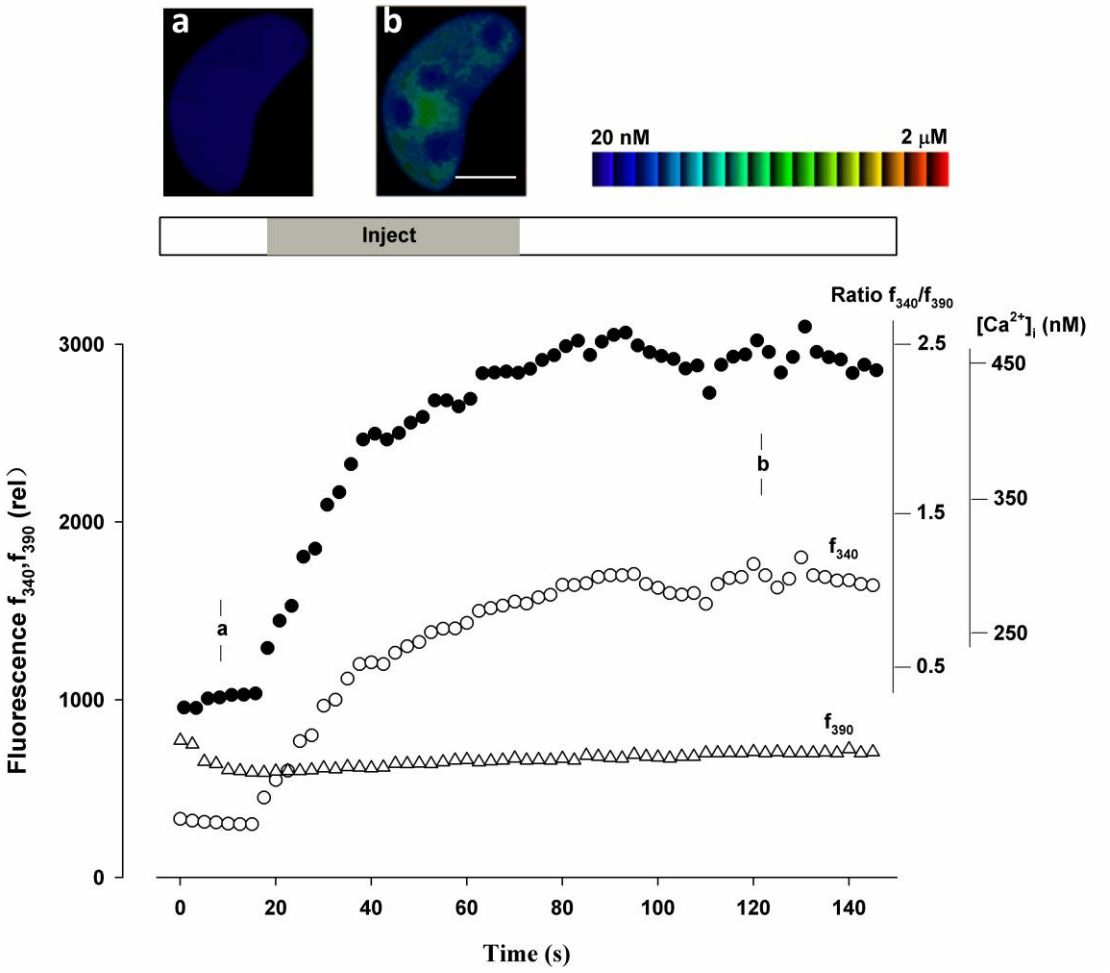

Figure 5. 12 $[Ca^{2+}]_i$ recording from one *slac1-1* mutant guard cell using Fura-2 fluorescence ratiometry.

Fluorescence at 340 nm (f_{340}, ○), 490 nm (f_{390}, Δ), and the fluorescence ratio (f_{340}/f_{390} and calibrated $[Ca^{2+}]_i$, ●) recorded at 10-s intervals from 1.5-μm depth around the cell periphery. Representative images (above) taken at time points indicated (a and b). Intensity modulated pseudocolor scale (*left to right*), concentration 20 nM to 2 μM. Period of Fura-2 injection as indicated.

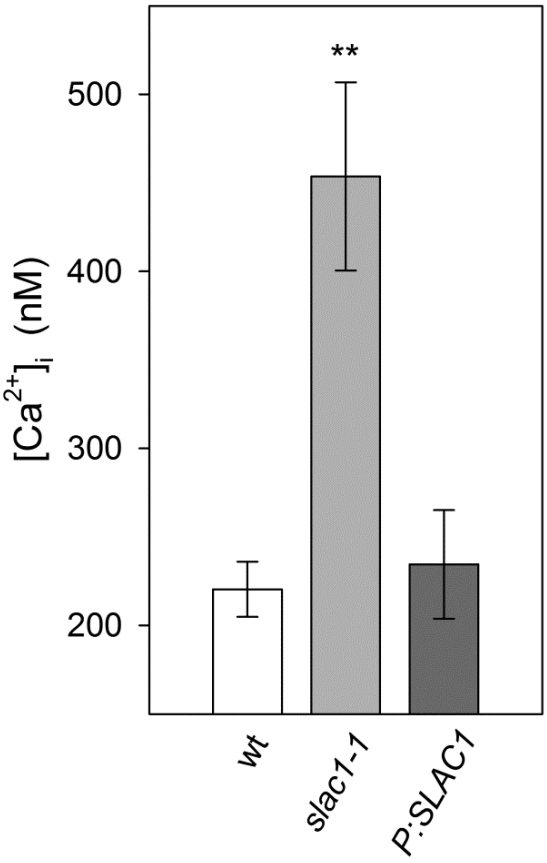

Figure 5. 13 The comparison of $[Ca^{2+}]_i$ in wild-type, *slac1-1* and pSLAC1.

Mean ±SE (n ≥5) for resting $[Ca^{2+}]_i$. Values for *slac1-1* guard cells differed significantly (P<0.001) from that of wild-type and pSLAC1.

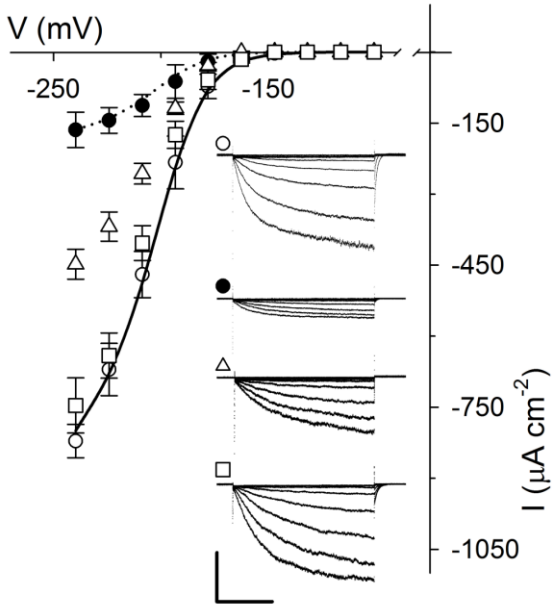

Figure 5. 14 Altered $I_{K,in}$ are consequent on elevation of cytosolic pH and free Ca^{2+} concentration in the *slac1-1* mutant.

Mean ±SE (n≥8) of steady-state currents for $I_{K,in}$ under voltage clamp show recovery of wild-type characteristics in the *slac1-1* mutant on suppressing $[Ca^{2+}]_i$ and pH_i elevations. Wt (○) and *slac1-1* (●) data included from figure 5.2 for reference. *slac1-1* guard cells were loaded with 10 mM BAPTA to buffer $[Ca^{2+}]_i$ (△) and additionally exposed to 3 mM butyrate outside (□) to lower pH_i (Figure 5.10-5.13). Inset: Current traces recorded under voltage clamp and cross-referenced by symbol. Scale: vertical, 500 μA cm^{-2}; horizontal, 2 s.

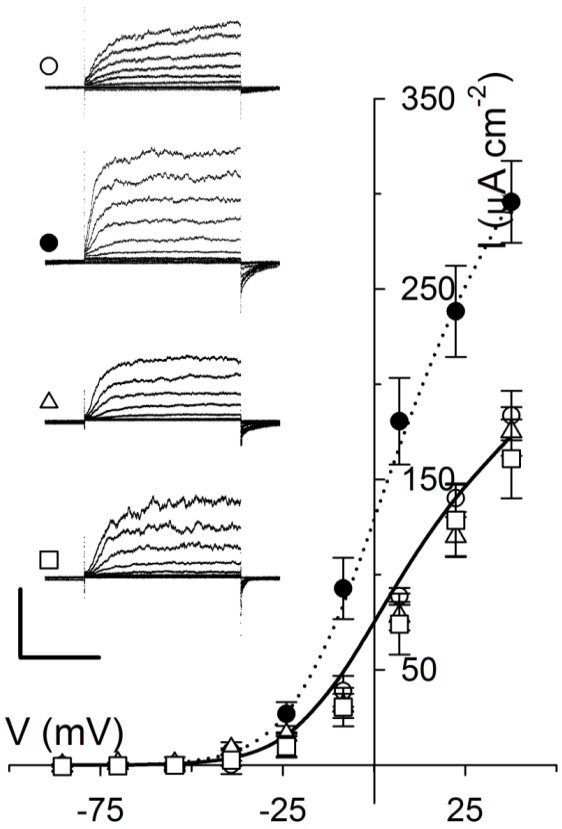

Figure 5. 15 Altered $I_{K,out}$ are consequent on elevation of cytosolic pH and free Ca^{2+} concentration in the *slac1-1* mutant.

Mean ±SE (n≥7) of steady-state currents for $I_{K,out}$ under voltage clamp show recovery of Wt current characteristics in *slac1-1* mutant guard cells on suppressing pH_i elevation. Wt (○) and slac1-1 (●) data included from Figure 5.3 for reference. *slac1-1* guard cells exposed to 3 mM butyrate outside (□) to lower pH_i [see also figure 5.10-5.13] and additionally when loaded with 10 mM BAPTA to buffer $[Ca^{2+}]_i$ (△). Inset: Current traces recorded under voltage clamp and cross-referenced by symbol. Scale: vertical, 200 μA cm^{-2}; horizontal, 2 s.

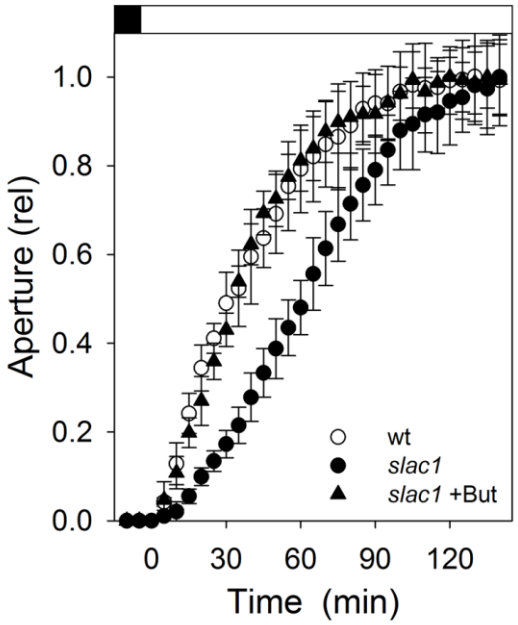

Figure 5. 16 Stomatal opening in epidermal peels on transition to 300 µmol $m^{-2}s^{-1}$ light in the presence of 3 mM butyrate (But).

Data normalised to initial and final apertures after correcting for But-induced aperture increase. Results for Wt and the *slac1-1* mutant included from Figure 5.6 for comparison. Opening halftime: *slac1-1* +But, 23±0.8 min. Apertures (initial/final in µm): Wt, 2.7±0.3 / 4.5±0.3; *slac1-1*, 4.3±0.3 / 5.1±0.3; *slac1-1* +But, 4.5±0.2 /5.6±0.2.

5.4 Discussion

The detail now available for, and complexity of guard cell transport defy any simple explanation of how guard cells achieve the range of stomatal apertures observed *in vivo*, let alone a clear understanding of the properties of the guard cell system as a whole. This gap in understanding is evident especially in the counterintuitive behaviour of stomata of the *slac1* mutant. *slac1* guard cells lack the major anion channel that mediates anion efflux during stomatal closure, yet paradoxically the cells show profound changes in K^+ channel activities and a slowed rate of stomatal opening. With Prof. Blatt, I took a computational approach to quantitative dynamic modelling of the guard cell that incorporates all of the properties for transporters at the plasma membrane and tonoplast, the salient features of osmolite metabolism, pH and Ca^{2+} buffering. The results demonstrate the true predictive power of this systems modelling approach to guide a detailed mechanistic analysis of the signaling pathways responsible, and in so doing they highlight a previously unrecognised homeostatic network that regulates membrane transport for stomatal function. The SLAC1 channel has no direct connection with solute uptake, and especially not with $I_{K,in}$ and K^+ influx; however, modelling uncovered the feedback pathway to the K^+ channels, and we confirm experimentally the link through the effect of *slac1* in elevating pH_i and $[Ca^{2+}]_i$ (see Appendix Figures). This network moderates the effect of the *slac1* mutation by suppressing $I_{K,in}$ and the rise in transpiration during the first hours of daylight, thus explaining the otherwise counterintuitive effects of *slac1* on stomatal movement.

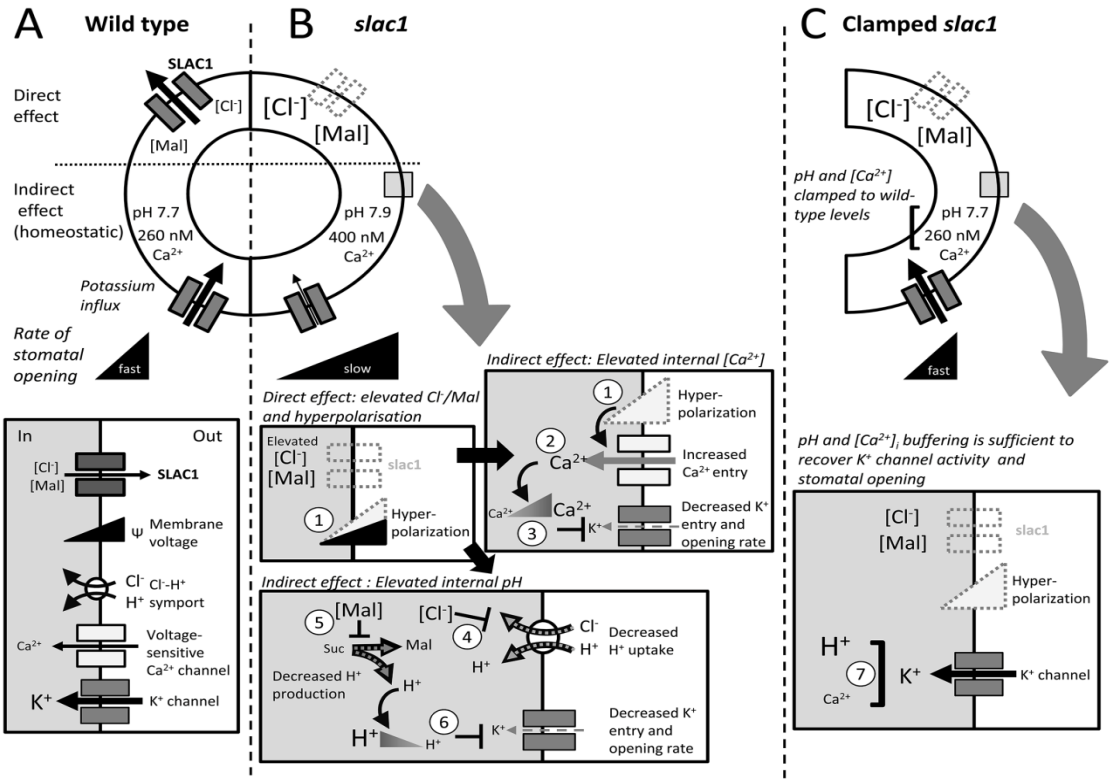

Figure 5. 17 Eliminating the SLAC1 anion channel affects K^+ channel activity, K^+ uptake and the rate of stomatal opening through its impact on cytosolic pH and $[Ca^{2+}]_i$ as predicted by the OnGuard model (Hills et al., 2012, Chen et al., 2012a). Note that effects on tonoplast transport and on $I_{K,out}$ are not included for clarity, but are complementary. (A) SLAC1 is a major pathway for Cl^- efflux during stomatal closure and is facilitated when Ca^{2+} channels activate to raise $[Ca^{2+}]_i$. The K^+ channel $I_{K,in}$ and H^+-coupled Cl^- symport are pathways for osmotic solute uptake during opening (note black arrows indicate wild-type, grey arrows indicate *slac1*). (B) The *slac1* mutation eliminates an inward current (anion efflux), leading directly to membrane hyperpolarisation (①) and Cl^- and Mal accumulation in the guard cell. Membrane hyperpolarization promotes Ca^{2+} entry by activating plasma membrane Ca^{2+} channels (②) and elevates $[Ca^{2+}]_i$, which in turn suppresses $I_{K,in}$ (③). Elevated Cl^- and Mal suppress H^+- coupled Cl^- symport (④) and Mal synthesis (⑤), thereby reducing the H^+ load on the cytosol and raising pH_i. The rise in pH_i also suppresses $I_{K,in}$ (⑥). The predicted increases in $[Ca^{2+}]_i$ and pH_i were confirmed experimentally.(C) Suppressing the rise in $[Ca^{2+}]_i$ and pH_i by buffering (⑦) was sufficient to recover K^+ channel activity and the rate of stomatal opening, thus validating the model. (Figure from Wang et al., 2012)

5.4.1 Anion Transports Link With pH_i

In the model – just as *in vivo* – changes in $[Ca^{2+}]_i$ and pH_i arise through interactions between the various transporters, metabolism and associated buffering characteristics (Hills et al., 2012, Chen et al., 2012a). The model accounts for the emergent effects of the *slac1* mutant on pH_i as a consequence of Cl^- and Mal hyperaccumulation, much as has been observed *in vivo* (Negi et al., 2008). A detailed analysis of the model outputs is presented in Appendix. It predicted pH_i in the mutant to rise with Mal transinhibition of Mal synthesis and of Cl^--mediated transinhibition of H^+-coupled anion transport. Strongly affected was the H^+-Cl^- antiport at the tonoplast, which normally transports inorganic anions into the vacuole in exchange for H^+ (De Angeli et al., 2006, Jossier et al., 2010). Overall, the result was to reduce the metabolic and transport H^+ load on the cytosol, including H^+ return to balance the H^+-ATPase at the plasma membrane (see Appendix Figure 5), hence raising pH_i. Thus, one important conclusion to be drawn from this first of the model predictions, and from its experimental validation, is of the central importance played by H^+-coupled anion transport in controlling pH_i. A detailed knowledge of Cl^- uptake in plants is restricted to a few cell types (Sanders et al., 1989) but, like that of NO_3^- (Meharg and Blatt, 1995), it is generally recognised to be mediated in symport with H^+. In fact, H^+-coupled anion transport at both membranes has been suggested to contribute to pH_i homeostasis (Barbier-Brygoo et al., 2011, Chen et al., 2012a), although direct and quantitative evidence has been lacking until now.

5.4.2 Anion Transports Link With $[Ca^{2+}]_i$

Perhaps most obvious is the link between the *slac1* mutant and elevated $[Ca^{2+}]_i$. $[Ca^{2+}]_i$ is known as a second messenger which affects many cellular processes. In the guard cells micromolar $[Ca^{2+}]_i$ suppresses $I_{K,in}$ (Grabov and Blatt, 1997) and promotes I_{Cl} (Hedrich et al., 1990, Schroeder and Keller, 1992), indicating the effect of a elevated $[Ca^{2+}]_i$ on ion transports. Our results directly point out that, in *slac1-1* mutant, the loss of anion channel results in a dramatic increase in pH_i as well as $[Ca^{2+}]_i$. Physiological range of resting $[Ca^{2+}]_i$ in guard cell is situated around 100 nM to 200 nM (Blatt, 2000). Above this concentration, it will affect the activity of $I_{K,in}$ and I_{Cl} (Blatt and Thiel, 1993, Blatt, 1999, Blatt, 2000, Chen et al., 2010). Thus, not supressingly, the 2-fold $[Ca^{2+}]_i$ in *slac1-1*

mutant (Figure 5.12-5.13) will cause $I_{K,in}$ decreased partly. But is there a "feedback" mechanism that ion channels, at least anion channels, to affect $[Ca^{2+}]_i$?

The model ascribes the elevated $[Ca^{2+}]_i$ of the mutant to loss of the SLAC1-mediated (inward) current and consequent negative shift in membrane voltage, thus promoting Ca^{2+} entry across the plasma membrane (Figure 5.4,Appendix Figure 1 and 6). By contrast with the situation for pH_i, the effect of membrane hyperpolarisation in promoting Ca^{2+} influx and elevating $[Ca^{2+}]_i$ in guard cells is well-documented (Chen et al., 2010, Grabov and Blatt, 1998, Grabov and Blatt, 1999, Hamilton et al., 2000). I note that Vahisalu, et al. (2008) reported little difference in $[Ca^{2+}]_i$ between wild-type and *slac1* mutant guard cells when recorded using the Cameleon YC3.6 Ca^{2+}-sensitive reporter. However, their measurements were determined under experimental conditions known to drive $[Ca^{2+}]_i$ – indeed, *via* control of membrane voltage (Grabov and Blatt, 1998, Grabov and Blatt, 1999, Allen et al., 2001) – effectively clamping $[Ca^{2+}]_i$ either to high or low values. Thus, their measurements cannot speak to the free-running $[Ca^{2+}]_i$, either in the wild-type or *slac1* mutant guard cells.

5.4.3 Summary

In guard cells, the SLAC1 anion channel which facilitates anion loss and stomatal closure and does not contribute to stomatal opening - nonetheless slows stomatal opening and suppresses the channels that mediate K^+ uptake for opening. The model showed how anion accumulation in the mutant suppressed the H^+ load on the cytosol and promoted Ca^{2+} influx to elevate pH_i and $[Ca^{2+}]_i$, in turn regulating the K^+ channels. We have confirmed these predictions, measuring pH_i and $[Ca^{2+}]_i$ *in vivo*, and report that experimental manipulation of pH_i and $[Ca^{2+}]_i$ is sufficent to recover K^+ channel activities and stomatal opening in the *slac1* mutant. These data uncover a previously unrecognised signaling network that ameliorates the effects of the *slac1* mutant on transpiration, and they underscore the importance of H^+-coupled anion transport for pH_i homeostasis.

I stress that my results uncover a homeostatic signalling network which, in itself, is sufficient to explain the physiopathology of the *slac1* mutant and its phenotypic

characteristics in altered K^+ transport and stomatal opening. These findings do not rule out other consequences of the *slac1* mutation, such as might be effected through more subtle changes in pH_i or $[Ca^{2+}]_i$ sensitivities of one or more of the underlying channels; however, they demonstrate that any such changes are not, in themselves, essential to understanding the effect of the *slac1* mutant either on K^+ channel activities or on stomatal movement. Our findings also pave the way, through similar dynamic modelling and validation, to addressing many other unresolved observations in stomatal physiology. This strategy is certain to yield a greater understanding of the impacts of transport at the plasma membrane. Furthermore, it should prove a powerful new tool with which to analyse transport at the tonoplast for which direct access in vivo is not possible. Challenges, for example, include resolving the controversial roles for the TPC1 cation channel in stimulus-response coupling (Peiter et al., 2005) and the counterintuitive effects of the TPK1 K^+ channel and CLCc anion antiporter, the deletion of either of which slows stomatal closure but with counterintuitive effects on K^+ (Gobert et al., 2007) and anion content (Jossier et al., 2010). Analysis of these problems will help refine our current model of the guard cell as well as our understanding of stomatal function.

CHAPTER 6:

GENERNAL DISCUSSION

6.1 Summary

Guard cells adjust stomatal pore in response to changes in the surrounding environment or to intrinsic signals. Rapid stomatal regulation is important for plant to balance the demand of carbon dioxide uptake with minimal loss of water, especially in situations of limited water resources. This process of opening and closing is subtly controlled by an ion channel system, including $I_{K,in}$, $I_{K,out}$ and anion channels, that changes the guard cell osmotic pressure and movement of water in or out of the cells. From work carried out over the past three decades, we know now that to close the aperture, guard cells activate anion channels to depolarize plasma membrane. The depolarized membrane then activates $I_{K,out}$ promoting K^+ release and it deactivates the K_{in} channels inhibiting K^+ uptake. Thus activation of anion channel is crucial step for stomatal closing.

Early studies indicated that there are at least two types of anion channel present in guard cell plasma membrane (Schroeder and Keller, 1992, Schroeder and Hedrich, 1989). These channels were dividing into two major grouping as rapid (R)-type and slow (S)-type according to differences of their voltage-dependent activation and deactivation. Although there are differences in their physiological function, both R- and S-type anion channels are activated when the plasma membrane voltage becomes more positive. These anion channels are more easily distinguished through comparing activation time. The speed of R-type channel activation, as its name implies, is approximately thousand times faster than S-type channels (Schroeder and Keller, 1992, Hedrich et al., 1990, Hedrich and Marten, 1993). In addition, activation of R-type anion channels is strongly voltage dependent, while the voltage-dependence of S-type channels is much weaker.

Various stimuli activate anion channels to cause a reduction in cell turgor. Among these signals the ABA and Ca^{2+} are considered as key players to control the anion channels. The drought hormone ABA can activate both R- and S-type anion channels in the plasma membrane of guard cells. It has been found that the protein (de-)phosphorylation plays a central role in this process. ABA activates the kinase OST1 promoting ABA regulation of guard cell transport and OST1 phosphorylates both anion and K^+ channels directly (Mustilli et al., 2002, Geiger et al., 2009, Sato et al., 2009). Upstream of OST1, the

regulatory phosphatases ABI1 and ABI2 were identified to negatively control ABA signaling (Umezawa et al., 2009, Geiger et al., 2009). We now know that the START PYR/PYL/RCAR protein family of ABA receptors interact directly with PP2C-type protein phosphatases and most likely initiates the signal cascade triggered by ABA (Park et al., 2009). Although it has been less clear how ABA regulates the anion channels from the molecular perspective, all evidence has suggested that Ca^{2+} might be involved in this process.

In this thesis, I have focused on (i) anion channel regulation from metabolic viewpoint to understand how channel control might be coordinated especially with malate (Mal) synthesis and degradation; (ii) the relationship between ABA and $[Ca^{2+}]_i$ –mediated anion channel control with reference to the phosphatase-associated START family of receptors; and (iii) how anion channel activity feeds back within the guard cell through a homeostatic network controlling the K^+ channels.

6.2 The Role of Cell Metabolism in Anion Channel Regulation

Early research uncovered evidence that guard cells sense changes in the ambient CO_2 concentration (Hedrich et al., 1994). These, and other studies showed that decreases in the CO_2 deactivated S-type anion channels and hyperpolarized the guard-cell plasma membrane (Raschke et al., 2003), suggesting that low CO_2 levels trigger hyperpolarization of guard cells. It was argued that as a result of this hyperpolarization, stomata opened to enhance diffusion of CO_2 into the leaf and thereby promote photosynthetic carbon fixation. However, recent studies have indicated that guard cells probably do not sense CO_2 directly, but instead respond to HCO_3^- synthesized from CO_2 within the cytosol by carbonic anhydrases (Hu et al., 2010). This process was shown to be dependent on the OST1 protein kinase (Xue et al., 2011) suggesting that high CO_2 concentrations stimulate phosphorylation events, which in turn lead to changes in ion transport, including the activation of SLAC1. How do these findings connect with evidence that an increased apoplastic Mal levels can be observed at high CO_2 levels when stomata are closed (Hedrich et al., 1994)? The answer has not been clear, but one explanation lies in a more direct connection to metabolism.

Mal has a multitude of functions in plant metabolism and homeostasis. It plays a key role in the mitochondrial tricarboxylic acid (TCA) cycle, in crassulacean acid metabolism (CAM) and C4 metabolism, in osmotic regulation, in pH homeostasis, and also as an important root exudates (Martinoia and Rentsch, 1994). In guard cell, Mal is widely recognized for of its role as an osmoticum in generating turgor pressure for stomatal movements (Hetherington and Woodward, 2003, Schroeder et al., 2001, Blatt, 2000, Willmer and Fricker, 1996, Sokolovski et al., 2008). Thus Mal synthesis, accumulation and transport are important for stomatal movements. Indeed anion currents were found to be linked to Mal so that low concentrations of Mal outside the guard cells affected the voltage dependence of anion currents (Hedrich and Marten, 1993, Raschke et al., 2003). These earlier studies thus focused on Mal release to the apoplast and were interpreted from this perspective, essentially ignoring any effects of Mal from the cytosolic side of the membrane. For external Mal, similar results were obtained in my experiments when treating cells with low Mal from outside. However, I found that with increasing Mal this enhancement of anion current declined. This evidence suggested to me that any dependence on external Mal concentrations was less significant and the cytosolic organic acid content was more likely to be of importance. Subsequent results confirmed that raising Mal from the cytosolic side of the membrane could block the anion current, implying a role of cytosolic organic acids in the regulation of these channels.

Oxaloacetate (OAA) is the four-carbon precursor in the formation of cytosolic Mal from phosphoenolpyruvate and is the immediate product of Mal oxidation. In addition, it is linking between the two respiratory pathway, glycolysis and TCA. Thus OAA takes a key role in metabolism regulation, and, probably, in anion currents regulation. My observations indicated that even a small increase in cytosolic OAA led to a dramatic decrease in anion currents. Most important, the apparent K_i for OAA action on the anion channels matched closely the midpoint in the variation of OAA concentrations expected during the shift from Mal synthesis to Mal degradation. All these results support the central role of OAA in stomatal movements. Thus, I interpret the findings as follows. During the early part of the day, cellular metabolism generates Mal through the synthesis and elevation in OAA concentrations; the effect in this case is to block the anion channels and to suppress

stomatal closing. During the latter part of the day, as cellular metabolism switches to Mal degradation, organic acids are drawn through the OAA intermediate, leading to a decreasing concentration of OAA and enhancing the activity of anion channels for anion efflux and stomatal closure.

From my experiments, it is confirmed that the Mal and OAA affect anion channel activity. Of course, these are only two of a number of cytosolic organic acids that might be tested; there remain a large number of other organic acids that may also regulate anion currents, including fumarate and citrate. Thus, it is impossible to confirm that OAA is the only (or even the major) organic acid regulating the anion channels. What is important is that my findings place metabolism and its cytosolic products squarely at the centre of anion channel control, unlike ealier studies that focused on these compounds as 'byproducts' with secondary actions in anion channel control. Clearly, more work will be needed in the future, especially on how various organic acids reciprocally regulate the various ion channels and their physiological roles in stomatal movements.

6.3 The Role of ABA in Anion Channel Regulation

ABA regulates numerous physiological processes in plants. In guard cells, ABA has been widely recognized to trigger anion channel activity for stomatal closure. To acivate anion channels, ABA engages two parallel signaling pathways, one of which was recently indentified as the PYR/PYL-PP2C/SnRK pathway. All evidence now suggests that ABA is perceived by members of the START PYR/PYL/RCAR protein family and its binding leads the receptor proteins to interact directly with PP2C-type protein phosphatases (Park et al., 2009). The PP2Cs ABI1 and ABI2 act as negative regulators in ABA signalling and inactivate downstream SnRK2 kinases by direct dephosphorylation (Umezawa et al., 2009, Geiger et al., 2009). The ABA signal is thus passed to anion channels, as well as K^+ channels (Sato et al., 2009), by SnRK-mediated phosphorylation activity (Mustilli et al., 2002, Geiger et al., 2009). The other major pathway for ABA signalling passes through $[Ca^{2+}]_i$. It has long been known that ABA elevates $[Ca^{2+}]_i$ through the combined effects of Ca^{2+} entry at the plasma membrane and Ca^{2+} release from endomembrane stores (Blatt, 2000, MacRobbie, 2000). Notably, ABA activates Ca^{2+} channels at the plasma membrane,

facilitating Ca^{2+} influx and triggering Ca^{2+}-induced Ca^{2+} release (Grabov and Blatt, 1997, Grabov and Blatt, 1998, Grabov and Blatt, 1999, Hamilton et al., 2001, Hamilton et al., 2000).

Although these are separated pathways, there are several connections between them. The PP2C-SnRK has been shown to be located in the key position among these connections, and the PP2Cs ABI1 and ABI2 also affect $[Ca^{2+}]_i$. For example, the *abi1-1* and *abi2-1* mutations impair ABA-induced stomatal closure in Arabidopsis and were shown to affect ABA-induced ROS production and ROS activation of plasma membrane Ca^{2+} channels that mediate Ca^{2+} influx (Pei et al., 2000, Murata et al., 2001). Similar results were found on *ost1* mutant (Mustilli et al., 2002) indicating the protein phosphatase–kinase pair PP2C and SnRK play a role in $[Ca^{2+}]_i$ regulation. Thus the ABA receptor which initiates protein phosphorylation events is also connected to $[Ca^{2+}]_i$ elevation, although little mechanistic detail has been to hand.

My works on *pyr1/pyl1/pyl2/pyl4* quadruple mutant supports the role of the cytosolic ABA receptor PYL/PYR function as an initiator of ABA-$[Ca^{2+}]_i$ events and it links the START proteins to Ca^{2+} through ROS-mediated channel activation. Although we cannot exclude other ABA receptors, the main ABA signal from cytosol side is passing through PYL/PYR-PP2C-SnRK. Therefore, the PYL/PYR, PP2Cs and SnRKs combined as ABA "STARTor", followed with two parallel pathways: Ca^{2+} dependent and Ca^{2+} independent to active anion channels (Figure 6.1).

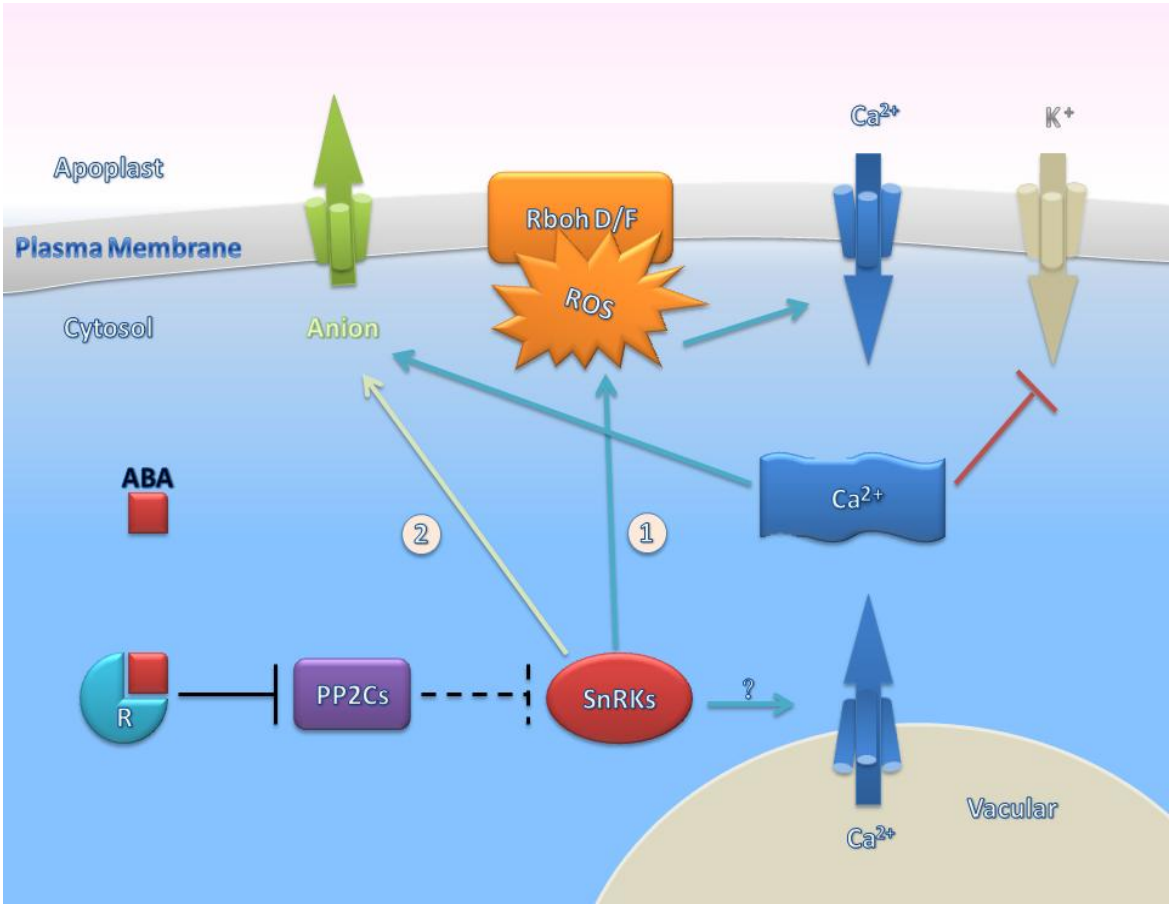

Figure 6. 1 ABA signalling cascade from cytosol.

Once ABA combines with the PYL/PYR protein (R), it immediately suppresses the activity of the 2C-type protein phosphatases (PP2Cs) releasing protein kinases of the SnRK family (SnRK). The SnRKs then (1) activate the anion channels, and (2) trigger ROS production which promotes Ca^{2+} channels and elevates $[Ca^{2+}]_i$. The elevated $[Ca^{2+}]_i$ also serves to activate anion channels.

6.4 A Homeostatic Network Link to Anion Channel

As noted above, the anion channels in guard cells contribute to stomatal movements by providing a pathway for export of osmotic solutes, especially Cl^- and Mal. When activated, the anion channels also serve to drive the membrane voltage positive and to promote K^+ efflux. The *slac1* mutant was first identified because its guard cells fail to close stomata, and detailed analysis showed that the mutant lacks the major S-type anion channel (Vahisalu et al., 2008, Negi et al., 2008). Remarkably, these guard cells also showed profound changes in K^+ channel activities and a slower rate of stomatal opening. Indeed the SLAC1 channel has no direct connection with solute uptake, and especially not with $I_{K,in}$ and K^+ influx. My experiments and model predictions derived from Prof. Blatt's work, provide evidence of an homeostatic network that regulates the K^+ channels, connecting them with the anion channels, and I have confirmed experimentally this link through the effect of *slac1* in elevating pH_i and $[Ca^{2+}]_i$.

Cytosolic Ca^{2+} and pH have long been known to serve parallel signalling pathways that affect K^+ and anion channel behaviour (Blatt, 2000). Elevating $[Ca2^+]_i$ leads to an inactivation current carried by $I_{K,in}$ and to the activation of I_{Cl} (Grabov and Blatt, 1997, Pei et al., 1997). Once positive of the K^+ equilibrium voltage, the flux of Cl^- and other anions is balanced by a parallel flux of K^+ through $I_{K,out}$ and results in a net loss of osmotically active solutes. How the anion channels could influence on $[Ca^{2+}]_i$ homeostasis is less obvious. From my experiments, I could show that loss of anion efflux and accumulation of Cl^- and Mal leads to a $[Ca^{2+}]_i$ elevation, which in turn suppressed $I_{K,in}$ and stomatal opening. Similarly, my work demonstrated that pH_i, like $[Ca^{2+}]_i$, was increased in *slac1* mutant as a consequence of anion accumulation. Most important, an analysis of the model outputs predicting the rise in pH_i and $[Ca^{2+}]_i$ showed that these effects could be connected to trans-inhibition of the H^+ loads generated by metabolism and transport. Thus, again, the findings emphasize that transport and metabolism signal to each other. In this case, they suggest a homeostatic signalling network that links SLAC1 and the K^+ channels through the intermediates of pH_i and $[Ca^{2+}]_i$ to regulate stomatal movement.

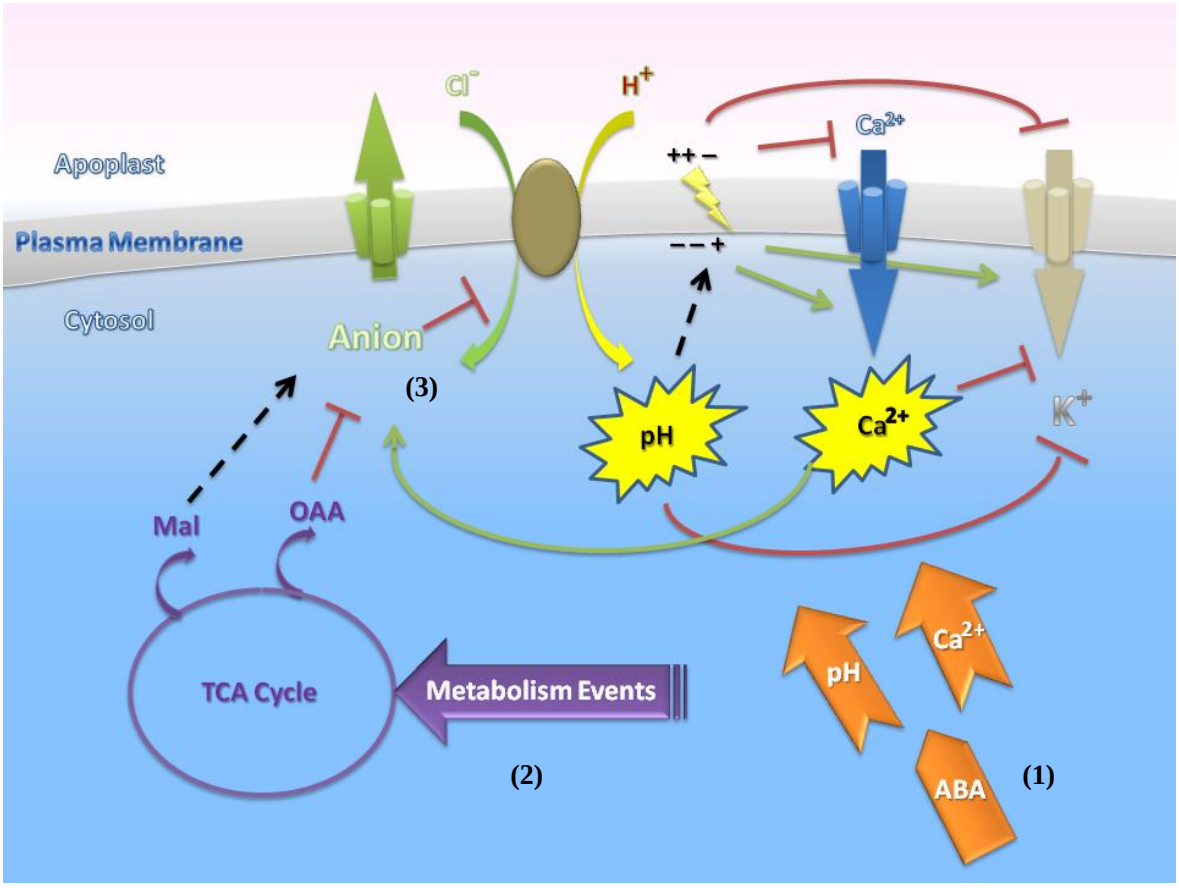

Figure 6. 2 Signalling cascade summarized from this thesis.

(1) ABA leads to two parallel signalling pathways dependent on pH and Ca^{2+} (details see Chapter 1). (2) Metabolism results in cytosolic organic acid systhesis and degradation. The small amount of OAA present during the synthesis phase is expected to suppress anion currents. By contrast, Mal exhibits a biphasic effect on anion channel activities depending on its concentration, and these effects are not consistent with a role in regulating the channels in vivo. (3) Cytosolic ion homeostasis impacts on ion channel regulation. Once anion concentration is changed, it will affects H^+-coupled Cl^- transport activities and, consequently, cytosolic $[H^+]$. Cl^- channel activity also affects membrane voltage and, consequently, the capacity for elevating $[Ca^{2+}]_i$. Elevating pH and $[Ca^{2+}]_i$ nactivates K_{in} channels and activates K_{out} channels.Positive activation is noted by an arrow; bars indicate repression and dotted lines indicate activation under different circumstance.

REFERENCES

ACHE, P., BECKER, D., IVASHIKINA, N., DIETRICH, P., ROELFSEMA, M. R. G. & HEDRICH, R. 2000. GORK, a delayed outward rectifier expressed in guard cells of *Arabidopsis thaliana*, is a K^+-selective, K^+-sensing ion channel. *Febs Letters,* 486**,** 93-98.

ALBERTS, B., JOHNSON, A., LEWIS, J., RAFF, M., ROBERTS, K. & WALTER, P. 2002. *Molecular Biology of the Cell, 4th edition,* New York, Garland Science.

ALLAWAY, W. G. 1973. Accumulation of malate in guard cells of *Vicia faba* during stomatal opening. *Planta,* 110**,** 63-70.

ALLEN, G. J., AMTMANN, A. & SANDERS, D. 1998. Calcium-dependent and calcium-independent K^+ mobilization channels in *Vicia faba* guard cell vacuoles. *Journal of Experimental Botany,* 49**,** 305-318.

ALLEN, G. J., CHU, S. P., HARRINGTON, C. L., SCHUMACHER, K., HOFFMAN, T., TANG, Y. Y., GRILL, E. & SCHROEDER, J. I. 2001. A defined range of guard cell calcium oscillation parameters encodes stomatal movements. *Nature,* 411**,** 1053-1057.

ALLEN, G. J., KUCHITSU, K., CHU, S. P., MURATA, Y. & SCHROEDER, J. I. 1999a. *Arabidopsis abi1-1* and *abi2-1* phosphatase mutations reduce abscisic acid-induced cytoplasmic calcium rises in guard cells. *Plant Cell,* 11**,** 1785-1798.

ALLEN, G. J., KWAK, J. M., CHU, S. P., LLOPIS, J., TSIEN, R. Y., HARPER, J. F. & SCHROEDER, J. I. 1999b. Cameleon calcium indicator reports cytoplasmic calcium dynamics in *Arabidopsis* guard cells. *Plant Journal,* 19**,** 735-747.

ALLEN, G. J. & SANDERS, D. 1994. Two voltage-gated, calcium-release channels coreside in the vacuolar membrane of broad bean guard cells. *Plant Cell,* 6**,** 685-694.

ALLEN, G. J. & SANDERS, D. 1995. Calcineurin, a type 2B protein phosphatase, modulates the Ca^{2+}-permeable slow vacuolar ion channel of stomatal guard cells. *Plant Cell,* 7**,** 1473-1483.

ALLEN, G. J. & SANDERS, D. 1996. Control of ionic currents in guard cell vacuoles by cytosolic and luminal calcium. *Plant Journal,* 10**,** 1055-1069.

AMODEO, G., ESCOBAR, A. & ZEIGER, E. 1994. A cationic channel in the guard cell tonoplast of *Allium cepa*. *Plant Physiology,* 105**,** 999-1006.

AMTMANN, A. & BLATT, M. R. 2009. Regulation of macronutrient transport. *New Phytologist,* 181**,** 35-52.

APEL, K. & HIRT, H. 2004. Reactive oxygen species: Metabolism, oxidative stress, and signal transduction. *Annual Review of Plant Biology,* 55**,** 373-399.

ARMSTRONG, F. & BLATT, M. R. 1995. Evidence for K^+ channel control in *Vicia* guard cells coupled by G-proteins to a 7tms receptor mimetic. *Plant Journal,* 8**,** 187-198.

ARMSTRONG, F., LEUNG, J., GRABOV, A., BREARLEY, J., GIRAUDAT, J. & BLATT, M. R. 1995. Sensitivity to abscisic acid of guard cell K^+ channels is suppressed by *abi1-1,* a mutant *Arabidopsis* gene encoding a putative protein phosphatase. *Proceedings of the National Academy of Sciences of the United States of America,* 92**,** 9520-9524.

ASAI, N., NAKAJIMA, N., KONDO, N. & KAMADA, H. 1999. The effect of osmotic stress on the solutes in guard cells of *Vicia faba L*. *Plant and Cell Physiology,* 40**,** 843-849.

ASAI, N., NAKAJIMA, N., TAMAOKI, M., KAMADA, H. & KONDO, N. 2000. Role of malate synthesis mediated by phosphoenolpyruvate carboxylase in guard cells in the regulation of stomatal movement. *Plant and Cell Physiology,* 41**,** 10-15.

ASSMANN, S. M. 1995. Cyclic-AMP as a 2nd messenger in higher-plants-status and future-prospects. *Plant Physiology,* 108**,** 885-889.

BARBIER-BRYGOO, H., DE ANGELI, A., FILLEUR, S., FRACHISSE, J.-M., GAMBALE, F., THOMINE, S. & WEGE, S. 2011. Anion Channels/Transporters in Plants: From Molecular Bases to Regulatory Networks. *In:* MERCHANT, S. S., BRIGGS, W. R. & ORT, D. (eds.) *Annual Review of Plant Biology, Vol 62.*

BARRAGAN,V., LEIDI, E.O., ANDRES, Z., RUBIO, L., DE LUCA, A., FERNANDEZ, J. A., CUBERO, B. & PARDO, J. M. 2012. Ion Exchangers NHX1 and NHX2 Mediate Active Potassium Uptake into Vacuoles to Regulate Cell Turgor and Stomatal Function in *Arabidopsis*. *Plant cell,* 24**,** 1127-1142

BARRS, H. D. & WEATHERLEY, P. E. 1962. A re-examination of the relative turgidity technique for estimating water deficits in leaves. *Australian Journal of Biological Sciences,* 15**,** 413-428.

BECKER, D., DREYER, I., HOTH, S., REID, J. D., BUSCH, H., LEHNEN, M., PALME, K. & HEDRICH, R. 1996. Changes in voltage activation, Cs^+ sensitivity, and ion permeability in H5 mutants of the plant K^+ channel KAT1. *Proceedings of the National Academy of Sciences of the United States of America,* 93**,** 8123-8128.

BEILBY, M. J. & WALKER, N. A. 1981. Chloride transport in *Chara* I. kinetics and current-voltage curves for a probable proton symport. *Journal of Experimental Botany,* 32**,** 43-54.

BEWELL, M. A., MAATHUIS, F. J. M., ALLEN, G. J. & SANDERS, D. 1999. Calcium-induced calcium release mediated by a voltage-activated cation channel in vacuolar vesicles from red beet. *Febs Letters,* 458**,** 41-44.

BLATT, M. R. 1987. Electrical characteristics of stomatal guard cells: The ionic basis of the membrane potential and the consequence of potassium chlorides leakage from microelectrodes. *Planta,* 170**,** 272-287.

BLATT, M. R. 1988. Potassium-dependent, bipolar gating of K^+ channels in guard cells. *Journal of Membrane Biology,* 102**,** 235-246.

BLATT, M. R. 1990. Potassium channel currents in intact stomatal guard cells: rapid enhancement by abscisic acid. *Planta,* 180**,** 445-455.

BLATT, M. R. 1991. Ion channel gating in plants: physiological implications and integration for stomatal function. *Journal of Membrane Biology,* 124**,** 95-112.

BLATT, M. R. 1992. K^+ channels of stomatal guard cells. Characteristics of the inward rectifier and its control by pH. *Journal of General Physiology,* 99**,** 615-644.

BLATT, M. R. 1999. Reassessing roles for Ca^{2+} in guard cell signalling. *Journal of Experimental Botany,* 50**,** 989-999.

BLATT, M. R. 2000. Cellular signaling and volume control in stomatal movements in plants. *Annual Review of Cell and Developmental Biology,* 16**,** 221-241.

BLATT, M. R. 2004. *Membrane transport in plants*. Blackwell Publishing.

BLATT, M. R. 2008. Ion transport at the plant plasma membrane. *Life Sciences*. DOI: 10.1002/9780470015902.a0001307.pub2

BLATT, M. R. & ARMSTRONG, F. 1993. K^+ channels of stomatal guard cells abscisic acid evoked control of the outward rectifier mediated by cytoplasmic pH. *Planta,* 191**,** 330-341.

BLATT, M. R. & BEILBY, M. J. 2007. Mitochondrial sequestration of BCECF after ester loading in the giant alga *Chara australis*. *Protoplasma,* 232**,** 131-136.

BLATT, M. R. & CLINT, G. M. 1989. Mechanisms of fusicoccin action kinetic modification and inactivation of potassium channels in guard cells. *Planta,* 178**,** 509-523.

BLATT, M. R., GARCIA-MATA, C. & SOKOLOVSKI, S. 2007. *Membrane transport and Ca^{2+} oscillations in guard cells*. Rhythms in plants: phenomenology, mechanisms, and adaptive significance, Springer.

BLATT, M. R. & GRABOV, A. 1997. Signalling gates in abscisic acid mediated control of guard cell ion channels. *Physiologia Plantarum,* 100**,** 481-490.

BLATT, M. R. & GRADMANN, D. 1997. K^+ sensitive gating of the K^+ outward rectifier in *Vicia* guard cells. *Journal of Membrane Biology,* 158**,** 241-256.

BLATT, M. R., MAUROUSSET, L. & MEHARG, A. A. 1997. High-affinity NO_3^--H^+ cotransport in the fungus *Neurospora*: Induction and control by pH and membrane voltage. *Journal of Membrane Biology,* 160**,** 59-76.

BLATT, M. R., RODRIGUEZNAVARRO, A. & SLAYMAN, C. L. 1987. Potassium-proton symport in *Neurospora*: kinetic control by pH and membrane potential. *Journal of Membrane Biology,* 98**,** 169-189.

BLATT, M. R. & SLAYMAN, C. L. 1983. KCl leakage from microelectrodes and its impact on the membrane parameters of a nonexcitable cell. *Journal of Membrane Biology,* 72**,** 223-234.

BLATT, M. R. & SLAYMAN, C. L. 1987. Role of "active" potassium transport in the regulation of cytoplasmic pH by nonanimal cells. *Proceedings of the National Academy of Sciences of the United States of America,* 84**,** 2737-2741.

BLATT, M. R. & THIEL, G. 1993. Hormonal control of ion channel gating. *Annual Review of Plant Physiology and Plant Molecular Biology,* 44**,** 543-567.

BLATT, M. R. & THIEL, G. 1994. K^+ channels of stomatal guard cells - bimodal control of the K^+ inward rectifier evoked by Auxin. *Plant Journal,* 5**,** 55-68.

BLATT, M. R., THIEL, G. & TRENTHAM, D. R. 1990. Reversible inactivation of K^+ channels of *Vcia* stomatal guard cells following the photolysis of caged inositol 1, 4, 5-trisphosphate. *Nature,* 346**,** 766-769.

BREARLEY, J., VENIS, M. A. & BLATT, M. R. 1997. The effect of elevated CO_2 concentrations on K^+ and anion channels of *Vicia faba* L. guard cells. *Planta,* 203**,** 145-154.

BUSH, D. S. 1995. Calcium regulation in plant cells and its role in signaling. *Annual Review of Plant Physiology and Plant Molecular Biology,* 46**,** 95-122.

CHEN, L. S., LIN, Q. & NOSE, A. 2002. A comparative study on diurnal changes in metabolite levels in the leaves of three crassulacean acid metabolism (CAM) species, *Ananas comosus, Kalanchoe daigremontiana and K.pinnata*. *Journal of Experimental Botany,* 53**,** 341-350.

CHEN, Y.-H., HU, L., PUNTA, M., BRUNI, R., HILLERICH, B., KLOSS, B., ROST, B., LOVE, J., SIEGELBAUM, S. A. & HENDRICKSON, W. A. 2010a. Homologue structure of the SLAC1 anion channel for closing stomata in leaves. *Nature,* 467**,** 1074-1080.

CHEN, Z.-H., HILLS, A., BAETZ, U., AMTMANN, A., LEW, V. L. & BLATT, M. R. 2012a. Systems dynamic modeling of the stomatal guard cell predicts emergent behaviors in transport, signaling, and volume control. *Plant Physiology,* 159**,** 1235-1251.

CHEN, Z.-H., HILLS, A., LIM, C. K. & BLATT, M. R. 2010b. Dynamic regulation of guard cell anion channels by cytosolic free Ca^{2+} concentration and protein phosphorylation. *Plant Journal,* 61**,** 816-825.

CHEN, Z., EISENACH, C., XU, X., HILLS, A. & BLATT, M. 2012b. Protocol: optimised electrophysiological analysis of intact guard cells from *Arabidopsis*. *Plant Methods,* 8:15 10.1186/1746-4811-8-15.

CHENG, N. H., PITTMAN, J. K., BARKLA, B. J., SHIGAKI, T. & HIRSCHI, K. D. 2003. The *Arabidopsis cax1* mutant exhibits impaired ion homeostasis, development, and hormonal responses and reveals interplay among vacuolar transporters. *Plant Cell,* 15**,** 347-364.

CLAYTON, H., KNIGHT, M. R., KNIGHT, H., MCAINSH, M. R. & HETHERINGTON, A. M. 1999. Dissection of the ozone-induced calcium signature. *Plant Journal,* 17**,** 575-579.

CLINT, G. M. & BLATT, M. R. 1989. Mechanisms of fusicoccin action: evidence for concerted modulations of secondary K^+ transport in a higher-plant cell. *Planta,* 178**,** 495-508.

COELLO, P., HEY, S. J. & HALFORD, N. G. 2011. The sucrose non-fermenting-1-related (SnRK) family of protein kinases: potential for manipulation to improve stress tolerance and increase yield. *Journal of Experimental Botany,* 62**,** 883-893.

COLCOMBET, J., LELIEVRE, F., THOMINE, S., BARBIER-BRYGOO, H. & FRACHISSE, J. M. 2005. Distinct pH regulation of slow and rapid anion channels at the plasma membrane of *Arabidopsis thaliana* hypocotyl cells. *Journal of Experimental Botany,* 56**,** 1897-1903.

COSGROVE, D. J. & HEDRICH, R. 1991. Stretch-activated chloride, potassium, and calcium channels coexisting in plasma membranes of guard cells of *Vicia faba* L. *Planta,* 186**,** 143-153.

COTELLE, V., PIERRE, J. N. & VAVASSEUR, A. 1999. Potential strong regulation of guard cell phosphoenolpyruvate carboxylase through phosphorylation. *Journal of Experimental Botany,* 50**,** 777-783.

COUSSON, A. 1999. Pharmacological study of two potential Ca^{2+} signalling pathways within stomatal closing in response to abscisic acid in *Commelina communis* L. *Plant Science,* 145**,** 67-74.

CROSS, A. R. & JONES, O. T. G. 1986. The effect of the inhibitor diphenylene iodonium on the superoxide-generating system of neutrophils. Specific labelling of a component polypeptide of the oxidase. *Biochemical Journal,* 237**,** 111-116.

CUTLER, S. R.,RODRIGUEZ, P. L.,FINKELSTEIN, R. R. & ABRAMS, S. R. 2010. Abscisic Acid: Emergence of a Core Signaling Network. *Annual Review of Plant Biology*, 61**,** 651-679

CZEMPINSKI, K., FRACHISSE, J. M., MAUREL, C., BARBIER-BRYGOO, H. & MUELLER-ROEBER, B. 2002. Vacuolar membrane localization of the *Arabidopsis* 'two-pore' K^+ channel KCO1. *Plant Journal,* 29**,** 809-820.

DARAM, P., URBACH, S., GAYMARD, F., SENTENAC, H. & CHEREL, I. 1997. Tetramerization of the AKT1 plant potassium channel involves its C-terminal cytoplasmic domain. *Embo Journal,* 16**,** 3455-3463.

DARLEY, C. P., SKIERA, L. A., NORTHROP, F., SANDERS, D. & DAVIES, J. M. 1998. Tonoplast inorganic pyrophosphatase in *Vicia faba* guard cells. *Planta,* 206**,** 272-277.

DE ANGELI, A., MONACHELLO, D., EPHRITIKHINE, G., FRACHISSE, J. M., THOMINE, S., GAMBALE, F. & BARBIER-BRYGOO, H. 2006. The nitrate/proton antiporter AtCLCa mediates nitrate accumulation in plant vacuoles. *Nature,* 442**,** 939-942.

DELLEDONNE, M., XIA, Y. J., DIXON, R. A. & LAMB, C. 1998. Nitric oxide functions as a signal in plant disease resistance. *Nature,* 394**,** 585-588.

DESIKAN, R., CHEUNG, M. K., BRIGHT, J., HENSON, D., HANCOCK, J. T. & NEILL, S. J. 2004. ABA, hydrogen peroxide and nitric oxide signalling in stomatal guard cells. *Journal of Experimental Botany,* 55**,** 205-212.

DESIKAN, R., GRIFFITHS, R., HANCOCK, J. & NEILL, S. 2002. A new role for an old enzyme: Nitrate reductase-mediated nitric oxide generation is required for abscisic acid-induced stomatal closure in *Arabidopsis thaliana*. *Proceedings of the National Academy of Sciences of the United States of America,* 99**,** 16314-16318.

DETTMER, J., HONG-HERMESDORF, A., STIERHOF, Y. D. & SCHUMACHER, K. 2006. Vacuolar H^+-ATPase activity is required for Endocytic and secretory trafficking in *Arabidopsis*. *Plant Cell,* 18**,** 715-730.

DIETRICH, P., DREYER, I., WIESNER, P. & HEDRICH, R. 1998. Cation sensitivity and kinetics of guard cell potassium channels differ among species. *Planta,* 205**,** 277-287.

DIETRICH, P. & HEDRICH, R. 1994. Interconversion of fast and slow gating modes of GCAC1, a guard cell anion channel. *Planta,* 195**,** 301-304.

DIETRICH, P. & HEDRICH, R. 1998. Anions permeate and gate GCAC1, a voltage-dependent guard cell anion channel. *Plant Journal,* 15**,** 479-487.

DIETRICH, P., SANDERS, D. & HEDRICH, R. 2001. The role of ion channels in light-dependent stomatal opening. *Journal of Experimental Botany,* 52**,** 1959-1967.

DITTRICH, P. & RASCHKE, K. 1977. Malate metabolism in isolated epidermis of *Commelina communis* L. in relation to stomatal functioning. *Planta,* 134**,** 77-81.

DODD, A. N., GARDNER, M. J., HOTTA, C. T., HUBBARD, K. E., DALCHAU, N., LOVE, J., ASSIE, J.-M., ROBERTSON, F. C., JAKOBSEN, M. K., GONCALVES, J., SANDERS, D. & WEBB, A. A. R. 2007. The *Arabidopsis* circadian clock incorporates a cADPR-based feedback loop. *Science,* 318**,** 1789-1792.

DODD, A. N., JAKOBSEN, M. K., BAKER, A. J., TELZEROW, A., HOU, S.-W., LAPLAZE, L., BARROT, L., POETHIG, R. S., HASELOFF, J. & WEBB, A. A. R. 2006. Time of day modulates low-temperature Ca*2+* signals in *Arabidopsis*. *Plant Journal,* 48**,** 962-973.

DODD, A. N., LOVE, J. & WEBB, A. A. R. 2005. The plant clock shows its metal: circadian regulation of cytosolic free Ca^{2+}. *Trends in Plant Science,* 10**,** 15-21.

DREYER, I., ANTUNES, S., HOSHI, T., MULLERROBER, B., PALME, K., PONGS, O., REINTANZ, B. & HEDRICH, R. 1997. Plant K^+ channel alpha-subunits assemble indiscriminately. *Biophysical Journal,* 72**,** 2143-2150.

DREYER, I. & BLATT, M. R. 2009. What makes a gate? The ins and outs of Kv-like K^+ channels in plants. *Trends in Plant Science,* 14**,** 383-390.

DREYER, I., POREE, F., SCHNEIDER, A., MITTELSTADT, J., BERTL, A., SENTENAC, H., THIBAUD, J. B. & MUELLER-ROEBER, B. 2004. Assembly of plant Shaker-like K_{out} channels requires two distinct sites of the channel alpha-subunit. *Biophysical Journal,* 87**,** 858-872.

DROZDOWICZ, Y. M., KISSINGER, J. C. & REA, P. A. 2000. AVP2, a sequence-divergent, K^+-insensitive H^+-translocating inorganic pyrophosphatase from *Arabidopsis*. *Plant Physiology,* 123**,** 353-362.

DUBY, G., HOSY, E., FIZAMES, C., ALCON, C., COSTA, A., SENTENAC, H. & THIBAUD, J.-B. 2008. AtKC1, a conditionally targeted Shaker-type subunit, regulates the activity of plant K^+ channels. *Plant Journal,* 53**,** 115-123.

EAMUS, D. & SHANAHAN, S. T. 2002. A rate equation model of stomatal responses to vapour pressure deficit and drought. *BMC ecology,* 2**,** 8-8.

EHRET, D. L. & BOYER, J. S. 1979. Potassium loss from stomatal guard cells at low water potentials. *Journal of Experimental Botany,* 30**,** 225-234.

EISENACH, C., CHEN, Z.-H., GREFEN, C. & BLATT, M. R. 2012. The trafficking protein SYP121 of *Arabidopsis* connects programmed stomatal closure and K plus channel activity with vegetative growth. *Plant Journal,* 69**,** 241-251.

FARQUHAR, G. D. & WONG, S. C. 1984. An empirical model of stomatal conductance *Australian Journal of Plant Physiology,* 11**,** 191-209.

FISCHER-SCHLIEBS, E., MARIAUX, J. B. & LUTTGE, U. 1997. Stimulation of H^+-transport activity of vacuolar H^+-ATPase by activation of H^+-PPase in *Kalanchoe blossfeldiana*. *Biologia Plantarum,* 39**,** 169-177.

FOREMAN, J., DEMIDCHIK, V., BOTHWELL, J. H. F., MYLONA, P., MIEDEMA, H., TORRES, M. A., LINSTEAD, P., COSTA, S., BROWNLEE, C., JONES, J. D. G., DAVIES, J. M. & DOLAN, L. 2003. Reactive oxygen species produced by NADPH oxidase regulate plant cell growth. *Nature,* 422**,** 442-446.

FRICKER, M. D., GILROY, S., READ, N. D. & TREWAVAS, A. J. 1991. Visualisation and measurement of the calcium message in guard cells. *Symposia of the Society for Experimental Biology,* 45**,** 177-90.

GARCIA-MATA, C., GAY, R., SOKOLOVSKI, S., HILLS, A., LAMATTINA, L. & BLATT, M. R. 2003. Nitric oxide regulates K^+ and Cl^- channels in guard cells through a subset of abscisic acid-evoked signaling pathways. *Proceedings of the National Academy of Sciences of the United States of America,* 100**,** 11116-11121.

GAXIOLA, R. A., PALMGREN, M. G. & SCHUMACHER, K. 2007. Plant proton pumps. *Febs Letters,* 581**,** 2204-2214.

GAYMARD, F., PILOT, G., LACOMBE, B., BOUCHEZ, D., BRUNEAU, D., BOUCHEREZ, J., MICHAUX-FERRIERE, N., THIBAUD, J. B. & SENTENAC, H. 1998. Identification and disruption of a plant shaker-like outward channel involved in K^+ release into the xylem sap. *Cell,* 94**,** 647-655.

GEDNEY, N., COX, P. M., BETTS, R. A., BOUCHER, O., HUNTINGFORD, C. & STOTT, P. A. 2006. Detection of a direct carbon dioxide effect in continental river runoff records. *Nature,* 439**,** 835-838.

GEIGER, D., BECKER, D., VOSLOH, D., GAMBALE, F., PALME, K., REHERS, M., ANSCHUETZ, U., DREYER, I., KUDLA, J. & HEDRICH, R. 2009a. Heteromeric AtKC1-AKT1 channels in *Arabidopsis* roots facilitate growth under K^+ limiting conditions. *Journal of Biological Chemistry,* 284**,** 21288-21295.

GEIGER, D., MAIERHOFER, T., AL-RASHEID, K. A. S., SCHERZER, S., MUMM, P., LIESE, A., ACHE, P., WELLMANN, C., MARTEN, I., GRILL, E., ROMEIS, T. & HEDRICH, R. 2011. Stomatal closure by fast abscisic acid signaling is mediated by the guard cell anion channel SLAH3 and the receptor RCAR1. *Science Signaling,* 4**,** ra(32).

GEIGER, D., SCHERZER, S., MUMM, P., MARTEN, I., ACHE, P., MATSCHI, S., LIESE, A., WELLMANN, C., AL-RASHEID, K. A. S., GRILL, E., ROMEIS, T. & HEDRICH, R. 2009b. Guard cell anion channel SLAC1 is regulated by CDPK protein kinases with distinct Ca^{2+} affinities. *Proceedings of the National Academy of Sciences of the United States of America,* 107**,** 8023-8028.

GEIGER, D., SCHERZER, S., MUMM, P., STANGE, A., MARTEN, I., BAUER, H., ACHE, P., MATSCHI, S., LIESE, A., AL-RASHEID, K. A. S., ROMEIS, T. & HEDRICH, R. 2009c. Activity of guard cell anion channel SLAC1 is controlled by drought-stress signaling kinase-phosphatase pair. *Proceedings of the National Academy of Sciences of the United States of America,* 106**,** 21425-21430.

GELLI, A. & BLUMWALD, E. 1997. Hyperpolarization-activated Ca^{2+}-permeable channels in the plasma membrane of tomato cells. *Journal of Membrane Biology,* 155**,** 35-45.

GILROY, S., FRICKER, M. D., READ, N. D. & TREWAYAS, A. J. 1991. Role of calcium in signal transduction of *Commelina* guard cells. *Plant Cell,* 3**,** 333-344.

GILROY, S., READ, N. D. & TREWAVAS, A. J. 1990. Elevation of cytoplasmic calcium by caged calcium or caged inositol trisphosphate initiates stomatal closure. *Nature,* 346**,** 769-771.

GLASS, A. D. M., SHAFF, J. E. & KOCHIAN, L. V. 1992. Studies of the uptake of nitrate in barley: IV. Electrophysiology. *Plant Physiology,* 99**,** 456-463.

GOBERT, A., ISAYENKOV, S., VOELKER, C., CZEMPINSKI, K. & MAATHUIS, F. J. M. 2007. The two-pore channel TPK1 gene encodes the vacuolar K^+ conductance and plays a role in K^+ homeostasis. *Proceedings of the National Academy of Sciences of the United States of America,* 104**,** 10726-10731.

GOH, C. H., KINOSHITA, T., OKU, T. & SHIMAZAKI, K. I. 1996. Inhibition of blue light-dependent H^+ pumping by abscisic acid in *Vicia* guard cell protoplasts. *Plant Physiology,* 111**,** 433-440.

GONZALEZ, W., RIEDELSBERGER, J., MORALES-NAVARRO, S. E., CABALLERO, J., ALZATE-MORALES, J. H., GONZALEZ-NILO, F. D. & DREYER, I. 2012. The pH sensor of the plant K^+-uptake channel KAT1 is built from a sensory cloud rather than from single key amino acids. *Biochemical Journal,* 442**,** 57-63.

GORTON, H. L., WILLIAMS, W. E. & ASSMANN, S. M. 1993. Circadian rhythms in stomatal responsiveness to red and blue light. *Plant Physiology,* 103**,** 399-406.

GOTOW, K., SAKAKI, T., KONDO, N., KOBAYASHI, K. & SYONO, K. 1985. Light-induced alkalinization of the suspending medium of guard cell protoplasts from *Vicia faba* L. *Plant Physiology,* 79**,** 825-828.

GRABOV, A. & BLATT, M. R. 1997. Parallel control of the inward-rectifier K^+ channel by cytosolic free Ca^{2+} and pH in *Vicia* guard cells. *Planta,* 201**,** 84-95.

GRABOV, A. & BLATT, M. R. 1998. Membrane voltage initiates Ca^{2+} waves and potentiates Ca^{2+} increases with abscisic acid in stomatal guard cells. *Proceedings of the National Academy of Sciences of the United States of America,* 95**,** 4778-4783.

GRABOV, A. & BLATT, M. R. 1999. A steep dependence of inward-rectifying potassium channels on cytosolic free calcium concentration increase evoked by hyperpolarization in guard cells. *Plant Physiology,* 119**,** 277-287.

GRABOV, A., LEUNG, J., GIRAUDAT, J. & BLATT, M. R. 1997. Alteration of anion channel kinetics in wild-type and *abi1-1* transgenic *Nicotiana benthamiana* guard cells by abscisic acid. *Plant Journal,* 12**,** 203-213.

GREFEN, C., CHEN, Z., HONSBEIN, A., DONALD, N., HILLS, A. & BLATT, M. R. 2010. A novel motif essential for SNARE Interaction with the K^+ channel KC1 and channel gating in *Arabidopsis*. *Plant Cell,* 22**,** 3076-3092.

GRYNKIEWICZ, G., POENIE, M. & TSIEN, R. Y. 1985. A new generation of Ca^{2+} indicators with greatly improved fluorescence properties. *Journal of Biological Chemistry,* 260**,** 3440-3450.

GUERN, J., FELLE, H., MATHIEU, Y. & KURKDJIAN, A. 1991. Regulation of intracellular pH in plant-cells. *International Review of Cytology-a Survey of Cell Biology,* 127**,** 111-173.

GUO, F. Q., OKAMOTO, M. & CRAWFORD, N. M. 2003. Identification of a plant nitric oxide synthase gene involved in hormonal signaling. *Science,* 302**,** 100-103.

HAMILTON, D. W. A., HILLS, A. & BLATT, M. R. 2001. Extracellular Ba^{2+} and voltage interact to gate Ca^{2+} channels at the plasma membrane of stomatal guard cells. *Febs Letters,* 491**,** 99-103.

HAMILTON, D. W. A., HILLS, A., KOHLER, B. & BLATT, M. R. 2000. Ca^{2+} channels at the plasma membrane of stomatal guard cells are activated by hyperpolarization and abscisic acid. *Proceedings of the National Academy of Sciences of the United States of America,* 97**,** 4967-4972.

HARUTA, M., BURCH, H. L., NELSON, R. B., BARRETT-WILT, G., KLINE, K. G., MOHSIN, S. B., YOUNG, J. C., OTEGUI, M. S. & SUSSMAN, M. R. 2010. Molecular characterization of mutant *Arabidopsis* plants with reduced plasma membrane proton pump activity. *Journal of Biological Chemistry,* 285**,** 17918-17929.

HARUTA, M. & SUSSMAN, M. R. 2012. The Effect of a Genetically Reduced Plasma Membrane Protonmotive Force on Vegetative Growth of *Arabidopsis*. *Plant Physiology,* 158**,** 1158-1171.

HEDRICH, R., BUSCH, H. & RASCHKE, K. 1990. Ca^{2+} and nucleotide dependent regulation of voltage dependent anion channels in the plasma membrane of guard cells. *Embo Journal,* 9**,** 3889-3892.

HEDRICH, R. & MARTEN, I. 1993a. Malate-induced feedback regulation of plasma membrane anion channels could provide a CO_2 sensor to guard cells. *Embo Journal,* 12**,** 897-901.

HEDRICH, R. & MARTEN, I. 1993b. Malate-induced feedback regulation of plasma membrane anion channels could provide a CO_2 sensor to guard cells. *Embo Journal,* 12**,** 897-901.

HEDRICH, R., MARTEN, I., LOHSE, G., DIETRICH, P., WINTER, H., LOHAUS, G. & HELDT, H. W. 1994. Malate-sensitive anion channels enable guard cells to sense changes in the ambient CO_2 concentration. *Plant Journal,* 6**,** 741-748.

HEINEKE, D., RIENS, B., GROSSE, H., HOFERICHTER, P., PETER, U., FLUGGE, U. I. & HELDT, H. W. 1991. Redox transfer across the inner chloroplast envelope membrane. *Plant Physiology,* 95**,** 1131-1137.

HERMAN, E. M., LI, X. H., SU, R. T., LARSEN, P., HSU, H. T. & SZE, H. 1994. Vacuolar-type H^+-ATPases are associated with the endoplasmic reticulum and provacuoles of root tip cells. *Plant Physiology,* 106**,** 1313-1324.

HETHERINGTON, A. M. & WOODWARD, F. I. 2003. The role of stomata in sensing and driving environmental change. *Nature,* 424**,** 901-908.

HILLE, B. 1967. The selective inhibition of delayed potassium currents in nerve by tetraethylammonium ion. *Journal of General Physiology,* 50**,** 1287-1300.

HILLS, A., CHEN, Z.-H., AMTMANN, A., BLATT, M. R. & LEW, V. L. 2012. OnGuard, a computational platform for quantitative kinetic modeling of guard cell physiology. *Plant Physiology,* 159**,** 1026-1042.

HODGKIN, A. L. & HUXLEY, A. F. 1939. Action potentials recorded from inside a nerve fibre. *Nature,* 144**,** 710-711.

HOMANN, U. & TESTER, M. 1998. Patch-clamp measurements of capacitance to study exocytosis and endocytosis. *Trends in Plant Science,* 3**,** 110-114.

HONSBEIN, A., BLATT, M. R. & GREFEN, C. 2011. A molecular framework for coupling cellular volume and osmotic solute transport control. *Journal of Experimental Botany,* 62**,** 2363-2370.

HONSBEIN, A., SOKOLOVSKI, S., GREFEN, C., CAMPANONI, P., PRATELLI, R., PANEQUE, M., CHEN, Z., JOHANSSON, I. & BLATT, M. R. 2009. A tripartite SNARE-K^+ channel complex mediates in channel-dependent K^+ Nutrition in *Arabidopsis*. *Plant Cell,* 21**,** 2859-2877.

HOPKINS, W. G. & HUNER, N. P. A. 2004. *Introduction to Plant Physiology 4th edition.*, John Wiley & Sons Inc.

HOSY, E., VAVASSEUR, A., MOULINE, K., DREYER, I., GAYMARD, F., POREE, F., BOUCHEREZ, J., LEBAUDY, A., BOUCHEZ, D., VERY, A. A., SIMONNEAU, T., THIBAUD, J. B. & SENTENAC, H. 2003. The *Arabidopsis* outward K^+ channel GORK is involved in regulation of stomatal movements and plant transpiration. *Proceedings of the National Academy of Sciences of the United States of America,* 100**,** 5549-5554.

HOTH, S., GEIGER, D., BECKER, D. & HEDRICH, R. 2001. The pore of plant K^+ channels is involved in voltage and pH sensing: Domain-swapping between different K^+ channel alpha-subunits. *Plant Cell,* 13**,** 943-952.

HOTH, S. & HEDRICH, R. 1999. Distinct molecular bases for pH sensitivity of the guard cell K^+ channels KST1 and KAT1. *Journal of Biological Chemistry,* 274**,** 11599-11603.

HU, H. H., BOISSON-DERNIER, A., ISRAELSSON-NORDSTROM, M., BOHMER, M., XUE, S. W., RIES, A., GODOSKI, J., KUHN, J. M. & SCHROEDER, J. I. 2010. Carbonic anhydrases are upstream regulators of CO_2 controlled stomatal movements in guard cells. *Nature Cell Biology,* 12**,** 87-U234.

HUANG, J. W. W., GRUNES, D. L. & KOCHIAN, L. V. 1994. Voltage-dependent Ca^{2+} influx into right-side-out plasma membrane vesicles isolated from wheat roots: characterization of a putative Ca^{2+} channel. *Proceedings of the National Academy of Sciences of the United States of America,* 91**,** 3473-3477.

IRVING, H. R., GEHRING, C. A. & PARISH, R. W. 1992. Changes in cytosolic pH and calcium of guard cells precede stomatal movements. *Proceedings of the National Academy of Sciences of the United States of America,* 89**,** 1790-1794.

ISHIBASHI, K., SUZUKI, M. & IMAI, M. 2000. Molecular cloning of a novel form (two-repeat) protein related to voltage-gated sodium and calcium channels. *Biochemical and Biophysical Research Communications,* 270**,** 370-376.

ISRAELSSON, M., SIEGEL, R. S., YOUNG, J., HASHIMOTO, M., IBA, K. & SCHROEDER, J. I. 2006. Guard cell ABA and CO_2 signaling network updates and Ca^{2+} sensor priming hypothesis. *Current Opinion in Plant Biology,* 9**,** 654-663.

JEANGUENIN, L., ALCON, C., DUBY, G., BOEGLIN, M., CHEREL, I., GAILLARD, I., ZIMMERMANN, S., SENTENAC, H. & VERY, A.-A. 2011. AtKC1 is a general modulator of *Arabidopsis* inward shaker channel activity. *Plant Journal,* 67**,** 570-582.

JOHANSSON, I., WULFETANGE, K., POREE, F., MICHARD, E., GAJDANOWICZ, P., LACOMBE, B., SENTENAC, H., THIBAUD, J. B., MUELLER-ROEBER, B., BLATT, M. R. & DREYER, I. 2006. External K^+ modulates the activity of the *Arabidopsis* potassium channel SKOR via an unusual mechanism. *Plant Journal,* 46**,** 269-281.

JOSSIER, M., KRONIEWICZ, L., DALMAS, F., LE THIEC, D., EPHRITIKHINE, G., THOMINE, S., BARBIER-BRYGOO, H., VAVASSEUR, A., FILLEUR, S. & LEONHARDT, N. 2010. The Arabidopsis vacuolar anion transporter, AtCLCc, is involved in the regulation of stomatal movements and contributes to salt tolerance. *Plant Journal,* 64**,** 563-576.

KANDEL, E. R., SCHWARTZ, J. H. & JESSELL, T. M. 2000. *Principles of Neural Science, 4th ed.*, McGraw-Hill, New York.

KAPLAN, B., SHERMAN, T. & FROMM, H. 2007. Cyclic nucleotide-gated channels in plants. *Febs Letters,* 581**,** 2237-2246.

KIM, T.-H., BOEHMER, M., HU, H., NISHIMURA, N. & SCHROEDER, J. I. 2010. Guard cell signal transduction network: Advances in understanding abscisic acid, CO_2, and Ca^{2+} signaling. *In:* MERCHANT, S., BRIGGS, W. R. & ORT, D. (eds.) *Annual Review of Plant Biology, Vol 61.*

KINOSHITA, T., NISHIMURA, M. & SHIMAZAKI, K. I. 1995. Cytosolic concentration of Ca^{2+} regulates the plasma membrane H^+-ATPase in guard cells of fava bean. *Plant Cell,* 7**,** 1333-1342.

KLINGLER, J. P., BATELLI, G. & ZHU, J.-K. 2010. ABA receptors: the START of a new paradigm in phytohormone signalling. *Journal of Experimental Botany,* 61**,** 3199-3210.

KLINK, R., HASCHKE, H. P., KRAMER, D. & LUTTGE, U. 1990. Membrane particles, proteins and ATPase activity of tonoplast vesicles of *Mesembryanthemum crystallinum* in the C3 and CAM state. *Botanica Acta,* 103**,** 24-31.

KOHLER, B. & BLATT, M. R. 2002. Protein phosphorylation activates the guard cell Ca^{2+} channel and is a prerequisite for gating by abscisic acid. *Plant Journal,* 32**,** 185-194.

KOLB, H. A., MARTEN, I. & HEDRICH, R. 1995. Hodgkin-Huxley analysis of a GCAC1 anion channel in the plasma membrane of guard cells. *Journal of Membrane Biology,* 146**,** 273-282.

KOURIE, J. & GOLDSMITH, M. H. M. 1992. K^+ channels are responsible for an inwardly rectifying current in the plasma membrane of mesophyll protoplasts of *Avena sativa*. *Plant Physiology,* 98**,** 1087-1097.

KOVERMANN, P., MEYER, S., HOERTENSTEINER, S., PICCO, C., SCHOLZ-STARKE, J., RAVERA, S., LEE, Y. & MARTINOIA, E. 2007. The *Arabidopsis* vacuolar malate channel is a member of the ALMT family. *Plant Journal,* 52**,** 1169-1180.

KRAMER, P. J. & BOYER, J. S. 1995. *Water relations of plants and soils*.

KUROSAKI, F. 1997. Role of inward K^+ channel located at carrot plasma membrane in signal cross-talking of cAMP with Ca^{2+} cascade. *Febs Letters*, 408**,** 115-119.

KWAK, J. M., MORI, I. C., PEI, Z. M., LEONHARDT, N., TORRES, M. A., DANGL, J. L., BLOOM, R. E., BODDE, S., JONES, J. D. G. & SCHROEDER, J. I. 2003. NADPH oxidase AtrbohD and AtrbohF genes function in ROS-dependent ABA signaling in *Arabidopsis*. *Embo Journal,* 22**,** 2623-2633.

LACOMBE, B., PILOT, G., GAYMARD, F., SENTENAC, H. & THIBAUD, J. B. 2000. pH control of the plant outwardly-rectifying potassium channel SKOR. *Febs Letters,* 466**,** 351-354.

LEBAUDY, A., HOSY, E., SIMONNEAU, T., SENTENAC, H., THIBAUD, J.-B. & DREYER, I. 2008a. Heteromeric K^+ channels in plants. *Plant Journal,* 54**,** 1076-1082.

LEBAUDY, A., VAVASSEUR, A., HOSY, E., DREYER, I., LEONHARDT, N., THIBAUD, J.-B., VERY, A.-A., SIMONNEAU, T. & SENTENAC, H. 2008b. Plant adaptation to fluctuating environment and biomass production are strongly dependent on guard cell potassium channels. *Proceedings of the National Academy of Sciences of the United States of America,* 105**,** 5271-5276.

LECKIE, C. P., MCAINSH, M. R., ALLEN, G. J., SANDERS, D. & HETHERINGTON, A. M. 1998. Abscisic acid-induced stomatal closure mediated by cyclic ADP-ribose. *Proceedings of the National Academy of Sciences of the United States of America,* 95**,** 15837-15842.

LEE, S. C., LAN, W., BUCHANAN, B. B. & LUAN, S. 2009. A protein kinase-phosphatase pair interacts with an ion channel to regulate ABA signaling in plant guard cells. *Proceedings of the National Academy of Sciences of the United States of America,* 106**,** 21419-21424.

LEE, Y. S., CHOI, Y. B., SUH, S., LEE, J., ASSMANN, S. M., JOE, C. O., KELLEHER, J. F. & CRAIN, R. C. 1996. Abscisic acid-induced phosphoinositide turnover in guard cell protoplasts of *Vicia faba*. *Plant Physiology,* 110**,** 987-996.

LEIGH, R. A. & JONES, R. G. W. 1984. A hypothesis relating critical potassium concentrations for growth to the distribution and functions of this ion in the plant cell. *New Phytologist,* 97**,** 1-13.

LEMTIRI-CHLIEH, F. & MACROBBIE, E. A. C. 1994. Role of calcium in the modulation of *Vicia guard* cell potassium channels by abscisic acid: a patch-clamp study. *Journal of Membrane Biology,* 137**,** 99-107.

LEUBE, M. P., GRILL, E. & AMRHEIN, N. 1998. ABI1 of *Arabidopsis* is a protein serine/threonine phosphatase highly regulated by the proton and magnesium ion concentration. *Febs Letters,* 424**,** 100-104.

LEUNG, J., BOUVIERDURAND, M., MORRIS, P. C., GUERRIER, D., CHEFDOR, F. & GIRAUDAT, J. 1994. *Arabidopsis* ABA response gene *ABI1* : features of a calcium modulated protein phosphatase. *Science,* 264**,** 1448-1452.

LEUNG, J. & GIRAUDAT, J. 1998. Abscisic acid signal transduction. *Annual Review of Plant Physiology and Plant Molecular Biology,* 49**,** 199-222.

LEYMAN, B., GEELEN, D., QUINTERO, F. J. & BLATT, M. R. 1999. A tobacco syntaxin with a role in hormonal control of guard cell ion channels. *Science,* 283**,** 537-540.

LI, J. X. & ASSMANN, S. M. 1996. An abscisic acid-activated and calcium-independent protein kinase from guard cells of fava bean. *Plant Cell,* 8**,** 2359-2368.

LI, L., KIM, B.-G., CHEONG, Y. H., PANDEY, G. K. & LUAN, S. 2006. A Ca^{2+} signaling pathway regulates a K^{+} channel for low K response in *Arabidopsis*. *Proceedings of the National Academy of Sciences of the United States of America,* 103**,** 12625-12630.

LINDER, B. & RASCHKE, K. 1992. A slow anion channel in guard cells, activating at large hyperpolarization, may be principal for stomatal closing. *Febs Letters,* 313**,** 27-30.

LIU, X., YUE, Y., LI, B., NIE, Y., LI, W., WU, W.-H. & MA, L. 2007. A G protein-coupled receptor is a plasma membrane receptor for the plant hormone abscisic acid. *Science,* 315**,** 1712-1716.

LOUGUET, P., COUDRET, A., COUOTGASTELIER, J. & LASCEVE, G. 1990. Structure and ultrastructure of stomata. *Biochemie Und Physiologie Der Pflanzen,* 186**,** 273-287.

LOZANO-JUSTE, J. & LEON, J. 2010. Enhanced abscisic acid mediated responses in *nia1nia2noa1-2* triple mutant impaired in NIA/NR and AtNOA1 dependent nitric oxide biosynthesis in *Arabidopsis*. *Plant Physiology,* 152**,** 891-903.

LUAN, S. 2009. The CBL-CIPK network in plant calcium signaling. *Trends in Plant Science,* 14**,** 37-42.

MA, Y., SZOSTKIEWICZ, I., KORTE, A., MOES, D., YANG, Y., CHRISTMANN, A. & GRILL, E. 2009. Regulators of PP2C phosphatase activity function as abscisic acid sensors. *Science,* 324**,** 1064-1068.

MAATHUIS, F. J. M. & SANDERS, D. 1994. Mechanism of high-affinity potassium uptake in roots of *Arabidopsis thaliana*. *Proceedings of the National Academy of Sciences of the United States of America,* 91**,** 9272-9276.

MACROBBIE, E. A. C. 1981. Ion fluxes in 'Isolated' guard cells of *Commelina communis* L. *Journal of Experimental Botany,* 32**,** 545-562.

MACROBBIE, E. A. C. 1983. Effects of light/dark on cation fluxes in guard cells of *Commelina communis* L. *Journal of Experimental Botany,* 34**,** 1695-1710.

MACROBBIE, E. A. C. 1990a. Calcium-dependent and calcium-independent events in the initiation of stomatal closure by abscisic acid. *Proceedings of the Royal Society of London Series B-Biological Sciences,* 241**,** 214-219.

MACROBBIE, E. A. C. 1990b. *Ion transport in stomatal guard cells.* Beilby, M. J., N. A. Walker and J. R. Smith (Ed.). Membrane Transport in Plants and Fungi; 7th International Workshop on Plant Membrane Transport, Sydney, New South Wales, Australia, 1986. 513p. University of Sydney: Sydney, New South Wales, Australia. Illus. Paper

MACROBBIE, E. A. C. 1998. Signal transduction and ion channels in guard cells. *Philosophical Transactions of the Royal Society of London Series B-Biological Sciences,* 353**,** 1475-1488.

MACROBBIE, E. A. C. 2000. ABA activates multiple Ca^{2+} fluxes in stomatal guard cells, triggering vacuolar K^{+}(Rb^{+}) release. *Proceedings of the National Academy of Sciences of the United States of America,* 97**,** 12361-12368.

MACROBBIE, E. A. C. 2006. Osmotic effects on vacuolar ion release in guard cells. *Proceedings of the National Academy of Sciences of the United States of America,* 103**,** 1135-1140.

MAESHIMA, M. 2000. Vacuolar H^{+}-pyrophosphatase. *Biochimica Et Biophysica Acta-Biomembranes,* 1465**,** 37-51.

MALONE, M., LEIGH, R. A. & TOMOS, A. D. 1991. Concentrations of vacuolar inorganic ions in individual cells of intact wheat leaf epidermis. *Journal of Experimental Botany,* 42**,** 305-309.

MARTINOIA, E., MAESHIMA, M. & NEUHAUS, H. E. 2007. Vacuolar transporters and their essential role in plant metabolism. *Journal of Experimental Botany,* 58**,** 83-102.

MARTINOIA, E. & RENTSCH, D. 1994. Malate compartmentation-responses to a complex metabolism. *Annual Review of Plant Physiology and Plant Molecular Biology,* 45**,** 447-467.

MATSUOKA, K., HIGUCHI, T., MAESHIMA, M. & NAKAMURA, K. 1997. A vacuolar type H^+-ATPase in a nonvacuolar organelle is required for the sorting of soluble vacuolar protein precursors in tobacco cells. *Plant Cell,* 9**,** 533-546.

MAYER, B. & HEMMENS, B. 1997. Biosynthesis and action of nitric oxide in mammalian cells. *Trends in Biochemical Sciences,* 22**,** 477-481.

MCAINSH, M. R., BROWNLEE, C. & HETHERINGTON, A. M. 1990. Abscisic acid induced elevation of guard cell cytosolic Ca^{2+} precedes stomatal closure. *Nature,* 343**,** 186-188.

MCAINSH, M. R., BROWNLEE, C. & HETHERINGTON, A. M. 1991. Partial inhibition of ABA-induced stomatal closure by calcium channel blockers. *Proceedings of the Royal Society B-Biological Sciences,* 243**,** 195-201.

MCAINSH, M. R., BROWNLEE, C. & HETHERINGTON, A. M. 1992. Visualizing changes in cytosolic free Ca^{2+} during the response of stomatal guard cells to abscisic acid. *Plant Cell,* 4**,** 1113-1122.

MCAINSH, M. R., CLAYTON, H., MANSFIELD, T. A. & HETHERINGTON, A. M. 1996. Changes in stomatal behavior and guard cell cytosolic free calcium in response to oxidative stress. *Plant Physiology,* 111**,** 1031-1042.

MCAINSH, M. R. & PITTMAN, J. K. 2009. Shaping the calcium signature. *New Phytologist,* 181**,** 275-294.

MEHARG, A. A. & BLATT, M. R. 1995. NO_3^- transport across the plasma membrane of *Arabidopsis Thaliana* root hairs kinetic control by pH and membrane voltage. *Journal of Membrane Biology,* 145**,** 49-66.

MEIDNER, H. & WILLMER, C. M. 1993. Circadian rhythm of stomatal movements in epidermal strips. *Journal of Experimental Botany,* 44**,** 1649-1652.

MERLOT, S., LEONHARDT, N., FENZI, F., VALON, C., COSTA, M., PIETTE, L., VAVASSEUR, A., GENTY, B., BOIVIN, K., MUELLER, A., GIRAUDAT, M. & LEUNG, J. 2007. Constitutive activation of a plasma membrane H^+-ATPase prevents abscisic acid-mediated stomatal closure. *Embo Journal,* 26**,** 3216-3226.

MEYER, S., MUMM, P., IMES, D., ENDLER, A., WEDER, B., AL-RASHEID, K. A. S., GEIGER, D., MARTEN, I., MARTINOIA, E. & HEDRICH, R. 2010. AtALMT12 represents an R-type anion channel required for stomatal movement in *Arabidopsis* guard cells. *Plant Journal,* 63**,** 1054-1062.

MIEDEMA, H. & ASSMANN, S. M. 1996. A membrane-delimited effect of internal pH on the K^+ outward rectifier of *Vicia faba* guard cells. *Journal of Membrane Biology,* 154**,** 227-237.

MORI, I. C., MURATA, Y., YANG, Y., MUNEMASA, S., WANG, Y.-F., ANDREOLI, S., TIRIAC, H., ALONSO, J. M., HARPER, J. F., ECKER, J. R., KWAK, J. M. & SCHROEDER, J. I. 2006. CDPKs CPK6 and CPK3 function in ABA regulation of guard cell S-type anion- and Ca^{2+} permeable channels and stomatal closure. *Plos Biology,* 4**,** 1749-1762.

MORSOMME, P. & BOUTRY, M. 2000. The plant plasma membrane H^+-ATPase: structure, function and regulation. *Biochimica Et Biophysica Acta-Biomembranes,* 1465**,** 1-16.

MUIR, S. R. & SANDERS, D. 1996. Pharmacology of Ca^{2+} release from red beet microsomes suggests the presence of ryanodine receptor homologs in higher plants. *Febs Letters,* 395**,** 39-42.

MURATA, Y., PEI, Z. M., MORI, I. C. & SCHROEDER, J. 2001. Abscisic acid activation of plasma membrane Ca^{2+} channels in guard cells requires cytosolic NAD(P)H and is differentially disrupted upstream and downstream of reactive oxygen species production in *abi1-1* and *abi2-1* protein phosphatase 2C mutants. *Plant Cell,* 13**,** 2513-2523.

MUSTILLI, A. C., MERLOT, S., VAVASSEUR, A., FENZI, F. & GIRAUDAT, J. 2002. *Arabidopsis* OST1 protein kinase mediates the regulation of stomatal aperture by abscisic acid and acts upstream of reactive oxygen species production. *Plant Cell,* 14**,** 3089-3099.

NAKAMURA, R. L., ANDERSON, J. A. & GABER, R. F. 1997. Determination of key structural requirements of a K^+ channel pore. *Journal of Biological Chemistry,* 272**,** 1011-1018.

NEGI, J., MATSUDA, O., NAGASAWA, T., OBA, Y., TAKAHASHI, H., KAWAI-YAMADA, M., UCHIMIYA, H., HASHIMOTO, M. & IBA, K. 2008. CO_2 regulator SLAC1 and its homologues are essential for anion homeostasis in plant cells. *Nature,* 452**,** 483-U13.

NEILL, S., DESIKAN, R. & HANCOCK, J. 2002a. Hydrogen peroxide signalling. *Current Opinion in Plant Biology,* 5**,** 388-395.

NEILL, S. J., DESIKAN, R., CLARKE, A. & HANCOCK, J. T. 2002b. Nitric oxide is a novel component of abscisic acid signaling in stomatal guard cells. *Plant Physiology,* 128**,** 13-16.

NEILL, S. J., DESIKAN, R. & HANCOCK, J. T. 2003. Nitric oxide signalling in plants. *New Phytologist,* 159**,** 11-35.

NILSON, S. E. & ASSMANN, S. M. 2007. The control of transpiration. Insights from *Arabidopsis*. *Plant Physiology,* 143**,** 19-27.

NISHIMURA, N., SARKESHIK, A., NITO, K., PARK, S.-Y., WANG, A., CARVALHO, P. C., LEE, S., CADDELL, D. F., CUTLER, S. R., CHORY, J., YATES, J. R. & SCHROEDER, J. I. 2010. PYR/PYL/RCAR family members are major *in vivo* ABI1 protein phosphatase 2C interacting proteins in *Arabidopsis*. *Plant Journal,* 61**,** 290-299.

OUTLAW, W. H. 2003. Integration of cellular and physiological functions of guard cells. *Critical Reviews in Plant Sciences,* 22**,** 503-529.

OUTLAW, W. H., DU, Z. R., MENG, F. X., AGHORAM, K., RIDDLE, K. A. & CHOLLET, R. 2002. Requirements for activation of the signal transduction network that leads to regulatory phosphorylation of leaf guard cell phosphoenolpyruvate carboxylase during fusicoccin stimulated stomatal opening. *Archives of Biochemistry and Biophysics,* 407**,** 63-71.

OUTLAW, W. H., JR. 1990. Kinetic properties of guard-cell phospho enolpyruvate carboxylase. *Biochemie Und Physiologie Der Pflanzen,* 186**,** 317-325.

PADMANABAN, S., CHANROJ, S., KWAK, J. M., LI, X., WARD, J. M. & SZE, H. 2007. Participation of endomembrane cation/H^+ exchanger AtCHX20 in osmoregulation of guard cells. *Plant Physiology,* 144**,** 82-93.

PALMGREN, M. G. 2001. Plant plasma membrane H^+-ATPases: Powerhouses for nutrient uptake. *Annual Review of Plant Physiology and Plant Molecular Biology,* 52**,** 817-845.

PANDEY, S., NELSON, D. C. & ASSMANN, S. M. 2009. Two novel GPCR-type G proteins are abscisic acid receptors in *Arabidopsis*. *Cell,* 136**,** 136-148.

PANDEY, S., ZHANG, W. & ASSMANN, S. M. 2007. Roles of ion channels and transporters in guard cell signal transduction. *Febs Letters,* 581**,** 2325-2336.

PANTOJA, O. & SMITH, J. A. C. 2002. Sensitivity of the plant vacuolar malate channel to pH, Ca^{2+} and anion channel blockers. *Journal of Membrane Biology,* 186**,** 31-42.

PAPAZIAN, D. M., SCHWARZ, T. L., TEMPEL, B. L., JAN, Y. N. & JAN, L. Y. 1987. Cloning of genomic and complementary DNA from Shaker, a putative potassium channel gene from *Drosophila*. *Science,* 237**,** 749-753.

PARK, S.-Y., FUNG, P., NISHIMURA, N., JENSEN, D. R., FUJII, H., ZHAO, Y., LUMBA, S., SANTIAGO, J., RODRIGUES, A., CHOW, T.-F. F., ALFRED, S. E., BONETTA, D., FINKELSTEIN, R., PROVART, N. J., DESVEAUX, D., RODRIGUEZ, P. L., MCCOURT, P., ZHU, J.-K., SCHROEDER, J. I., VOLKMAN, B. F. & CUTLER, S. R. 2009. Abscisic acid inhibits type 2C protein phosphatases via the PYR/PYL family of START proteins. *Science,* 324**,** 1068-1071.

PARMAR, P. N. & BREARLEY, C. A. 1993. Identification of 3-and 4-phosphorylated phosphoinositides and inositol phosphates in stomatal guard cells. *Plant Journal,* 4**,** 255-263.

PARMAR, P. N. & BREARLEY, C. A. 1995. Metabolism of 3-and 4-phosphorylated phosphatidylinositols in stomatal guard cells of *Commelina communis* L. *Plant Journal,* 8**,** 425-433.

PEI, Z. M., BAIZABAL-AGUIRRE, V. M., ALLEN, G. J. & SCHROEDER, J. I. 1998. A transient outward-rectifying K^+ channel current down-regulated by cytosolic Ca^{2+} in *Arabidopsis thaliana* guard cells. *Proceedings of the National Academy of Sciences of the United States of America,* 95**,** 6548-6553.

PEI, Z. M., KUCHITSU, K., WARD, J. M., SCHWARZ, M. & SCHROEDER, J. I. 1997. Differential abscisic acid regulation of guard cell slow anion channels in Arabidopsis wild-type and *abi1* and *abi2* mutants. *Plant Cell,* 9**,** 409-423.

PEI, Z. M., MURATA, Y., BENNING, G., THOMINE, S., KLUSENER, B., ALLEN, G. J., GRILL, E. & SCHROEDER, J. I. 2000. Calcium channels activated by hydrogen peroxide mediate abscisic acid signalling in guard cells. *Nature,* 406**,** 731-734.

PEI, Z. M., WARD, J. M., HARPER, J. F. & SCHROEDER, J. I. 1996. A novel chloride channel in *Vicia faba* guard cell vacuoles activated by the serine/threonine kinase, CDPK. *Embo Journal,* 15**,** 6564-6574.

PEITER, E., MAATHUIS, F. J. M., MILLS, L. N., KNIGHT, H., PELLOUX, J., HETHERINGTON, A. M. & SANDERS, D. 2005. The vacuolar Ca^{2+} activated channel TPC1 regulates germination and stomatal movement. *Nature,* 434**,** 404-408.

PILOT, G., GAYMARD, F., MOULINE, K., CHEREL, I. & SENTENAC, H. 2003. Regulated expression of *Arabidopsis* Shaker K^+ channel genes involved in K^+ uptake and distribution in the plant. *Plant Molecular Biology,* 51**,** 773-787.

PILOT, G., LACOMBE, B., GAYMARD, F., CHEREL, I., BOUCHEREZ, J., THIBAUD, J. B. & SENTENAC, H. 2001. Guard cell inward K^+ channel activity in *Arabidopsis* involves expression of the twin channel subunits KAT1 and KAT2. *Journal of Biological Chemistry,* 276**,** 3215-3221.

PONGS, O., KECSKEMETHY, N., MULLER, R., KRAHJENTGENS, I., BAUMANN, A., KILTZ, H. H., CANAL, I., LLAMAZARES, S. & FERRUS, A. 1988. Shaker encodes a family of putative potassium channel proteins in the nervous system of *Drosophila*. *Embo Journal,* 7**,** 1087-1096.

RASCHKE, K. 1979. Movements using turgor mechanisms. *Encyclopedia of Plant Physiology, New Series, Volume 7. Physiology of movements [Haupt, W.; Feinleib, M.E. (Editors)]*. 383-441.

RASCHKE, K. & SCHNABL, H. 1978. Availability of chloride affects the balance between potassium chloride and potassium malate in Guard Cells of *Vicia faba* L. *Plant Physiology,* 62**,** 84-87.

RASCHKE, K., SHABAHANG, M. & WOLF, R. 2003. The slow and the quick anion conductance in whole guard cells: their voltage-dependent alternation, and the modulation of their activities by abscisic acid and CO_2. *Planta,* 217**,** 639-650.

REA, P. A. & POOLE, R. J. 1993. Vacuolar H^+-translocating pyrophosphatase. *Annual Review of Plant Physiology and Plant Molecular Biology,* 44**,** 157-180.

RODRIGUEZ, P. L., BENNING, G. & GRILL, E. 1998. ABI2, a second protein phosphatase 2C involved in abscisic acid signal transduction in *Arabidopsis*. *Febs Letters,* 421**,** 185-190.

ROELFSEMA, M. R. G. & HEDRICH, R. 2005. In the light of stomatal opening: new insights into 'the Watergate'. *New Phytologist,* 167**,** 665-691.

ROELFSEMA, M. R. G., HEDRICH, R. & GEIGER, D. 2012. Anion channels: master switches of stress responses. *Trends in Plant Science,* 17**,** 221-229.

ROELFSEMA, M. R. G., LEVCHENKO, V. & HEDRICH, R. 2004. ABA depolarizes guard cells in intact plants, through a transient activation of R- and S-type anion channels. *Plant Journal,* 37**,** 578-588.

ROELFSEMA, M. R. G. & PRINS, H. B. A. 1997. Ion channels in guard cells of *Arabidopsis thaliana* (L) Heynh. *Planta,* 202**,** 18-27.

ROUGHAN, P. G. 1995. Acetate concentrations in leaves are sufficient to drive in vivo fatty acid synthesis at maximum rates. *Plant Science,* 107**,** 49-55.

SANDERS, D., HOPGOOD, M. & JENNINGS, I. R. 1989. Kinetic response of H^+-coupled transport to extracellular pH: Critical role of cytosolic pH as a regulator. *Journal of Membrane Biology,* 108**,** 253-261.

SANDERS, D., PELLOUX, J., BROWNLEE, C. & HARPER, J. F. 2002. Calcium at the crossroads of signaling. *Plant Cell,* 14**,** S401-S417.

SASAKI, T., MORI, I. C., FURUICHI, T., MUNEMASA, S., TOYOOKA, K., MATSUOKA, K., MURATA, Y. & YAMAMOTO, Y. 2010. Closing plant stomata requires a homolog of an aluminum-activated malate transporter. *Plant and Cell Physiology,* 51**,** 354-365.

SATO, A., SATO, Y., FUKAO, Y., FUJIWARA, M., UMEZAWA, T., SHINOZAKI, K., HIBI, T., TANIGUCHI, M., MIYAKE, H., GOTO, D. B. & UOZUMI, N. 2009. Threonine at position 306 of the KAT1 potassium channel is essential for channel activity and is a target site for ABA-activated SnRK2/OST1/SnRK2.6 protein kinase. *Biochemical Journal,* 424**,** 439-448.

SCHACHTMAN, D. P., SCHROEDER, J. I., LUCAS, W. J., ANDERSON, J. A. & GABER, R. F. 1992. Expression of an inward-rectifying potassium channel by the *Arabidopsis* KAT1 cDNA. *Science,* 258**,** 1654-1658.

SCHMIDT, C., SCHELLE, I., LIAO, Y. J. & SCHROEDER, J. I. 1995. Strong regulation of slow anion channels and abscisic acid signaling in guard cells by phosphorylation and dephosphorylation events. *Proceedings of the National Academy of Sciences of the United States of America,* 92**,** 9535-9539.

SCHMIDT, C. & SCHROEDER, J. I. 1994. Anion selectivity of slow anion channels in the plasma membrane of guard cells (large nitrate permeability). *Plant Physiology,* 106**,** 383-391.

SCHROEDER, J. I. 1988. K^+ transport properties of K^+ channels in the plasma membrane of *Vicia faba* guard cells. *Journal of General Physiology,* 92**,** 667-683.

SCHROEDER, J. I., ALLEN, G. J., HUGOUVIEUX, V., KWAK, J. M. & WANER, D. 2001a. Guard cell signal transduction. *Annual Review of Plant Physiology and Plant Molecular Biology,* 52**,** 627-658.

SCHROEDER, J. I. & FANG, H. H. 1991. Inward-rectifying K^+ channels in guard cells provide a mechanism for low-affinity K^+ uptake. *Proceedings of the National Academy of Sciences of the United States of America,* 88**,** 11583-11587.

SCHROEDER, J. I. & HEDRICH, R. 1989. Involvement of ion channels and active transport in osmoregulation and signaling of higher plant cells. *Trends in Biochemical Sciences,* 14**,** 187-192.

SCHROEDER, J. I. & KELLER, B. U. 1992. Two types of anion channel currents in guard cells with distinct voltage regulation. *Proceedings of the National Academy of Sciences of the United States of America,* 89**,** 5025-5029.

SCHROEDER, J. I., KWAK, J. M. & ALLEN, G. J. 2001b. Guard cell abscisic acid signalling and engineering drought hardiness in plants. *Nature,* 410**,** 327-330.

SCHULZ-LESSDORF, B. & HEDRICH, R. 1995. Protons and calcium modulate SV-type channels in the vacuolar-lysosomal compartment—channel interaction with calmodulin inhibitors. *Planta,* 197**,** 655-671.

SCHULZ-LESSDORF, B., LOHSE, G. & HEDRICH, R. 1996. GCAC1 recognizes the pH gradient across the plasma membrane: A pH-sensitive and ATP-dependent anion channel links guard cell membrane potential to acid and energy metabolism. *Plant Journal,* 10**,** 993-1004.

SCHWEIGHOFER, A., HIRT, H. & MESKIENE, L. 2004. Plant PP2C phosphatases: emerging functions in stress signaling. *Trends in Plant Science,* 9**,** 236-243.

SERRANO, R. 1989. Structure and function of plasma membrane ATPase. *Annual Review of Plant Physiology and Plant Molecular Biology,* 40**,** 61-94.

SHIMAZAKI, K.-I., DOI, M., ASSMANN, S. M. & KINOSHITA, T. 2007. Light regulation of stomatal movement. *Annual Review of Plant Biology.*

SHOPE, J. C., DEWALD, D. B. & MOTT, K. A. 2003. Changes in surface area of intact guard cells are correlated with membrane internalization. *Plant Physiology,* 133**,** 1314-1321.

SIEGEL, R. S., XUE, S., MURATA, Y., YANG, Y., NISHIMURA, N., WANG, A. & SCHROEDER, J. I. 2009. Calcium elevation-dependent and attenuated resting calcium dependent abscisic acid induction of stomatal closure and abscisic acid-induced enhancement of calcium sensitivities of S-type anion and inward-rectifying K^+ channels in *Arabidopsis* guard cells. *Plant Journal,* 59**,** 207-220.

SLAYMAN, C. L. & SLAYMAN, C. W. 1974. Depolarization of the plasma membrane of *Neurospora* during active transport of glucose: evidence for a proton dependent cotransport system. *Proceedings of the National Academy of Sciences of the United States of America,* 71**,** 1935-1939.

SMITH, F. A. 1973. The internal control of nitrate uptake into excised barley roots with differing salt contents. *New Phytologist,* 72**,** 769-782.

SOKOLOVSKI, S. & BLATT, M. R. 2004. Nitric oxide block of outward rectifying K^+ channels indicates direct control by protein nitrosylation in guard cells. *Plant Physiology,* 136**,** 4275-4284.

SOKOLOVSKI, S., HILLS, A., GAY, R., GARCIA-MATA, C., LAMATTINA, L. & BLATT, M. R. 2005. Protein phosphorylation is a prerequisite for intracellular Ca^{2+} release and ion channel control by nitric oxide and abscisic acid in guard cells. *Plant Journal,* 43**,** 520-529.

SOKOLOVSKI, S., HILLS, A., GAY, R. A. & BLATT, M. R. 2008. Functional interaction of the SNARE protein NtSyp121 in Ca^{2+} channel gating, Ca^{2+} transients and ABA signalling of stomatal guard cells. *Molecular Plant,* 1**,** 347-358.

SPANSWICK, R. M. 1981. Electrogenic ion pumps. *Annual Review of Plant Physiology and Plant Molecular Biology,* 32**,** 267-289.

STAMLER, J. S., LAMAS, S. & FANG, F. C. 2001. Nitrosylation: The prototypic redox-based signaling mechanism. *Cell,* 106**,** 675-683.

SWEETLOVE, L. J., BEARD, K. F. M., NUNES-NESI, A., FERNIE, A. R. & RATCLIFFE, R. G. 2010. Not just a circle: flux modes in the plant TCA cycle. *Trends in Plant Science,* 15**,** 462-470.

SZE, H., LI, X. H. & PALMGREN, M. G. 1999. Energization of plant cell membranes by H^+-pumping ATPases: Regulation and biosynthesis. *Plant Cell,* 11**,** 677-689.

SZE, H., SCHUMACHER, K., MULLER, M. L., PADMANABAN, S. & TAIZ, L. 2002. A simple nomenclature for a complex proton pump: VHA genes encode the vacuolar H^+-ATPase. *Trends in Plant Science,* 7**,** 157-161.

SZYROKI, A., IVASHIKINA, N., DIETRICH, P., ROELFSEMA, M. R. G., ACHE, P., REINTANZ, B., DEEKEN, R., GODDE, M., FELLE, H., STEINMEYER, R., PALME, K. & HEDRICH, R. 2001. KAT1 is not essential for stomatal opening. *Proceedings of the National Academy of Sciences of the United States of America,* 98**,** 2917-2921.

TALBOTT, L. D. & ZEIGER, E. 1993. Sugar and organic acid accumulation in guard cells of *Vicia faba* in response to red and blue light. *Plant Physiology,* 102**,** 1163-1169.

TALBOTT, L. D. & ZEIGER, E. 1996. Central roles for potassium and sucrose in guard cell osmoregulation. *Plant Physiology,* 111**,** 1051-1057.

TARCZYNSKI, M. C. & OUTLAW, W. H. 1990. Partial characterization of guard-cell phosphenolpyruvate carboxylase: kinetic datum collection in real time from single-cell activities. *Archives of Biochemistry and Biophysics,* 280**,** 153-158.

TESTER, M. & MACROBBIE, E. A. C. 1990. Cytoplasmic calcium affects the gating of potassium channels in the plasma membrane of *Chara corallina*: a whole-cell study using calcium-channel effectors. *Planta,* 180**,** 569-581.

THIEL, G., BLATT, M. R., FRICKER, M. D., WHITE, I. R. & MILLNER, P. 1993. Modulation of K^+ channels in *Vicia* stomatal guard cells by peptide homologs to the auxin binding protein C terminus. *Proceedings of the National Academy of Sciences of the United States of America,* 90**,** 11493-11497.

THIEL, G., MACROBBIE, E. A. C. & BLATT, M. R. 1992. Membrane transport in stomatal guard cells: the importance of voltage control. *Journal of Membrane Biology,* 126**,** 1-18.

THULEAU, P., WARD, J. M., RANJEVA, R. & SCHROEDER, J. I. 1994. Voltage-dependent calcium-permeable channels in the plasma membrane of a higher plant cell. *Embo Journal,* 13**,** 2970-2975.

UENO, K., KINOSHITA, T., INOUE, S., EMI, T. & SHIMAZAKI, K. 2005. Biochemical characterization of plasma membrane H^+-ATPase activation in guard cell protoplasts of *Arabidopsis thaliana* in response to blue light. *Plant and Cell Physiology,* 46**,** 955-963.

UMEZAWA, T., SUGIYAMA, N., MIZOGUCHI, M., HAYASHI, S., MYOUGA, F., YAMAGUCHI-SHINOZAKI, K., ISHIHAMA, Y., HIRAYAMA, T. & SHINOZAKI, K. 2009. Type 2C protein phosphatases directly regulate abscisic acid-activated protein kinases in *Arabidopsis*. *Proceedings of the National Academy of Sciences of the United States of America,* 106**,** 17588-17593.

UOZUMI, N., GASSMANN, W., GAO, Y. W. & SCHROEDER, J. I. 1995. Identification of strong modifications in cation selectivity in an *Arabidopsis* inward rectifying potassium channel by mutant selection in yeast. *Journal of Biological Chemistry,* 270**,** 24276-24281.

VAHISALU, T., KOLLIST, H., WANG, Y.-F., NISHIMURA, N., CHAN, W.-Y., VALERIO, G., LAMMINMAKI, A., BROSCHE, M., MOLDAU, H., DESIKAN, R., SCHROEDER, J. I. & KANGASJARVI, J. 2008. SLAC1 is required for plant guard cell S-type anion channel function in stomatal signalling. *Nature,* 452**,** 487-U15.

VAN KIRK, C. A. & RASCHKE, K. 1977. Stomatal aperture and malate content of epidermis effects of chloride and abscisic acid. *Plant Physiology (Rockville),* 59**,** 96-96.

VAN KIRK, C. A. & RASCHKE, K. 1978a. Presence of chloride reduces malate production in epidermis during stomatal opening. *Plant Physiology,* 61**,** 361-364.

VAN KIRK, C. A. & RASCHKE, K. 1978b. Release of malate from epidermal strips during stomatal closure. *Plant Physiology,* 61**,** 474-475.

VOLOTOVSKI, I. D., SOKOLOVSKY, S. G., MOLCHAN, O. V. & KNIGHT, M. R. 1998. Second messengers mediate increases in cytosolic calcium in tobacco protoplasts. *Plant Physiology,* 117**,** 1023-1030.

WANG, Y. & BLATT, M. R. 2011. Anion channel sensitivity to cytosolic organic acids implicates a central role for oxaloacetate in integrating ion flux with metabolism in stomatal guard cells. *Biochemical Journal,* 439**,** 161-170.

WANG, Y., PAPANATSIOU, M., EISENACH, C., KARNIK, R., WILLIAMS, M., HILLS, A., LEW, V. L. & BLATT. M.R. (2012). Systems dynamic modelling of a guard cell Cl^- channel mutant uncovers an emergent homeostatic network regulating stomatal transpiration. *Plant Physiology* 160**,** 1956-1967

WARD, J. M. 1997. Patch-clamping and other molecular approaches for the study of plasma membrane transporters demystified. *Plant Physiology*, 114**,** 1151-1159.

WARD, J. M., MAESER, P. & SCHROEDER, J. I. 2009. Plant ion channels: gene families, physiology, and functional genomics analyses. *Annual Review of Physiology*. 71**,**59–82

WARD, J. M. & SCHROEDER, J. I. 1994. Calcium-activated K^+ channels and calcium-induced calcium release by slow vacuolar ion channels in guard cell vacuoles implicated in the control of stomatal closure. *Plant Cell,* 6**,** 669-683.

WASILEWSKA, A., VLAD, F., SIRICHANDRA, C., REDKO, Y., JAMMES, F., VALON, C., FREY, N. F. D. & LEUNG, J. 2008. An update on abscisic acid signaling in plants and more. *Molecular Plant,* 1**,** 198-217.

WEBB, A. A. R., MCAINSH, M. R., MANSFIELD, T. A. & HETHERINGTON, A. M. 1996. Carbon dioxide induces increases in guard cell cytosolic free calcium. *Plant Journal,* 9**,** 297-304.

WENDEHENNE, D., PUGIN, A., KLESSIG, D. F. & DURNER, J. 2001. Nitric oxide: comparative synthesis and signaling in animal and plant cells. *Trends in Plant Science,* 6**,** 177-183.

WILKINSON, J. Q. & CRAWFORD, N. M. 1993. Identification and characterization of a chlorate-resistant mutant of *Arabidopsis thaliana* with mutations in both nitrate reductase structural genes NIA1 and NIA2. *Molecular & General Genetics*, 239**,** 289-297.

WILLMER, C. & FRICKER, M. 1996. *Stomata*. 2: 1-375. London, Chapman and Hall

WOJTASZEK, P. 1997. Oxidative burst: An early plant response to pathogen infection. *Biochemical Journal,* 322**,** 681-692.

WOLFE, J. 1982. The conjugation junction of Tetrahymena: Its structure and development. *Journal of Morphology,* 172**,** 159-178.

WOLFE, J. & STEPONKUS, P. L. 1981. The dynamics of area changes in the protoplast plasma membrane. *Proceedings of the International Botanical Congress,* 13**,** 245.

WOODWARD, A. W. & BARTEL, B. 2005. Auxin: Regulation, action, and interaction. *Annals of Botany,* 95**,** 707-735.

WOODWARD, F. I. 2002. Potential impacts of global elevated CO_2 concentrations on plants. *Current Opinion in Plant Biology,* 5**,** 207-211.

WU, Y., KUZMA, J., MARECHAL, E., GRAEFF, R., LEE, H. C., FOSTER, R. & CHUA, N. H. 1997. Abscisic acid signaling through cyclic ADP-Ribose in plants. *Science,* 278**,** 2126-2130.

XUE, S., HU, H., RIES, A., MERILO, E., KOLLIST, H. & SCHROEDER, J. I. 2011. Central functions of bicarbonate in S-type anion channel activation and OST1 protein kinase in CO_2 signal transduction in guard cell. *Embo Journal,* 30**,** 1645-1658.

YAMASAKI, H. & SAKIHAMA, Y. 2000. Simultaneous production of nitric oxide and peroxynitrite by plant nitrate reductase: in vitro evidence for the NR-dependent formation of active nitrogen species. *Febs Letters,* 468**,** 89-92.

ZHANG, D. P., WU, Z. Y., LI, X. Y. & ZHAO, Z. X. 2002. Purification and identification of a 42-kilodalton abscisic acid-specific-binding protein from epidermis of broad bean leaves. *Plant Physiology,* 128**,** 714-725.

ZHU, J. K. 2002. Salt and drought stress signal transduction in plants. *Annual Review of Plant Biology,* 53**,** 247-273.

APPENDIX

Quantitative Analysis *slac1-1* Mutant by OnGuard Model

To explore the physiological context of the *slac1-1* mutation, quantitative systems modeling of the guard cells was carried out. The modeling incorporating all of the known transporters at the plasma membrane and tonoplast, their biophysical and kinetic characteristics, the salient features of sucrose and malic acid (Mal) metabolism, as well as the homeostatic parameters of Ca^{2+} and pH buffering (Hills et al., 2012). The modeling was carried out by Prof. Blatt, who used an equivalent ensemble of model parameters (Chen et al., 2012a) to simulate the diurnal cycle of stomatal movements after scaling guard cell volume and stomatal aperture to the dimensions of the *Arabidopsis* stomatal complex while maintaining transporter surface densities. Simulations were carried out first with the full complement of membrane transporters including the SLAC1 current, and then with the SLAC1 current omitted. Results shown below are macrosocpic ouputs from the OnGuard model resolved over a standard diurnal cycle (12h light: 12 h dark) with 10 mM KCl, 1 mM CaCl2 and pH 6.5 outside (Chen et al., 2012a). For the results in the subsequent figures, the simulation was initiated with wild-type parameters and the SLAC1 component current eliminated at the start of day 3, yielding a new stable (mutant) cycle from day 4 onwards. Brief analysis is provided with each of the subsequent figures; further details will be found in (Chen et al., 2012a).

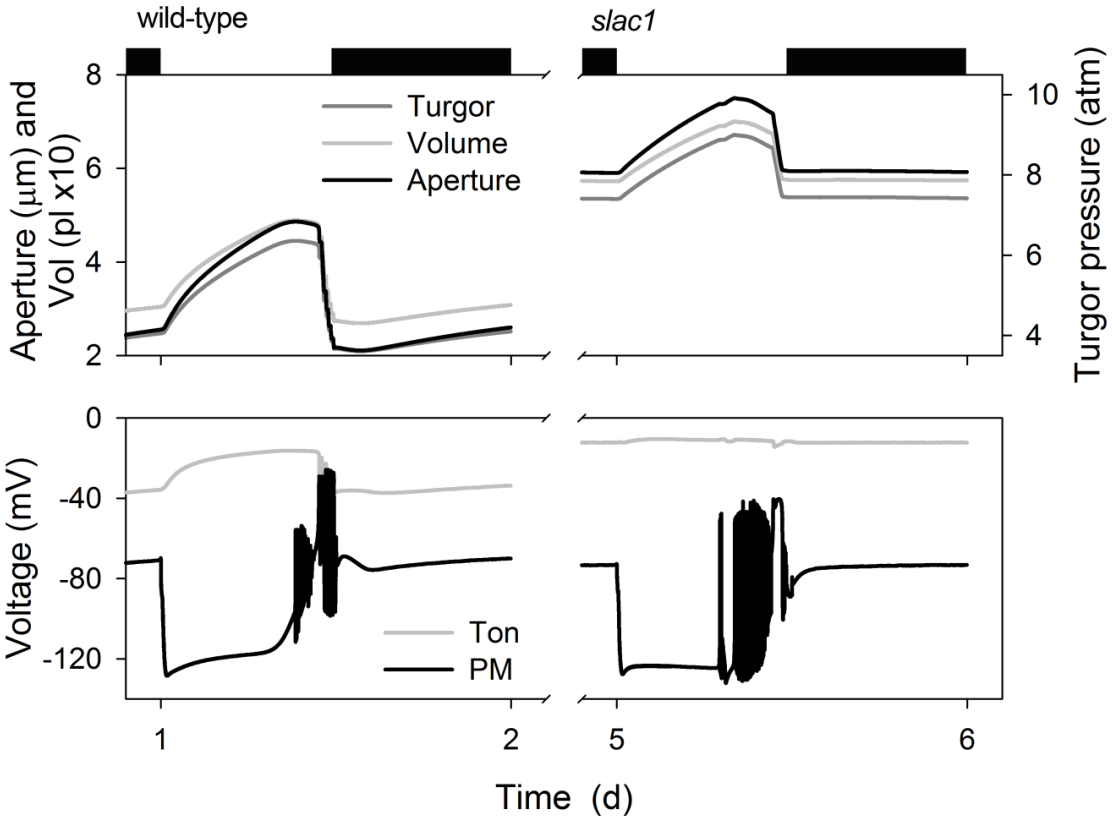
wild-type
slac1
Aperture (µm) and
Vol (pl x10)
Turgor
Volume
Aperture
Turgor pressure (atm)
Voltage (mV)
Ton
PM
Time (d)

Figure 1

Figure 1. Macrosocpic ouputs from the OnGuard model resolved over a standard diurnal cycle (12h light:12 h dark, indicated by bars above) with 10 mM KCl, 1 mM $CaCl_2$ and pH 6.5 outside (Chen et al., 2012a). Representative diurnal cycles are shown for the Wt (*left*) and the *slac1* mutant (*right*). For the results in this and the subsequent figures, the simulation was initiated with Wt parameters and the SLAC1 component current eliminated at the start of day 3, yielding a new stable (mutant) cycle from day 4 onwards. Brief analysis is provided with each of the subsequent figures; further details will be found in (Chen et al., 2012a). Shown are (A) stomatal aperture, turgor pressure and total guard cell volume, and (B) plasma membrane and tonoplast voltage. Stomatal apertures varied over a physiological range between roughly 2 μm and 5 μm in the Wt and were parallelled by physiologically reasonable changes in guard cell volume and turgor. Following stomatal closure at the end of the day, the model generated a small and gradual rise in aperture and the associated outputs that anticipated the start of the next day, much as has been observed *in vivo* (Gorton et al., 1993, Meidner and Willmer, 1993). The start of the day was associated with hyperpolarisation of the plasma membrane to voltages near -130 mV and the dark period was accompanied by depolarisation of the plasma membrane to voltages near the equilibrium voltage for K^+, consistent with the diurnal cycle in energetic outputs of the ATP-driven pumps (Blatt, 1987, Kinoshita et al., 1995, Clint and Blatt, 1989, Blatt and Clint, 1989, Spanswick, 1981). Note the plasma membrane remains hyperpolarised in the absence of inward (depolarising) current through the SLAC1 channel and later in the daylight period, the voltage underwent an extended period of oscillations, between roughly -120 and -50 mV. These oscillations were accompanied by parallel oscillations in elevated $[Ca^{2+}]_i$ and enhanced R-type anion channel activity (see Appendix Figure 3, 4 and 6). Guard cells of *Arabidopsis* are typically 5-6 μm in diameter and 10-12 μm in length, presenting roughly 10% the volume, 20% of the surface area of a *Vicia* guard cell and an input resistance of 20 GΩ or more. Thus, the less hyperpolarised voltages recorded in vivo under similar conditions probably reflects the effects of amplifier leakage current on the free-running voltage of these smaller cells (see Figure 5.4).

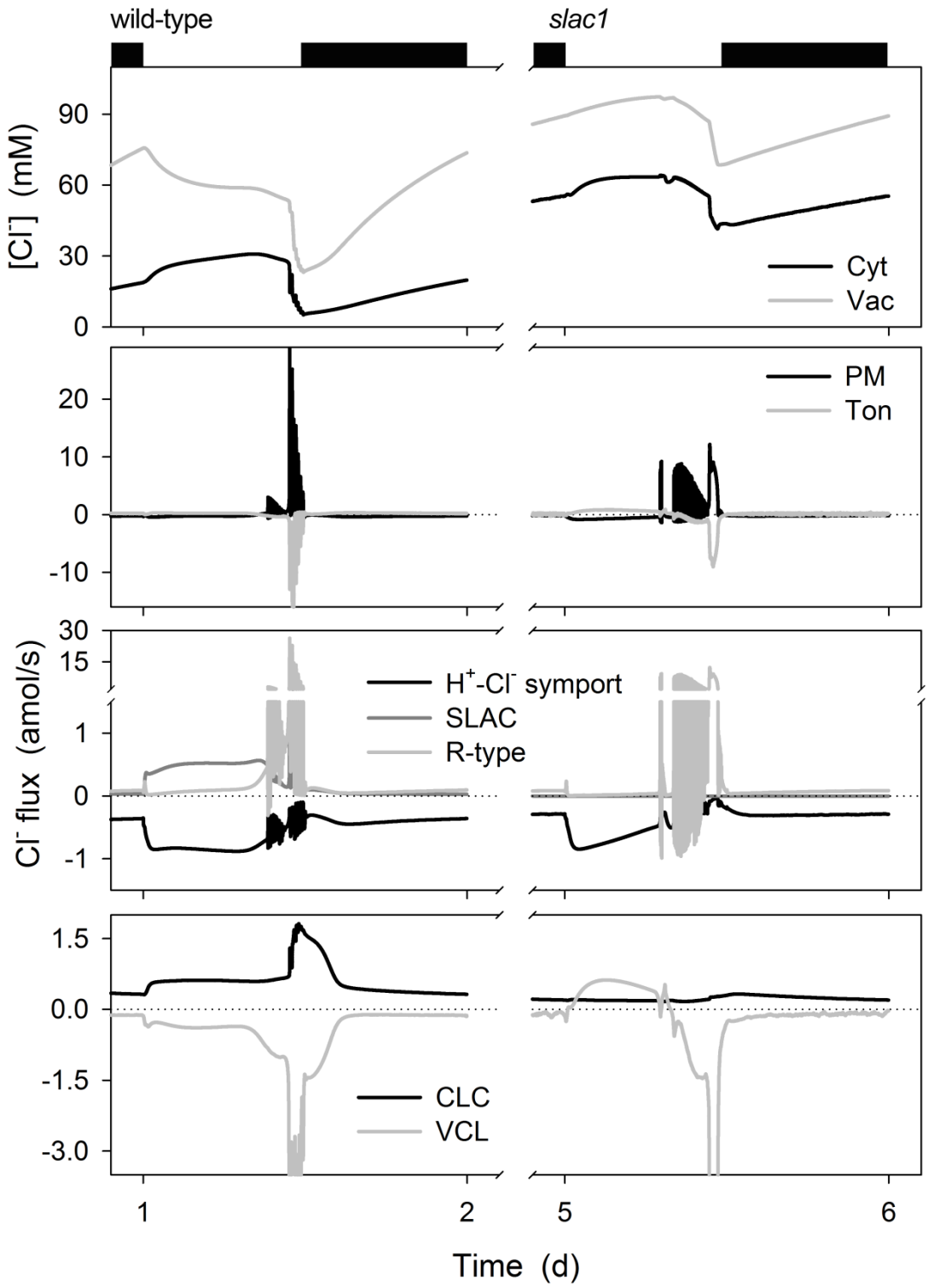
wild-type
slac1
[Cl⁻] (mM)
90
60
30
0
Cyt
Vac
20
10
0
-10
PM
Ton
Cl⁻ flux (amol/s)
30
15
1
0
-1
H⁺-Cl⁻ symport
SLAC
R-type
1.5
0.0
-1.5
-3.0
CLC
VCL
1
2
5
6
Time (d)

Figure 2

Figure 2. Chloride contents and analysis of Cl^- fluxes at the plasma membrane and tonoplast resolved over a standard diurnal cycle (12 h light: 12 h dark, indicated by bars above) (Chen et al., 2012a) for the Wt (*left*) and the *slac1* mutant (*right*) as described in Appendix Figure 1. Shown are (A) total cytosolic and vacuolar [Cl^-], (B) the net flux of Cl^- across the plasma membrane and tonoplast, (C) the flux of Cl^- through the Cl^- -permeable transporters at the plasma membrane, comprising the SLAC and R^- (ALMT-) type anion channels and H^+-Cl^- symporter, and (D) the flux of Cl^- through the Cl^- -permeable transporters at the tonoplast, comprising the VCL channel and CLC H^+-Cl^- antiporter. Positive flux is defined as movement of the ionic species (not the charge) out of the cytosol, either across the plasma membrane or the tonoplast. Note the expanded scales in (C) and (D). In the Wt, both cytosolic and vacuolar Cl^- concentrations exhibited complex, biphasic responses to the diurnal cycle, consistent with experimental observation, in effect leading to an exchange of Cl^- for Mal accumulated in the daytime and vice versa at night (compare Appendix Figure 3) (Raschke and Schnabl, 1978, Talbott and Zeiger, 1993, Talbott and Zeiger, 1996). Stomatal opening was accompanied by a net efflux of Cl^- from the vacuole to the cytosol and, later in the daylight period from the cytosol to the apoplast. Closure was marked by much larger fluxes of Cl^- from the vacuole to the cytosol and export across the plasma membrane; this pattern reversed after the first 1-2 h of dark. The rise in cytosolic Cl^- concentration during the first hours of the day arose from the rapid Cl^- influx across the tonoplast and a slower rise in the rate of Cl^- export across the plasma membrane. Eliminating the SLAC1 current led to a hyper accumulation of Cl^- in both the cytosol and vacuole (A). This effect was accompanied by a reduced Cl^- uptake via the H^+-Cl^- symport (C) and export to the vacuole via the CLC H^+-Cl^- antiport (D). The changes in H^+-coupled Cl^- transport can be understood, therefore, as a consequence of substrate trans-inhibition by the accumulated Cl^- in the two compartments. With the change in driving force, Cl^- flux through the VCL channel at the tonoplast was reversed during much of the daylight period (D), thus leading to accumulation of vacuolar Cl^- during the day (A). Thus, the net effect of the slac1 mutant was to trap Cl^- in the cell and to slow Cl^- exchange between the cytosol and vacuole.

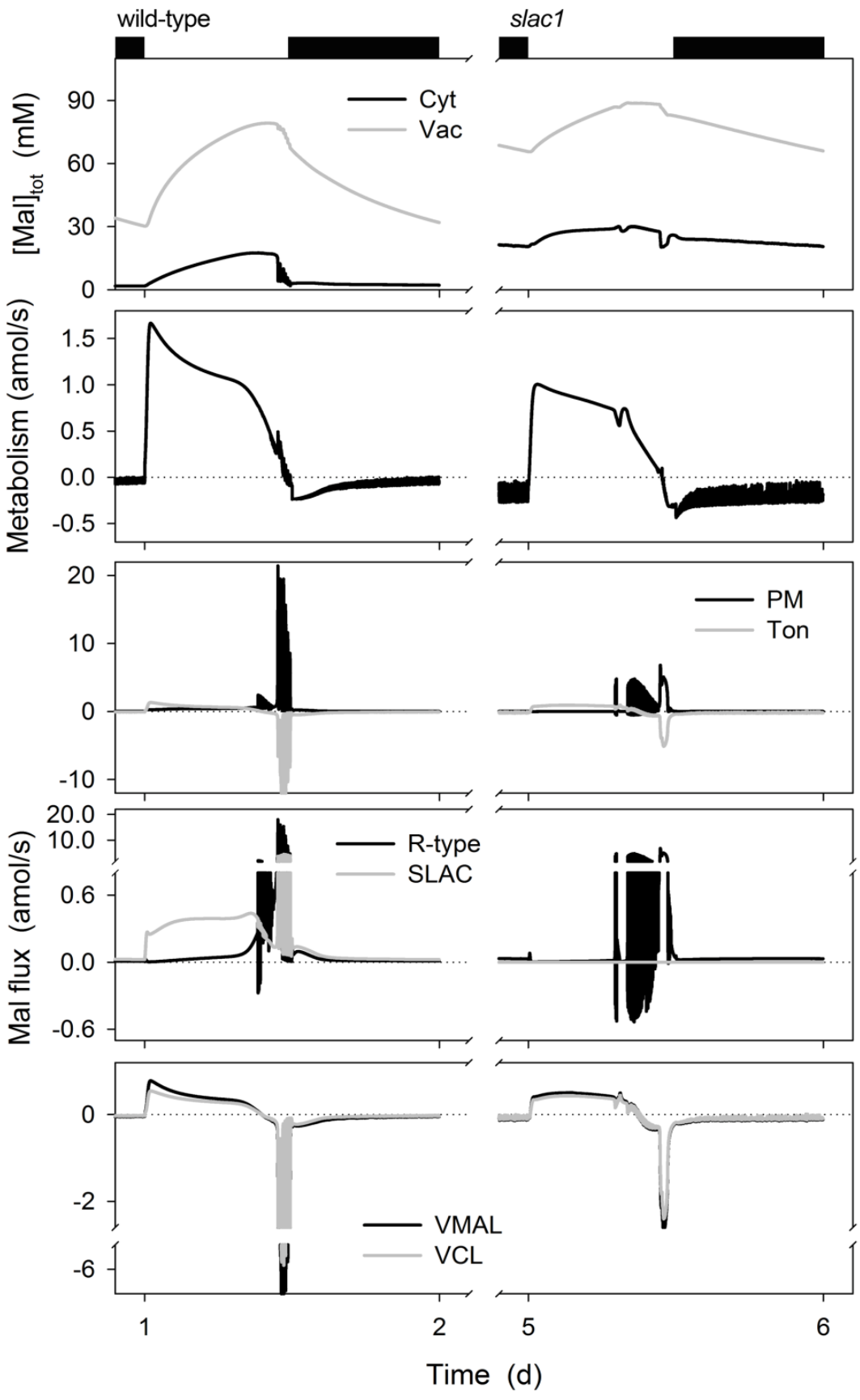
wild-type
slac1
Cyt
Vac
[Mal]tot (mM)
90
60
30
0
Metabolism (amol/s)
1.5
1.0
0.5
0.0
-0.5
20
10
0
-10
PM
Ton
Mal flux (amol/s)
20.0
10.0
0.6
0.0
-0.6
R-type
SLAC
0
-2
-6
VMAL
VCL
1
2
5
6
Time (d)

Figure 3

Figure 3 Malic acid synthesis, total malate (Mal) contents and analysis of Mal^{2-} fluxes at the plasma membrane and tonoplast resolved over a standard diurnal cycle (12 h light:12 h dark, indicated by bars above) (Chen et al., 2012a) for the Wt (*left*) and the *slac1* mutant (*right*) as described in Appendix Figure 1. Shown are (A) total cytosolic and vacuolar [Mal], (B) the rates of Mal synthesis and metabolism, (C) the net flux of Mal^{2-} across the plasma membrane and tonoplast, (D) the Mal^{2-} flux through the Mal^{2-}-permeable transporters at the plasma membrane, comprising the SLAC and R- (ALMT-) type anion channels, and (E) the Mal^{2-} flux through the Mal^{2-} - permeable transporters at the tonoplast, comprising the VMAL and VCL channels. Positive flux is defined as movement of the ionic species (not the charge) out of the cytosol, either across the plasma membrane or the tonoplast. In the Wt, the bulk of Mal production was diverted by transport of Mal^{2-} across the tonoplast, leading to a rise in total vacuolar Mal from 30 mM at the end of the night to near 90 mM before declining at the end of the daylight period; Mal in the cytosol rose from approximately 1 mM to values near 15 mM, much as has been estimated from experimental data (Hills et al., 2012). Mal accumulation was accompanied by a small increase in export across the plasma membrane, culminating at the end of the daylight period in a substantial efflux from the vacuole and cytosol during closure; much documented experimentally (Allaway, 1973, Van Kirk and Raschke, 1978b, Van Kirk and Raschke, 1977, Gotow et al., 1985, Tarczynski and Outlaw, 1990). At the plasma membrane, the OnGuard model predicted Mal efflux to be mediated largely by the SLAC-type anion channel during daylight with the added contribution of flux through the R- (ALMT-) type anion channel during stomatal closure. With the loss of the SLAC1 efflux pathway, Mal hyperaccumulated in the *slac1* mutant (A) despite the reduced synthesis (B). Its reduced efflux across the plasma membrane was a direct consequence of loss of the SLAC1 flux pathway and because of the shift in the balance of membrane voltages out of the range effective in activating the R- (ALMT-) type current (see Appendix Figure 1). The much reduced influx across the tonoplast from the vacuole to the cytosol at the end of the daylight period (D) arose entirely from the build-up of Mal in the cytosol (A) and the resulting decrease in driving force.

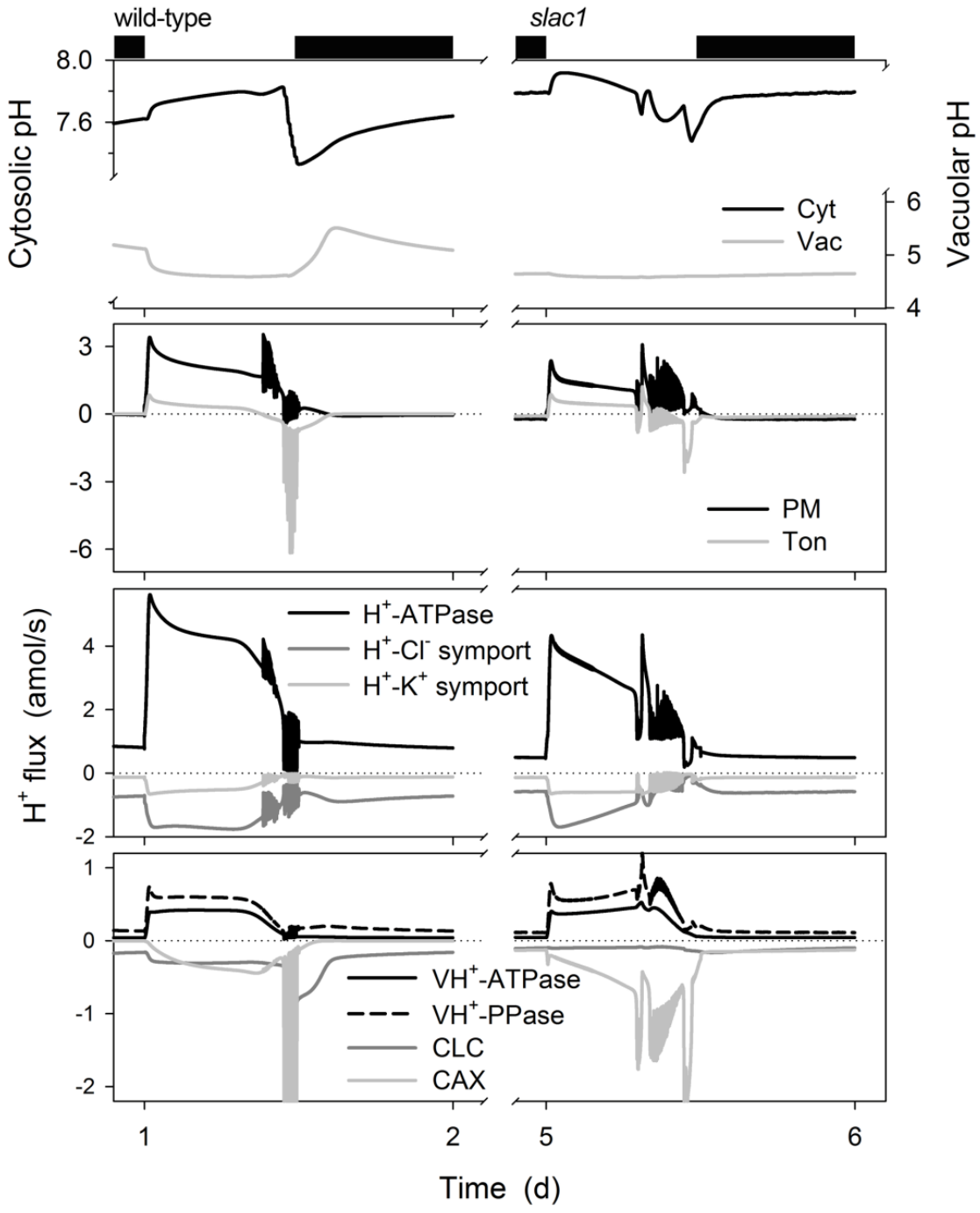
wild-type
slac1
8.0
7.6
Cytosolic pH
Vacuolar pH
Cyt
Vac
6
5
4
3
0
-3
-6
PM
Ton
H+-ATPase
H+-Cl- symport
H+-K+ symport
H+ flux (amol/s)
4
2
0
-2
1
0
-1
-2
VH+-ATPase
VH+-PPase
CLC
CAX
1
2
5
6
Time (d)

Figure 4

Figure 4 Cytosolic and vacuolar pH, and analysis of H^+ fluxes across the plasma membrane an d tonoplast resolved over a standard diurnal cycle (12 h light:12 h dark, indicated by bars above) (Chen et al., 2012a) for the Wt (*left*) and the *slac1* mutant (*right*) as described in Appendix Figure 1. Shown are (A) cytosolic and vacuolar pH, (B) the net H^+ flux across the plasma membrane and tonoplast, (C) the H^+ flux through the H^+-permeable transporters at the plasma membrane, comprising the H^+-ATPase, and the H^+-K^+ and H^+-Cl^- symporters, and (D) the H^+ flux through the H^+ permeable transporters at the tonoplast, comprising the VH^+-ATPase, VH^+-PPase, the CLC H^+-Cl^- antiporter and the CAX H^+-Ca^{2+} antiporter. Positive flux is defined as movement of the ionic species (not the charge) out of the cytosol, either across the plasma membrane or the tonoplast. The OnGuard model faithfully reproduced the characteristics anticipated for both cytosolic and vacuolar pH in the Wt. It predicted the vast bulk of the H^+ production associated with daytime Mal synthesis (Appendix Figure 3) to be exported via the plasma membrane H^+-ATPase, with roughly 20% transported to the vacuole (B-D). In the vacuole, Mal comprises the major pH buffer and its accumulation is associated with acidification of the vacuolar contents (Van Kirk and Raschke, 1978a, Outlaw, 1990, Talbott and Zeiger, 1993, Willmer and Fricker, 1996). Diurnal changes in vacuolar pH in the model resulted primarily from Mal transport and charge balance with H^+ (Appendix figure 3). The organic acid is thought to be transported as the fully deprotonated (Mal^{2-}) form -with the VMAL channel as the primary pathway for tonoplast Mal^{2-} flux implying charge balance via the tonoplast VH^+- ATPase and H^+-PPase, consistent with estimates from experimental data in several plant species and cell types (Rea and Poole, 1993, Martinoia et al., 2007). Even so, the bulk of H^+ production must be balanced by its export across the plasma membrane (see Appendix Figure 5). The model predicted roughly 30-40% of the H^+ export via the H^+-ATPase to be balanced by H^+ entry coupled with Cl^- uptake and, to a lesser extent, with K^+ uptake (C). Consistent with this observation, the suppressed influx of H^+ to the cytosol via the H^+-Cl^- symport (C) and CLC H^+-Cl^- antiport (D) was accompanied by an elevation in the mean cytosolic pH (A; Figure 5.17). Thus, the model predicts the rise in cytosolic pH to stem from the accumulated Cl^- in the cytosol (Appendix Figure 2) and the consequent substrate trans-inhibition of H^+-coupled anion transport (Appendix Figure 5) in addition to reduced H^+ generation via Mal synthesis (Appendix Figure 3).

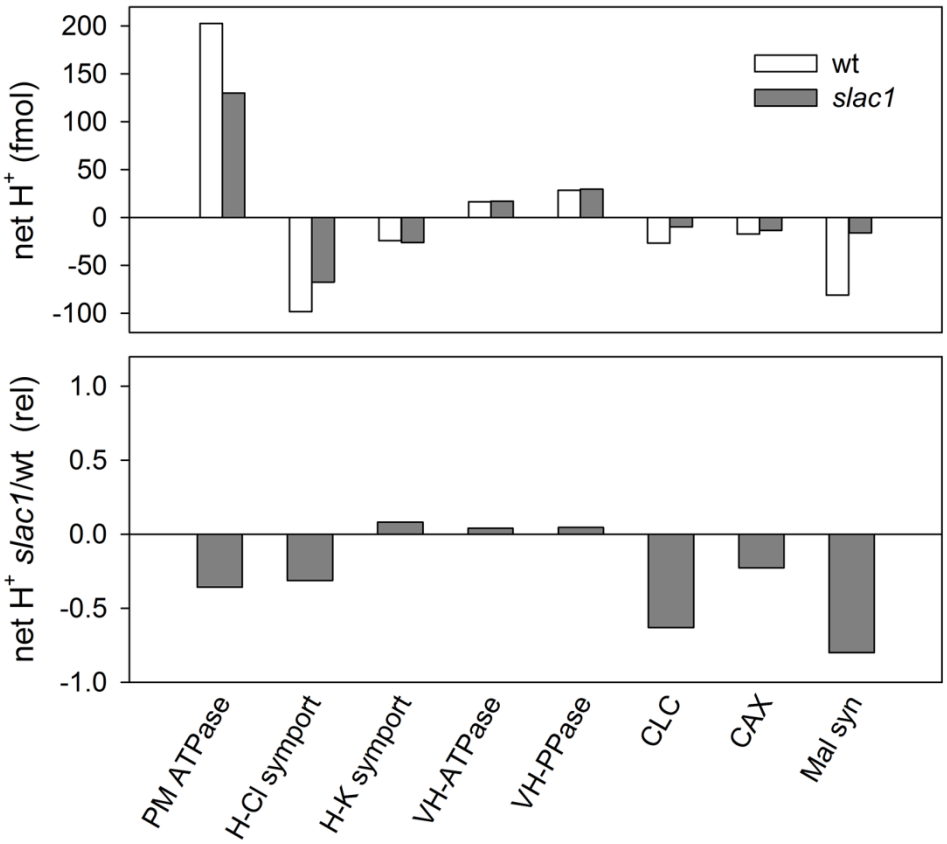

Figure 5 Total H^+ distribution summed over a 24-h period as predicted from the OnGuard model for the Wt and *slac1* mutant guard cell.

Shown are (A) the net H^+ generation and export distributed between Mal synthesis and H^+-coupled transport, and (B) the change in H^+ load in the *slac1* mutant relative to the Wt. A positive sign indicates H^+ removal from the cytosol and a negative sign corresponds to an H^+ load on the cytosol. Consistent with studies in several plant and fungal cell types (Smith, 1973, Blatt and Slayman, 1987, Sanders et al., 1989, Guern et al., 1991), roughly 30-40% of H^+ export via the plasma membrane H^+-ATPase was balanced by H^+ return coupled in symport with Cl^- and, a similar fraction of H^+ export to the vacuole via the VH^+-ATPase and H^+-PPase was balanced by H^+ return through the H^+-Cl^- antiporter. The bulk of the remaining H^+ load was generated by Mal synthesis. The model predicted the *slac1* mutant to lead to disproportionate decreases in H^+ loads imposed by Mal synthesis and coupled H^+ transport compared with H^+ export by the H^+-ATPase across the plasma membrane, resulting in the overall shift to more alkaline cytosolic pH values (Appendix Figure 4 and 5.9-5.15).

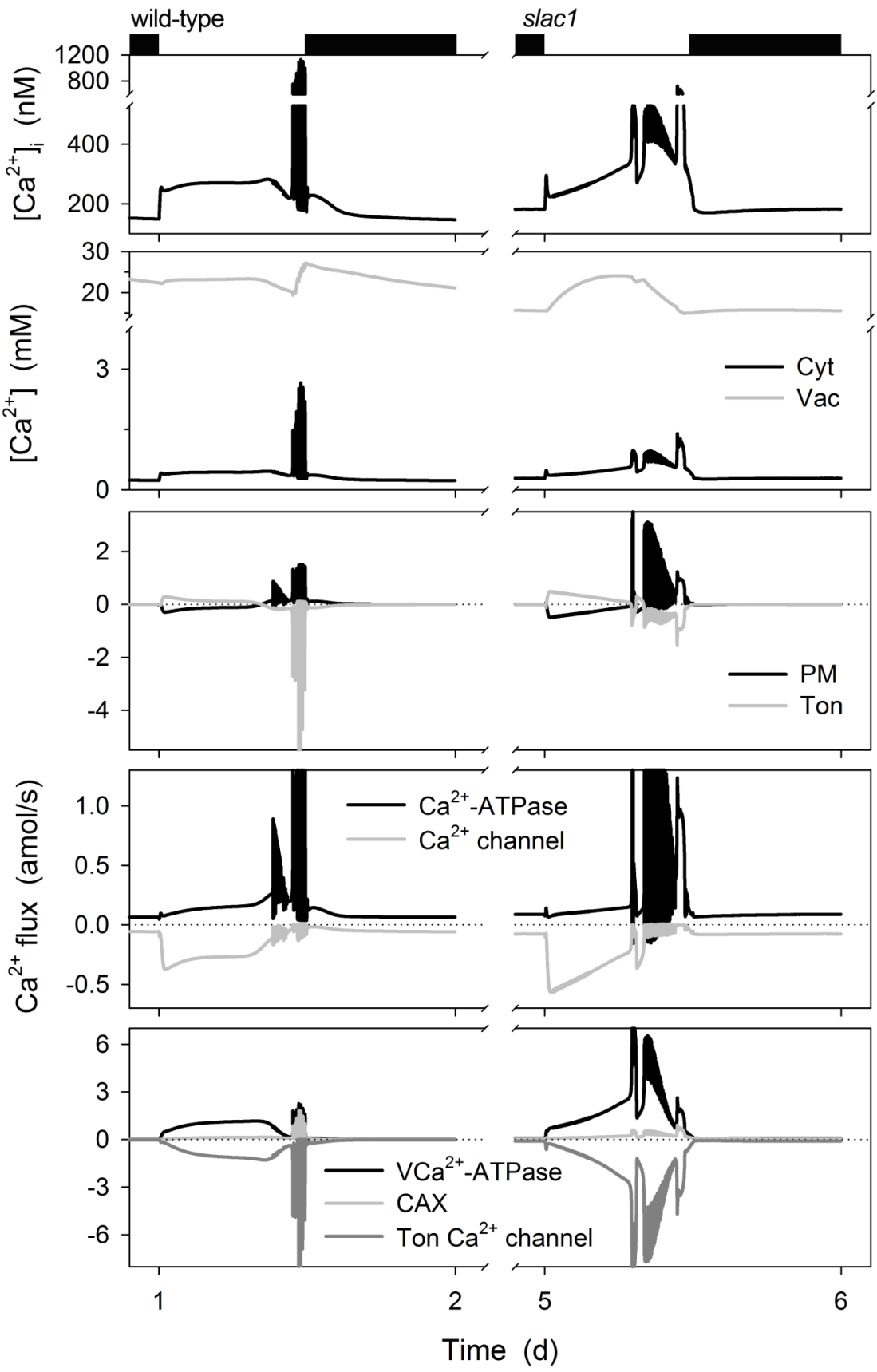
wild-type
slac1
1200
800
400
200
[Ca2+]i (nM)
30
20
3
0
[Ca2+] (mM)
Cyt
Vac
2
0
-2
-4
PM
Ton
1.0
0.5
0.0
-0.5
Ca2+ flux (amol/s)
Ca2+-ATPase
Ca2+ channel
6
3
0
-3
-6
VCa2+-ATPase
CAX
Ton Ca2+ channel
1
2
5
6
Time (d)

Figure 6

Figure 6. Total cytosolic and vacuolar [Ca^{2+}], cytosolicfree [Ca^{2+}], and analysis of Ca^{2+} fluxes across the plasma membrane and tonoplast resolved over a standard diurnal cycle (12 h light:12 h dark, indicated by bars above) (Chen et al., 2012a) for the Wt (*left*) and the *slac1* mutant (right) as described in Appendix Figure 1. Shown are (A) the cytosolic-free [Ca^{2+}] ([$Ca^{2+}]_i$), (B) the total cytosolic and vacuolar [Ca^{2+}], (C) the net flux of Ca^{2+} across the plasma membrane and tonoplast, (D) the Ca^{2+} flux through the Ca^{2+} -permeable transporters at the plasma membrane, comprising the hyperpolarisation-activated Ca^{2+} channel and the Ca^{2+}- ATPase, and (E) the flux of Ca^{2+} through the Ca^{2+}- permeable transporters at the tonoplast, comprising the Ca^{2+}-ATPase, the CAX H^{+}-Ca^{2+} antiporter, and the TonVCa Ca^{2+} channel. Flux through the TPC channel accounts for less than two percent of the total Ca^{2+} flux across the tonoplast and has therefore been omitted for purposes of clarity. Positive flux is defined as movement of the ionic species (not the charge) out of the cytosol, either across the plasma membrane or the tonoplast. For the wild-type, the OnGuard model predicted $[Ca^{2+}]_i$ to rise from a resting value near 160 nM in the dark to a mean daylight value near 260 nM (A). Stomatal closure was accompanied by a series of voltage (Appendix Figure 1) and $[Ca^{2+}]_i$ excursions before recovery in dark levels for total [Ca^{2+}] and $[Ca^{2+}]_i$. These characteristics are broadly consistent with experimental observations of action potential-like oscillations in membrane voltage and $[Ca^{2+}]_i$ elevations (Gilroy et al., 1991, Thiel et al., 1992, Irving et al., 1992, McAinsh et al., 1992) and diurnal variations in $[Ca^{2+}]_i$ (Dodd et al., 2006, Dodd et al., 2005). Further details will be found in (Chen et al., 2012a). Vacuolar Ca^{2+} circulation dominated over transport at the plasma membrane by at least one order of magnitude, an observation generally in accord with the major roles for endomembrane sequestration and release in Ca^{2+} homeostasis (Sanders et al., 2002, Blatt et al., 2007, McAinsh and Pittman, 2009) and its importance in potentiating $[Ca^{2+}]_i$ signals (Gilroy et al., 1991, McAinsh et al., 1991, Grabov and Blatt, 1997, Grabov and Blatt, 1998, Grabov and Blatt, 1999, Garcia-Mata et al., 2003). At the plasma membrane (D), the Ca^{2+} flux was dominated by the Ca^{2+} channels during much of the daylight hours and by the Ca^{2+}-ATPase at the end of the day and in the first hours of dark, determined primarily by changes in voltage across the plasma membrane (Appendix Figure 1). In the *slac1* mutant, the prolonged daytime elevation of $[Ca^{2+}]_i$ (A) was associated with a higher Ca^{2+} influx through Ca^{2+} channels at the plasma

membrane (C,D). These observations lead to the prediction that the elevated daytime $[Ca^{2+}]_i$ of the *slac1* mutant can be ascribed to the increased electrical driving force for Ca^{2+} entry across the plasma membrane.

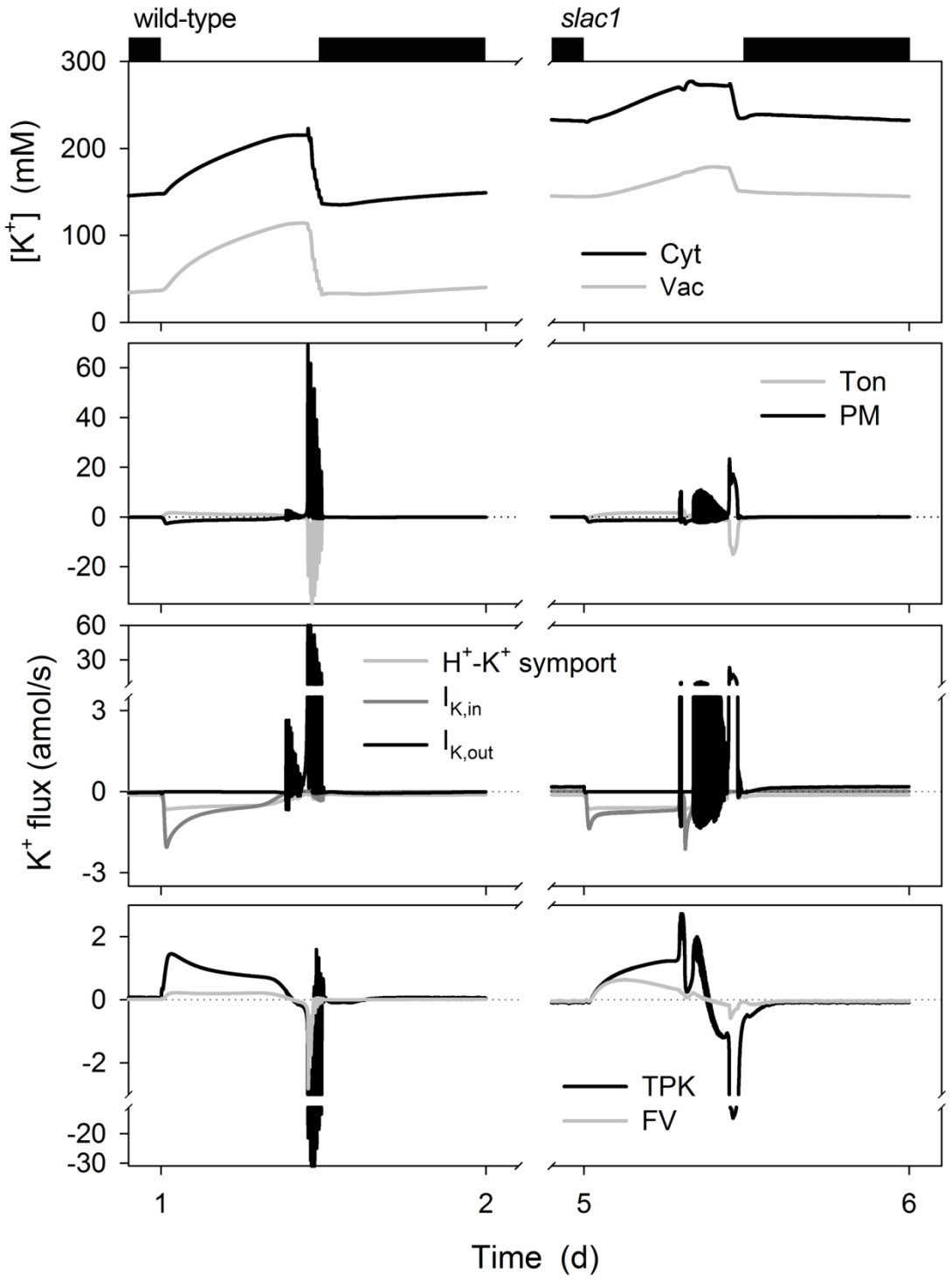
wild-type
slac1
[K+] (mM)
300
200
100
0
Cyt
Vac
60
40
20
0
-20
Ton
PM
K+ flux (amol/s)
60
30
3
0
-3
H+-K+ symport
IK,in
IK,out
2
0
-2
-20
-30
TPK
FV
1
2
5
6
Time (d)

Figure 7

Figure 7 K^+ contents and analysis of K^+ fluxes at the plasma membrane and tonoplast resolved over a standard diurnal cycle (12 h light:12 h dark, indicated by bars above) (Chen et al., 2012a) for the Wt (*left*) and the slac1 mutant (*right*) as described in Appendix Figure 1. Shown are (A) cytosolic and vacuolar [K^+], (B) the net K^+ flux across the plasma membrane and tonoplast, (C) the K^+ flux through the K^+- permeable transporters at the plasma membrane, comprising the two K^+ channels and the H^+- K^+ symporter, and (D) the K^+ flux through the K^+ permeable transporters at the tonoplast, comprising the TPK and FV channels. K^+ flux through the TPC channel accounted for less than one percent of either of the other channel fluxes, and has therefore been omitted for purposes of clarity. Positive flux is defined as movement of the ionic species (not the charge) out of the cytosol, either across the plasma membrane or the tonoplast. In the Wt, the cytosolic K^+ concentration varied between approximately 140 mM and 230 mM; in the vacuole, K^+ concentrations ranged between approximately 40 and 120 mM (A). The major proportion of K^+ influx across the plasma membrane was shunted across the tonoplast to the vacuole during the day and this pattern reversed in the first hours of dark, as expected from experimental observation (Chen et al., 2012a, Hills et al., 2012). At the plasma membrane (C), K^+ influx was dominated by $I_{K,in}$ in the first half of the day, this flux relaxing to roughly that through the H^+-K^+ symport in the second half of the day. Closure was marked by the predominance of K^+ efflux through $I_{K,out}$, which relaxed to a near-zero value during the night. The model predicted the *slac1* mutant to retain substantial levels of K^+ in both cytosol and vacuole (A) consistent with experiment (Vahisalu et al., 2008, Negi et al., 2008); it yielded a reduced K^+ influx (C) via $I_{K,in}$ (compare with Figure 5.2).The reduced efflux across the plasma membrane at the end of the daylight period (B), despite the enhancement of $I_{K,out}$, was associated with the reduced Cl^- and Mal efflux (Appendix Figure 2-3) balancing charge.